Kinetics and mechanisms of early stages of resorcinol-formaldehyde polymerization

Katarzyna Zofia Gaca

Degree of Doctor of Philosophy

2012

Declaration of Authors Rights

Signed:

Date:

Acknowledgements

Most of all, I would like to thank Jan Sefcik who supervised my work in every possible detail. He motivated me every single day, challenged me to think both creatively and critically, saw me through rough patches and shared my joy of each success. Without his support and sincerity I would not be writing this thesis.

I would also like to thank John Parkinson, whose expertise in NMR proved invaluable for this work. I am glad that he shared his knowledge with me and was always eager to discuss all intricacies of NMR.

Regular meetings and input provided by Ashleigh Fletcher and Alison Nordon were very inspiring and affected my ways of thinking, opening my eyes to brand new ideas.

My practical work would not be possible if it was not for the technical staff of the department – I would like to thank especially Jim Murphy and John Wilkie not only for their assistance at the lab but also for their bonhomie. I am more than happy when I reminisce working with Craig Irving who taught me how to tame wild beasts called NMR spectrometers.

My deepest gratitude goes to every single person in the Department of Chemical and Process Engineering who made working with both enjoyable and inspiring.

I also wish to thank Peter Hall for his financial support of my work.

Living away from home, my family and friends proved to be one of the greatest challenges I have faced so far. I understood how blessed I am to have them in my life – I felt their love and support at every step of the way. I cannot thank enough my Parents for everything they have done for me; for the great things and those tiny ones.

And last but not least, I want to thank my Partner who stood by me in my darkest moments and celebrated my successes, no matter the distance that separated us. *Nie znoszę Cię.*

Abstract

This work focuses on the main aspects of mechanism and kinetics of resorcinol-formaldehyde sol-gel polymerization. Nuclear Magnetic Resonance, Dynamic Light Scattering, pH and gel time measurements, as well as IR and Raman spectroscopies were used to examine this process. Experiments and methods were chosen so that both chemical (NMR, IR, Raman) and physical changes (DLS, gel time) would be investigated.

First of all equilibria in formaldehyde-water-methanol were examined with a fully quantitative ^{13}C NMR and thus speciation of formaldehyde solutions as a function of its concentration in water and in methanol was successfully determined. The results confirm lack of detectable concentrations of formaldehyde in the aldehyde form and prove presence methylene glycol, its oligomers (up to trimer) and their methoxylated forms. The higher the concentration of the starting formaldehyde stock solution, the longer are the chains of oligomers. Dilution in water leads to depolymerisation to mostly methylene glycol and free methanol, while diluting in methanol yields mostly monomethoxylated form of methylene glycol and free methanol. Based on these results, confirmed by IR and Raman, values of equilibrium constants between all species found in the solution were determined. ^{1}H NMR spectroscopy was used to both verify these results and to establish the changes of on these values in range of temperatures from 283K to 328K. Additionally performed experiments with DLS showed no phase separation caused by potential de-mixing of any of these three liquids.

Formaldehyde-water-sodium carbonate solutions which were mimicking the composition of reacting mixtures without resorcinol, were also examined. The results of ^{13}C NMR proved that the linewidth of the spectra at given

peaks broadened upon addition of sodium carbonate and this effect was stronger for solutions with greater concentration of the catalyst. DLS experiments proved presence of objects with significant diameter despite filtration of the samples. These are thought to be droplets of a second phase, having a different refractive index and thus being visible in the DLS and their presence may explain changes in relaxation time T_2, causing linewidth broadening in NMR experiments.

Monitoring of the changes in the composition of reacting mixtures and detection of new species forming in the solutions was done primarily by ^{13}C NMR, ^{1}H NMR and HSQC. Unexpectedly, presence of hydroxymethyl derivatives, both mono- and di-substituted, just a few minutes after addition of formaldehyde was confirmed. Moreover, site C(5) was also found to be substituted. The results of experiments performed at 293K and 328K showed that the concentrations of both total formaldehyde and resorcinol decreased rapidly within first few minutes of mixing the two solutions, followed by a more gradual decrease over time. When plotted in scaled time, the rates of consumption of both reactants are very similar regardless of the catalyst concentrations at a given temperature, confirming that sodium carbonate serves as a catalyst for the resorcinol-formaldehyde substitution reaction. Experiments performed in 293K showed very little changes in concentrations of protons at resorcinol C(5) site, while those at 328K showed a decrease proportional to the one for C(2,4/6). This suggests that di-substituted resorcinol appears to be subject to condensation or further substitution in higher temperature, which leads to formation of either highly reactive or insoluble intermediate which then leaves solution and forms another (micro)phase, since liquid NMR signal from C(5) sites is lost.

The DLS experiments proved that regardless of the R/C and R/W ratios, the growth of primary particles which subsequently form a solid network in the gel follows the same pattern. Moreover, the average hydrodynamic radius of these particles is similar across all samples. It was found that the higher the temperature, the concentration of reactants or the catalyst, the sooner the particles reach their final radius. Analysis of autocorrelation functions development in time allowed to confirm the gelation times and to determine the intermediate stage between the *sol* and *gel* forms. These novel results disprove previous suggestions that the catalyst directly controls the size of particles forming the gel structure. Experiments on the reacting systems were completed by measurements of pH changes in the course of the reaction. As it turned out, regardless of the catalyst and reactants concentration, all reacting samples exhibited a pH drop of the same magnitude within the first 30-40 minutes. A number of theories explaining this phenomenon are formed in this work, however, none of them seems to be fully explain it.

Table of Contents

Table of figures

List of tables

CHAPTER 1. INTRODUCTION

1.1. Introduction

The history of sol-gel processing dates back to the first half of the 19th century, when Ebelmen synthesised the first silica gel in a sol-gel process from $SiCl_4$ in an alcohol followed by evaporation of the solvent [2]. However, this synthesis was virtually forgotten until late 1930s. The first time it was introduced in practice outside laboratory and patented was in 1939 by Geffcken and Dislich, who developed a method for preparation of oxide films for the Schott glass company in Germany. The purpose of this process was to coat large panes of window glass with thin oxide films. At the same time, mineralogists became increasingly interested in application of the sol-gel processing to obtain homogenous solid powders, which were required for studies of solid phase equilibria [2]. The 1950s saw the sol-gel processing application for the production of radioactive powders of UO_2 and ThO_2 (used for nuclear fuels) – the main advantage of this method was avoiding producing large amounts of excessive dust [2]. Interestingly, this research was also done during the war but was kept secret for many years in fear of revealing advances in nuclear technology. The 1970s saw a great increase in the sol-gel technology research mostly because the ceramics industry appreciated its potential: once again Dislich and others developed a synthesis method of multicomponent glasses *via* controlled hydrolysis and condensation of alkoxides. Further research conducted by Yoldas and Yamane resulted in monolith materials obtained from sol-gel synthesised gels, providing an appropriate drying was applied. Important subsequent development of sol-gel technology development is owed to this, and this process is now used in preparation of many porous materials.

In late 1980s a breakthrough happened in the sol-gel technology research, opening doors to a completely new field of organic gels. In 1989 Richard Pekala published an important article in which he described sol-gel synthesis of an aerogel based on organic materials rather than previously used silica-based reactants [3]. The results were very encouraging and the publication of this paper was followed by series of patents granted to Pekala and his associates. Since then the sol-gel research has grown to be even more intensive, with over 50000 papers published worldwide since the 1990s.

The reason for which Pekala's publication was so ground-breaking is not because it was the first time that a porous organic material was obtained – polyacrylic hydrogels or polystyrene gel-based packaging in gel chromatography were well known in the 1980s. It was because , unlike other organic gels, the resorcinol-formaldehyde gels synthesized by Pekala did not swell or shrink when solvent was exchanged, as it is known for example in polystyrene based polymers. Moreover, Pekala managed to supercritically dry this gel and obtained a transparent, very low density foam (aerogel) with cell (or pore) sizes below 100 nm.

The sol-gel synthesis method is beneficial in many aspects and has the potential of replacing some of the currently used synthesis routes. The most attractive features of this method is usage of water as solvent and good potential for effective solvent recovery, compared to when less eco-friendly organic solvents are used. From the economical point of view this is as important as the fact that the whole reaction takes place in rather low temperatures (below boiling point of the solution, which would be just below 100°C in case of water-based synthesis), therefore the energy cost is relatively low. Additionally, this technology does not require high pressure, therefore

general and inexpensive laboratory equipment is sufficient. The control of homogeneity of the mixture is extremely easy, as is its control over stoichiometry. Lastly, a number of appearances can be obtained – from monoliths, thin films to beads and fine powders.

1.2. Properties and Applications of Organic Gels

Extensive studies of organic gels resulted in a great number of possible applications for these materials. The spectrum of their uses is very vast, as it is possible to match the properties' requirements of the material by appropriately modifying the conditions of the synthesis and post-production processing. Not only the conditions of the synthesis process can alter the properties of the resulting material but also use of different reactants. Apart from resorcinol-formaldehyde studied in this work, other materials used in organic gels synthesis are the following: phenol-formaldehyde [4], melamine-formaldehyde [5], phenol-furfural [6], cresol-formaldehyde [7], epoxides, polyurethanes, polyacrylates, polystyrenes, polyimides and those based on natural polymers, like agar or agarose [8]. It is clear that with so many materials at choice and with possibility of modifying the synthesis process, the number of obtainable materials seems virtually limitless.

Organic gels are highly porous (>80% [9]) with pore sizes that can be controlled by modification of certain parameters of the synthesis process. The high porosity is linked with very low bulk densities, making these materials very light which also improves their thermal insulation properties. The pore sizes of organic gels obtained in a sol-gel process tend to be very low (100 nm or less) [3] [10] [11], however these are still accessible. For example, porosity

with specified pore sizes is a desirable feature in filtration applications and in nanotechnology research.

High porosity is closely related to surface area of the material and in case of organic gels the range within which most specific areas are found is 400-1200 $m^2 \cdot g^{-1}$ [9]. For comparison, the area of a tennis court is ca. 260 m^2 which means that one gram of an organic aerogel has an area comparable with at least two tennis courts. This property is invaluable in many applications. Most of all, it makes carbon aerogels excellent adsorbents, which can be used for gas storage (e.g. hydrogen and carbon dioxide) or as very versatile sorbents.

Carbonisation or pyrolysis step during preparation of organic gels is aimed at transforming an organic gel into a carbon structure. Organic gels may have functional groups and thus contain various atoms including oxygen and oxygen bound to hydrogen. In order to remove these a gel is typically heated in high temperature (600-2100°C) under a flow of an inert gas, like nitrogen or helium [9]. This process influences the final properties of the material, therefore it needs to be appropriately adjusted and controlled. During or after the pyrolysis a gel can also undergo activation. Thermal activation is done using either way gases (air, steam or carbon dioxide) in elevated temperature (750-1000°C), while chemical activation is carried out by immersing the gel in an acid solution. Another type of activation is electrochemical and this one is done by immersing the gel in a dilute electrolyte solution and performing cyclic oxidation and reduction processes [9]. In all cases activation aims at altering the structure of the gel and its properties, so that it matches requirements posed by its application.

One of the most interesting and important features of carbonized organic gels is their electrical conductivity [12]. They are electrically conductive in a similar way to charcoal or graphite, in a sense that they are better conductors than plastics (insulators) but much worse than metals. What makes carbon aerogels much different from graphite is the fact that their electrical conductivity is closely related to density of the material [11]. Research proved that carbon aerogels with high and low bulk density have different nanostructure, which causes the latter ones to have a lesser internal connectivity which strongly affects the way the electric charge is transported by the material. Additionally, the lower the bulk density, the greater surface area, therefore if an application requires both high surface area and good electrical conductivity, certain compromises must be made. Fortunately, there is a growing number of techniques which allow to overcome this issue. One of them is activation of high density aerogels which leads to exposure of very small pores (a few nm in diameter), leading to a material with both good electrical conductivity and surface area [13] [14]. Another option is to synthesize the organic gels doped with highly conductive materials, like metals [15] [16] [17]. Being electrically conductive and having very large surface areas, organic aerogels are ideal novel materials for electrodes in electrochemical double-layer supercapacitors [18] [19] [20], making their research of great importance in terms of energy storage and management. They are also used to produce electrodes for batteries [21] and for capacitative deionization units [22], as well as materials for hydrogen fuel storage [23] due to their porosity and high surface areas. All in all, a great potential lies in these materials in terms of energy management, which is currently a matter of great interest.

Being greatly versatile, organic aerogels are ideal materials for catalyst support [24]. They have high surface area per unit of mass, meaning that even small mass can carry significant amount of catalyst or active sites. Even more importantly, their macroscopic properties, i.e. appearance, can also be adjusted: they can be obtained in many forms, from monolith blocks [25], through beads to fine powders and films [26]. Very often metals are used as catalysts and in most cases it is crucial that they are not present in the final product. For example, platinum is used as a catalyst in hydrogenation of vegetable oils and the product – margarine – is edible, therefore must be metal-free. This translates into the need to immobilize the catalyst on a carrier which can be in form of a mesh, honeycomb, powder or beads, which are removed from the products of reaction. In many cases, catalyst deposition on a support material is an arduous process. Sol-gel technology is a significant step towards solving these problems: by addition of a metal precursor into the initial solution, the obtained material is uniform in its structure and in distribution of the catalyst (metal). Properties, like porosity, surface area and morphology can be adjusted to the requirements by modifying the synthesis conditions.

Less popular applications of organic aerogels are those in which they are a more expensive replacement for materials which serve their purpose quite well. An excellent example is carbon aerogels application as nano-composite energetic materials used as explosive materials [27]. The greatest advance of these materials lies in their uniformity in terms of structure and distribution of components, as well as in low-dust manufacturing process. However, this method is unlikely to be widely applied as it is not a significant improvement over currently used processes and does not offer a considerable economical advantage.

1.3. Research Challenges

Extensive studies dedicated to the sol-gel technology mostly concerned the silica-based and other (mixed) oxide materials, as for a long time they were of primary interest. Pekala's discovery in late 1980s was without any doubt very important, however it seems that not much interest was dedicated to detailed understanding of the mechanisms leading to organic gels, as it was assumed that the process follows the same pattern as in the inorganic sol-gel synthesis. There is a limited number of publications dedicated to investigation of these mechanisms, as from the practical point of view it seemed of lesser importance: the synthesis method worked well, the assumption of analogy to the silica-based gels seemed to explain the process satisfactorily. It was much more worthwhile, according to many, to focus on tailoring the final properties of the materials by varying the conditions of the reaction. This was mostly done by trial and error and it resulted in an enormous number of publications, which resemble recipes rather than offer an insight on the mechanisms which cause the properties to respond to changes in reaction conditions in a certain manner. The number of factors which can be changed is significant, making studying the influence of reaction conditions on the properties of the final material an arduous task. The factors which need to be considered, include amount and type of catalyst, solvent, temperature, ratios of reactants, to name a few.

A vast majority of papers published on resorcinol-formaldehyde gels synthesis base on the mechanism suggested by Pekala, in which formaldehyde is shown in the aldehyde form [3], although it is known that free formaldehyde in aqueous solutions is scarce [28] [29].This reaction is shown in Figure 1.

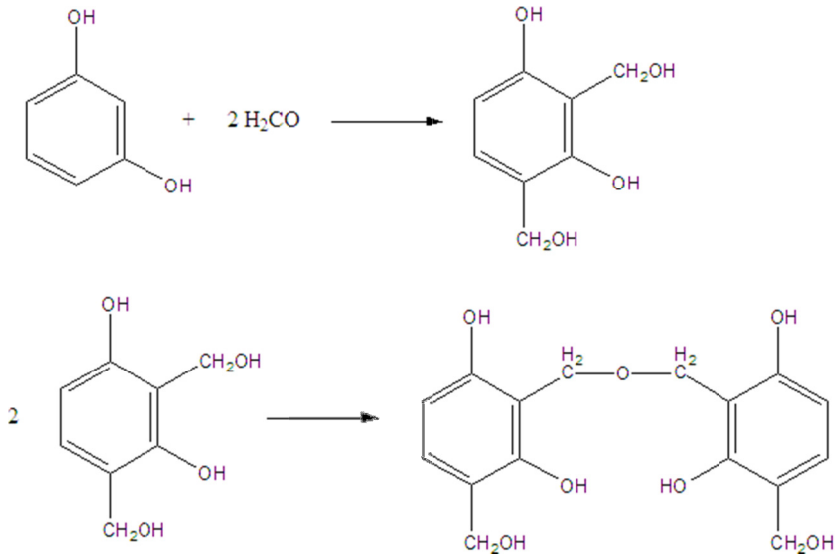

Figure 1. The most commonly shown mechanism of resorcinol-formaldehyde substitution and condensation.

However, actual distribution of formaldehyde-related species in commercially available solutions as a complex function of their concentration and methanol content, which is added to suppress formaldehyde polymerisation. Literature on formaldehyde chemistry dates back many years with a few valuable publications from mid-20th century [30], when most of formaldehyde synthesis methods were further developed on a large scale, as formaldehyde became increasingly important in plastics industry. The experimental methods which were then used are still applicable these days, however, more sophisticated methods, including spectroscopy techniques, have greatly advanced since then. There is a number of more recent articles concerning formaldehyde-water equilibria but these studies mostly use *in situ* produced aqueous solutions of formaldehyde from depolymerisation of poly(oxymethylene), without addition of methanol. Because the commercially used formaldehyde solutions have significant amounts (1-15%wt.) of methanol [28], studies dealing with water-glycol

equilibria are not directly applicable to these solutions and quantitative information on methanol influence is lacking. Not many publications were focused on detection and quantification of concentrations of all different species found in differently concentrated formaldehyde aqueous solutions, and even less did this for aqueous solutions with both formaldehyde and methanol.

In terms of investigation of the reaction mechanism and the gel formation, these seemed to be treated with far less interest than tailoring the properties of the material resulting from the synthesis. This is reasonable from the practical point of view, as once the synthesis process was adjusted to obtain material with certain properties, there appeared to be little practical need for investing time and money into understanding why, as long as the main goal, the specific application, was achieved. There is a number of published correlations between conditions of the reaction and surface area, density and other properties, but they mostly lack reasonable and well-founded explanation.

It would be useful to study the sol-gel polymerization of resorcinol and formaldehyde in two parts: one study should investigate strictly the chemical reactions between the reactants, while the other should examine closely the process of gel formation, which could be of physical or chemical nature. Of course the results of both studies should be linked together to provide most valuable addition to the current state of knowledge. However, not many articles are concerned with mechanism of the reaction, assuming that the mechanism suggested by Pekala and repeated many times by others is valid. The research performed on kinetics of reactions between formaldehyde and resorcinol has been limited and should be revisited as more advanced

experimental methods are now available and it is reasonable to assume that more accurate information can be now obtained, thus providing new insights into the reactions' mechanisms and kinetics.

Most authors agree that the role of the catalyst is primarily to alter the pH of the reacting mixture to enhance the substitution of resorcinol. Not many investigated the changes in the pH values in the course of the reaction, even though all acknowledge the paradox that basic catalyst is required to form a gel, which is believed to be formed through acid-catalysed hydrolytic condensation of substituted resorcinol. All the same, most papers state that the higher the concentration of the basic catalyst, the faster the gel formation is [31] [9]. Interestingly, certain studies prove that not all basic compounds can be used as catalysts, as some reacting solutions with ammonia-based catalyst, despite having pH adjusted to an appropriate value, do not form gels [32] [33] [34]. This proves that the role of the catalyst is more complex than that of providing an appropriate basicity of the solution. Moreover, there are several studies which investigated acid catalysts and proved that in most cases gel structures were also formed [35] [36]. Since gelation was observed for all other types of catalysts based on metal cations, it may be that it is necessary to form a sort of intermediate species which then form the gel or it may modify the stability of the colloidal suspension of primary particles before their aggregation and subsequent gelation.

Since it is the porosity and surface area that is so important for applications of the organic gels, many papers focused on studying the relationship between the catalyst and the pore size distribution and surface area of the resulting material. All the same, very few studied the particle growth of clusters which are believed to link and form the gel network structure,

therefore most of the studies were rather static and focused on the *before-and-after* rather than on what was happening between. Most of the conclusions on the relationship between pore sizes and catalyst concentration and type are based on the appearance of materials, which were treated after the synthesis, i.e. solvent exchanged, dried and (sometimes) carbonised. It is known that post-synthesis treatment of the gels influences the final properties of the gels, therefore it might obscure the actual relationship between the catalyst or pH and the final properties. It is essential to investigate how does the growth of these clusters look like *in situ*, while the reaction takes place and before the network is formed.

1.4. Main contributions of the thesis

This thesis contains answers to some of the research challenges described above as well as it poses new ones which are summarized in Chapter 7.

The greatest contribution in terms of experimental methods development is undoubtedly work done towards fully quantitative ^{13}C NMR spectroscopy, which can be successfully used by others to examine both reaction kinetics as well as glycol equilibria in non-reacting solutions of formaldehyde. This development was a fully comprehensive process which included measurements of T_2 and Nuclear Overhauser Effect, as well as development of methods and tools to overcome these issues.

A significant input of this work is confirmation that formaldehyde in the form of an aldehyde is not present in aqueous solutions but forms a vast number of glycols or their oligomers, as well as their methoxylated forms. In terms of glycol equilibria in formaldehyde solutions this work provides an exact speciation of both methanolic and aqueous solutions which were

obtained using commercially available formaldehyde, unlike previous publications which focused on those prepared *in situ* and often without addition of methanol. Another contribution of this research is determination of equilibrium constants of the reactions in formaldehyde-water-methanol solutions not only in 293K but also in a range of temperatures from 283K to 328K. Evaluation of both IR and Raman spectroscopies for their potential use in determining composition of formaldehyde solutions was also done and showed that when compared with NMR, these techniques appear not to be very informative.

In terms of examining the catalyst influence, a significant discovery was made when formaldehyde-water-sodium carbonate solutions were prepared and investigated. The results from NMR showed line broadening due to changing T_2 time which can be attributed to phase separation. Results obtained from the Dynamic Light Scattering support this theory, as upon addition of sodium carbonate into an otherwise uniform formaldehyde-water solution, objects of a few tens of nanometres in diameter are found. This set of experiments is novel in the light of previous research and provides significant input into the discussion on what is the actual role of the catalyst, as a possible phase separation inducer.

Experiments on reaction kinetics provided interesting results. First of all, it is clear from these results that formaldehyde and resorcinol react with each other in room temperature and the NMR results show a significant depletion of both reactants even at a very early stage of the reaction. This is important mostly because it is in contrast with previous work's suggestions and additionally is useful when developing a synthesis process (i.e. mixing time of the reactants in room temperature needs to be taken into account as

already reaction time). Another valuable discovery is that resorcinol can be di-substituted in this time, which was not expected. Moreover, substitution at position C(5) of resorcinol has also been detected. Interestingly enough, no products of condensation were detected, however, significant depletion of total resorcinol was observed during reaction in 328K, suggesting that the products of condensation must have migrated into the phase undetectable by the NMR. Further research is required to confirm that, however, this is a milestone in this matter's research. Dynamic Light Scattering experiments showed that the pattern of colloidal particles growth and their average hydrodynamic radius are independent on both R/W and R/C ratios. This finding is very interesting as it disproves a theory derived by some that the catalyst directly controls the sizes of particles forming a gel network. Interesting observations were made when measurements of pH were performed in the course of the reaction. Regardless of the R/C or R/W ratio, all reacting samples exhibit a pH drop of the same magnitude within the same timeframe. No explanation has been provided here, however a few theories are explored.

1.5. Thesis Structure

Following this Chapter, the thesis structure is formed by the sections described below.

Chapter 2 contains a literature review which aims at familiarizing the reader with issues dealt with in this thesis. Appropriate references are made, should the reader wish to access the publications by himself.

Chapter 3 is focused on describing the methods used by the author to perform research. Both theoretical background of the methods as well as

practical sample preparation and data analysis procedures are provided here.

In Chapter 4 an extensive analysis of glycol equilibria in formaldehyde-water and formaldehyde-methanol solutions is presented.

Chapter 5 contains an analogous analysis of formaldehyde-water-sodium carbonate solutions.

Chapter 6 is focused on thoroughly investigating the kinetics and reaction mechanism in formaldehyde and resorcinol reactions in water.

Chapter 7 contains overall conclusions which were drawn basing on findings presented in this thesis. Additionally suggestions for further research work are included.

Chapter 8 includes list of references used in this work, which are also recommended for those wishing to continue this work.

1.6. Useful terms, definitions and abbreviations

A list of key concepts used in this thesis may help a reader to make the best use of this work. Most of the definitions below are quoted from the IUPAC Gold Book [1] which contains widely accepted definitions of terms used in chemistry.

Monomer - a molecule which can undergo polymerization thereby contributing constitutional units to the essential structure of a macromolecule [1].

Polymerisation – it is a process in which chemically reacting monomer molecules form very large, often three-dimensional structures or chains called **macromolecules** or **polymers**.

Depolymerisation – a process of converting a polymer into a monomer or a mixture of monomers [1].

Sol-gel process – it is a process through which a network is formed from solution by a progressive change of liquid precursor(s) into a sol, to a gel, and in most cases finally to a dry network [1]

Resin – it is a soft solid or highly viscous substance, usually containing prepolymers with reactive groups [1]. This term is still used by a number of researchers to describe cured thermosetting polymers (e.g. phenolic or epoxy resins), even though this is strongly discouraged as it is misleading.

Gel - non-fluid colloidal network or polymer network that is expanded throughout its whole volume by a fluid [1]. It is worth adding that a gel has a finite yield stress, which is often very small.

Aerogel – it is a gel comprised of a microporous solid in which the dispersed phase is a gas [1].

Xerogel – it is an open network formed by the removal of all swelling agents from a gel [1].

Carbonization - a process by which solid residues with increasing content of the element carbon are formed from organic material usually by pyrolysis in an inert atmosphere [1].

Colloidal suspension - a system in which particles of colloidal size (roughly between 1 nm and 1 μm) of any nature (e.g. solid, liquid or gas) are dispersed in a continuous phase of a different composition (or state). The name dispersed phase for the particles should be used only if they essentially have the properties of a bulk phase of the same composition [1].

NMR – Nuclear Magnetic Resonance

HSQC – Heteronuclear Single Quantum Coherence

NOE – Nuclear Overhauser Effect

2D-WISE – Two-Dimensional Wide-Line Separation

FID – Free Induction Decay

DEPT - Distortionless Enhancement by Polarization Transfer

NOESY – Nuclear Overhauser Effect Spectroscopy

HOESY – Heteronuclear Overhauser Effect Spectroscopy

ROESY – Rotating Frame Nuclear Overhauser Effect Spectroscopy

RF (pulse) – radiofrequency pulse

IR – Infra-Red (spectroscopy)

FT-IR – Fourier-Transform Infra-Red Spectroscopy

NIR – Near Infra-Red

MIR – Mid Infra-Red

FIR – Far Infra-Red

ATR - Attenuated Total Reflectance

DLS – Dynamic Light Scattering

QUELS, QELS – Quasi Elastic Light Scattering

PCS – Photon Correlation Spectroscopy

MALDI-TOF – Matrix Assisted Laser Desorption-Ionization – Time of Flight

SAXS – Small Angle X-Ray Scattering

SANS – Small Angle Neutron Scattering

PTFE – poli(tetrafluoroethylene)

POM – poli(oxymethylene)

TMS - tetramethylsilane

B – benzene

MG – mono-glycol

DG – di-glycol

TG – tri-glycol

MMG – methoxylated mono-glycol

MDG – methoxylated di-glycol

MTG – methoxylated tri-glycol

MeOH – methanol

CHAPTER 2. THEORETICAL BACKGROUND

2.1. Chemistry of formaldehyde

Formaldehyde is an aliphatic aldehyde with the smallest number of carbon atoms per molecule: just one. It was first discovered in 1859 by Butlerov and no later than half a century later it was manufactured on an increasingly large scale [37]. Because of its properties it can enter a variety of reactions, giving a vast spectrum of products, out of which plastics and pharmaceuticals are currently of the greatest interest.

Pure formaldehyde at normal pressure and temperatures above -19°C is a gas with a very strong and suffocating odour, and due to its carcinogenic and toxic properties, it must be handled with extreme care [30] [37]. In this state, it has a formula $H_2C=O$ – the carbon atom is bound by a double bond to an oxygen atom, forming a carbonyl group. In this group, the carbon atom has an sp^2 configuration, which means that all atoms are placed upon the same plane, with angles between the bonds of 120°. Due to its structure, it is very reactive, thus it is impossible to purchase formaldehyde as a gaseous monomer. It is stable as a gas only when stored at 80-100°C and kept dry, otherwise it easily polymerizes and forms poly(oxymethylene). This polymer is very well known in industry as a construction material with good chemical and mechanical resistance, with relative ease of forming. The rate of poly(oxymethylene) formation depends on the purity of the gas and it is greatly enhanced by even trace amounts of polar impurities, like acids, alkalis or water. Depolymerisation of poly(oxymethylene) is a method of in situ manufacture of formaldehyde monomer but it is a slow process if not catalysed and if performed in temperatures lower than 300°C. Therefore,

should one wish to work with formaldehyde in the form of gaseous aldehyde, this is the only possible source.

Chemical properties of gaseous formaldehyde are exceptional because despite being a very small molecule, it has both nucleophilic and electrophilic centres. This is a very interesting feature, as most aldehydes tend to be nucleophilic reactants, whereas formaldehyde can take part in both electro- and nucleophilic substitution reactions. Figure 2 shows the structure of formaldehyde with electrophilic centre (on the H atom) marked with red dotted circle and nucleophilic centre (on the O atom) with the blue one.

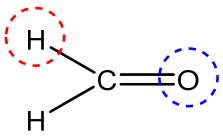

Figure 2. Formaldehyde molecule with nucleophilic (blue) and electrophilic (red) centres.

The most popular formaldehyde manufacture processes avoids obtaining formaldehyde as a gas by its immediate absorption in water in an absorbing column located directly after the reactor. Starting in the early 20th century, formaldehyde was manufactured *via* methanol oxidation. This method is still the most popular with only slight differences in metals used as catalysts or the temperatures. However, in the mid-20th century, another formaldehyde production process was introduced where formaldehyde was obtained through vapour-phase, non-catalytic oxidation of butanes and propane. This method failed to supplant the methanol-based one, as it required a very complex process for separation of the product. Therefore, the two most

popular methods of formaldehyde production are partial methanol oxidation with air over either silver or metal oxide catalysts [30] [37]. The process which uses silver catalyst could also work using copper; the typically used metal oxides are vanadium pentoxide and a combination of iron and molybdenum oxides. Both processes require high temperatures (silver ca. 600°C, metal oxide ca. 400°C) but can be carried out at near atmospheric pressure. There are several differences in the processes, mostly due to the nature of the catalyst. In case of the process using silver catalyst, the reactor feed is very rich in methanol and virtually all of oxygen is reacted, while feed to the metal oxide catalyst has to be of a low methanol concentration and nearly full conversion of methanol is achieved. In both cases, the mixture leaving the reactor enters the absorber, in which it is absorbed in water. This is necessary in order to eliminate the polymerization of free formaldehyde. The process using silver catalyst gives a mixture richer in methanol, while the metal oxide process can provide a mixture with less than 1%wt. of methanol. However, as it is explained further on, methanol is a desirable by-product which should be present in the final solution of formaldehyde, especially so that its content can be controlled.

There is a number of commercially available solutions of formaldehyde, which differ mostly by the concentration of formaldehyde and methanol. The overall concentration of formaldehyde is expressed as a weight fraction (typically as per cent) of the free formaldehyde in the overall solution. The same definition applies to the amount of methanol. Summary of the most common commercially available formaldehyde solutions and forms is shown in Table 1. Depending on the requirements and the nature of the reaction in which formaldehyde is needed, there is a number of available sources of formaldehyde. The most popular is the 35-37%wt. aqueous solution, mainly

because it is convenient in handling while being sufficiently reactive. Its main disadvantage is high water content, which is not a problem when working with water-based syntheses like the sol-gel polymerization of formaldehyde and resorcinol.

Table 1. Properties of various formaldehyde solutions and forms.

Type	Chemical formula	Resin preparation	
		Advantages	Disadvantages
Gaseous (not commercially available)	CH_2O	• High purity	• Unstable
35-37%wt. aqueous solution	$HO(CH_2O)_nH$ $n \approx 2$	• Easy handling, • Moderate activity • Stable at room temperature	• High water content
50%wt. aqueous solution	$HO(CH_2O)_nH$ $n \approx 3$	• Increased capacity (less water)	• Elevated temperature of storage • Formation of formic acid
Poly(oxymethylene) (POM)	$HO(CH_2O)_nH$ $n \approx 20\text{-}100$	• Increased capacity • Water-free	• Dangerously high activity • Solids handling
Trioxane	$(CH_2O)_3$	• Water-free	• Catalyst requirements • High costs

The high reactivity of formaldehyde translates not only into its polymerization into poly(oxymethylene) but also to very rapid hydration when mixed with water. The aldehyde molecule is solvated with water at molar ratio of 1:1 and this process leads to formation of methylene glycol and its oligomers. The length of the oligomer molecules depends on the concentration of the methylene glycol (i.e. availability of water molecules) and becomes larger with increasing overall formaldehyde concentration. The

reaction which leads to formation of methylene glycol and its oligomers is shown in Equation 1.

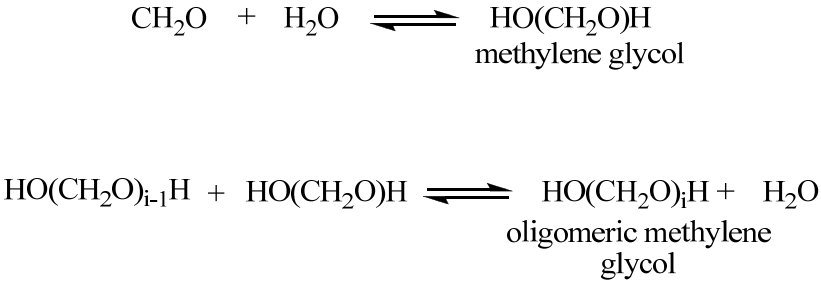

Equation 1. Reactions of formaldehyde in water.

All aqueous formaldehyde solutions without addition of methanol or those highly concentrated can become cloudy after a certain period of time. This phenomenon is caused by formation of 1,3,5-trioxane and poly(oxymethylene), which are both insoluble in water. This impacts the quality of the solution, as it decreases the formaldehyde content usually to an unknown level. In order to eliminate this problem, methanol which is a by-product in the manufacture process is left in the solution. Its concentration can be modified in order to allow reactions between methylene glycol and its oligomeric forms with methanol to occur. The products of this reaction have one of the hydroxyl groups methoxylated, which makes them less prone to polymerisation, thus allowing to control the molecular weight of the species in the solution. These structures are called hemiformals and their formation from any given alcohol (typically methanol and ethanol) and formaldehyde is shown in Equation 2.

$$CH_2O + ROH \overset{H^+}{\leftrightarrow} HO(CH_2O)R$$

Equation 2. Reaction of formaldehyde with alcohols leading to a hemiformal structure. Note that R = -CH_3, -CH_2CH_3, -Ph, etc.

Presence or addition of methanol in the solution also enhances the reaction of poly(oxymethylene) depolymerisation to formaldehyde, additionally protecting the solution from loss of reactive formaldehyde species.

There is a large number of chemical species which can be found in formaldehyde aqueous solutions, as the equations above show. There are several papers published with data on equilibria between formaldehyde-relates species in aqueous formaldehyde solutions but in most of these methanol is not taken into account, as formaldehyde solutions were prepared *in situ* by decomposition of poly(oxymethylene). All authors agree that these species are in mutual equilibria. and it was also suggested that these equilibria might be sensitive to the pH of the solution.

Since all of these formaldehyde-based species are in mutual equilibria, the length of the oligooxyglycols and their methoxylated forms changes . depending on the concentration of the formaldehyde. It is known that the greater the formaldehyde concentration, the longer species can be found. First of all, methylene glycol $HO(CH_2O)H$ (MG) is formed in the reaction of formaldehyde as aldehyde with water:

$$\boldsymbol{CH_2O + H_2O = MG} \tag{3}$$

This reaction is extremely fast and the value of its equilibrium constant is very high [38] as the dominant species in MG in the presence of water [37]. Two molecules of MG can react together to form di-glycol $HO(CH_2O)_2H$ (DG). Because there is an ether group formed from two condensing hydroxyl groups, one water molecule is formed per one DG molecule formed:

$$MG + MG = DG + H_2O \tag{4}$$

One molecule of DG may further react with a molecule of MG and form a tri-glycol (TG). Similarly to DG formation, one water molecule is formed as a by-product of two hydroxyl groups condensing and forming an ether bridge:

$$DG + MG = TG + H_2O \quad (3)$$

Due to presence of methanol, further reactions leading to formation of longer oligooxyglycols are less prominent and instead formation of methoxylated species (so-called hemiformals) dominates:

$$MG + MeOH = MMG + H_2O \quad (6)$$

$$DG + MeOH = MDG + H_2O \quad (7)$$

$$TG + MeOH = MTG + H_2O \quad (8)$$

It is important to be able to determine the values of the equilibrium constants for all of the above reactions as this allows to predict the speciation of the formaldehyde solutions at a variety of concentrations, including those used in synthesis of resorcinol-formaldehyde gels. It is also worth to determine the influence of the temperature on these values.

The information presented above is based on a number of publications and studies on the glycol equilibria in the formaldehyde-methanol-water mixtures. The matter of glycol equilibria is a complex issue and therefore it was extensively studied over the years. For clarity of this section, the development of the state of knowledge on this issue is presented in a chronologic manner.

One of the most popular spectroscopic methods which can be used to identify the composition of a solution are the infra-red and Raman spectroscopies, which are complementary to each other. Their main disadvantage is that they are bond-selective, therefore hardly ever they are sufficient for identification of a complex solution or molecules without additional information. Unfortunately this is the case of formaldehyde aqueous solutions, which may explain why there is a limited number of publications dedicated to determination of the composition of these mixtures. In many cases the studies were performed on solutions of formaldehyde prepared by dissolution of paraformaldehyde in water. In practice these solutions are different from the commercially available formaldehyde solutions because they usually have different concentrations and do not contain methanol. A good attempt to determine the speciation changes of the formaldehyde solution caused by changes in the overall formaldehyde concentration by Raman spectroscopy is a study by Lebrun et al. [39]. This study carefully assigns most of the signals found in the Raman spectra of aqueous formaldehyde solutions from very low to high concentrations and compares the results with previous work of Matsuura et al. [40] and Möhlmann et al. [41]. The findings of these studies are consistent and they indicate that Raman spectroscopy can be used to determine the overall concentration of formaldehyde-related species, as well as confirm presence of poly(oxymethylene) glycols. It would be very beneficial to conduct similar research on solutions containing also methanol. The difficulty with this is that the signals from methoxy-groups might overlap with other signals.

In terms of the IR spectroscopy investigations of formaldehyde aqueous solutions, there are not many thorough studies. Most of these publications

focus not on determination of the exact speciation of the solutions but on other aspects, like reactions of formaldehyde with specific substrates [42] [43]. One can find publications on chemical compounds (glycols) which can be found in the formaldehyde aqueous solutions. However, these studies were dedicated to isolated compounds, while the formaldehyde solutions are very complex and therefore many signals may overlap or their positions (i.e. wavenumbers) change. A very good example of a publication dedicated to spectroscopic studies of only one compound – methoxymethanol – is work by Johnson et al. [44].

A potentially far more informative spectroscopy method is the Nuclear Magnetic Resonance, as it is nucleus-specific and not bond-specific. It is a method that has been developed greatly over the last few decades and it has been used to investigate the equilibria in formaldehyde aqueous solutions and the formation kinetics of poly(oxymethylene) glycols and their methoxylated forms.

The extensive NMR research on the aqueous formaldehyde solutions speciation was begun by Dankelman et al. [45], who investigated formaldehyde solutions using the ^{1}H NMR and gas chromatography. The results of this work include low quality (poor resolution, large noise in the baseline) spectra, however, most of the peaks were assigned properly and could be used as a starting point for later research. The main conclusions of the Dankelman et al. were that even heptamers of the polyoxymethylene glycols could be found if an appropriate technique was used (direct silylation with N,O-bis(trimethylsily1)trifluoroacetamide). The main disadvantage of this work was the fact that it investigated solutions with very low methanol concentrations (up to 1%wt.), which is much lower than the composition of

the commercially available formaldehyde solutions. This study was followed by Le Botlan et al. [46], who also used NMR to study the speciation of formaldehyde aqueous solutions. The authors decided to apply ^{13}C NMR rather than ^{1}H due to the complications caused by the water (-OH/D) signal in the proton spectra. Le Botlan et al. [46] discussed briefly a number of issues related to the use of ^{13}C NMR spectroscopy, such as relaxation time T_1. Spectra collected and published by Le Botlan et al. [46] were of better quality than those previously published, however, they were still of significantly lower quality than can be achieved nowadays. Nonetheless, the spectra were properly assigned and an attempt at quantification of the data and calculation of equilibrium constants was done.

In the early 1990s there were a few notable publications on the formaldehyde-water-methanol equilibria and kinetics of glycols formation. Several were from the same research group and focused on using NMR as a tool to describe the speciation of the aqueous solutions of formaldehyde [47] [48] [49]. In these studies, the spectra – both ^{1}H and ^{13}C – were assigned basing on the correlation between measured and calculated chemical shifts. Hasse et al. [47] performed high accuracy density measurements in order to calculate chemical reactions rate constants in aqueous formaldehyde solutions and then evaluated this data using both a model derived from the density measurements and a second-order reaction kinetic model. Additionally, this study also used previously unpublished NMR data to evaluate the results. There were quantitative discrepancies found and therefore further research was suggested to address these issues. A later study by Hahnenstein et al. [48] studied the chemical equilibria in formaldehyde in water, deuterium oxide and methanol, under assumption that these solutions behave as the ideal ones. The quantitative results showed

the differences between predicted and measured concentrations or their ratios of up to 10%, when the results of NMR spectroscopy were used. Authors also used an old sodium sulphite titration method [30] to determine the overall formaldehyde concentration and the results were no more than 2% different from predicted. These results suggest that the NMR method used by Hahnenstein et al. [48] needed further development, should one use it as a quantitative analysis tool. Nonetheless, this study provided values for most of the equilibrium constants in formaldehyde-water and formaldehyde-methanol mixtures. However, the study did not include commercially available formaldehyde solutions and was performed using formaldehyde solutions prepared by the authors. Unfortunately, the investigated solutions were binary and were manufactured by dissolution of paraformaldehyde in water or methanol at elevated temperature. Therefore, the equilibrium constants presented by Hahnenstein et al. [48] cannot be related to the solutions made from commercially available formaldehyde. A later publication also by Hahnenstein et al. [49] addressed similar issues and produced similar results.

The question of the vapour-liquid equilibria of a binary system (formaldehyde-water mixtures) was studied by Albert et al. [50]. This work is mentioned here mostly because it used NMR spectroscopy to identify the speciation of the investigated solutions, however, just as it is in case of previous studies, the formaldehyde aqueous solutions were prepared by dissolution of paraformaldehyde in water without addition of methanol. Only later studies were focused on ternary systems with formaldehyde, i.e. formaldehyde-water-alcohol solutions. A study by Balashov et al. [51] was focused on association of formaldehyde in mixtures of water and alcohol, which is basically the case of commercially available formaldehyde solutions.

This study included a range of alcohols, like methanol, ethanol and ethylene glycol. The most important finding of this study is that further addition of methanol into formaldehyde-water-methanol mixture causes not only the reaction between formaldehyde and methanol and formation of hemiacetals, but also shifts equilibria towards lower oligomers. Moreover, Balashov et al. [51] managed to calculate the equilibrium constants of formaldehyde step polycondensation. The ^{13}C NMR spectra were assigned in this paper basing on previous work and appear to be accurate. A study by Maiwald et al. [52] also investigated ternary systems using the ^{13}C NMR spectroscopy, however, just as previously, the authors of this study did not use commercially available formaldehyde solutions but manufactured their own samples. Maiwald et al. [52] ensured the correctness of the NMR spectra assignment by performing a two-dimensional heteronuclear ^{1}H-^{13}C correlation NMR experiment. The authors acknowledged that there was a need to improve the description of the distribution of formaldehyde among poly(oxymethylene) glycols and poly(oxymethylene) hemiformals. The study by Maiwald et al. [52] is very valuable also because it covers a range of temperatures from 298K to 383K. In an article published shortly afterwards, Maiwald et al. [53] discuss the possibility of using NMR spectroscopy as a fast and accurate on-line method for reaction and process monitoring. This paper is interesting mostly because it shows an example of water signal suppression, which can be helpful when analysing aqueous formaldehyde solutions with ^{1}H NMR.

The kinetics of oligomerization reactions in solutions of formaldehyde were also investigated by Ott et al. [54] using the on-line ^{1}H NMR. This research also based on formaldehyde solutions made by the authors rather than on the commercially available solutions. The main result of this work was that reaction rate constants of the degradation of poly(oxymethylene) glycols and

poly(oxymethylene) hemiformals were determined for a broad temperature and pH range, basing on the experimental results. Ott et al. also confirmed that the rate constants strongly depended not only on the temperature, as it was expected, but also on the pH of the solution. Another study on the kinetics of reactions in formaldehyde solutions was conducted by Maiwald et al. [55]. In this study, quantitative ^{1}H NMR spectroscopy was used to investigate reaction kinetics of formation and decomposition of 1,3,5-trioxane in methanol-free aqueous formaldehyde solutions. It is known that this species can be formed especially when no alcohol is added to the formaldehyde solution [30] [37]. This study allowed to confirm, as it will be shown later on in the results discussion section, that there is no significant amount of 1,3,5-trioxane in the commercially available formaldehyde solutions in water with methanol.

2.2. Chemistry of resorcinol

The physical properties of resorcinol are similar to those of phenol because these two are of alike structures. Benzene-1,3-diol (IUPAC recommended name for resorcinol) at room temperature is a white solid material in form of relatively thick flakes. Exposure to sun can cause slight discolouration and cause appearance of a pale yellow tint. It is well soluble in water (110 g per 100 ml in 20°C), alcohols and ethers. The melting point is estimated to be 110°C (383K), while boiling point is 277°C (550K) [56].

Resorcinol was first synthesised in a laboratory in 1864 and then, since a large potential was expected for its use, a significant effort was made to develop an industrial process which was implemented for the first time in 1878 [56]. In over a century, a number of resorcinol synthesis methods was

developed, however, only two are widely used nowadays. The most popular and economically viable process is the benzenedisulfination, while the second is hydroperoxidation of meta-diisopropylbenzene. Both of these processes have been developed and constantly improved over the years, therefore their overall efficiency is very good and the purity of the final product is more than satisfactory. Despite the fact that the benzenedisulfination process is the most economical one, other processes were developed over the years and, as a consequence, there is a number of them available, however, none of them matches the benzenedisulfination process. Among those processes one can mention hydrolysis of meta-phenylenediamine, keto-acid cyclization and dehydrogenation and cyclohexanone oxidation.

Resorcinol has two hydroxyl groups attached to carbon atoms 1 and 3 in a benzene ring, therefore it is also known as 1,3-dihydroxybenzene. Presence of the hydroxyl groups in the molecule changes the distribution of the δ and π-electrons in the aromatic ring and this change causes the activation of sites ortho and para towards reactions of electrophilic substitution. Since resorcinol has two hydroxyl groups positioned in meta configuration in respect to each other, it is a unique molecule. The reactive sites are activated doubly because each of the hydroxyl groups activates three positions: two adjacent and one opposite to itself. Therefore, in case of resorcinol, the reactive sites are located at carbons 2, 4 and 6, as it is shown in Figure 3. When comparing reactivity of formaldehyde with phenolic compounds, resorcinol is the most reactive among phenol (reactivity 1), p-methyl phenol (0.35), m-cresol (2.88) and 3,5-dimethyl phenol (7.75), having a relative reactivity 12.2 times greater than phenol [56].

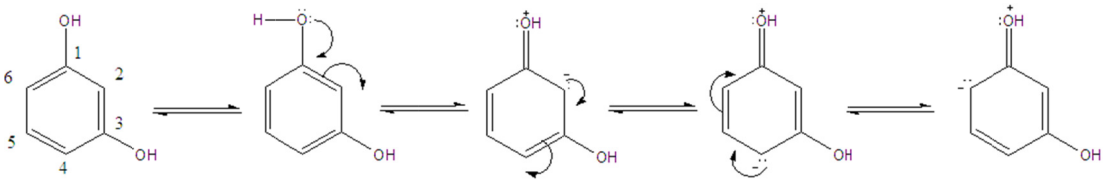

Figure 3. Mesomeric structures of resorcinol: activating effect of hydroxyl groups at positions 1 and 3.

Additionally, electron density is the highest at carbon atom 2, however, presence of hydroxyl groups at carbon atoms 1 and 3 causes steric hindrance and this site is expected to be less reactive than those at carbon atoms 4 and 6, especially when larger substituents are considered (e.g. t-butyl group). It is expected that electrophilic substitution takes place predominantly at sites 4, 6 and 2, with the last one being slightly less reactive. It is, however, possible that reactions at site 5 take place but are far less likely in normal conditions. Due to high reactivity caused by double activation of sites 2, 4 and 6, it is very difficult to obtain a mono-substituted resorcinol and this can lead to difficulties in separating the products of resorcinol reactions with electrophilic agents, such as formaldehyde.

Resorcinol undergoes a number of reactions, including alkylation, esterification, halogenation, acylation, nitration and sulfonation. All these occur mostly at positions 2, 4 and 6.

2.3. Chemistry of sodium carbonate

Sodium carbonate which is also known as soda ash, is a sodium salt of a weak inorganic acid, the carbonic acid. In room temperature this substance is in the form of white powder, which is highly hygroscopic. The melting point depends on the type of sodium carbonate: the higher the degree of

hydration, the lower the melting point. For decahydrate ($Na_2CO_3 \cdot 10\ H_2O$) the melting point is the lowest at 34°C, while for the anhydrous form it is above 800°C (various sources give different values, from 825°C [37] to 851°C [57]). Sodium carbonate dissolves easily in water, due to the fact that the bonds between sodium and oxygen atoms in the carbonate group are ionic, producing alkaline solution: an aqueous solution containing as little as 1%wt. has a pH of 11.37 at 25°C [37]. This can be considered as a high value, however it is to be expected because this is a salt of a strongly alkaline metal.

Upon dissolution in water, the carbonate group is present in three forms (CO_3^{-2}, HCO_3^- and CO_2). The form H_2CO_3 is practically not present, therefore the carbonate is distributed between these three forms according to the following equilibria [58]:

$$HCO_3^- \leftrightarrow CO_3^{-2} + H^+,\ pK_a = 10.33 \quad (9)$$

$$CO_2 + H_2O \leftrightarrow HCO_3^- + H^+,\ pK_a = 6.35 \quad (10)$$

In practice this means that in solutions with pH lower than 6.35 the most abundant form of the carbonate is CO_2, while with pH above 10.33 the CO_3^{-2} form is predominant. In case of solutions with pH ranging between 6.35 and 10.33, the HCO_3^- is the dominant form .

Sodium carbonate can be obtained from natural sources and can also be manufactured in a synthetic processes [59]. The most commonly used natural source of sodium carbonate is trona – $Na_2CO_3 \cdot NaHCO_3 \cdot 2\ H_2O$. This mineral requires processing and the most commonly used is a method in which monohydrate is formed as an intermediate crystalline form [37]. There were a few attempts at a fully-synthetic method but the one that became very

popular is the Solvay method. This method bases on relatively cheap and available materials, like limestone ($CaCO_3$), salt brine (NaCl) and ammonia (in relatively small amounts). The whole process has a number of steps, however, one can describe it overall with one equation: $2\ NaCl + CaCO_3 \rightarrow Na_2CO_3 + CaCl_2$. The main by-product of this process, calcium chloride, is either way deposited in waste beds or used as road salt in the winter but unfortunately its amount can exceed the amount of the main product by as much as 50%wt.. However, the process was improved in 1930s and the by-product is NH_4Cl instead of $CaCl_2$. This is a great advantage from the economical point of view, as ammonium chloride can be refined and then used as a fertilizer, which is more valuable than calcium chloride [59]. Depending on the process in which sodium carbonate was obtained, the impurities can include water (below 2%) and small (<0.5%wt.) amounts of sodium chloride and sulphite, calcium, magnesium and even iron.

2.4. Resorcinol-formaldehyde gels via sol-gel polymerisation

Synthesis of organic gels in a sol-gel process was proposed first by Pekala in late 1980s [60]. This method was used before then in synthesis of inorganic (oxide-based) gels, and it was because of its feasibility that it became popular also in organic syntheses. The sol-gel process is fairly simple in terms of realization, as it does not require high pressure or high temperature. The upper limit for the temperature which can be used in a specific synthesis is dictated by the boiling point of the solution at a given pressure. In most cases, atmospheric pressure is sufficient therefore the whole synthesis can be carried out in typical laboratory glassware. Moreover, water can be used as a solvent, therefore use of expensive and potentially hazardous solvents

may not be required. All these make the sol-gel process economically viable and also environmentally reasonable.

The whole process involves the transition of a system from a liquid solution (the *sol*) of the molecular reactants to colloidal dispersion of primary particles and finally into a soft solid (the *gel*) phase, as shown in Figure 4.

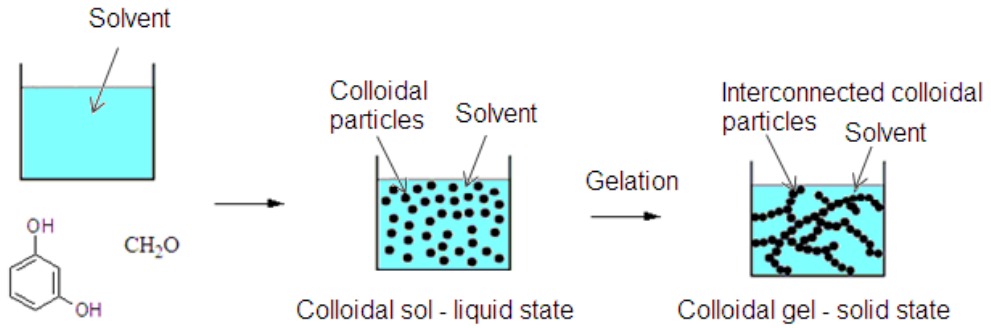

Figure 4. The sol-gel transition.

In a typical sol-gel process, the dissolved chemical reactants undergo a series of reactions and initially form colloidally sized (of nm dimensions) primary particles. The approximate radius of unsolvated resorcinol molecule is below 1 nm (ca. 5.8 Å), which increases slightly by substitution with formaldehyde. Condensation of resorcinol-formaldehyde molecules then leads to formation of a colloidal suspension although exact mechanism of how this happens is not currently known. These particles subsequently aggregate ultimately leading to a transition into a new gel phase, in which a solid three-dimensional network spans the solvent volume. This description of the process prevails in the literature, although in case of resorcinol-formaldehyde gels it is unclear what controls the formation of primary

particles or their subsequent aggregation. There is another theory which suggests that instead of simple particles growth and aggregation, the solution separates into two phases and one of them forms the solid part of the gel network [9] [61]. Among factors which are reported to influence the sol-gel process itself and thus the properties of the resulting material, one can name the temperature, concentration of the reactants and also the type of solvent. Concentration of the catalyst, which mainly affects the pH of the solution is also of great importance, especially in synthesis of organic gels. There are other factors which can affect the process but these three seem to be the ones which are the easiest to control and are proven to affect the structure of the resulting gel. Therefore these are investigated most often.

It is very important to understand the manner in which primary particles grow because it is their diameter that strongly affects the pore sizes in the resulting gel. When these particulates start joining and form a solid network, the way they are arranged and their diameters determine how much space is left between them. This space is nothing else but pores of the gel and the ability to fully control their size, and thus accessibility of the pore, is crucial for many researchers as it determines the possible applications of the material.

In order to understand how the temperature, catalyst and reactants concentrations influence the properties of the resulting gel, one needs to explore the sol-gel process itself and not only the properties of the obtained material. Most researchers focus on how the final properties of the gel change when certain process conditions are altered, which is by all means reasonable from the practical point of view. Not many have focused on the influence of these conditions on the reactions and the process of gel formation itself.

Relatively often, the gel formation and resorcinol-formaldehyde reactions are treated as the same single process, while it is likely that there are several sub-processes that may be influenced in different ways by adjustment of certain factors. This could in turn lead to confusing and/or misleading conclusions. An excellent example of a non-uniform effect is the influence of pH. In order to facilitate formaldehyde substitution ideally an resorcinol anion should be formed, however due to high pK_a of resorcinol this is unlikely in low pH, therefore basic conditions are called for. The gel formation, on the other hand, is related to condensation of hydroxymethyl resorcinol derivatives, which is said to be acid catalysed, thus requiring low pH.

It would be very beneficial to describe how each of the factors affects the sol-gel process and not only to assess its influence on the properties of the material. As mentioned earlier, most of the research was done on the resulting materials and because there is a number of processing steps between the gel formation itself and actually investigating properties of the final material, it is very difficult to draw conclusions from work done by more than one research group. It is because most of the published work does not have consistent post-synthesis processing methods, i.e. they have different ways of solvent exchange, activating, additional crosslinking, drying or carbonizing. All these influence the pore size and surface area of the final material and it is not possible to determine the effect of, for example, catalyst concentration on the gel formation itself. Therefore in this work I performed a series of *in-situ* experiments, investigating the mixtures during their reaction at the early stages of the process rather than focusing on the resulting materials.

2.4.1. Role of temperature

The temperature plays a key role in most of the chemical reactions, as they are often related to certain thermal effects. For most of the reactions, increasing the temperature of the reaction causes the rate of the reaction to increase as well. This is caused by the fact that the molecules are moving faster in higher temperatures, therefore there is a greater chance of effective collision per unit of time and this results in a faster reaction rate [62]. The dependence of the reaction rate on the temperature can be described by the Arrhenius equation:

$$\ln k = \ln A - \frac{E_a}{RT} \tag{11}$$

where k is the reaction rate constant, A is the pre-exponential factor, E_a is the activation energy, R is the universal gas constant and T is the temperature. Very often the relationship $\ln k \; vs. \; (1/T)$ is linear, therefore E_a/R can be determined from the slope of the relationship and it is clear that the greater the activation energy, the stronger the dependence of the reaction rate constant and temperature. If the plot of $\ln k$ $(1/T)$ is not linear, the energy activation can still be determined using a local slope and thus it would be dependent on the temperature as well.

The temperature can influence the sol-gel synthesis of the resorcinol-formaldehyde in more than just one way. It can influence both kinetics and equilibrium of chemical reactions: addition of formaldehyde to resorcinol and condensation of hydroxymethyl resorcinol. It can also influence the physical processes leading to gel formation, whether it is aggregation or phase separation. The temperature can also affect solubility of both reactants

and products. Since the most common synthesis processes are conducted at elevated temperatures, this is not an issue when it comes to the reactants which are fully soluble/miscible at ambient temperature. The solubility of the products on the other hand is not known in this case. Previous research on temperature influence on the resorcinol-formaldehyde gels synthesis is very limited, as most researchers followed the well-established synthesis procedure at a fixed temperature [60].The purpose of most of the previous work done in this field was to develop a method which would produce materials with desired properties, while keeping the production time as short as possible. Since the reaction rate increases with the temperature, it was natural to increase the reaction temperature as far as possible, i.e. to 90°C, which is just below the boiling point of the reacting mixture.

In order to verify how does the temperature affect the porous properties of the resulting gel a research was done [34] in which the reaction was conducted at two temperatures, i.e. 25°C (298K) and 50°C (323K). None of these is the typical synthesis temperature, however gels can be obtained in both of them. As it turned out there was hardly any difference in the porous properties of resulting dry gels. Another study on the temperature influence on the porous properties was done on resorcinol-formaldehyde gels which were prepared using very high R/C ratios (1000-3000) [63]. In this case, the synthesis process was changed from one day at 22°C followed by one day at 50°C and another day at 90°C to simply heating the sample at 90°C directly after mixing. The main conclusions from this work were that the resulting materials had slightly smaller particle sizes and pores, which was probably due to the fact that the particulates forming the gel were not allowed enough time to grow before condensation took place. The temperature needs to be lowered if the boiling point of the solvent is lower, as it is in case of acetone:

the temperature needs to be lowered from ca. 80°C to ca. 40°C, however, good quality gels can still be obtained [9].

Unfortunately, none of the studies were performed to analyse the temperature influence on the reactions taking place in the mixture. None of the papers published focused on how does the temperature affect the gel formation stage from a purely physical point of view, either. Even research which focused on the growth of particulates forming the gel using DLS did not examine the influence of temperature [64].

2.4.2. Role of catalyst and initial pH of the reacting solution

When investigating the influence of the catalyst on the porous properties of an organic gel, there are a few key issues that need to be taken into account. The catalyst is added to the reacting mixture to provide the most suitable conditions for the reaction. This means adjusting the pH to the desired level, which can later on affect the whole process. The type of the catalyst needs to be chosen appropriately, as is its concentration.

The most popular catalysts used in resorcinol-formaldehyde gels are those which provide alkaline solution upon dissolution in water. The very first studies [60] proved that the gels are best synthesised in the pH above 6.0, however, the initial pH values above 7.5 were not examined then. Some of the later studies [65] [66] [67] were also performed in conditions of the initial pH not exceeding 7.5, however, a couple of studies [32] [33] covered also experiments in which the initial pH was as high as 9.0. The main conclusions from these studies were that in pH below 6.0 the gel did not form after temperature treatment and instead the solution became opaque or a precipitate formed. When the initial pH was above 8.0, the gel either way did

not form [32] or contained virtually no pores [33]. Results of research done by Lin et al. [65] proved that for carbon xerogels synthesised with an initial pH 7.0-7.5 virtually no pore volume was found. Only when the pH was decreased by addition of nitric acid, both the pore volume and the surface area increased, with the most dramatic increase from 0 to 600 $m^2 \cdot g^{-1}$ when pH dropped from 7.0 to 6.5; it remained at this level until pH dropped to 5.5. The pore volume increased linearly with the decrease of pH in the range 7.0-5.7. Lin et al. [65] also discovered that the lower the initial pH, the broader pore size distribution. Results of Zanto et al. [66] confirmed these findings, underlining that the most significant factor affecting the surface area and pore volume is the initial pH, and not weight percentage of solids or the pyrolysis temperature. This proves that it is crucial to fully understand and explore the reaction mechanism because it is the most influential step. Research performed by Job et al. [67] revealed that the specific surface area can be changed by varying the initial pH values. An increase of pH from 5.45 to 7.35 caused the specific surface area to increase from 330 $m^2 \cdot g^{-1}$ to 470 $m^2 \cdot g^{-1}$, however, a maximum of 510 $m^2 \cdot g^{-1}$ was found at pH equal to 6.50. A more recent research by Zubizaretta et al. [33] investigated the influence of the initial pH on the surface area of resorcinol-formaldehyde gels. The main conclusion was that the surface area of the gels synthesised at pH 6-7 was much higher than of those synthesised at pH equal to 9.

Several researchers [36] [35] investigated acidifying agents (acetic acid) as catalysts. These experiments covered pH range lower than 5.0 and proved that gels can be formed also in such conditions, however, their porous properties are – depending on a chosen R/C ratio – slightly different than of those synthesised in basic conditions. For instance, they exhibit very weak relationship between the pore size and R/C ratio. It is worth mentioning that

at very high R/C ratios (above 1000), acid- and base-catalysed resorcinol-formaldehyde gels have almost the same properties as far as electrical conductivity, elastic moduli, micropore size and volume, and the density of primary particles are concerned [36]. When R/C ratios are kept low, the particles appear to be joined together with their centres (on SEM images), looking like small spheres being molten. Both diameters of these spheres as well as pore sizes are lower, especially when concentration of the reactants is increased.

None of the studies focused on the influence of the pH on the actual mechanism of the gel formation itself but only on the final properties of the gels and partially on the gelation time. Interestingly enough, there is very limited data on how the pH changed in the course of the reaction.

It turns out that it is not only the pH of the initial solution that may influence the properties of the resulting material, but also the chemical compound used to do this. The most commonly chosen catalysts are alkaline, because the preferred reaction conditions are mildly basic, while both resorcinol and formaldehyde produce acidic environment upon dissolution in water. Most researchers use the same catalyst as Pekala did in 1989 and afterwards [60] [68], i.e. sodium carbonate. This compound is easy in terms of handling, available and relatively inexpensive, therefore it is so common [3] [69] [70] [71] [72] [73] [74] [64] [75]. Nonetheless, other basifying agents were investigated. Among them one can find sodium hydrogencarbonate [34] [76] potassium carbonate [76] [77] and potassium hydrogencarbonate [76]. Alkaline hydroxides are also popular with the researchers – hydroxides of sodium, potassium, lithium, calcium, barium, magnesium and strontium were extensively studied [34] [78]. Since the prevailing hypothesis is that the

catalysts primary role is to provide appropriate pH, even ammonia was studied as a potential catalyst [34]. Research performed by Tamon et al. [34] proved, however, that alkaline metal cations are indispensable for the synthesis and gel formation, as process in which ammonia was used failed to produce a gel.

In their study, Grenier-Loustalot et al. [79] identified relationship between the size of the cation in the alkaline metal hydroxides acting as catalysts in phenol-formaldehyde reactions and the rate of the reactions between these two compounds. Even though the study concerns a different material, it is worth to mention its main findings due to the similarity of resorcinol and phenol. Grenier-Loustalot et al. [79] found that the relationship between the constant of formaldehyde disappearance and the radius of the alkaline metal cation is almost linear. The smaller the radius, the greater the constant. Moreover, for divalent cations, like Mg^{+2}, Ca^{+2} or Ba^{+2}, the constant values were greater than for monovalent like K^{+}, Li^{+} or Na^{+}. Grenier-Loustalot et al. [79] suggested that this relationship may be caused by formation of a certain intermediate species, a chelate which facilitates reactions between phenol, formaldehyde and their derivatives. This is an interesting suggestion, even though it concerns a different reactant (phenol) than the one which is the focus here.

Fairen-Jimenez et al. [77] found that for the same concentration of the reactants, gels produced with sodium carbonate were denser than those synthesised with potassium carbonate as catalyst. They also had smaller pore volume and smaller pore diameters. This research was followed by a far more extensive one by Job et al. [78]. This study focused on alkali metal hydroxides and alkali earth metal hydroxides and it allowed to draw

conclusions on the influence on the type of metal used on the synthesis process. Job et al. [78] found that the size of the metal cation does not influence the pore characteristics of the resulting gel, however its charge and its concentration do. Gels synthesised using alkali earth metals (charge +2) had larger pore sizes than those synthesised in presence of alkali metals (charge +1). The initial pH was kept constant, meaning that the concentration of alkali metal hydroxides was twice the concentration of alkali earth metal hydroxides. The explanation for this effect provided by Job et al. [78] relates the effect of ions on the pore structure with electrostatic effects on the microphase separation process prior the gelation. It is known that salts destabilise colloidal suspensions and may lead to their coagulation and Job et al. [78] claim that this is what controls the gelation step. They reason that the repulsion between colloidal particles is being screened over the Debye–Hückel distance, which is inversely proportional to $\sqrt{\sum nq^2}$, where n is the concentration of ions and q is their charge. Therefore, due to the fact that earth metal cations have charge +2, they are more effective in screening these repulsive forces, leading to destabilisation of the suspension and gel formation at an earlier stage of the reaction than in case of alkali metals with charge +1. As a consequence, the obtained gels have larger pores, even when the same initial pH was ensured.

Findings of Job et al. [78] were mostly in agreement with findings of a more recent study by Morales-Torres et al. [75], in which five alkali carbonates were used as catalysts (Li, Na, K, Rb, Cs). The results showed that the gelation occurred faster for gels prepared using salts with smaller counter-ions, i.e. Li or Na, than for larger counter-ions, like Cs or Rb. The slower the gelation, the larger the primary particles, therefore also larger pores. Morales-Torres et al. [75] found that the porous characteristic of the material

depends on the size of the counter-ion in the carbonate used as a catalyst, which is in contrast to findings of Job et al. [78], who stated that the size of the metal cation did not influence the pore characteristics. In their study, Morales-Torres et al. [75], suggest that the growth of the resorcinol-formaldehyde gels takes place *via* formation of anionic species induced by the catalyst. Therefore, there must be electrostatic interactions present and it might be worth to consider application of surfactants in order to provide better control over the process.

Acid-catalysed synthesis of organic gels is possible as well, however there are a few differences between the processes. A study on acid-catalysed sol-gel process of resorcinol-formaldehyde gels synthesis in aqueous solutions was done [36]. Brandt et al. discovered that the greater the concentration of the catalyst – acetic acid – the smaller the particles form the gel network. At the same time, the dependence of the pore sizes of the gel on the R/C ratio is much weaker than for gels synthesised using basic agents.

Another study, in which resorcinol-formaldehyde gel was synthesised using hydrochloric acid as catalyst and acetonitrile as solvent was done by Mulik et al. [35]. His results proved that these gels were virtually indistinguishable by IR and ^{13}C CPMAS NMR from the base-catalysed materials. Mulik et al. [35] reason that the acid-catalysed route to gel formation is acceleration of the reaction *via* increasing the positive charge of the electrophile rather than activation of the aromatic ring by enhancing the ability to donate electrons of the substituents (OH to O^-), as it is in case of the base-catalysed synthesis. On the other hand, results provided by Fairen-Jimenez et al. [77], before Mulik et al. study [35], proved that the acidic catalyst affected only the gelation process. This study [77] also proved that

when using acidic catalyst, oxalic acid or para-toluenesulfonic acid, the density of the resulting material is greater than in case of alkaline carbonate catalysts by a factor of two or even three, suggesting that use of acidic catalyst greatly enhances cross-linking and condensation.

A number of studies proved that there is a dependence of the porous properties of the resorcinol-formaldehyde gels on the concentration of the catalyst. In most cases, the catalyst influence is examined not as an absolute concentration but as the resorcinol-to-catalyst molar ratio. This makes it complicated when comparing the results of various research groups, as their synthesis methods also vary by resorcinol and/or formaldehyde concentrations.

There is a large number of studies which deal with the effect of the R/C ratio on the properties of the final material but they are mostly consistent in their findings. A study performed by Saliger et al. [31] showed that the growth of particles forming the gel could be controlled by the concentration of the catalyst, appropriate concentration of the reactants and the temperature. The amount of catalyst was claimed to control the size of the particles constituting the gel network under assumption that more catalyst translates into more active sites in which these particles are formed, leading to structures with smaller particles and thus pores. In very long synthesis process Saliger et al. [31] managed to obtain materials with cluster sizes in the μm range, while typically nm scaled particles are found. Findings of Saliger et al. [31] were confirmed by findings of Bock et al. [80], who found that for lower R/C ratios (i.e. higher catalyst concentrations) the gel structures were finer (corresponding to smaller primary particles).

A very good review by Al-Muhtaseb et al. [9] summarises the findings of research on the resorcinol-formaldehyde gels, focusing on the influence of each synthesis and processing step on the properties of the resulting gel, not only on the catalyst influence. The overall conclusion from their review is that the structure of gels synthesised in presence of low concentration of catalyst (i.e. high R/C ratio) resembles "string-of-pearls". This means that there is a number of rather large (16-200 nm in diameter) particles connected with thin strings, which is not the case for more fibrous in appearance materials obtained in conditions of high catalyst concentration. In that case the diameter of the particles and the links between them is virtually the same and varies around much smaller values of only 3-5 nm. These findings are supported by a number of studies [68] [81] [82] [83] [84]. The reasoning behind this finding is that lower catalyst concentration allows longer growth of the primary particles prior to gel formation. As a result the pore sizes are greater. Additionally, these studies mostly confirm that the higher the R/C ratio, the wider the pore size distribution in the resulting material, suggesting that in conditions of low catalyst concentration polydispersity occurs in the colloidal suspension before gelation [85].

The effect of the R/C ratio on the surface area is significant, however, it varies across studies. In many cases, a maximum value was found for certain conditions and it appears that more factors than just R/C ratio determined this [86]. It also seems that pH is a more influential factor than R/C ratio [9].

A later study by Job et al. [67] is in agreement with these findings and attempts to give an explanation of this phenomenon. When high concentration of catalyst is used the rate of hydroxymethyl derivatives formation as well as the extent of substitution are high, which translates into

highly-branched clusters. These structures condense easily, therefore they do not persist in the nucleation regime and form smaller clusters. When low concentration of catalyst is used, the effect is contrary: lowly-branched structures, which persist in the nucleation regime for a longer time, allowing growth without condensation and gelation.

Significant majority of the available studies focus on the influence of the R/C ratio on the properties of the gel and not on the mechanism itself. There is a very limited number of studies, which use Dynamic Light Scattering to examine the changes caused by altering the R/C ratio on the gelation mechanism. One of the studies was done by Berthon et al. [74], who studied mostly influence of the solvent and type of catalyst on the gels. This study is very limited in case of water-sodium carbonate solvent-catalyst couple, as it investigates only one R/C ratio. Nonetheless, Berthon et al. [74] suggested that the mechanism of gel formation is different for acid and base-catalysed syntheses. A far more relevant study was conducted by Yamamoto et al. [64], in which Dynamic Light Scattering experiments were done on samples with varying catalyst (sodium carbonate) and resorcinol concentrations. The main findings of this study are that the rate of growth of the primary particles depends on the catalyst and resorcinol concentrations. Moreover, this relationship is not linear throughout the whole synthesis process. Yamamoto et al. [64] also found that as the reaction reaches approximate gelation time, the shape of the decay time spectrum becomes bimodal, indicating formation of a less-mobile structure, probably the gel network.

2.4.3. In situ investigations of resorcinol-formaldehyde reaction

There are several good previous publications on the reactions leading to formation of formaldehyde resins, however most of them focused on phenol-based materials. Moreover, most of the studies were performed relatively long time ago before more advanced analytical methods were available. A very informative method is the Nuclear Magnetic Resonance spectroscopy (NMR) which can provide both qualitative and quantitative description of the reacting mixture. An early study of the reactions leading to formation of resorcinol-phenol-formaldehyde resins was performed by Anderson et al. [87]. In this study a number of peaks in ^{1}H NMR spectra was assigned, however, no spectra were provided. Information on the methodology of measurements (such as pulse programme, delay time etc.) is scarce and, moreover, the method was used to identify the products of the reactions rather than monitor its progress in time. A later study by Sojka et al. [88] was performed in order to examine the mechanism of reactions in phenolic resin formation, however, the study covered reactions of phenol and hexamethylenetetramine and not formaldehyde. Nonetheless, this study provides useful information and suggestions on the experimental methodology and the analysis of the results.

A study by Kim et al. [89] was performed also on phenol-formaldehyde resins and it provided information mostly on the assignments of the free-formaldehyde related signals as well as issues related to the use of NMR. It is important to emphasise that since this study the NMR technique has greatly improved and most of the problems reported there are not obstacles these days. A later study by Fisher et al. [90] was performed using better equipment, therefore the resulting spectra had better resolution and a more

thorough analysis was possible. Moreover, Fisher et al. [90] performed not only the classic 1D experiments – ^{1}H and ^{13}C NMR – but also 2D experiments, such as Double Quantum Filtered Correlation Spectroscopy (DQF COSY). As a result of this study, identification of most products was possible and also information on the limitations of the non-typical NMR techniques was obtained. A later study by Grenier-Loustalot et al. [79] on the catalyst influence on the mechanism and kinetics of the phenol-formaldehyde reactions used ^{13}C NMR as a tool. This was an insightful study on the application of the NMR technique as a quantitative analysis tool and as a tool that allows kinetics investigations.

A study by Luukko et al. [91] is also focused on the phenol-formaldehyde resins, however, it deals with optimization of the ^{13}C NMR experimental conditions. It investigates the effect of addition of a paramagnetic agent (chromium (III) acetylacetonate – $Cr(AcAc)_3$) on the relaxation times of species found in the reacting mixture. The main result of this study is that the relaxation times can be shortened considerably and, as a consequence, so can the experimental procedure. However, authors do not take into consideration the fact that chromium (III) acetylacetonate affects the pH of the reacting mixture and that presence of Cr^{+3} may affect the actual mechanism of the reaction. A similar study, also using chromium (III) acetylacetonate as a relaxing agent was later conducted by Rego et al. [92]. This study was without a doubt helpful in assignment of the formaldehyde-related species, however, it also focused on the phenol-formaldehyde resins and not resorcinol-formaldehyde. Additionally, this study discusses briefly a number of issues which should be dealt with if one wants to collect fully quantitative ^{13}C NMR spectra.

There is a very limited number of studies which focused on the resorcinol-formaldehyde reactions mechanism, mostly because it has always been assumed to be analogous to the that of phenol-formaldehyde resins. A very important and extensive ^{13}C NMR study of resorcinol-formaldehyde resins formation was performed by Werstler [93]. His work became a foundation for many others that followed him, including Pekala [60]. In this work Werstler [93] performed a very thorough ^{13}C NMR investigation of reacting mixtures of resorcinol and formaldehyde. Not only did he identify the issues with the method he used (namely NOE) but he also assigned chemical shifts for the most probable products of the reaction. He also showed that ^{13}C NMR can be used to determine speciation of the reacting mixture and also to quantify the concentrations of given species, allowing to examine the kinetics of the reactions.

A thorough study of resorcinol-formaldehyde reactions was done by Christiansen [94], using ^{13}C-enriched formaldehyde and sodium hydroxide as catalyst. Although conditions used were not identical with those used to synthesise resorcinol-formaldehyde gels, Christiansen [94] identified the products of reactions between formaldehyde and resorcinol and was also able to determine the approximate rate at which they appeared in the solution. As in case of studies performed by Luukko et al. [91] and Rego et al. [92], there is certain doubt regarding the results because of the type of the reference standard which was used. Christiansen [94] used sodium salt of the 3-(trimethylsilyl)-1-propanesulfonic acid (DSS) as an internal standard. In the light of previous studies on the influence of the catalyst metal cations concentration, one should be cautious when interpreting quantitative results of this study. Nonetheless, this research provided good quality spectra along with their assignments and good quantitative analysis of results.

Christiansen [94] detected and quantified not only the hydroxymethyl derivatives of resorcinol but also products of their condensation, along with methylene linkages. A later study by Pizzi et al. [95] provided extensive information on a variety of phenol-based resins (linear phenol–resorcinol–formaldehyde, urea-branched phenol–resorcinol–formaldehyde and phenol–resorcinol–furfural). The study used both ^{13}C NMR and MALDI-TOF techniques to examine the structures of these materials, however, the NMR spectra are of relatively low quality, as they are only supportive for the MALDI-TOF technique. A later work by Moudrakowski et al. [96] focused on structure analysis of resorcinol-formaldehyde aerogels using continuous flow ^{139}Xe NMR, solid-state ^{13}C NMR and two-dimensional wide-line separation (2D-WISE) NMR techniques. These methods are far more advanced than used previously, however, they do not provide information on the mechanism of the reactions leading to gel formation. Nevertheless, this study provides very valuable input on the assignment of ^{13}C NMR spectra collected in solid state, which can be extrapolated onto the liquid state NMR experiments. Moudrakowski et al. [96] concluded that the degree of polymerization and the mobility of the functional groups responsible for cross-linking are closely related to the R/C ratio. A low R/C ratio results in a high degree of cross-linking, which translates into lower mobility in the network. This is in agreement with other studies, which did not use highly-advanced NMR techniques.

Most of studies presented here were performed on samples of the reacting mixture after their dissolution in a deuterated organic solvent and not water, therefore there is doubt whether the results represent the actual changes in the mixture in the course of the reaction. One could expect that a significant change in the reaction environment would influence the reaction mechanism.

Moreover, there is a very limited number of publications directly dealing with the resorcinol-formaldehyde reactions. Therefore, it can be can concluded that the literature suffers from lack of *in situ* quantitative analysis of reaction mechanisms and kinetics in resorcinol-formaldehyde systems and therefore this study aims at filling that void.

In order to determine the mechanism of gel formation from a physical as well as chemical point of view, one should observe the growth of primary particles which grow in time and subsequently aggregate to form a solid network immersed in the solvent and residues of the reactants. This can be done in a number of ways out of which Dynamic Light Scattering (DLS) seems to be the most insightful. A number of SAXS and SANS studies were performed [97] [74] [98] [61] to investigate the final structure of the gels and its dependence on reaction conditions, however, these studies were not performed on reacting systems. Despite being a very useful tool, there is a relatively low number of publications on the DLS application in studies of the gel formation in resorcinol-formaldehyde reactions. One of the studies, which also covered SAXS experiments, is the one by Berthon et al. [74]. This study showed that the shape of the autocorrelation function changes as the reaction proceeds and that the mechanism of gel formation in presence of alkaline catalyst is different than in presence of an acidic catalyst. However, unlike the study by Yamamoto et al. [64], it does not describe the growth pattern of the primary particles in the colloidal suspension before gelation. In their study, Yamamoto et al. [64] showed the growth of the diameter of the primary particles as a function of both time and catalyst concentration. From their results one can conclude that there is a relationship between the growth rate, time required to form a firm network and the catalyst concentration. This work is an excellent example of how the gel formation could be

investigated from a more physical approach, however, there were not many similar studies performed later on. A study by Czakkel et al. [99] focused on copper-doped resorcinol-formaldehyde aerogels and DLS was used in this study but not to determine the growth rate of the primary particles but the influence of copper acetate (CuAc) on their diameter. Therefore, there is a need to perform time-resolved DLS experiments in order to examine more closely the physical mechanisms leading to particle growth and subsequent gel formation.

CHAPTER 3. EXPERIMENTAL METHODS

3.1. Gel (gelation) time

The term "gel time" or "gelation time" refers to how long it takes for a sample to become a gel in given conditions.

3.1.1. Methodology

Gel is a soft solid material formed from two interpenetrating phases. A solid phase is usually a macromolecular or particulate network spanning a continuous second phase which is usually liquid, therefore one can say it is a special case of a dispersed system. Colloidal materials can form gels usually as a result of coagulation leading to interconnected clusters. This process can be controlled to a certain degree in terms of aggregation kinetics and resulting cluster structure. A number of factors can induce, speed up or slow down the process of gel formation in most colloidal suspensions. These factors include electrostatic interactions leading to destabilization of the suspension (i.e. addition of salts, modification of pH, addition of a flocculant) or others, like ultrasounds, temperature treatment, to name a few.

For the purpose of this research the gelation time needed to be estimated to assess influence of various factors (temperature, composition) on the gelation process, but also to ensure that results of other experiments performed on the reacting mixtures were viable. For instance, both NMR and DLS require the investigated solutions to be liquid in order to provide reliable results. Otherwise, a special type of NMR spectroscope probe needs to be used, while the DLS results would not provide reliable information about the

particle or cluster size, since the Stokes-Einstein equation which is the basis of results interpretation, is no longer fulfilled.

There is a number of methods which can be employed to detect the moment when gelation occurs in a colloidal suspension. A widely used and direct method is based on visual observation [100]. A sample of a reacting liquid mixture is kept at a sealed vial at a given temperature and when no flow is observed upon tilting to angle of 45°, the sample is considered to have become a gel and the time at which this is observed is the gel time. This method is also useful because the observer can notice other changes to the solution during the reaction (clarity, colour) as well as to get the sense of when the viscosity of the sample starts to increase strongly, which is in case of NMR experiments already a limitation in application. The method is adequate when an estimate of gel time needs to be determined, rather than the exact point of gelation. Apart from the factors mentioned above, which can be directly linked to the compositions of the samples and the temperature, a number of other factors may play an important role. The gel time measured with the chosen method (visual observations) was proven to depend also on the dimensions of the vials which held the sample, whether they were sealed and the headspace above the reacting mixture. Therefore, all gel time measurements were performed on the same or very similar volumes held in identical, sealed vials. Detection of the gel time can be also determined by more precise rheological methods [101]. These are far more accurate in determining the exact gel time, however they require interacting with the mixture during gelation which can affect the process of gel formation and thus influence results. Non-invasive methods include methods based on light transmission changes [102]. It has been observed that upon gelation increased scattering intensity is observed [103], therefore the

gel time can be determined by observation of the intensity of scattered light in time. Certain methods based on light transmission require use of dyes which, being chemical compounds, may as well influence the gelation process [102]. Taking all these facts into consideration, it was decided to use the visual method as it is the most suitable for our purposes here.

3.1.2. Sample preparation and measurements

Prior to preparation of the reacting mixtures, the glassware was washed with de-ionized water to ensure that no impurities were present. Meanwhile, the oven was pre-heated to 55°C, 80°C or 90°C; this temperature was kept constant.

The required amount of de-ionized water was measured in a measuring cylinder and poured into a 100 ml beaker. Then resorcinol was weighed, transferred to the beaker, a magnetic bar was placed in the beaker as well, and the vessel was then placed on the magnetic stirrer. After all solid flakes of resorcinol have fully dissolved (5 min), sodium carbonate was weighed by an analytical scale and transferred to the beaker with dissolved resorcinol. After ensuring that all sodium carbonate has dissolved (10 min), the required amount of formaldehyde solution was measured with an automatic pipette and added to the mixture inside the beaker. Stirring continued for 30 min from the moment formaldehyde solution was added. A 10 ml sample of the solution was transferred using an automatic pipette into a screw-topped poly(propylene) flask (25 ml; diameter 25 mm, height 100 mm). The vial was immediately sealed (screw-top was secured) and then placed in an electric oven pre-heated to a desired temperature or left at the laboratory bench in room temperature.

The process of gelation was monitored by visual observations of changes in the solution flowability and gelation time was taken here as time measured from the moment a sample of reacting mixture is placed in an electric oven set to the desired temperature and periodically checked until lack of flow at tilting (by approximately 45°) is observed.

3.2. pH measurements

3.2.1. Concept of pH and pH measurements methods

Svante Arrhenius won the Nobel Prize in 1903 for his theory on electrolytic dissociation. The three postulates which he has created and which are the basis of his theory are: (1) acids, bases and salts decompose into positive and negative ions under the influence of water, (2) the number of electric charge accumulated on positive ions is equal to that accumulated by negative ions, therefore the solution as a whole has a zero net charge and (3) weak electrolytes dissociate in water to a very small degree. Arrhenius has then defined acid as a substance which dissociates forming a hydrogen ion (H^+) while substances producing hydroxyl ions (OH^-) are bases. According to this theory water is both an acid and a base.

In 1909, which is just a few years after Arrhenius published his postulates and formed his theory, Søren Sørensen introduced a characteristics which allowed to define the strength of acids and bases. Basing on the definition that acids donate protons and that bases donate hydroxyl ions, Sørensen concluded that the total concentration of hydrogen ions in the solution should indicate to what degree the acid or base dissociated. Introducing the definition of pH as $-\log_{10}[H^+]$ allowed segregation of acids and bases depending on their potential to dissociate in water, naming it their strength.

This definition of pH was predominant for many years, until research proved that hydrogen ions are not present in aqueous solutions in a free form but as hydronium ions (H_3O^+).

Due to the fact that it is impossible to define the absolute concentration of H_3O^+ and that currently most pH measurements are performed via galvanometric methods, IUPAC introduced a definition of pH as [1] [104]:

$$pH(X) = pH(S) + \frac{(E_S - E_X)\cdot F}{RTln10} \tag{12}$$

where F – Faraday constant ($9.65\cdot10^4$ C·mol^{-1}), R – universal gas constant (8.31 J·mol^{-1}·K^{-1}), T – temperature in K, E_S and pH(S) – electromotive power of a standard cell immersed in a standard solution and pH of this solution in a given temperature specified by IUPAC, respectively.

This general definition shows that pH is a dimensionless unit and is only a comparative characteristic, not directly related to concentration or activity of hydronium ions or any others. However, as IUPAC points it out [1], in a narrow range of dilute solutions with concentrations lower than 0.1 mol·dm^{-3} and pH between 2 and 12, it is reasonable to assume that pH measured with galvanometric methods satisfies the following equation:

$$pH = -log_{10}\left[\frac{\gamma_1\cdot[H^+]}{1\ mol\ dm^{-3}}\right] \pm 0.02 \tag{13}$$

where $[H^+]$ corresponds to hydronium ion concentration in mol·dm^{-3} and γ_1 is activity coefficient of these ions.

Bearing in mind the above statements and equations, one may use pH measurements as indication of changes in hydronium ions, as without knowledge of activity coefficients it is not possible to fully quantify them.

The value of pH in liquid solutions can be estimated visually by adding substances called acidity indicators. These chemical species change their colour (and thus the colour of the solution) depending on the concentration of hydrogen ions. These are very convenient for quick assessment of pH of the solution, however, they do have a number of limitations. The main issue is the fact that they do not cover the whole pH range but just certain intervals, therefore a knowledge or indication of expected pH value is required. Another serious disadvantage of all these indicators is the fact they do not provide information about exact value of pH of the solution, therefore they cannot provide quantitative data.

If quantitative information on the acidity of solution is required, a variety of galvanometric methods can be used [104] [105]. Galvanometry is in general method of measuring the strength of electric currents and it can be used to determine the pH value of a solution, owing to the fact that ions are charge carriers and the strength of the current depends on their concentration.

The practical implementation of galvanometry to measure pH of solutions is fairly straightforward: the pH measurement is simply measurement of hydrogen half-cell potential immersed in the investigated solution. The reference left hand side half-cell is usually a saturated calomel one ($Hg_2Cl_2(s)$) which has a potential of E(cal), while the right side half-cell is the hydrogen one, which potential is described by the abovementioned equations.

In practice a more convenient method is used – instead of hydrogen half-cell a glass electrode is implemented. Its potential changes proportionally to pH and it is sensitive to changes in hydrogen ions activity. The main two advantages of the glass electrode over the calomel and hydrogen cell is (1) the possibility of calibrating it with any given solution of known pH and (2) feasibility of usage (unlike gaseous hydrogen electrode). It is most often filled with a phosphate buffer containing chloride ions. It is assumed that when pH of the solution in which the electrode is immersed is equal to 7, its potential (E) is equal to 0. Sensitivity of the glass electrode to activity of hydrogen ions is an effect of complex processes between the glass membrane and solution and buffer on both of its sides. The membrane itself is permeable to sodium and lithium ions (Na^+ and Li^+) but not to hydrogen ions. Both sides of the membrane are covered with a very thin layer of hydrated silica oxide, which changes its properties due to changes of hydrogen ions activity. Changes in this external layer on the outside of the electrode (i.e. in the solution) are passed on by sodium and lithium ions to the internal layer of the electrode, thus the hydrogen ions indirectly affect the potential of the membrane [104].

3.2.2. Sample preparation and experimental procedure

The pH meter used was a commercially available Hanna Instruments (model pH 20; resolution ±0.01 pH, accuracy ±0.02 pH, temperature range 0-100°C) unit equipped with a glass electrode (model HI 1110B: single reference (Ag/AgCl), gel electrolyte, pH 0-13, -5 - 100°C) suitable for measurements in solutions containing alcohols.

All experiments were taken at room temperature conditions (18-25°C) with temperature being monitored and recorded during the measurements. It was crucial to ensure all the data was collected in the same conditions in order to allow reliable comparison and correlation. It is a known fact that activity coefficient of hydrogen ions depends on temperature and composition of the solution. According to information provided by the manufacturer of the electrode used (Hanna Instruments Inc.), the temperature-caused error from the electrode varies basing on the Nernst Equation and is calculated to be 0.03 pH units per 10°C per each unit of pH away from 7. This means that if the solution has a pH of 9 at 20°C, then at 30°C it would be 9.06. Bearing in mind that for certain dilutions the concentration and composition remained constant between measurements, the only factor that might have affected the activity coefficient and thus the pH reading, was temperature, therefore all effort was made to ensure this parameter also remained constant between measurements and that its spread was less than 10°C.

Non-reacting systems

Formaldehyde-water and formaldehyde-methanol solutions

All solutions of formaldehyde diluted in water or in methanol were prepared in a glass beaker and then transferred into 25 ml poly(propylene) sealable vials, where they were kept for measurements at certain time intervals after preparation. Appropriate amounts of formaldehyde and solvent were drawn with an automatic pipette into the beaker, then magnetic bar was placed in the vessel and the mixture was left to stir on a magnetic stirrer for 10 min. Then the contents were transferred into 25 ml poly(propylene) flasks, sealed and labelled. Measurements of pH were taken in room temperature by

placing the glass electrode and temperature control device into the flask. For each composition three measurements were performed and then an average value was obtained. In order to determine the stability of pH of the prepared compositions, measurements were taken at certain time intervals: right after the solution was prepared (t = 0h), 24h and 48h later.

Resorcinol-water and resorcinol-sodium carbonate-water solutions

Appropriate amount of resorcinol was weighed in a beaker, then de-ionised water was drawn with an automatic pipette and added. Magnetic bar was placed inside the beaker, then the vessel was placed on a magnetic stirrer and moderate stirring was allowed for 10 min, until all of resorcinol dissolved. Then the solution was transferred into a 25 ml poly(propylene) vial, sealed and labelled. Measurements were then taken in the same manner as for formaldehyde-water and formaldehyde-methanol solutions.

Formaldehyde-water-sodium carbonate solutions

Sodium carbonate was weighed on an analytical scale and then transferred into a glass beaker, where de-ionised water was drawn into with an automatic pipette. Magnetic bar was placed inside the beaker, then the vessel was placed on a magnetic stirrer and moderate stirring was allowed for 10 min, until all solids dissolved. Then the solution was transferred into a 25 ml poly(propylene) vial, sealed and labelled. Measurements were then taken in the same manner as for formaldehyde-water and formaldehyde-methanol solutions.

Resorcinol-sodium carbonate-water, formaldehyde-water and sodium carbonate-water solutions after temperature treatment

Solutions of resorcinol and sodium carbonate in water, as well as formaldehyde and sodium carbonate in water were prepared as previously described. The mixtures right after preparation were divided evenly into poly(propylene) vials, ensuring that each sample was of the same volume (automatic pipette), sealed and labelled. All vials but one were then placed in an electric oven pre-heated to 90°C and the moment the oven was closed was marked as "time zero" and a stopwatch was started. In the meantime, pH measurement of contents of the vial which had not been placed in the oven, was performed. The results of this measurements correspond to sample "time zero", which means that the sample did not undergo temperature treatment (time spent in the oven is equal to zero minutes). Subsequently, remaining samples were taken out of the oven, one at a time, five minutes apart. Each vial was cooled down in an ice-bath until its contents reached desired temperature (room temperature) and then the value of pH was measured.

Reacting systems

An appropriate amount of resorcinol was weighed and placed in a 250 ml glass beaker, equipped in a magnetic bar. Then an appropriate volume of de-ionised water was measured with a cylinder and added into the beaker. The vessel was then placed on a magnetic stirrer and the contents were stirred moderately for 5 min. In the meantime an appropriate amount of sodium carbonate was weighed on an analytical scale, added to the solution and the stirring continued for another 10 min. Then formaldehyde stock solution was

measured with an automatic pipette and added into the solution; the stirring continued for another 30 min. Once stirring process was completed, the solution was divided into samples of equal volume and poured into 25 ml poly(propylene) sealable flasks. Each vial contained a sample of 5-8 ml. The measurement procedure was as described earlier, however, the cleaning of the glass electrode was more carefully washed, due to the fact that steadily increasing viscosity of the reacting mixture in the course of reaction tended to stick to and clog the key of the electrode, posing a risk of affecting the readings. This is discussed in more detail in the results section.

3.3. IR spectroscopy

3.3.1. Methodology

Infrared spectroscopy is a non-destructive analytical method examining interactions between infrared (IR) light and matter, providing information on the type and quantity of different types of bonds present due to their selective absorbance of electromagnetic radiation [106].

All chemical bonds within matter constantly vibrate at specific frequencies. They undergo a number of vibrations like bending, stretching and contracting [107]. When matter is exposed to infrared radiation, which happens at all times as this type of radiation corresponds to the heat transfer, vibrational motion of bonds is more excited. Even though this motion is very complex, it can be broken down into a number of constituent vibrations, eventually allowing identification of chemical compounds present in the investigated sample.

The term *infrared light* refers to electromagnetic radiation with wavelengths greater than those of visible light (700 nm) but smaller than 1 mm. It is common practice to use reciprocals of wavelengths (in cm), which are called wavenumbers and have units of cm^{-1}. This value defines the number of cycles of a given light wave per one centimetre and following this definition, infra-red radiation can be sub-divided into the following sections [108]:

- Near infrared – NIR: 14000-4000 cm^{-1}
- Mid infrared – MIR: 4000-400 cm^{-1}
- Far infrared – FIR: 400-4 cm^{-1}

The most useful range for purpose of this research is the mid-infrared because it covers the vibrational frequencies of most chemical bonds. The far infrared contains only a few absorptions useful from our point of view: carbon-halogen absorptions and absorptions associated with rotational changes within the molecule. Near infrared is much closer to the visible light and contains mainly absorptions that are harmonic overtones of fundamental vibrations which are found also in the mid-infrared range [108] [106].

A plot of measured infrared intensity (expressed in either transmittance or absorbance of the sample) versus wavenumber is a result of an experiment and is called infrared spectrum. If a molecule absorbs infrared light and starts to vibrate, it gives rise to a peak at certain wavenumber, which corresponds with the frequency of induced vibrations. Assignment of these peaks to vibrations of certain bonds allows identification of chemical compounds present within the investigated matter. A simple example of a transmittance and absorbance spectra is shown in Figure 5

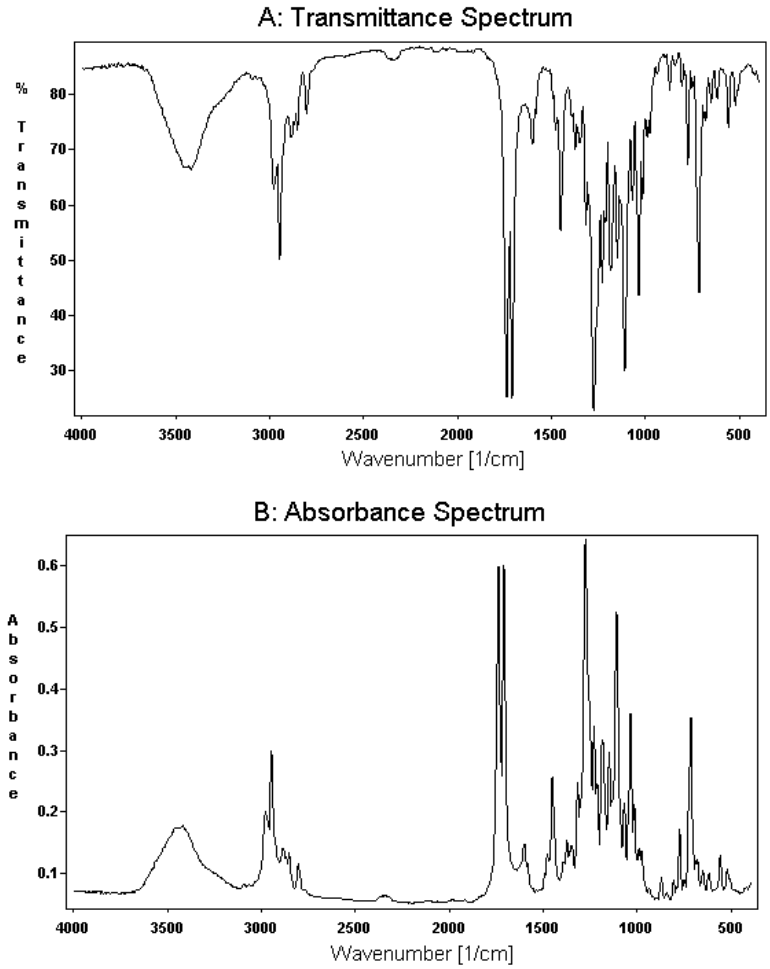

Figure 5 An example of (A) transmittance and (B) absorbance IR spectrum of the same compound [109].

Assignment of peaks found in an IR spectrum needs to take into account also intensity of the signals, not only their wavenumber. Intensities of peaks can vary depending on the type of bond they are related to. The reasons for this are the differences in changes of dipole moments: in some cases the change can be very small and then the intensity is low; when the change is considerable, the intensity is high [107]. Another factor contributing to the intensity and area of the registered signals is concentration of the bonds vibrating at given frequencies, which makes this method a very useful

analytical tool. For a single-component solution the relative intensities of peaks are not concentration-dependent [107]. However, in a mixture of a few chemical compounds, changes of concentration of some of them may lead to changes in proportions of the peaks, as peaks are assigned rather to a certain type of bond which can be present in a few different molecules.

Experimental procedure is fairly simple, due to introduction of Fourier transform IR spectroscopy technique. Initially, when IR spectroscopy was first introduced, a sample was swept by a monochromatic light beam which wavelength was incrementally changed during the measurement. Currently a vast majority of IR spectrometers operate under much faster method in which a sample is illuminated with a beam of radiation covering all wavelengths within the investigated IR range. Once the beam passes the sample it is interfered with a beam that did not pass through a sample and then the sum undergoes a Fourier transformation, which leads to formation of the final spectrum which can be subsequently analysed. This method requires more advanced equipment and appropriate software but it is much faster and more accurate than the older method.

An additional advance in the infrared spectroscopy was introduction of the Attenuated Total Reflectance (ATR) method. In traditional infrared spectroscopy sample preparation is crucial to obtain reliable data, since the intensity of the registered spectra depends on the thickness of the sample, which is usually no more than a few tens of microns. Analysis of solid materials requires grinding them and then dispersing in a mineral oil to form a paste, which is then spread between two windows made from potassium bromide (KBr), sodium chloride (NaCl) or calcium fluoride (CaF_2). Another option is grinding the investigated solid and dispersing it in ground KBr; the

powder is then pressed at a special press at a very high pressure to re-crystallize KBr, which results in a clear KBr disc which can be analyzed by infrared. Experiments on liquid samples are considerably easier to conduct, as samples are placed in cells forming thin films in which it is crucial to ensure the pathlength is constant, especially if a quantitative analysis is done. All these methods suffer from poor reproducibility of results, as sample preparation – especially of solids – is complex and requires considerable accuracy and practice. Samples of dispersed solids need to be homogenous, the proportions of matrix (namely KBr) and investigated solid need to be appropriate, which is a challenge due to the hygroscopic nature of used materials. A convenient solution to these issues was provided by the Attenuated Total Reflectance (ATR) method, which basically uses an accessory which measures the changes that occur in a totally internally reflected infrared beam when it comes into contact with a sample. The beam is directed onto an optically dense crystal with a high refractive index at a certain angle (see Figure 6). The internal reflectance forms an evanescent wave which penetrates the sample for only a few microns. The wave is then attenuated or altered in regions of the infrared spectrum in which the sample absorbs energy. The changed energy of each evanescent wave is collected and sent back to the infrared beam, then to the detector which compares the reflected signal with sent signal and constructs an infrared spectrum, as discussed earlier [110]. The most commonly used materials as crystals in ATR devices are zinc selenide (ZnSn), Germanium and diamond. The last one is probably the best material as it is very durable, scratch-resistant and chemically insensitive, unlike ZnSN and Ge.

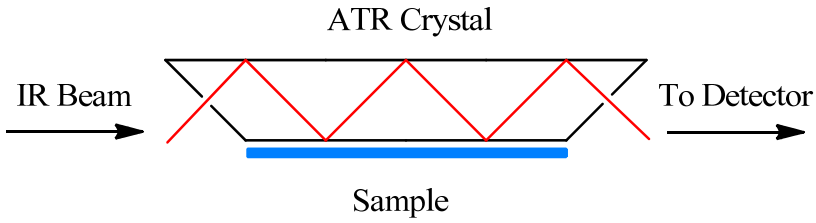

Figure 6. A scheme of an ATR crystal.

3.3.2. Equipment used

All experiments were performed using a MB3000 mid-IR Fourier Transform spectrometer manufactured by ABB Inc., equipped with class 3B laser (760 nm, 2 mW output power) and an ATR (attenuated total reflection) probe linked with the FTIR by custom-made optical fibre cable (see Figure 7).

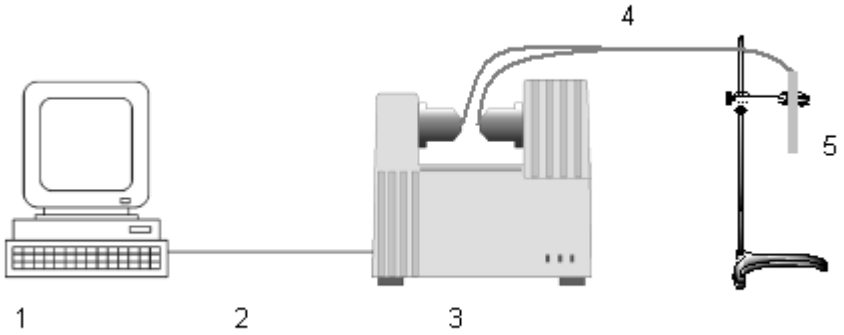

Figure 7. Scheme of FTIR equipment used in experiments: (1) computer with MB Horizon software, (2) crossover cable, (3) MB3000 mid-IT FTIR, (4) optical fibre cable, (5) ATR diamond probe.

3.3.3. Sample preparation

Non reacting systems

Methanol and water

De-ionised water was measured with an automatic pipette into a 25 ml beaker, which was equipped with a magnetic bar (cigar-shaped, 14x5 mm, PTFE surface) and placed on a magnetic stirrer. Methanol was measured with an automatic pipette and added to the water. The beaker was then covered with a layer of parafilm and mixed intensively for approximately 3 min. Then measurements took place without transferring the composition into another vessel due to relatively high volatility.

Formaldehyde and water

De-ionised water was measured with an automatic pipette into a 25 ml beaker, which was equipped with a magnetic bar (cigar-shaped, 14x5 mm, PTFE surface) and placed on a magnetic stirrer. Formaldehyde stock solution was measured with an automatic pipette and added to the water. The beaker was then covered with a layer of parafilm and mixed intensively for approximately 5 min, poured into 25 ml poly(propylene) flask, labelled and sealed.

Formaldehyde and methanol

An appropriate amount of formaldehyde stock solution was measured with an automatic pipette into a 25 ml beaker, which was equipped with a magnetic bar (cigar-shaped, 14x5 mm, PTFE surface) and placed on a

magnetic stirrer. Methanol was measured with an automatic pipette and added to formaldehyde. The beaker was then covered with a layer of parafilm and mixed intensively for approximately 5 min. As in case of methanol-water solutions, measurement was performed immediately afterwards in the same vessel due to relatively high volatility.

Resorcinol and water

Resorcinol was weighed on a scale in a 100 ml beaker, which was later equipped with a magnetic bar (cigar-shaped, PTFE surface) and placed on a magnetic stirrer. De-ionised water was measured with a measuring cylinder and poured into the beaker. The contents were moderately stirred for 5 min, until all resorcinol has dissolved. The contents were then transferred into a 25 ml poly(propylene) flask, labelled and sealed. The procedure was slightly different than in case of formaldehyde, methanol and water due to lower volatility of resorcinol-water composition.

Sodium carbonate and water

De-ionised water was measured with an automatic pipette into a 25 ml beaker, which was equipped with a magnetic bar (cigar-shaped, 14x5 mm, PTFE surface) and placed on a magnetic stirrer. Sodium carbonate was weighed on an analytical scale and added to the water in the beaker. Moderate stirring took place for 10 minutes and then the sample was transferred into a 25 ml poly(propylene) flask, labelled and sealed.

Resorcinol, sodium carbonate and water

Resorcinol was weighed on a scale in a 100 ml beaker, which was later equipped with a magnetic bar (cigar-shaped, PTFE surface) and placed on a magnetic stirrer. De-ionised water was measured with a measuring cylinder and poured into the beaker. The contents were moderately stirred for 5 min, until all resorcinol has dissolved. Then sodium carbonate was weighed on an analytical scale and added into the beaker. Stirring was continued for another 10 min, until all solids have dissolved. The contents were then transferred into a 25 ml poly(propylene) flask, labelled and sealed.

Resorcinol, formaldehyde and water

Resorcinol was weighed on a scale in a 100 ml beaker, which was later equipped with a magnetic bar (cigar-shaped, PTFE surface) and placed on a magnetic stirrer. De-ionised water was measured with a measuring cylinder and poured into the beaker. The contents were moderately stirred for 5 min, until all resorcinol has dissolved. Then formaldehyde solution was measured with an automatic pipette and added to the solution and stirring continued for another 30 min. The contents were then transferred into a 25 ml poly(propylene) flask, labelled and sealed.

Reacting systems

Prior to preparation of the reacting mixtures, the glassware was washed with de-ionized water to ensure that no impurities were present. Meanwhile, the oven was pre-heated to 90^{o}C; this temperature was kept constant.

The exact amount of de-ionized water was measured in a measuring cylinder and poured into a 100 ml beaker. Then resorcinol was weighed, transferred to the beaker, a magnetic bar was placed in the beaker as well, and the vessel was then placed on the magnetic stirrer. After all solid flakes of resorcinol have fully dissolved (5 min), sodium carbonate was weighed by an analytical scale and transferred to the beaker with dissolved resorcinol. After ensuring that all sodium carbonate has dissolved (10 min), the exact amount of formaldehyde solution was measured with an automatic pipette and added to the mixture inside the beaker. Stirring continued for 30 min from the moment formaldehyde solution was added. The solution was divided (using an automatic pipette) into samples of equal volume and poured into screw-topped poly(propylene) flasks (volume: 25 ml). Flasks were immediately sealed (screw-top was secured). Each sample contained on average 5-8 ml of the solution.

3.3.4. Measurements and cleaning procedures

Measurements parameters

For reasonable data quality consistence, all measurements were performed at room temperature (controlled with a classic mercury thermometer) with the same set of parameters: 16 scans, resolution 8 cm^{-1}, de-ionised water as a background. Collected data was saved as CSV file containing values of intensity and wavenumbers.

Non-reacting solutions measurement procedure

All measurements of reactants' solutions were performed as soon as possible after their preparation was completed. No heating treatment was performed

prior to measurements and all samples were at room temperature when analysed.

An ATR probe attached via fibreglass cables to the infrared spectrometer was immersed in the solution in each poly(propylene) flask, which was gently agitated during the measurement to minimize the effect of local concentration differences, should they be present. After approximately 30-45 seconds measurement was performed. Once completed, the vial with reactant solution was disposed of in an appropriate manner and the ATR probe was rinsed with de-ionised water and left to dry.

Reacting systems measurement procedure

In order to slow down or quench the polymerization process, each sample had to be cooled down before the measurement. After certain time has passed since the samples were placed in the oven, one of them was taken out and placed in the ice-bath: a 250 ml poly(propylene) beaker filled with water and ice. The sample was delicately agitated in the bath to accelerate the heat exchange process (cooling). When temperature was in range of 20-30^{o}C (measured using a classic glass mercury thermometer), the sample was removed from the ice-bath and taken for measurement. The vial was opened and the ATR probe was immersed in the sample. The flask was gently agitated before and during the measurement, to ensure that the possible differences in local concentration of reactants would not affect the results. After approximately 30-45 seconds measurement was taken. When measurement was completed, the probe was thoroughly rinsed with de-ionised water and left to dry.

3.4. Raman spectroscopy

3.4.1. Methodology

Raman spectroscopy is a non-destructive analysis method that uses non-elastic photon scattering, called the Raman Effect. It is complementary to IR spectroscopy as it is able to detect certain types of vibrations which do not yield a signal in the IR.

As it is discussed in the DLS section of this work, light can be scattered by molecules or particles in an elastic manner without changing their frequency or energy – this phenomenon is called the Rayleigh scattering and is the principle behind the construction and application of DLS. However, it can occur that some of the scattered photons do change their energy (or frequency) and this was first experimentally proved in 1928 by Chandrasekhar Raman, who was awarded a Nobel Prize in 1930 for his work in the field [111]. Only about 1 in 10^7 of the incident photons which collide with the molecules loses some of its energy and leaves the matter with altered – lower – frequency, giving rise to Stokes radiation. Incident photons may collect energy from excited molecules and leave the matter with higher energy level, thus higher frequency, forming anti-Stokes radiation. Those photons which do not change their energy, i.e. scatter elastically, form Rayleigh radiation which covers frequencies lying symmetrically between Stokes and anti-Stokes region (Figure 8). It is worth mentioning that the intensity of the Rayleigh band is roughly 10^3 times greater than Stokes and anti-Stokes bands' [111]. The width and number of signals in Stokes and anti-Stokes bands depend on the investigated molecule.

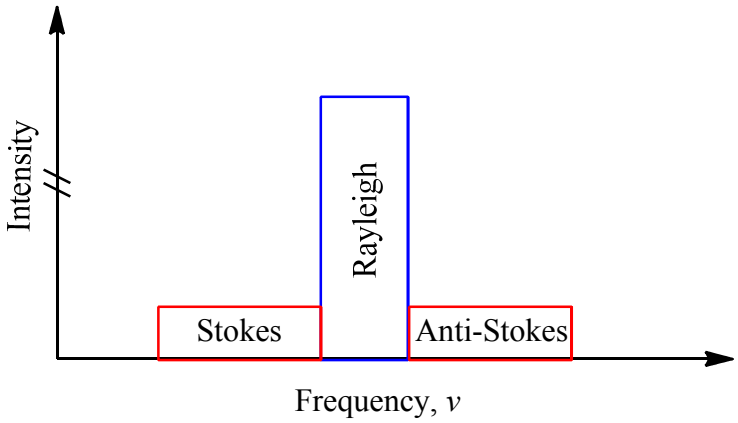

Figure 8. A diagram representing the relationship between Stokes, Anti-Stokes and Rayleigh radiation.

An important concept that needs to be discussed when dealing with Raman spectroscopy is polarizability of the molecules. All polar molecules have a permanent dipole moment, which depends on the difference of electronegativity of atoms constituting it and is expressed in Debye units. For example, a dipole moment of carbon monoxide (CO) is equal to 0.112 D. The addition of another oxygen atom makes the molecule symmetric (carbon dioxide, CO_2) causing it to have a zero dipole moment (therefore non-polar). Another type of dipole moment is an induced one: a non-polar molecule may attain a dipole moment if it is affected by an electric field generated by a nearby polar molecule or ion [62]. If a molecule can acquire an induced dipole moment it is said to be polarizable. The magnitude of the generated temporary dipole moment is proportional to the energy of the electric field inducing it and to a constant value, α – polarizability of the molecule. It is very important to remember that polarizability depends on a few factors, which include the amount of electrons in the molecule and also its orientation with respect to the field, unless the molecule is tetra-, octa- or icosahedral.

The two possible types of molecular movements which can be observed in Raman spectroscopy are rotational and vibrational. For a molecule to be visible in the rotational Raman spectra, it needs to have an anisotropic polarizability. This means, that this characteristic of the molecule has to be dependent on the orientation of the molecule with respect to the electric field inducing a dipole moment. As mentioned above, tetra-, octa- or icosahedral molecules and all spherical rotors have an isotropic polarizability and are rotationally Raman inactive. All other molecules, even homonuclear diatomic ones, like O_2 or H_2, are rotationally Raman active and can be seen in Raman spectroscopy. For molecules to be visible in vibrational Raman spectroscopy, the polarizability needs to change when the molecule vibrates. During vibrations, the molecules swell and contract, which leads to changes in of the control of nuclei over electrons, which means changes of polarizability [62] [111].

The most convenient source of a monochromatic electromagnetic wave in Raman spectroscopy are lasers, which emit waves of UV and visible light wavelengths (used in dispersive spectrometers) to infra-red range (Fourier Transform spectrometers). The light passes the sample and then is detected at a certain angle (typically 0°, 90° and 180°). The registered signal is plotted as a function of intensity against Raman shift (wavenumber, cm^{-1}) [112] and it consists of a very strong signal at shift equal to 0 cm^{-1}, which corresponds to the incident light (Rayleigh scattering), a strong band of Stokes radiation (at lower frequencies, thus higher Raman shift) and a very weak band of anti-Stokes radiation (lower Raman shift), as shown in Figure 9. In practice not all spectrum is registered but only the section of Stokes radiation which is of interest due to higher signal intensity.

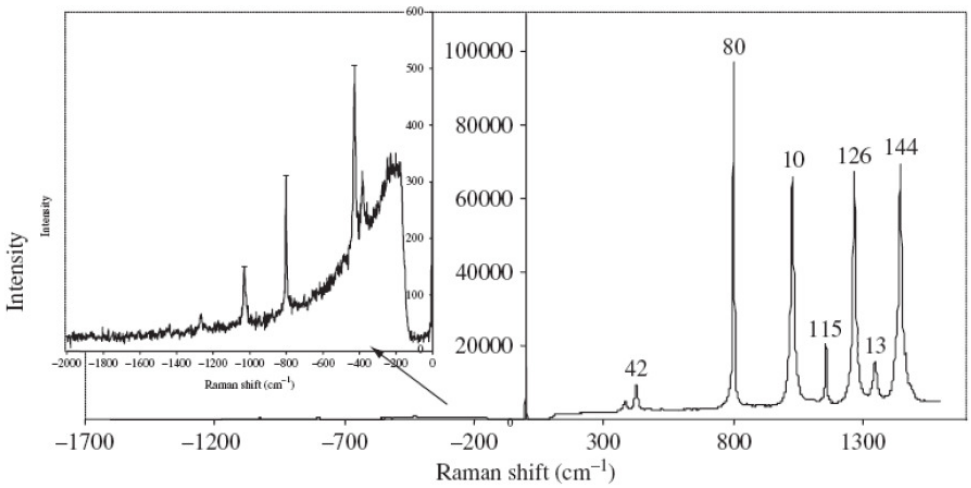

Figure 9. Stokes and anti-Stokes part of Raman spectrum of cyclohexane [112]. Stokes radiation bands are on the right hand side, anti-Stokes on the left hand side.

3.4.2. Equipment used

All spectra were collected using a Surface Enhanced Resonance Raman Spectroscopy (SERRS), which allowed a higher intensity of collected spectra even in small concentrations. Spectra were recorded using a Leica DM/LM microscope equipped with an Olympus 20x/0.4 long working distance objective, which was used to collect 180^0 backscattered light from macrosampler. The spectrometer system was Renishaw inVia equipped with helium-neon (He-Ne) laser emitting waves at λ=632.8 nm coupled to Renishaw Ramascope System 2000.

3.4.3. Sample preparation

Methanol and water

De-ionised water was measured with an automatic pipette into a 25 ml sealable glass vial, which was equipped with a magnetic bar (cigar-shaped, 14x5mm, PTFE surface) and placed on a magnetic stirrer. An appropriate volume of methanol was measured with an automatic pipette and added to the water. The vial was then sealed and mixed intensively for approximately 5 minutes. Then the vial was taken for the experiments.

Formaldehyde and water

De-ionised water was measured with an automatic pipette into a 25 ml sealable glass vial, which was equipped with a magnetic bar (cigar-shaped, 14x5mm, PTFE surface) and placed on a magnetic stirrer. Formaldehyde stock solution was measured with an automatic pipette and added to the water. The vial was then sealed with a cap and contents were mixed intensively for approximately 5 minutes and then taken for experiments.

Formaldehyde and methanol

An appropriate amount of formaldehyde stock solution was measured with an automatic pipette into a 25 ml sealable glass vial, which was equipped with a magnetic bar (cigar-shaped, 14x5mm, PTFE surface) and placed on a magnetic stirrer. Methanol was measured with an automatic pipette and added to formaldehyde. The vial was then sealed and mixed intensively for approximately 5 minutes and then taken for experiments.

3.4.4. Measurement procedure

Once a solution was prepared it was transferred using an automatic pipette into a poly(styrene) cuvette, sealed with parafilm and placed inside the sample holder of Raman spectroscope. Then spectra were collected, exported as CSV files and processed using Origin 8.1 software.

3.5. Dynamic Light Scattering

3.5.1. Methodology

The phenomenon of light scattering has been studied by mankind for centuries [113]. An early fundamental theory, explaining one of nature's most picturesque phenomenon, came from Lord Rayleigh (John William Strutt, 3rd Baron Rayleigh) in early 20th century. Basing on his observations and experiments, he concluded that the light (or any other electromagnetic radiation) is being scattered by particles much smaller than the wavelength of the light, like atoms or chemical compounds causing the colour of the sky to change. One of the most important points in his theory is the fact that this elastic scattering (named after Lord Rayleigh) is inversely proportional to the fourth power of the light's wavelength. This means that longer wavelengths (yellow, red) scatter less, while short scatter more (blue, violet). By this, Lord Rayleigh explained the phenomenon of colour of the sky: when the sun is up, the further from the sun, the more light is scattered and since blue and violet are colours which scatter the most, these are predominant. The closer you look towards the sun, the more yellow and red hue you may observe – the colour which was not scattered away. The change in the colour of the sky near the horizon during the sunset or sunrise is caused by the increased distance (amount of air) that the light must travel. It is significantly larger,

therefore the amount of Rayleigh scattering is also increased – most of the blue and violet lights are removed by scattering and the observer sees mostly orange and red colours. Rayleigh scattering is in many aspects similar to the mechanism described in the 19th century by John Tyndall, on whose work he most certainly must have based. This British physicist discovered and described a phenomenon in which light passing through a colloidal suspension with particles of diameter ranging between ca. 40 and 900 nm undergoes scattering. Knowing that light is a combination of electromagnetic radiation with different wavelengths and thus colours, Tyndall concluded that most of the longer wavelength light is transmitted, while most of the shorter wavelength light is reflected (scattered back) from the suspended particles. The Tyndall effect (as it is called) has found commercial applications and has been used for a long time now. The most significant practical application is related to determination of air quality (via turbidimeter).

Both Rayleigh's postulates and Maxwell's theory on electromagnetism opened doors to a new spectrum of research techniques: the light scattering investigation methods, which rely on observation and interpretation of the intensity of light scattered by objects in solutions and colloidal suspensions. Appropriate collection, processing of the data and then interpretation of results, provides extensive information on particles' sizes and their distribution in a given (colloidal) sample. Information on sizes of particles suspended in a solution can be key in a number of situations, including assessment of production processes (slight diameter changes, subject to processing parameters) and determination of mechanisms of gel or crystalline structure formation. These methods were greatly improved since

a source of coherent and monochromatic light – laser – was discovered and implemented.

The mechanism used in light scattering methods is fairly straightforward and can be understood as a simple mechanism of adsorption and re-emission of electromagnetic radiation, i.e. light. A beam of monochromatic and coherent light, i.e. a laser beam, is directed at a sample of colloidal dispersion. Some of the light, passing through the sample, is being scattered by suspended particles in all directions, while most of it (depending on the contents of the suspended matter) passes through unaffected. Depending on the size of particles, the intensity of the scattered light in all directions may be uniform – this is the case of Rayleigh scattering, which occurs when the sizes of particles are much smaller when compared with the wavelength of the incident light. In case of much larger particles – with diameters larger than ca. 250 nm – the intensity of scattered light is not uniform and it is angle dependent. It is very important to underline the fact, that the particle sizes and their distribution can be obtained from the collected data through numerical fitting under assumption that the particles present in the colloidal suspension are subject to Brownian motions only and that their movement in the solution is not affected by any other factors.

The most significant methods worth mentioning are Static Light Scattering and Dynamic Light Scattering techniques. Both are used to measure dimensions of particles and other objects suspended in solutions, however, there are some important differences between them.

Dynamic Light Scattering (DLS), also known as Quasi Elastic Light Scattering (QELS) ad Photon Correlation Spectroscopy (PCS), is an experimental

method which allows to determine the mean hydrodynamic radius of particles in a sub-micron range. In contrast to the Static Light Scattering, this method registers fluctuations of the intensity of scattered light at a given angle over time. These fluctuations, registered by an appropriate detector are caused by the fact that light scattering particles in the investigated colloidal suspension are small enough to be subject to random thermal motions, called the Brownian motions. As all particles move around in an unorganized manner (randomly), the distances between them change constantly. Scattered light, being an electromagnetic wave undergoes both constructive and destructive interferences, therefore as the positions of the particles change, the overall intensity registered at a certain point of the detector plane, will change. Depending on the size of the particle, it may scatter more or less light at a given angle, contributing proportionally to the registered light pattern. With the detector set at a given angle, intensity is registered and then it is analysed by a digital correlator. This device determines the intensity autocorrelation function, which can be simply described as an average of the signal with a delayed version of itself as a function of delay time, which is the delay between registering of each reading of the detector's plane. Should the colloidal suspension be perfectly monodisperse, this function plotted against delay time would form a single exponential decay. If a solution is polydisperse, which is very often the case, the function forms a series of exponential decays – each of them corresponding to a group of particles with the same or very similar hydrodynamic radius. Fitting these decays with simple linear, quadratic or cubic functions, allows to determine the hydrodynamic radius basing on the assumption that the Stokes-Einstein's equation holds true, which is the case for suspensions in which Brownian motions are dominant. Should there be another motion restraining force (e.g.

interactions between chains forming a gel network or very large or charged particles), the autocorrelation function ceases to be an exponential one and begins to resemble a power law, at which point data fitting in order to obtain particle sizes is void, as Stokes-Einstein equation is not fulfilled.

Static Light Scattering (SLS) is a method similar to DLS in the sense that the sample is also illuminated by a laser light and particles in the colloidal suspension also scatter the light in all directions. The main difference is that SLS measures intensity of scattered light averaged over time and not time-dependent fluctuations of scattered light intensity. This method, unlike DLS, is not used to measure the sizes (hydrodynamic radii) of particles but their averaged molecular weight, radius of gyration and second virial coefficient. This is possible since the scattered light is proportional to molecular weight and the concentration of that molecule in the solution. In order to measure and calculate all these values, a series of experiments where intensity of scattered light is accumulated over a given period of time (tens of seconds) for a number of samples with different concentrations, must be performed. Moreover, in order to obtain credible and accurate results for large molecules, one must carry out measurements at a range of angles. In terms of investigating particle growth and aggregation kinetics, this method seems to be less practical than DLS for a number of reasons. Most of all, the main aim of this research is to establish the mechanism of gel formation during the reaction, growth of primary particles and its dependency on catalyst and concentration, as well as temperature. Determination of hydrodynamic radii yields more information about the mechanism, as it is also an indication of mobility of the particles, while averaged molecular weight would not provide this information. Moreover, DLS can provide information about polydispersity of the particle sizes in the sample, rather than provide with

averaged values (it is subject to proper data analysis). Additionally, in order to obtain accurate results, a number of concentration-dependent repetitions should be made, which is assumed to change the kinetics of the reaction, making the possible results subject to another factor. The final argument against using SLS is that the time which is required to accumulate data for a single sample is considerably longer than in DLS. If, for example, in SLS let us assume measurements over 30 s (usually it is between 10 s and 30 s in order to minimize the fluctuations) for angles between 30^{o} and 150^{o} at a 10^{o} increment. A single experiment would take 390 s (6.5 min) and it would be reasonable to take three measurements, which means that in order to obtain good quality data an experiment that lasts almost 20 min is required. In situation where relatively rapid kinetics need to be investigated, this may turn out to be too long.

A proper analysis of the data collected in course of DLS experiments is key to reliable and valuable results. In order to do this, it is necessary to understand the process of light scattering inside the DLS equipment and every step of processing the data.

When the sample is inserted into the DLS holder, it is immersed in a thermostated toluene bath and once the holder is closed, the laser beam illuminates the sample. The incident laser light beam can be described by a wave vector $\vec{k}_i$ (Figure 10) of magnitude defined as $k_i = \frac{2\pi n}{\lambda_0}$, where λ_0 is the wavelength in vacuum and n is a medium refractive index. This can be simplified to $k_i = \frac{\omega_0 n}{c}$, where ω_0 is circular frequency of the incident wave in vacuum and c is the speed of light in vacuum.

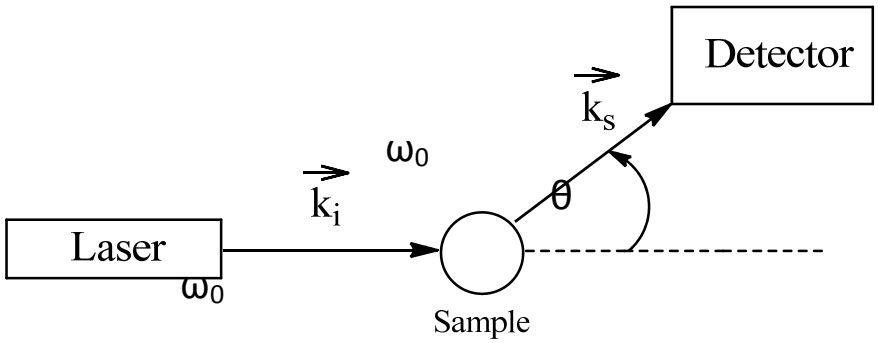

Figure 10. Simplified light scattering scheme

The light is elastically scattered by colloidal particles and other objects present in the sample. The angle between the direction of the scattered and incident light vectors is called θ and the wave vector of the scattered light at this angle is $\vec{k}_s$. It is safe to assume that the magnitude of the incident and scattered wave vectors are practically the same, as changes in frequency are very low in most DLS experiments and do not typically exceed 10^6 Hz, while optical frequencies are considerably greater – 10^{14}-10^{15} Hz [113].

In order to describe and quantify the scattering of incident light, a scattering vector defined as $\vec{q} = \overrightarrow{k_\iota} - \overrightarrow{k_s}$ is introduced. The magnitude of this vector, under a valid assumption that magnitudes of wave vectors of incident and scattered beam are equal, is described by the following equation:

$$\boldsymbol{q = \frac{4\pi n}{\lambda} sin\left(\theta/_2\right)} \tag{14}$$

where n is the refractive index, λ is the wavelength of the light and θ is the scattering angle, at which the detector is positioned in respect to the sample.

The scattered light is being detected by a very sensitive device, usually a photomultiplier tube which is sensitive to electromagnetic radiation and can respond to ultraviolet, visible and near-infrared light. The mechanism of

detection can be described in a simplified manner as multiplying the current produced by the incident light by a factor of even tens to hundreds of million times in multiple dynode stages, allowing to register light of even single photons. Due to very low noise, high detection area (which can be tailored to the exact needs), high gain and high frequency response, these devices have found many applications – from nuclear and particle physics to medical diagnostics and imaging.

The detected signal of the scattered light is virtually a function of only two variables: time (t) and scattering angle (θ). If the measurements are performed in a time-averaged manner (Static Light Scattering - SLS) over long time periods, the observed intensity is a function of scattering angle and can be described as:

$$I(\theta) = \lim_{T\to\infty} \frac{1}{T} \int_0^T I(\theta, t)\, dt \qquad (15)$$

This type of experiments, as mentioned before, provides information about static properties of the investigated particles, like their average molecular weight or radius of gyration.

Experiments performed at a given scattering angle (or a set of these) where time fluctuations of I(θ,t) are registered are called Dynamic Light Scattering (DLS) experiments and they provide information on dynamic properties of the investigated sample, namely the particle diffusion coefficient, from which – under certain assumptions – an average hydrodynamic radius can be calculated.

If all particles in the investigated sample were immobile, bearing in mind that the circular frequency (ω_0) of the laser light is constant, the circular

frequency of the elastically scattered light would be exactly the same as of the incident light. In this case, if a registered spectrum would be a function of circular frequency (ω), the result would be a single line or point at ω_0 (Figure 11). However, it is known that colloidal particles and other particles of sub-micron dimensions are subject to random thermal motions, called the Brownian motions. These were observed and described in late 19th century by Robert Brown, who was a British biologist, and then explained independently by two physicists: Albert Einstein (in 1905) and Marian Smoluchowski (1906). They explained the phenomenon of moving dust and specks in water by the fact that these objects are being constantly bombarded with small but very intensively moving water particles. Despite the fact that an approximate size of a water molecule is only 1.6 Å and the size of a speck (as an example) can be anything from a few to a few hundred of microns, a speck will move in water as is it surrounded by a very large number of randomly moving water molecules. Albert Einstein assumed this model to be true, while Marian Smoluchowski thought that the movement is not caused by the speck colliding with water molecules but by fluctuations of water density caused by their random movement [114]. Bearing in mind, that particles scattering the light are in constant, random and temperature-dependent motion, the frequency of the light they scatter will seem slightly different to an immobile observer. This is called the Doppler's effect and is a phenomenon in which there is a difference in frequency of the wave emitted by a moving object and received by a fixed observer. If a wave needs a medium to propagate (e.g. sound), the magnitude of the frequency shift depends on the speed of the source and the observer in relation to the medium in which these waves travel. In case of light or any other electromagnetic waves, which do not need any medium and can propagate

also in vacuum, the magnitude of this effect depends only on the difference between speeds of the source and the observer. Therefore, if we assume that the Brownian motions are dominant in the sample and the light is being scattered by moving particles, the circular frequency of the light incident and scattered is different and can be written as $\omega = \omega_0 + \Delta\omega$, where the $\Delta\omega$ is a frequency shift resulting from the Doppler's effect. The change of the frequency in this case depends only on the motion characteristics of the scattering particle: the scattering vector ($\vec{q}$) and its velocity ($\overrightarrow{v}$), what is represented by $\Delta\omega = \vec{q} \cdot \vec{v}$. In terms of the spectrum registered, should all particles move in the exact same manner, the $\Delta\omega$ would be constant and the registered spectrum would contain only a signal at $\omega_0+\Delta\omega$ (Figure 11). However, this situation is not possible in practical applications of DLS. In fact, all particles move in a chaotic manner – with different speeds and directions, which change randomly due to the fact that the particles collide and are interacting with small water molecules. Moreover, this is also dependent on the sizes of the particles: larger particles move slower as they are more inert, while smaller move faster. Therefore, the frequencies of the scattered light are not uniform and the theoretical registered spectrum of frequencies would resemble a typical bell-shaped curve or a Gaussian distribution curve (Figure 11).

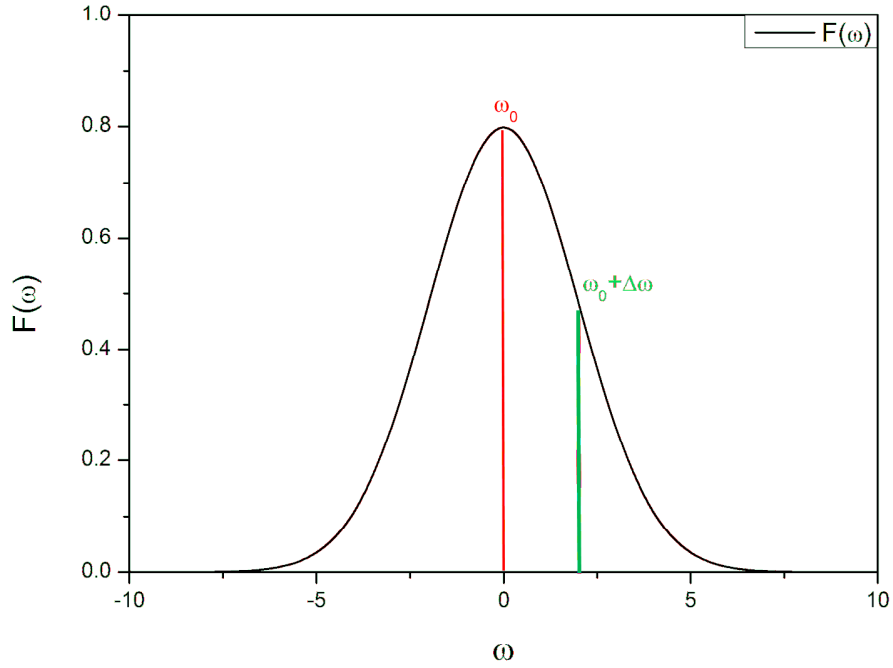

Figure 11. An example of theoretical spectrum resulting from DLS experiments.

The Brownian motion displacements can be quantified by means of the diffusion coefficient (D), however, this type of quantification can lead to only averaged results (i.e. if the dispersion is polydisperse, only an average hydrodynamic diameter can be obtained). It can be proved that the diffusion coefficient is related to the half of the width at the half of the height ($\Delta\omega_{1/2}$) of the bell curve: $\Delta\omega_{1/2} = Dq^2$, where q is the magnitude of the scattering vector [113].

Recording of spectra shown as an example above proved to be very troublesome and only spectra of high quality yield reliable results. The main obstacle in obtaining these is the fact that the scattered light needs to be filtered away at a given angle. This can be done by means of special filters

which would pass through waves at a given frequency ω+δω (x-axis), where δω is a bandwidth of the filter. In order to collect data with high ω accuracy, the δω needs to be as small as possible, which would mean that the collected signal is very weak and noisy (y-axis). Unfortunately, aiming at high accuracy of the recorded signal (high signal to noise ratio; y-axis) means collecting information from a broader ω+δω (x-axis) region.

Nonetheless, these problems were overcome due to the fact that theory says that information on dynamic properties of the particles scattering the light can be obtained also from the Fourier transform of the spectrum. In practice, the registered signal is sent from the detector to a digital autocorrelator which transforms the received signal into an intensity autocorrelation function $G_2(\tau)$:

$$G_2(\tau) = \langle I(t) \cdot I(t+\tau) \rangle \tag{16}$$

This is an autocorrelation function of the intensity of scattered light I(t) and it is an average value of the intensity registered at an observation time t, I(t), and the intensity registered after a time delay τ, i.e. I(t+τ), which can be written as:

$$g_2(\tau) = \frac{G_2(\tau)}{A} \text{ where } A = \langle I(t)^2 \rangle, \text{ so } G_2(\tau) = A \cdot [1 + g_1(\tau)^2] \tag{17}$$

Due to the way in which normalized autocorrelation function $g_2(\tau)$ is calculated, it can decay to 1 (when $G_2(\tau) = \langle I(t)^2 \rangle$). Therefore another autocorrelation function, decaying to zero – $g_1(\tau)$ – is created:

$$g_1(\tau) = \sqrt{g_2(\tau) - 1} \tag{18}$$

This autocorrelation function is recorded during the experimental procedure and it can be used to calculate distribution of hydrodynamic radii of particles present in the dispersion.

Should the sample be monodisperse, autocorrelation function $g_1(\tau)$ would decay exponentially because the Brownian motions are dominant. The autocorrelation function could be then written as $g_1(\tau) = B \cdot e^{-\Gamma\tau}$. The rate of decay, Γ, is proportional to product of D and q^2; B is the intercept at $g_1(0)$, D is the diffusion coefficient of the particles and q is the scattering vector (described earlier). Providing that Brownian motions are the only motions of the particles suspended in the investigated solution, Stokes-Einstein equation relating diffusion coefficient (D) to hydrodynamic radius (r_h) holds true:

$$D = \frac{k_B T}{6\pi\eta r_h} \tag{19}$$

where k_B is the Boltzmann constant ($1.3806503 \times 10^{-23}$ m^2 kg s^{-2} K^{-1}), T is the temperature (K) and η is the dynamic viscosity of the dispersing fluid at a given temperature T (Pa·s). If this is the case for a given dispersion, the shape of autocorrelation function $g_1(\tau)$ looks as shown in Figure 12-A.

In situations in which particles in the dispersion are either way too large to follow Brownian motions exclusively or if they interact with each other, causing additional restrictions to their movement, the autocorrelation function $g_1(\tau)$ fails to follow the exponential trend. Instead it may resemble shapes of power law functions, as shown in Figure 12-B**.** In this situation quantitative analysis of data obtained in the experimental procedure is not appropriate, as Stokes-Einstein equation cannot be implemented due to its limitations.

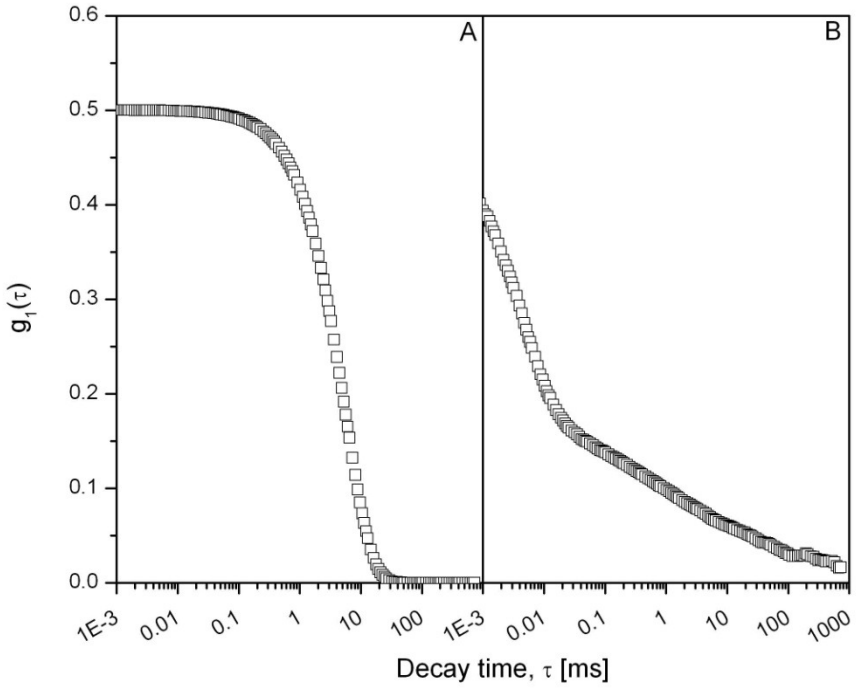

Figure 12. Autocorrelation function decay: (A) an exponential decay for a monodisperse solution, (B) a non-exponential decay for a gelling solution.

Quantitative data can be obtained by a number of mathematical fitting methods, among which the most commonly used are contin and cumulant methods [113]. For the purpose of this research, the cumulant method was chosen. In this procedure, the initial decay (after removing the first 3-5 datapoints) of the autocorrelation function $g_1(\tau)$ is fitted by polynomial functions of up to the third order and the best fit is then selected for further quantitative analysis. For monodisperse solutions in which the Stokes-Einstein equation holds true, it was shown previously that $g_1(\tau) = B \cdot e^{-\Gamma\tau}$, therefore the function $ln(g_1(\tau))$ plotted against τ forms a straight line described by $f(x) = ax + b$, where slope $a = -\Gamma$ [s^{-1}] and $x = \tau$ [s]. Using these equations one can calculate hydrodynamic radius, knowing that $\Gamma = D \cdot q^2$ and $D = \frac{k_B T}{6\pi\eta r_h}$, therefore $r_h = \frac{k_B T q^2}{6\pi\eta\Gamma}$.

As mentioned earlier, once the autocorrelation function ceases to be exponentially decaying in the course of reaction, the function $ln(g_1(\tau))$ is no longer linear when plotted against τ and the slope coefficient should not be used to calculate the hydrodynamic radius. Examples of both ideally fitted $ln(g_1(\tau))$ and a fit for a dispersion in which Stokes-Einstein equation is not valid, are shown in Figure 13.

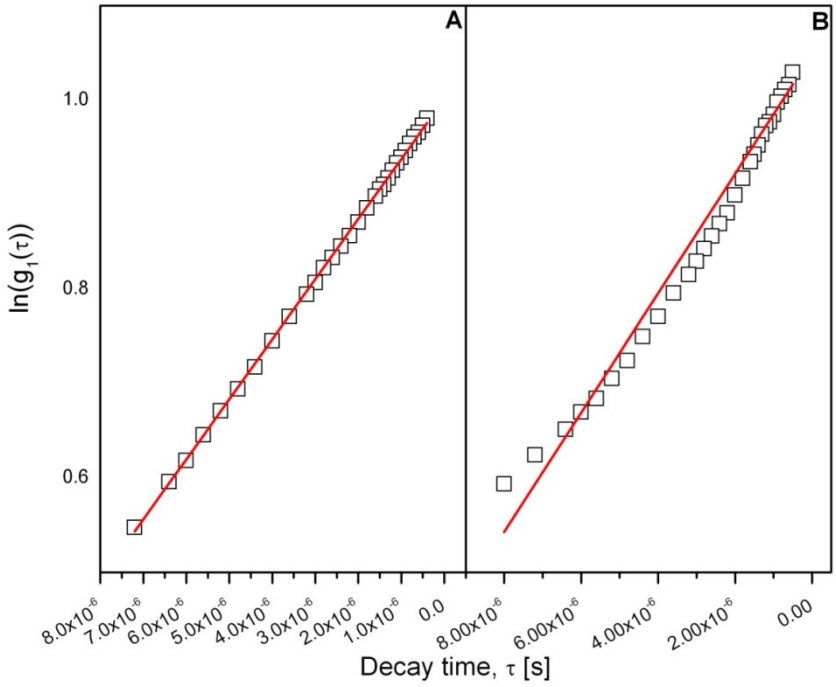

Figure 13. Example of fitting autocorrelation function for (A) a monodisperse solution with free Brownian motions, (B) a gelling sample.

3.5.2. Equipment and sample preparation

Equipment used

In Dynamic Light Scattering experiments autocorrelation functions $g_1(\tau)$ were measured using a digital correlator (ALV/LSE-5004 Light Scattering

Electronics and Multiple Tau Digital Correlator manufactured by ALV-GmbH). The wavelength λ of incident laser light was 632.8 nm and the scattering angle θ was set to 90°. The initial decay of the autocorrelation function was fitted using the cumulants method and the corresponding intensity averaged mean diffusion coefficient was estimated. From this, the mean hydrodynamic radius was calculated using the Stokes-Einstein equation, as described previously.

Filtration

Filtration of the samples was performed in order to minimize the risk of impurities affecting the results from measurements. These could originate from many sources, including large clusters of undissolved solids or even dust in the laboratory. All solid chemicals used were of high quality (all >99%wt.), so that the amount of by-products from their manufacture process, which may be insoluble, was minimal. Elimination of the dust from the working environment proved to be virtually impossible; however, dust which was in the glassware was washed away with filtered de-ionised water. Additionally, the glass vials used for measurements were also rinsed with filtered solution that was about to be investigated in them (in order to minimise dilution of the sample with de-ionised water). DLS is also sensitive to the quality of the glass used for experiments. The most important factors are the thickness of the vials' walls (the best is uniform) and possible defects of the surface. Therefore, any glass vial that was used in the DLS was checked for scratches and other defects. All that did not seem appropriate were discarded of and not used in the research.

Since DLS can detect particles of sub-micron diameter range, filtration had to be performed with filters guaranteeing elimination of such objects. Therefore filtration was conducted manually for each sample using poly(propylene) and rubber-free syringes and syringe filters with sub-micron openings in the membrane. For this purpose disposable Anotop™ filters with 0.45 μm and 0.02 μm membrane openings were purchased from Whatman®. These had poly(propylene) housing, inorganic (0.02 μm) or PTFE (0.45 μm) membranes and could work in pH range of 3.5-9.5 and in temperatures between 4 and 40°C.

Depending on the sample and experiment type, filtration could take place before or after mixing reagents. This is indicated in the sample preparation section below.

Sample preparation

Non-reacting samples

Resorcinol in water

Appropriate amount of resorcinol was weighed in a scale, transferred into a glass beaker. The de-ionised water was added (automatic pipette), magnetic bar inserted into the beaker and the vessel was placed on a magnetic stirrer. The contents of the beaker were stirred moderately for 10 min and then a sample was drawn with a poly(propylene) and rubber-free syringe. A 0.02 μm filter was placed at the outlet of the syringe for manual filtering. A scratch-free glass vial was rinsed with filtered de-ionised water and then rinsed again with ca. 1 ml of filtered resorcinol and water solution. After that ca. 2 ml of solution were filtered into the glass vial, sealed and rinsed on the

outside with ethanol or acetone to remove any marks and traces from handling the sample and inspected visually for any observable defects. Sample prepared in this way was placed in the DLS sample holder and experiment was performed.

Resorcinol and sodium carbonate in water

A given amount of resorcinol was weighed on a scale, transferred into a glass beaker and an appropriate amount of de-ionised water was added (automatic pipette). The beaker was then placed on a magnetic stirrer and moderate stirring was allowed for 10 min. Then an appropriate amount of sodium carbonate was weighed on an analytical scale, added into the solution and stirring continued for another 5 min. After this time sample was drawn with a poly(propylene) and rubber-free syringe. A 0.02 μm filter was placed at the outlet of the syringe for manual filtering. The glass vial for DLS measurement was rinsed with filtered de-ionised water and then rinsed again with ca. 1 ml of filtered resorcinol and sodium carbonate solution. Then ca. 2 ml of sample was filtered directly into the vial, sealed and rinsed on the outside with ethanol or acetone. After visually ensuring that no marks on the outside of the vial are present, the sample was placed in the DLS sample holder and experiment was run.

Formaldehyde

Appropriate amount of formaldehyde stock solution was transferred into a clean and dry glass vial with wide neck to facilitate handling. Then a sample was drawn from the vial with a poly(propylene) and rubber-free syringe, and a 0.02 μm filter was placed at the outlet of the syringe for manual filtering. As previously, a glass vial for DLS measurements was rinsed with

filtered de-ionised water and then rinsed again with ca. 1 ml of filtered formaldehyde stock solution. Following that ca. 2 ml of formaldehyde stock solution was filtered directly into the vial, sealed and rinsed on the outside with ethanol or acetone. Only after visual check for any marks on the outside of the vial, the sample was placed in the DLS sample holder and experiment was run.

Formaldehyde and water

An appropriate volume of formaldehyde stock solution was transferred from the stock bottle to a glass beaker by an automatic pipette and then an appropriate amount of de-ionised water (or water and deuterium dioxide in 7:3 volumetric ratio) was added (also by an automatic pipette). A magnetic bar was placed inside the beaker, the vessel placed on a magnetic stirrer and sealed from the top with parafilm to minimise evaporation of methanol from formaldehyde stock solution. Stirring was set to moderate and allowed for 10 min. Then a sample was drawn by a poly(propylene) and non-rubber syringe and a 0.02 μm filter was placed at the outlet of the syringe for manual filtering. A glass vial for DLS measurement was rinsed with filtered de-ionised water and then rinsed again with ca. 1 ml of filtered formaldehyde and water solution before the sample was filtered directly into the vial. Once that took place, the vial was sealed and rinsed on the outside with ethanol or acetone to remove any marks from handling the glassware. Once it was ensured that the vial does not have any visible defects on the surface, it was placed in the DLS sample holder and experiment was conducted.

Formaldehyde and sodium carbonate in water

Sodium carbonate was weighed on an analytical scale, transferred into a glass beaker and de-ionised water (or water and deuterium dioxide in 7:3 volumetric ratio) was added (by an automatic pipette). A magnetic bar was placed inside the beaker and the vessel was moved onto a magnetic stirrer. The contents were stirred moderately for 5 min, until all of sodium carbonate was dissolved. Then the solution was drawn by a poly(propylene) and non-rubber syringe and a 0.02 μm filter was placed at the outlet of the syringe for manual filtering. The solution was filtered into a clean (dust-free), dry glass vial and sealed. Formaldehyde stock solution was filtered (poly(propylene) and non-rubber syringe, a 0.02 μm filter) into a separate clean (dust-free), dry glass vial and sealed. Appropriate volumes of both filtered liquid solutions were mixed together in another clean and dry vial for 15 min. A DLS vial was rinsed with de-ionised water and then rinsed with ca. 1 ml of solution prepared from the filtered samples, and then a sample of ca. 2 ml formaldehyde and sodium carbonate in water solution was transferred into the vial. As usual, the glass was rinsed on the outside with ethanol or acetone and checked for any defects before placing it in the sample holder of the DLS and running the experiment.

Reacting solutions

The required amount of de-ionized water (W) was measured in a measuring cylinder and poured into a glass beaker. Resorcinol (R) was weighed, transferred to the beaker and stirred using a magnetic stirrer for 5 min until resorcinol had fully dissolved. Sodium carbonate (C) was weighed and transferred to the beaker with dissolved resorcinol. After 10 min of further

stirring to dissolve sodium carbonate, the required amount of formaldehyde solution (F) was measured in a measuring cylinder and added to the mixture and stirring continued for another 30 min.

In all DLS experiments, before starting thermal treatment, solutions were filtered in two steps: first using 0.45 μm pore size syringe filter and then 0.02 μm pore size syringe filter. Solutions were filtered directly into clean vials pre-washed with de-ionized water and filtered resorcinol-formaldehyde solution. Vials were then sealed with a cap and parafilm, placed in the measurement cell where they were thermostated at 55°C and measurements were taken at certain time intervals. DLS experiments with solutions reacting at 80°C were conducted in an alternative manner, since in-situ measurements were not possible at that temperature. After filtration solutions were divided into few parallel samples which were placed in an electric oven pre-heated to 80°C. The vials were then taken out from the oven at certain time intervals, one at a time, rapidly cooled down to ambient temperature using an ice bath in order to quench the reaction and taken for DLS measurements performed at 25°C. In all these experiments, careful filtration preceded the thermal treatment of reacting mixtures.

3.6. Nuclear Magnetic Resonance

3.6.1. Methodology

The basic principle of NMR spectroscopy is fairly simple, even though the details of physics behind it are fairly advanced and their detailed treatment is outside of the scope of this work. However, there is a number of publications which provide useful sources for understanding of physical background of nuclear magnetic resonance [104] [115] [116].

Basic description of nuclei quantum properties

Nuclear Magnetic Resonance is a spectroscopy that relies on the fact that all nuclei have spins – a term that is described by the quantum physics as angular momentum. For each nucleus, the magnitude of spin is quantized in certain units (ħ, which is Planck's constant divided by 2π) and is equal to $\sqrt{[I(I+1)]} \cdot \hbar$. The spin quantum number (I) can be equal to a certain, set value: 0, 1/2, 1, 3/2, 2 etc. The value of this number depends on the number of unpaired protons and neutrons; however, this method of prediction can fail when it is hard to guess the number of unpaired protons and neutrons. The same nuclear spin quantum number can be assigned to a number of different nuclei, for example, I=1 is assigned to both ^{2}H and ^{14}N, while ^{12}C and ^{16}O have I=0 [115]. If the magnitude of spin is equal to zero, which can happen when I=0, the nucleus does not have angular momentum which means no magnetic momentum, and thus no NMR spectrum. In this research, two NMR techniques were used: ^{13}C and ^{1}H. Nuclei of these two types have I=1/2 and therefore they do have NMR spectra.

Since spin angular momentum is a vector, one may quantify its direction and its magnitude. The angular momentum, $\boldsymbol{I}$, has 2I+1 possible projections onto a chosen z-axis. This means that when quantifying $\boldsymbol{I}$, its component on the z-axis, I_z, can be quantized: $I_z = m \cdot \hbar$, where m is the magnetic quantum number which has 2I+1 values in integral steps between +I and –I: $m = I, I-1, I-2, \ldots, -I+1, -I$ [115]. In case of ^{1}H and ^{13}C nuclei, which have I=1/2, there are only two permitted directions of the spin along the z-axis: $I_z = \pm\frac{1}{2}\hbar$.

Spin angular momentum is closely related to the magnetic moment of the nucleus, which makes it visible in the NMR spectroscopy. The magnetic moment - $\boldsymbol{\mu}$ - is a vector directly proportional to angular momentum $\boldsymbol{I}$: $\boldsymbol{\mu} = \gamma \boldsymbol{I}$, where γ is a constant describing ratio of magnetic dipole moment to angular momentum of a nucleus (gyromagnetic ratio) [115].

Nuclei in a magnetic field orientation, equilibrium and relaxation

Placing a nucleus in a magnetic field influences the orientations of spins. If there is no magnetic field applied, all spin orientations have the same energy. If a magnetic field described by a vector **B** is applied, the energy (E) of a magnetic moment ($\boldsymbol{\mu}$) is proportional to the negative product of the two vectors: $E = -\boldsymbol{\mu} \cdot \boldsymbol{B}$. Should the applied field be very strong, like it is in case of NMR spectroscopy, the chosen z-axis coincides with the field direction and can no longer be chosen freely, therefore: $E = -\mu_z \cdot B$. It is known that $\mu_z = \gamma I_z$ and $I_z = m \cdot \hbar$, therefore the energy of the nucleus in a strong magnetic field of magnitude equal to B can be expressed as: $E = -m\hbar\gamma B$ [115]. The selection rule is $\Delta m = \pm 1$, which means that the energy state of a nucleus can be changed by one level at a time. Therefore the two allowed energy levels are separated by a gap equal to $\hbar\gamma$B [115]. It is known that the resonance condition is $\Delta E = h\nu$ [104] [115], therefore $\Delta E = h\nu = \hbar\gamma B$, which can be transformed into $\nu = \frac{\gamma B}{2\pi}$. This equation allows prediction of the frequency of the electromagnetic radiation resulting from change of spin orientation and thus energy level.

Once a number of nuclei is placed in a strong magnetic field, their spins will spread among the permitted energy levels (strictly related to the spin orientation, as explained above) according to the rules of Boltzmann's

distribution. Therefore, if there are two available energy levels for a nucleus, the ratio of population at a higher level to the lower level is proportional to $e^{-\Delta E/k_B T}$, where ΔE is the energy gap (ħγB) and k_B is the Boltzmann's constant ($1.3806505(24)\cdot10^{-23}$ J·K^{-1}). Before placing the sample in the magnetic field, the strongly dominating spin population is the one of the lower energy. The process of reaching thermodynamic equilibrium distribution is not instantaneous and requires certain amount of time. Should the spin population be disturbed (like it is during an NMR experiment), the re-distribution of the spin populations to the equilibrium state will also require certain amount of time.

There is a number of complex mechanisms which take place when an excited nucleus returns to its original state. The two mechanisms which are significant from the practical point of view are the spin-lattice and spin-spin relaxation mechanisms. Term *relaxation* is used to describe a nonradiative return to the equilibrium state, i.e. no energy is emitted [62].

The spin-lattice relaxation is a mechanism which involves reinstatement of the spins distribution at thermal equilibrium by exchanging the excess energy with the surroundings, hence the name. The time-constant used to describe quantitatively this exponential process is T_1. It is also called the longitudinal relaxation, as it corresponds to the recovery of the z-component of the nuclear spin magnetization vector towards its equilibrium state. The T_1 value depends on a number of factors including **B**, therefore it is good practice to measure it before proceeding with quantitative analysis of collected data. Allowing not enough delay time for nuclei to reinstate the equilibrium state during the experiment leads to cut-off FIDs, which after

Fourier transformation results in peaks of too low intensity in the analysed spectrum.

The spin-spin relaxation mechanism is also called the transverse relaxation, as it corresponds to the recovery of the x,y-component of the magnetization vector (perpendicular to the magnetic field of the spectroscope) to the equilibrium state, which is equal to zero. It is a far more complex process than spin-lattice relaxation but fundamentally it corresponds to loss of coherence between transverse components of spin magnetization vectors. The spins are at truly thermal equilibrium only when the spin state populations are distributed as mentioned before and when the spin orientations are all at random angles round the direction of the applied field. This type of relaxation is also exponential and is described quantitatively using a time-constant T_2. Unlike T_1 it is less dependent on **B** and is in most cases significantly shorter.

Spectrometer construction and experimental principles

Magnetic fields used in NMR spectroscopy are very strong (between 1 and 20 T; at the moment of writing, the strongest NMR spectrometer is located in National High Magnetic Field Laboratory, Florida, and has a field of 21.1 T and frequency of 900 MHz) and in order to generate them, the spectrometer needs to be equipped in a superconducting magnet. This type of magnet is made of a set of coils of superconducting wire which needs to be cooled below its critical temperature in order to operate; hence liquid helium (4K) and liquid nitrogen (196 K) are used as coolants. Moreover, the field needs to be homogenous and stable, which is provided by superconducting coils arranged in an appropriately constructed solenoid.

In order to ensure stability of the magnetic field, a field-frequency lock is used. The applied field strength is controlled through NMR frequency of a specific nucleus. Usually a ^{2}H (D, deuterium) is used in form of a deuterated solvent or reference compound. During the measurement, this frequency is picked by the controlling panel and should any variation in this signal occur due to instability (drift) of the magnetic field, additional coils in the solenoid of the magnet are used to compensate for this drift [115].

When NMR spectroscopy was introduced and developed in early stages (1950-70s), most commonly used method was the one using continuous waves. A weak radiofrequency field with fixed amplitude was used and in order to detect nuclei at certain resonance frequencies either way the frequency was kept constant while the strength was incrementally changed or the other way around. Experiments performed in this manner took long time (longer than relaxation times T_1 and T_2). Advances in construction of NMR spectrometers allowed development of pulse programmes in which radiofrequency radiation is applied in a specific manner in short and intensive intervals [115].

A simplified scheme of the idea behind NMR spectroscope is shown in Figure 14. A sample tube is inserted between two superconducting magnet coils and is being held and spun (optional; increases homogeneity of the field by means of averaging the imperfections in thickness of the glass tube). The most important part of the probe is the coil surrounding the sample: it is where the pulses of RF transmitter are applied, which leads to formation of a magnetic field due to the alternating current in the coil wire. The frequency and phase of this generated field are the same as the signal from the RF transmitter. It causes excitation of the spins – nuclear magnetization, which

in turn induces an oscillating voltage (namely the NMR signal) in a coil. This signal is passed on to the receiver, where it is amplified and mixed with a reference voltage, corresponding to the pulses which were applied to excite the spins. Once the reference voltage is subtracted, the signal is amplified again, converted from an analogous signal into a digital and processed using appropriate software [115].

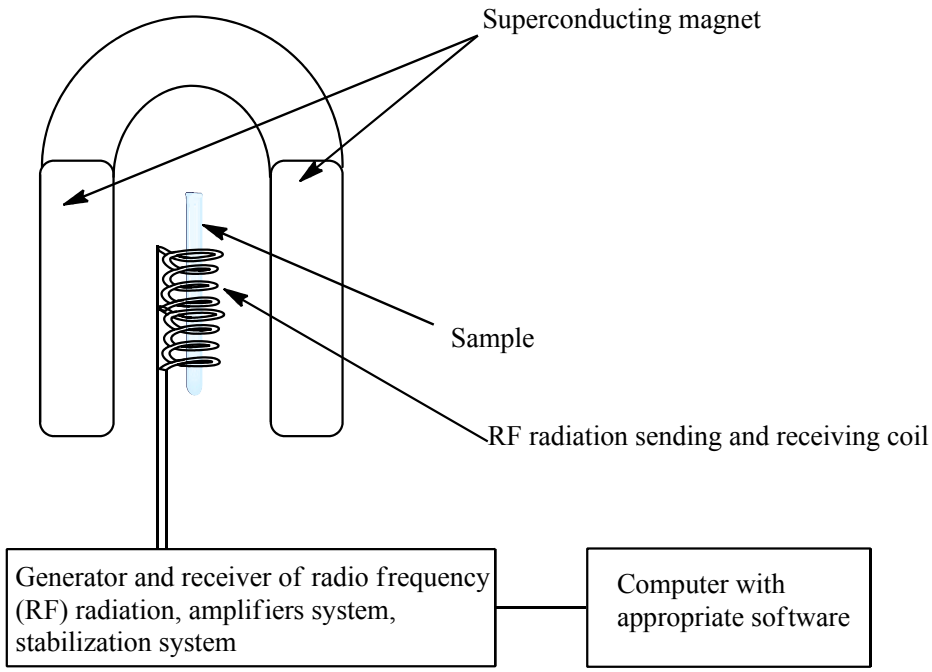

Figure 14. A simplified scheme of an NMR spectroscope

As it was mentioned before, the NMR frequency of a nucleus in a molecule is defined as $\nu = \frac{\gamma B}{2\pi}$. It is very important to bear in mind that the exact frequency is subject to a number of factors, from which the most significant is the position of the nucleus in a molecule (i.e. its neighbouring nuclei). This effect arises due to the fact that the magnetic field experienced by a certain nucleus is slightly different than the field applied. The reason for this is the fact that the nucleus is surrounded by electrons circulating around it. Since electrons are in motion, they induce a small magnetic field in the opposite

direction to the field applied, as it is described by the Maxwell's equations. Therefore, the nucleus is shielded from the applied field and the difference between the field applied and field experienced is quantified by a shielding constant σ. The value of this constant is very difficult to measure and is very impractical in use, therefore a more useful parameter was introduced: δ. This value is defined as a difference in resonance frequencies between an investigated nucleus and a reference frequency, divided by the reference frequency, so that it would be a normalized value, independent of the properties of the magnetic field used to examine the nuclei: $\delta = 10^6 \cdot \frac{(\nu - \nu_{ref})}{\nu_{ref}}$. The chemical shift (δ) is a dimensionless parameter, values of which are very often quoted in "parts per million" (ppm), hence 10^6 in the equation. For example, 1 ppm on a spectrum obtained in an experiment performed at a 600 MHz spectrometer corresponds to frequency of 600 Hz, while 1 ppm in a spectrum from a 400 MHz spectrometer – to 400 Hz. Therefore, if a nucleus is placed in a magnetic field of a NMR spectrometer, its energy change is strongly related to the properties of the field, therefore the frequency at which is resonates is different for spectrometers with different field frequency. However, the examined nucleus will still have the same chemical shift, say 1 ppm, in all the collected spectra, though its resonance frequency is different – 600 Hz or 400 Hz, for example [106] [108].

The reference signal is usually obtained by adding an appropriate chemical compound into an investigated sample (internal reference) or by inserting a separated capillary glass tube with a chemical compound into the test tube (external reference). Depending on the type of experiment (which nuclei are examined), type of solvent and experimental parameters (namely temperature), a number of compounds can be used. The most popular are

tetramethylsilane $(CH_3)_4Si$ (TMS), benzene-d_6 (C_6D_6), acetone- d_6 ($(CD_3)_2CO$) and dimethyl sulfoxide-d_6 ($(CH_3)_2SO$). For purposes of this research, TMS was chosen as an external standard for all experiments performed in 293 K due to its boiling point at 298-299 K; experiments performed in 328 K were conducted in presence of benzene as an external reference. The signal of the reference compound should be clearly visible (reasonable intensity) in the collected spectra and it should also be well separated from peaks of examined sample. Typically chemical shift for TMS is set to be zero and all other signals have chemical shift presented as in relation to TMS' shift. In case of experiments performed at higher temperatures, where temperature-dependency of chemical shift of benzene and other peaks was proved, chemical shift for benzene peak was set to 7 ppm. Very often, in quantitative NMR analysis, the reference is used not only to reference chemical shifts of detected nuclei, but also to match certain area (of reference signal) to known concentration.

Quantitative considerations

NMR spectroscopy has a potential to be a quantitative measure, providing the pulse program is adjusted to match specific requirements. In principle, the integrated intensity of a resonance signal is proportional to molar concentration and number of given nuclei resonating at considered frequency [108] [115]. In other words, integral area divided by number of nuclei detected at a given chemical shift is directly proportional to the molar concentration. In contrast to other popular spectroscopy methods (e.g. UV-Vis, fluorescence) NMR does not use the Beer-Lambert Law [104], therefore knowledge of molar absorption coefficient (ε) or access to pure components is not required. Moreover, the number of available standards for reference is

considerable, allowing examination of any given sample. The most favourable nuclei for quantitative analysis are those which have high relative abundance and, consequently, yield signal of large intensity, which in turn means high signal to noise ratio and lower errors. For example, both ^{1}H and ^{19}F have relative abundance of nearly 100%, while ^{13}C – only 1.1%, which means that in a sample containing carbon atoms, only 1.1% of them are visible in NMR, while the remaining 98.9%, mostly ^{12}C, is undetectable. Another important parameter that should be taken into account when choosing a nucleus to detect, are the relaxation times – T_1 and T_2. T_1 is often referred to as a constant of spin-lattice relaxation, in which one of the components of magnetization vector (along z-axis) returns to thermodynamic equilibrium with its surroundings. In other words, T_1 describes the average lifetime of nuclei at a higher energy level. The spin-spin relaxation is a mechanism in which the transverse component of the magnetization vector (x,y-plane) returns to its equilibrium state (equal to zero). Both types of relaxations decay exponentially and the rates of decay are T_1 and T_2, respectively. These values tend to be considerably longer for carbon than for proton nuclei. It does not mean that ^{13}C NMR cannot be used as a quantitative measure – it is simply more challenging as it requires longer and more elaborate experimental procedures. When developing procedures for collection of quantitative NMR data, a number of parameters has to be taken into account and carefully considered, including a number of scans, acquisition and repetition times and pulse width. All this is discussed further on.

3.6.2. Sample preparation

As explained earlier, in order to provide high stability of the magnetic field during the experiments, a field lock at certain frequency is attained. Very often the nucleus at which frequency the field is locked is deuterium. Because the solution of formaldehyde which is used in this research is aqueous, the most appropriate and neutral chemical compound containing deuterium is deuterium oxide (D_2O). The amount of deuterium oxide that is required to attain lock of the field may vary, however the higher the concentration the better the signal, therefore the lock is easier to achieve and maintain. Ideally, all water would be replaced by deuterium oxide – in case of ^1H NMR experiments, this would be a great advantage as a broad signal resulting from –OH exchanging groups would not be dominant. However, this solution is not practical in terms of purpose of this research, as reactions leading to formation of organic gels are performed in aqueous solutions and results from NMR performed in this manner would be less applicable if the solvent was replaced. Rather than eliminating all water, only part of it was replaced by deuterium oxide. Previous studies proved that replacement of 20% by weight of the solvent with D_2O was sufficient [94]. Due to the fact that in this research the total amount of water in all mixtures comprises water added as a solvent or diluent and water found in formaldehyde stock solution (roughly 50%wt.), the amount of water as a solvent replaced with D_2O was increased to 30%vol. In practice this means that the solvent or diluent was de-ionised water mixed with D_2O at volumetric ratio of 7 to 3.

Non-reacting systems

Formaldehyde-water

Appropriate volumes of formaldehyde stock solution and water-deuterium oxide mixture were measured with an automatic pipette into a glass vial equipped in a magnetic bar. The vial was then sealed and placed on a magnetic stirrer, where moderate stirring took place for approximately 10 min. Once the stirring finished a small volume (ca. 0.5 ml) of the solution was used to rinse the inside of an NMR tube and then the tube was filled with the examined mixture. A coaxial insert containing TMS was inserted into the NMR tube, allowing the excess of the solution to spill and ensuring that no air bubbles were trapped. Once insert was in place, the sealing cap was pulled on in the right position, the tube cleaned on the outside with acetone, labelled and taken to the NMR spectroscope for measurements.

Formaldehyde-methanol

Appropriate volumes of formaldehyde stock solution and methanol were measured with an automatic pipette into a glass vial equipped in a magnetic bar. In order to provide lock a small amount of deuterium oxide was added (see composition tables in the Appendices for details). The vial was sealed and placed on a magnetic stirrer, where moderate stirring was took place for 10 min. As in previous type of mixtures, a small volume (ca. 0.5 ml) was taken to rinse the NMR tube, and then the glass tube it was filled with the solution. A coaxial insert with TMS was inserted, ensuring that no air bubbles were trapped while the excess of the mixture was allowed to spill out. Once the insert was in place, the sealing cap was pulled into right

position, the tube was washed on the outside with acetone, labelled and taken to the NMR spectrometer.

Formaldehyde-water-sodium carbonate

Appropriate amounts of de-ionised water and deuterium dioxide were measured using an automatic pipette into a glass vial equipped with a magnetic bar and stirred moderately for 5 min on a magnetic stirrer. An appropriate amount of sodium carbonate was weighed on an analytical scale and then transferred into the glass vial with water and D_2O; stirring continued for another 10 min, until all solids have dissolved. An appropriate volume of formaldehyde stock solution was measured with an automatic pipette and added to the mixture in the glass vial. The vial was now sealed to minimize possible evaporation of volatile methanol from the formaldehyde stock solution and stirring continued for 5 min. Once this time was reached, a small volume (ca. 0.5 ml) of the solution was taken to rinse the NMR tube; then the tube was filled with the mixture. A coaxial insert containing TMS was inserted into the NMR tube, allowing the excess of the solution to spill and ensuring that no air bubbles were trapped. Once insert was in place, the sealing cap was pulled on in the right position, the tube cleaned on the outside with acetone, labelled and taken to the NMR spectroscope for measurements.

Resorcinol-water

Appropriate volumes of water and deuterium dioxide were measured with an automatic pipette into a glass vial into which a magnetic bar was placed. Resorcinol was weighed, added into the vial and then the vial was sealed and placed on a magnetic stirrer, where stirring took place for 10 min. Once

stirring was complete and all resorcinol was dissolved, a small amount (0.5 ml) of solution was taken to rinse the NMR tube. Once washed, it was filled with resorcinol solution and a coaxial insert was inserted, ensuring that no air bubbles were formed and allowing the excess solution to spill.

Reacting systems

Experiments at 20°C (293K)

The required amounts of de-ionized water and deuterium dioxide (at volumetric ratio 7 to 3) were measured with an automatic pipette into a glass vial. Resorcinol was weighed, transferred into the vial and stirred using a magnetic stirrer for 5 min until it had fully dissolved. Sodium carbonate was weighed on an analytical scale and transferred to the beaker with dissolved resorcinol. After 10 min of further stirring to dissolve sodium carbonate, the required amount of formaldehyde solution was measured with an automatic pipette and added to the mixture. The vial was sealed and shaken vigorously for about 30 s and then a small volume (0.5 ml) of the mixture was taken to rinse the NMR tube. Once rinsed, it was filled with the reacting mixture and a coaxial insert was inserted, allowing excess to spill and ensuring that no air bubbles were trapped. The NMR tube was rinsed with acetone on the outside, labelled and immediately placed in the spectrometer for measurements. The approximate time between adding formaldehyde and starting the experiment was about 3 min.

Experiments at 55°C (328K)

The required amounts of de-ionized water and deuterium dioxide (at volumetric ratio 7 to 3) were measured with an automatic pipette into a glass

vial. Resorcinol was weighed, transferred into the vial and stirred using a magnetic stirrer for 5 min until it had fully dissolved. Sodium carbonate was weighed on an analytical scale and transferred to the beaker with dissolved resorcinol. After 10 min of further stirring to dissolve sodium carbonate, the required amount of formaldehyde stock solution was measured with an automatic pipette and added to the mixture. The vial was sealed and shaken vigorously for about 30 s and then a small volume (0.5 ml) of the mixture was taken to rinse the NMR tube. Once rinsed, it was filled with the reacting mixture and a coaxial insert with benzene was inserted, allowing excess to spill and ensuring that no air bubbles were trapped. The NMR tube was rinsed with acetone on the outside, labelled and immediately placed in the spectrometer for measurements. The approximate time between adding formaldehyde and starting the experiment was about 3 min and the temperature in the spectrometer sample holder was preset to 55°C (328K) before sample insertion.

Experiments at 90°C (363K)

Due to technical limitations, the probe in the NMR spectrometer did not allow experiments at 90°C (363K) and, moreover, prepared coaxial inserts contained chemical compounds with boiling points below that temperature (26-28°C and 80°C for TMS and benzene, respectively [117]). An additional factor which contributed to the reasons for choosing this method was the fact that this is the way in which DLS, pH and IR experiments were performed when investigating reaction at 90°C (363K).

The required volumes of de-ionized water and deuterium oxide were measured using an automatic pipette and poured into a glass beaker.

Resorcinol was weighed, transferred to the beaker and stirred using a magnetic stirrer for 5 min until it had fully dissolved. Sodium carbonate was weighed on an analytical scale and transferred to the beaker with dissolved resorcinol. After 10 min of further stirring to dissolve sodium carbonate, the required amount of formaldehyde stock solution was measured with an automatic pipette and added to the mixture and stirring continued for another 30 min. Once stirring was completed, the solution was poured into a 25 ml poly(propylene) flask, sealed, labelled and placed in an electric oven preheated to 90°C (363K). Samples of constant volume were taken at specific time intervals (0, 10, 20 and 30 min) and mixed with water and deuterium oxide at volumetric ratio 1:2 in room temperature. Each sample was then transferred into a clean NMR tube, equipped in a coaxial insert containing TMS, washed with acetone and taken to the NMR spectroscope for measurements.

3.6.3. Measurement procedures

Equipment used

In order to collect data of high quality and ensure homogeneity of the field during the experiments is easily attained, appropriate NMR glass tubes needed to be used. High precision borosilicate glass tubes manufactured by Wilmad® were chosen. The upper limit of frequency for them was 600 MHz, the outer diameter 5 mm with wall thickness of 0.38 mm and 7 in. long (information from manufacturer).

Borosilicate glass coaxial inserts (Figure 15) to hold an external insert were also manufactured by Wilmad® and were designed to be compatible with the used tubes. The length of the stem (capillary part of the insert) was

50 mm; the capacities of reference and sample were 60 μL and 530 μL, respectively. In practice this means that the signal from the sample is approximately 8.83 times stronger than the reference's, therefore in quantitative analysis the signal from the sample needs to be divided by this factor.

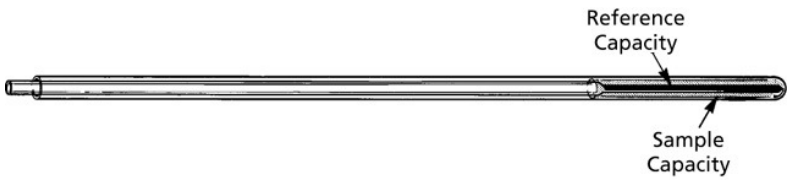

Figure 15. A scheme of a coaxial insert (Source: Sigma-Aldrich Company Ltd.)

All experiments were performed using a three channel multinuclear Bruker® Avance-III 600 MHz instrument. It is equipped in a 14.1 T Bruker UltraShield® magnet and two changeable probes: BBO-z-ATMA-[^{31}P-^{183}W/^{1}H] and TBI-z-[^{1}H, ^{13}C, ^{31}P-^{15}N]. Both probes are suitable for performing experiments on liquid samples but with different sensitivities towards ^{1}H and ^{13}C nuclei.

DEPT-90 and DEPT-135 experiments were performed using a two channel multinuclear Bruker® Avance/DRX500 (500 MHz) spectrometer. It is equipped in a 11.7 T Oxford unshielded magnet and a DUL-^{13}C/^{1}H-z gradient probe.

Types of experiments performed

^{13}C NMR T_1 measurements

Spin-lattice relaxation time (T_1) of ^{13}C nuclei was measured using a well-known method in which a pulse sequence can be represented as 180° - τ - 90° [115] [116] [118]. In simplification, this means that the equilibrium magnetization is inverted by the 180°, leaving the magnetization vector along the negative z-axis. Then during a certain τ time the magnetization vector is allowed to partially relax in the spin-lattice manner. Then a 90° pulse is applied – its aim is to rotate the magnetization vector along the y-axis. Once this is done, a free induction decay time is recorded and Fourier transformed to produce a spectrum with peaks whose intensities I(τ) are proportional to the τ-dependent function of magnetization vector magnitude along the z-axis – $M_Z(\tau)$ [118] [115]. The experiment runs this pulse program a number of times with different values of τ, chosen by the user. It is known that the spin-lattice relaxation process is exponential, therefore the following can be derived [115]:

$$M_Z(\tau) = M_0 \cdot \left[1 - 2 \cdot e^{-\tau/T_1}\right] \tag{20}$$

It is the main assumption that $M_Z(\tau)$ is proportional to the intensity of the registered signals, therefore the practical form of the above equation, which is used to obtain T_1 is [118]:

$$I(\tau) = I_0 + P \cdot e^{-\tau/T_1} \tag{21}$$

Where I_0 and P are constants.

Data collected during the experiment was fitted by the provided software (TopSpin® ver. 2.0) and correlated to the above function, from which T_1 was calculated for each signal in the ^{13}C spectrum.

The chosen parameters for T_1 relaxation time measurement experiments were:

- Number of scans: 256
- Number of dummy scans: 4
- Delay times - τ:
  - For resorcinol: 500 ms, 3 s, 6 s, 12 s, 20 s, 30 s, 50 s, 60 s, 90 s and 120 s
  - For formaldehyde: 0.1 s, 2 s, 5 s, 10 s, 20 s, 30 s, 60 s and 90 s
- Acquisition time: 0.27 s
- Temperature: 293K
- Spectral width: 33333 Hz (^{13}C) and 6194 Hz (^{1}H)
- FID resolution: 1.02 Hz (^{13}C) and 774 Hz (^{1}H)

Nuclear Overhauser Effect measurement

A relatively straightforward and traditional method to evaluate the magnitude of the Nuclear Overhauser Effect was used. The method has several disadvantages but because it was performed only to verify whether NOE could be an issue when analysing the data and the obtained values were not used in quantitative processing of any spectra, it was deemed suitable. The experimental procedure involves applying a 180° pulse to a selected peak in the spectrum. This type of pulse causes the most dramatic

perturbation there is: excess population in the lower energy level is now in the higher one, while the depleted population is now in the lower energy level. After a relatively short time this perturbation propagates to the close by nuclei in the molecule and thus affects their population distribution. At this point a 90° "read" pulse is applied and information on the amount of perturbation on the nearby nuclei is registered in the shape of a spectrum with enhanced or diminished peak areas. Then a basic spectrum is subtracted from the "enhanced" one and the difference in the peak areas or their intensity provides information on the magnitude of the NOE.

1D experiments

Two types of 1D experiments were performed – one were detecting ^{1}H nuclei and the other were investigating ^{13}C nuclei.

All ^{1}H NMR experiments were performed using BBO-z-ATMA-[^{31}P-^{183}W/^{1}H] probe due to its better sensitivity towards ^{1}H nuclei. The parameters of experimental procedure were as follows:

- Number of scans: 16
- Number of dummy scans: 2
- Delay time: 1 s
- Acquisition time: 2.65 s
- Temperature range: 293-328K
- Spectral width: 12335 Hz
- FID resolution: 0.19 Hz

^{13}C NMR Distortionless Enhancement by Polarization Transfer (DEPT) experiments are very useful when differentiating between carbons of different order (i.e. primary, secondary and tertiary). In this experiment polarization of the proton is transferred onto the carbon nuclei, therefore only carbons bound to protons are visible (all quaternary carbons are invisible). The angle of the pulse can be adjusted to one of three main values – 45°, 90° and 135° – to show carbon nuclei of certain order in phase (i.e. intensity of positive values). DEPT-90 uses a 90° angle and resulting spectrum contains CH groups in phase, while DEPT-135 uses a 135° angle and results in a spectrum where CH and CH_3 groups are in phase, while CH_2 gives rise to negative peaks.

The chosen parameters for DEPT-90 and DEPT-135 experiments were:

- Number of scans: 256
- Number of dummy scans: 4
- Delay time: 2 s
- Acquisition time: 0.27 s
- Temperature: 300K
- Spectral width: 30120 Hz
- FID resolution: 1.84 Hz

Inverse Gated Decoupling experiments were performed in order to achieve full relaxation due to long delay time and to eliminate the Nuclear Overhauser Effect.

All ^{13}C NMR experiments were performed using TBI-z-[^{1}H, ^{13}C, ^{31}P-^{15}N] probe due to its better sensitivity towards ^{13}C nuclei. The parameters of experimental procedure were as follows:

- Number of scans: 1024
- Number of dummy scans: 4
- Delay time: 60 s
- Acquisition time: 0.49 s
- Temperature: 278-293K
- Spectral width: 33333 Hz
- FID resolution: 1.02 Hz

The delay time was chosen to be in range of 1-5 T_1, which was measured in another experiment described earlier in this section. Inverse gated decoupling was used in order to eliminate Nuclear Overhauser Effect (its magnitude was also measured - ◎). A high number of scans allowed good signal to noise ratio even for dilute solutions.

2D experiments

Heteronuclear Single Quantum Coherence (HSQC) method is commonly used to record one-bond correlation between proton and ^{13}C [116]. The main advantage of this method is the fact that the proton is the observed nucleus,

which grants relatively short acquisition time and thus time-efficient experiment. The main purpose of performing this type of NMR experiments in this research was allowing for accurate assignments of both ^{1}H and ^{13}C spectra. It was especially useful in assignment of peaks overlapping and hidden under the water peak in ^{1}H spectra and very useful in assigning the region of **C**H_2 signals in oligomeric structures in ^{13}C spectra. Because only protons directly bound to ^{13}C nuclei give rise to signal in this experiment, water peak was eliminated. This method, despite a number of attempts at adjusting delay times, failed to be fully quantitative.

Heteronuclear Single Quantum Coherence (HSQC) experiments were performed using BBO-z-ATMA-[^{31}P-^{183}W/^{1}H] probe. The parameters of experimental procedure were as follows:

- Number of scans: 4
- Number of dummy scans: 16
- Delay time: 1.5-4 s
- Acquisition time: 0.17 s
- Temperature: 293K
- Spectral width: 6009 Hz
- FID resolution: 2.93 Hz

CHAPTER 4. GLYCOL EQUILIBRIA IN AQUEOUS SOLUTIONS

This Chapter focuses on investigation of speciation of formaldehyde related species in formaldehyde stock solutions diluted with various amounts of water or methanol. It was reported in previous publications that the speciation in these solutions is subject to interplay between glycol oligomerization and esterification and therefore depends on relative amounts of total formaldehyde, methanol and water. The main aim here was to investigate how speciation in these solutions depends on the concentration of formaldehyde, methanol and temperature in order to better understand what species are present in reacting solutions used in formation of resorcinol-formaldehyde gels (see Chapter 6).

Nuclear Magnetic Resonance was used to examine the speciation in formaldehyde solutions. ^{13}C NMR was chosen as the primary method for quantitative characterisation of non-reacting systems and after assignments were made, a quantitative distribution of species found in the solutions were obtained. Due to the fact that fully quantitative ^{13}C NMR experiments were lengthy, ^{1}H NMR experiments were performed in order to validate this method for kinetics experiments (see Chapter 6). In order to properly assign complex ^{1}H NMR spectra, HSQC experiments were performed and deconvolution of the -OH/D signal in proton spectra was done. Quantitative information, provided by the ^{13}C NMR experiments was used to calculate the equilibria constants for reactions among major species found in formaldehyde solutions under conditions investigated.

Both IR and Raman spectroscopies were also used to investigate formaldehyde solutions. These two methods were used because of their wide

popularity and good accessibility and speed. Information collected with these experiments aimed at identifying what information about formaldehyde species can be gained using IR and Raman spectroscopies and assess their potential for quantitative analysis. Due to the fact that collected spectra were fairly complex, deconvolution had to be performed in order to properly detect and assign all signals.

Dynamic Light Scattering was used to ascertain whether there is any significant clustering or phase separation happening in formaldehyde solutions. Measurements of pH of formaldehyde solutions were performed in order to monitor the effect of solution composition on the acidity of the solutions. These experiments are important because the ability to control and predict pH of the formaldehyde solutions is crucial when using it to synthesise organic gels, where the pH of reacting solutions impacts on the final properties of the gel.

4.1. Nuclear Magnetic Resonance

4.1.1. ^{13}C NMR T_1 relaxation times and Nuclear Overhauser Effect

In order to decide on the delay time in NMR experiments, knowledge of the relaxation time is essential, especially if the data which is to be collected is meant to be quantitatively accurate. As it was mentioned in the methodology description (Chapter 3), the delay time is primarily determined by the spin-lattice relaxation time constant, T_1. In case of proton spectra, this can be negligible as the spin-lattice relaxation is rapid; however carbon nuclei tend to require much longer time to fully relax.

The experiments were performed on formaldehyde solutions prepared by dilution of the formaldehyde stock solution with water or methanol, both at 1:10 volumetric ratios. In this experiment a number of delay times (0.1 s, 2 s, 5 s, 10 s, 20 s, 30 s, 60 s and 90 s) were chosen after each time the pulse was finished, allowing exactly as much time for the spins to return to the equilibrium state. For each peak intensity was recorded after each delay time was applied and then the data was plotted and fitted with the following equation:

$$I(\tau) = I_0 + P \cdot e^{-\tau/T_1} \tag{22}$$

An example of a resulting plot for peak corresponding to carbon nucleus in methanol is shown in Figure 16. As it can be seen, the intensity reaches a maximum after certain delay time (approximately 60 s) and further extension of this time does not influence the registered intensity.

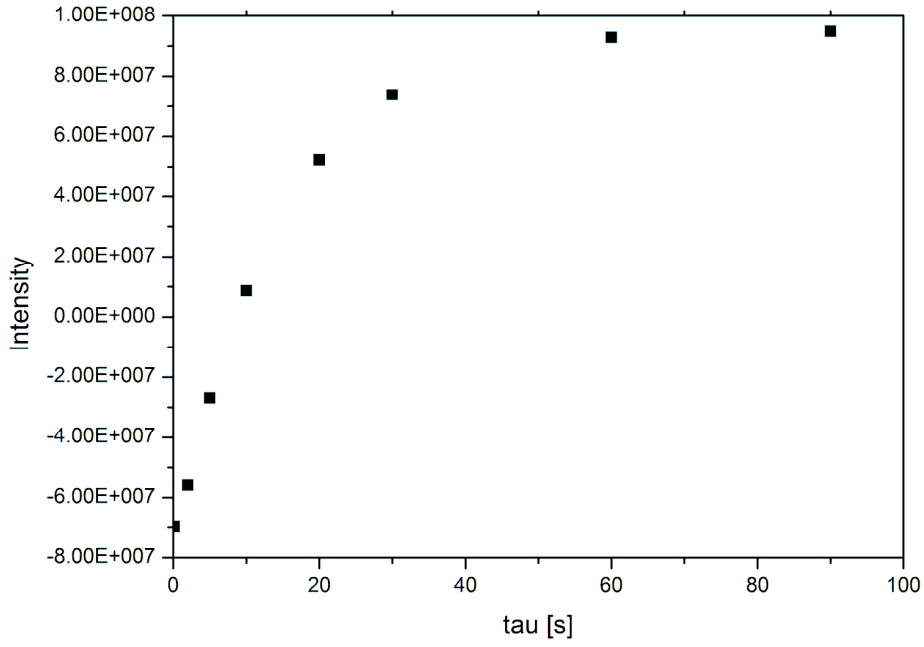

Figure 16. Peak intensity dependency of the chosen delay time (τ): carbon nucleus in methanol.

The data plotted in the way shown in Figure 16 was fitted using the Bruker® TopSpin ver. 2.0 software and the values of T_1 constants for each peak were obtained. The results of these operations are shown in Table 2. It can be seen that the longest relaxation time constant T_1 is observed for carbon nucleus in methanol and it is more than twice larger than the same constant for MG or MMG.

Table 2. Values of measured relaxation time T_1 for ^{13}C nuclei in formaldehyde-related species.

Name	**Compound**	**Calculated δ [ppm]**	**T_1 [s]**
MeOH	**C**H_3OH	46.7	15.0
MMG	**C**H_3O-CH_2-OH	55.3	1.7
MDG	**C**H_3O-CH_2-OCH_2-OH	55.6	3.7
MG	OH-**C**H_2-OH	82.0	6.1
DG	HO-**C**H_2-O-**C**H_2-OH	85.2	4.5
MDG	CH_3O-CH_2-O**C**H_2-OH	85.5	2.75
MMG	CH_3-O-**C**H_2-OH	91.4	6.04
MDG	CH_3O-**C**H_2-OCH_2-OH	93.6	3.32

As a consequence of these long relaxation times, an appropriate delay time during the experiments needed to be chosen. The most common practice is to choose delay time equal to $5 \cdot T_1$ [115], as this is the time in which most of the excited nuclei spins return to the equilibrium state. In case of this research, the longest spin-lattice relaxation time-constant was found to be 15 s, which means that the delay time in the experiments should be 75 s if all nuclei were to be relaxed. However, this was tested in order to verify if such a long delay time is indeed required. In order to do so, an experiment eliminating Nuclear Overhauser Effect was ran on a formaldehyde-water solution (1:6 vol. ratio) with two different delay times: 75 s and 60 s. Then the areas of the peak

corresponding to the carbon nucleus in methanol were integrated and compared. Due to virtually no differences, the shorter delay time was decided on in order to provide a more time-efficient experimental procedure. These 15 s may seem insignificant but for a typical 1024-scan ^{13}C NMR experiment, approximately 4 hours are saved.

The relaxation time is not the only thing that can affect the intensity of collected signals, leading to errors in quantitative analysis. The Nuclear Overhauser Effect is a relatively complex mechanism which causes amplification of signals of certain nuclei spins in NMR and is often used to determine the conformation of large molecules like proteins *via* a number of NMR techniques exploiting this phenomenon (NOESY, HOESY, ROESY, to name just a few). However, for the purpose of this research, where the investigated molecules are relatively small, do not have three-dimensional conformation and are easy to identify in the NMR spectra, this effect is an obstacle that stands in the way of obtaining reliable quantitative information on speciation in formaldehyde solutions. The Nuclear Overhauser Effect is caused by the fact that once RF pulse saturates one nucleus spin, the dipolar interactions with spins of further nuclei cause perturbations of those spins, allowing the transfer of spin polarization further on. As an effect, the signals from spins of neighbouring nuclei are enhanced. The propagation of spin polarization *via* this mechanism is not limited by the number of chemical bonds separating the nuclei but the actual space and distance between them, hence the usefulness in establishing three-dimensional conformation of biological structures.

The magnitude of Nuclear Overhauser effect needed to be assessed in order to obtain reliable quantitative information from ^{13}C NMR. The main purpose

of this experiment was to determine if NOE is present and if it is significant. The results of experiments proved that the answers to both questions are positive, which in conclusion led to application a pulse program which eliminates this effect (inverse gated decoupling).

As it was explained previously, the intensity of a peak in an NMR spectrum is proportional to the difference in population of nuclei at different energy levels. Therefore the perturbation of equilibrium between the two states caused by the Nuclear Overhauser Effect (NOE) can be measured by recording two spectra in very specific conditions and then comparing them. The most popular 1D NOE experiment involves irradiation of one peak at its resonant frequency with a low power radio frequency in order to equalize the populations of the two energy states. This process is called saturation and is continued until the perturbation populations of nearby nuclei in the molecule does not change any further, i.e. reaches a steady-state. The next step in the experiment is application of a 90° pulse and an FID is recorded and transformed into a classic NMR spectrum. This data is then used to measure the amount of perturbation on the nuclei in the vicinity. Despite being relatively popular, this method has a number of disadvantages which need to be considered before its application. Most of all, the conditions in which two spectra subtracted from each other are collected must be identical. The NMR spectrometer which was used in this research is of a very high standard, however since the spectra are collected at different times, one must anticipate subtraction artefacts due to the risk of differences in the vibrations (of the building and spectrometer), power of the RF signal, sensitivity, temperature or the magnetic field. It is safe to assume that these differences are minimal if any at all. Another disadvantage is that even with a high resolution spectrometer it is difficult to obtain irradiation of a very specific

peak, especially if the considered region is very crowded. This was however overcome by running the experiments on dilute solutions with a relatively simple speciation. All these factors were taken into consideration, however it was anticipated that the enhancement effect might be significant and thus these factors were unlikely to affect the results significantly. Moreover, the main purpose of this experiment was to assess whether there was a need to run a special (inverse gated decoupling) pulse program to obtain quantitative data.

The results from experiments performed on formaldehyde solutions prepared by dilution with water and methanol at volumetric ratio of 1 to 10, proved that the NOE effect is significant and should not be ignored if quantitative data is at stake. Bearing in mind that the magnitude of the NOE can depend also on the type of diluent, an experiment on formaldehyde-methanol at the same volumetric ratio was performed in order to determine whether the diluent influence is significant. The results of these experiments are summarised by Table 3 and Table 4.

Table 3. Comparison of NOE values measured for formaldehyde solutions prepared by dilution of the formaldehyde stock solutions with water at 1:10 [vol/vol] in ^{13}C NMR.

Assignment	**Measured chemical shift δ [ppm]**	**Type of enhancement (positive/negative)**	**NOE [%]**
CH_3-OH	48.9	negative	9.9
CH_3O-CH_2-OH	54.6	positive	19.0
HO-**C**H_2-OH	81.9	positive	34.0
HO-**C**H_2-O-**C**H_2-OH	85.6	positive	34.0
CH_3O-**C**H_2-OH	89.6	positive	22.8
CH_3O-**C**H_2-OCH_2-OH	93.3	positive	28.9

Table 4. Comparison of NOE values registered for formaldehyde solutions prepared by dilution of the formaldehyde stock solutions with methanol at 1:10 [vol/vol] in ^{13}C NMR.

Assignment	**Measured chemical shift δ [ppm]**	**Type of enhancement (positive/negative)**	**NOE [%]**
CH_3-OH	49.1	negative	4.8
CH_3O-CH_2-OH	54.3	positive	20.1
CH_3O-**C**H_2-OH	90.1	positive	34.0

The magnitude of the NOE was calculated by comparison of the intensities of the collected spectra (with and without saturation) and expressed as per cent of the intensity of the spectrum in which the NOE was eliminated. It can be clearly seen that the order of magnitude is so significant, that these values, despite being subject to a very small error impossible to quantify for the reasons mentioned earlier, can be treated as a very clear indication to use a special pulse program to collect quantitative data.

When analysing data from Table 3 and Table 4 one can notice that only one peak was subject to a decrease in its intensity and that peak was in both cases generated by methanol. Interestingly enough, the magnitude of NOE was roughly twice larger in solutions diluted with water compared to those diluted with methanol. It is important to note that the magnitude of NOE for other species can be as high as 34.0%, with the lowest value being as much as 19.0%. This means that in practice, previous studies which did not eliminate NOE in the experimental procedures may contain results subject to very high errors and ought to be treated with caution.

4.1.2. Qualitative analysis

In order to assign peaks in both ^{13}C and ^{1}H NMR spectra, calculations were made to predict the approximate chemical shift (δ, ppm). The values were predicted using ChemBioDraw Ultra ver. 12.0 (CambridgeSoft). It was also assumed that the chemical shift of TMS is zero. Calculated chemical shifts for each carbon nucleus are shown further on in Table 5.

The first experiments performed were DEPT-135 and their main purpose was to confirm which signals belong to carbon atoms in $-CH_2$ and $-CH_3$ groups. DEPT-135 experiment yields a spectrum in which $-CH_3$ and –CH groups give positive signal, while $-CH_2$ give negative peaks. As it was expected and can be seen in Figure 17, the group of signals found in range of 40-60 ppm corresponds to carbon atoms in $-CH_3$ groups, while all signals recorded at chemical shift greater than 70 ppm and lower than 100 ppm are related to carbon atoms in $-CH_2$ groups.

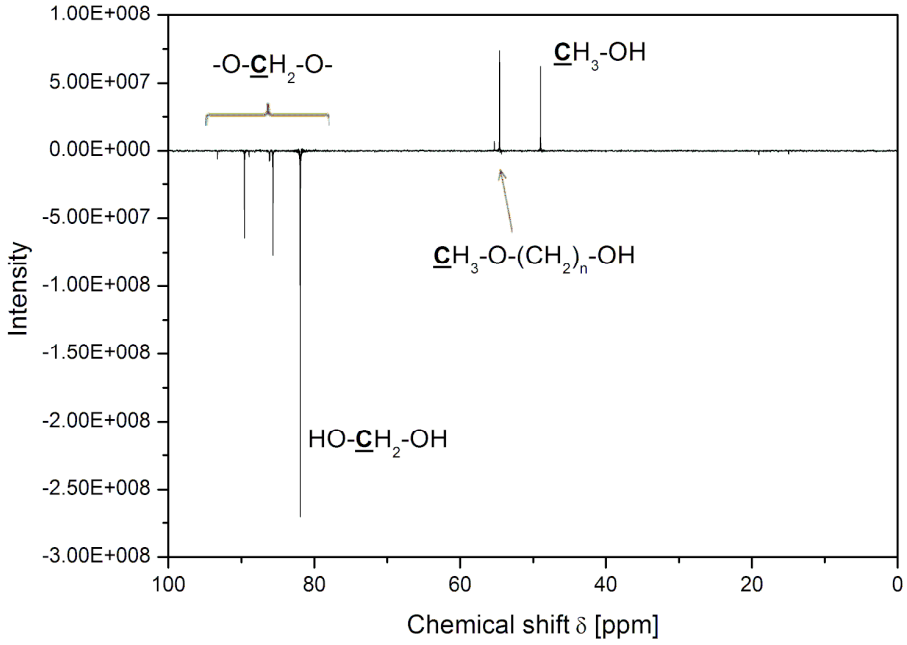

Figure 17. ^{13}C NMR DEPT-135 spectrum of formaldehyde solutions prepared by dilution of the formaldehyde stock solutions with water at 1:6 volumetric ratio.

Despite having calculated chemical shifts of all possible signals, certain difficulties in distinguishing between signals in the 80-100 ppm appeared. As it can be seen in Table 5, there are a few signals which have similar chemical shift and it was initially difficult to make unique assignments. In order to assign this region accurately additional experiments were performed. For a number of formaldehyde solutions prepared by dilution with either water or methanol, Heteronuclear Single Quantum Coherence (HSQC) experiments were done. This type of measurement, as it was mentioned before, helps to detect and correlate proton nuclei attached to carbons. In other words, the resulting spectrum is a 2D plot with signals registered only for protons attached directly to carbon nuclei. The chemical shift values on the x-axis

correspond to ^{1}H spectrum, while the y-axis to the ^{13}C. The greatest advantage of this method in this particular case was elimination of the OH/D signal, which was dominant in proton spectra and overlapped with potentially interesting -C$\underline{H}_2$ signals. The results proved to be very valuable as knowledge of carbon nuclei assignments and quantitative information on distribution of species helped to assign the proton NMR spectra, while information from the latter was useful in detailed description of the 80-100 ppm region in carbon NMR. The resolution of signals in HSQC was better than in a typical ^{13}C experiments mostly because the peaks were distributed along two axis and not one. The fact that the protons attached to carbon nuclei in this region are well separated, helped to observe the behaviour of these peaks as a function of dilution. As it can be seen in Figure 18, the peaks change their area with changing dilution. As expected, an increase in the amount of diluent (here: water) causes the spectrum to become less complex. Another factor affecting the appearance of these spectra is the type of diluent, as it can be seen in Figure 19 where HSQC spectra of two solutions prepared with dilution using the same volumetric ratios but different solvents are compared. This is in agreement with what was observed in 1D experiments, where the distribution of the formaldehyde-related species was a function of these two. These changes were compared with quantitative results from ^{13}C experiments and final assignment of both ^{1}H and ^{13}C spectra was then possible.

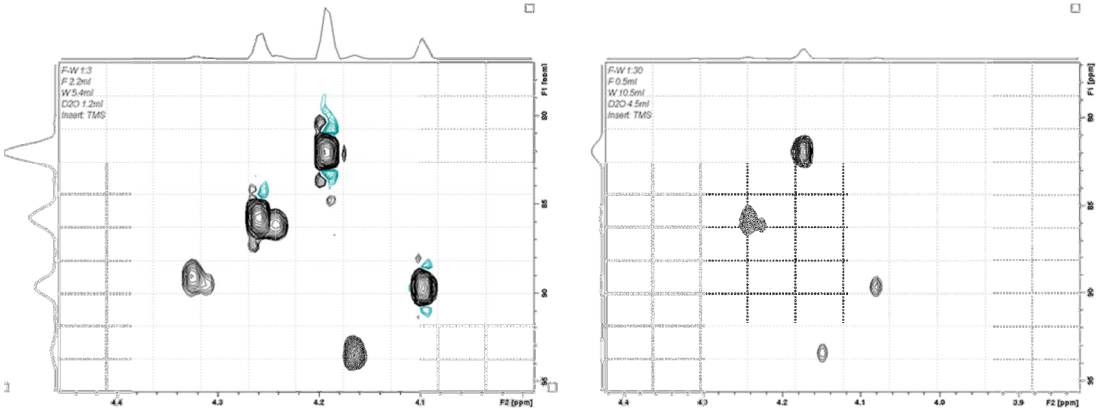

Figure 18. Formaldehyde-specific sections of HSQC spectra collected for formaldehydesolutions prepared by dilution of the formaldehyde stock solution with water at volumetric ratios 1:3 (left) and 1:30 (right).

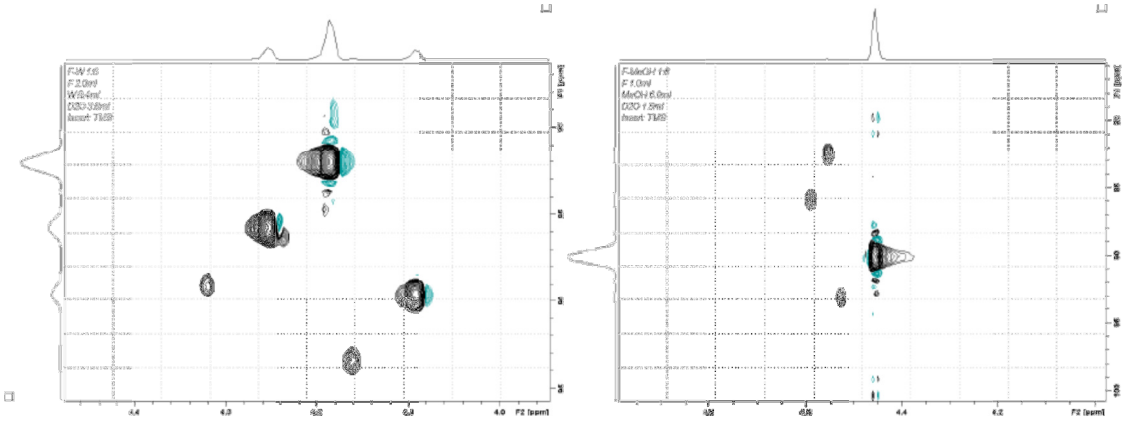

Figure 19. Formaldehyde-specific sections of HSQC spectra collected for formaldehyde solutions prepared by dilution of the formaldehyde stock solution with water (left) and methanol (right) at volumetric ratio 1:6.

The formaldehyde solution composition which is the closest to the one used in resorcinol-formaldehyde gels synthesis is the one corresponding to the formaldehyde stock solution with water at volumetric ratio1:6, therefore an HSQC spectrum of this solution is shown in Figure 20 with all peaks assigned. The two peaks on the right side are generated by protons in the –

OCH_3 groups and the peak which is assigned as MMG + MDG is – in greater magnification – constitutes of two slightly overlapping peaks. The expanded view of section with all signals from the CH_2 groups contains more signals and is by far more interesting. The most dominant signal is MG, while seemingly second in area or intensity peak (located to its left) is actually a group of three signals. There is a couple of peaks resulting from CH_2 groups in TG and MDG, which have exactly the same predicted carbon and proton chemical shifts: 85.5 ppm and 5.61 ppm, respectively. The third signal in this group is generated by the CH_2 group in DG, with predicted carbon and proton chemical shifts at 85.2 ppm and 5.61 ppm.

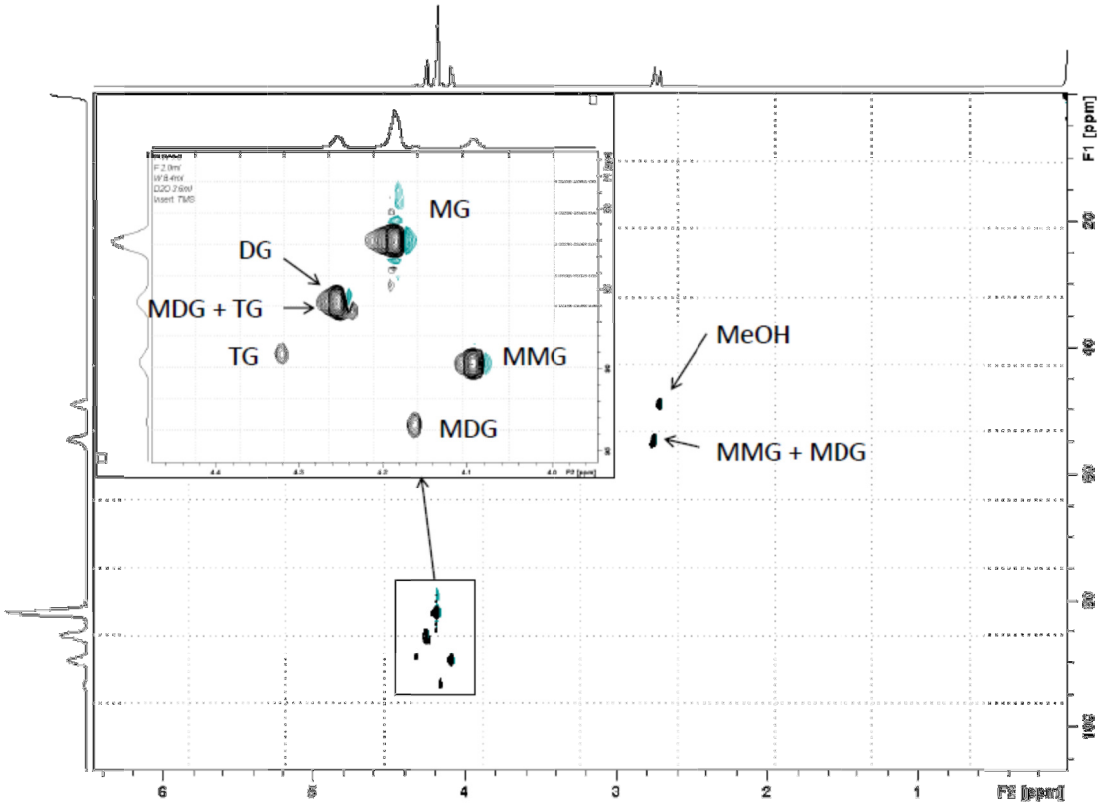

Figure 20. HSQC spectrum of formaldehyde-water solutions prepared by dilution of the formaldehyde stock solution with water at volumetric ratio 1:6 [vol/vol] with all peaks assigned.

The calculated values of chemical shift were to be treated only as a relative indication and it was expected that the measured values would be somewhat shifted. Therefore, after assignment of each peak for each solution a correlation chart was done to check these assignments. As it can be seen in Figure 21 and Figure 22 the plot of measured chemical shift values against theoretical ones forms a straight line, both for ^{13}C and ^{1}H NMR results.

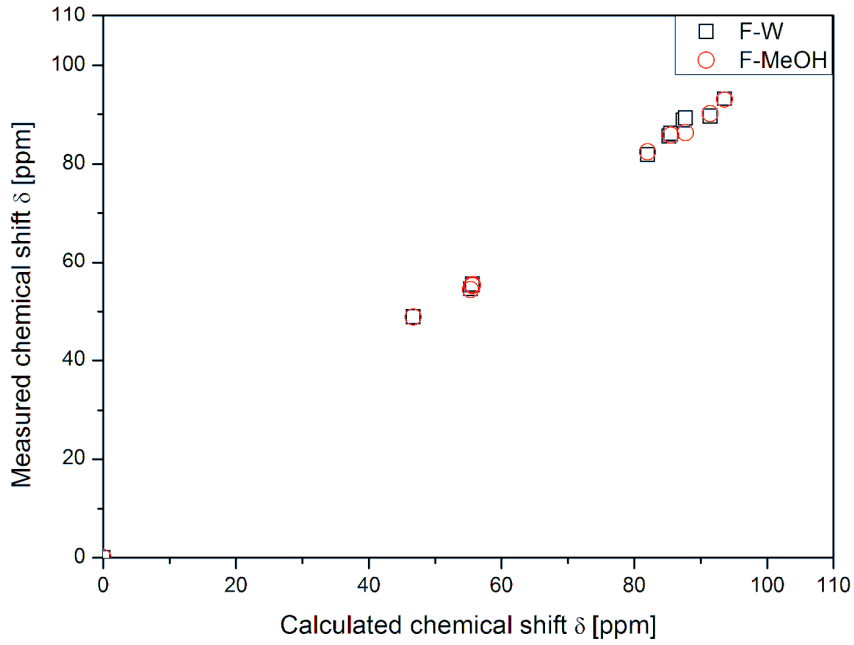

Figure 21. Correlation of assignments of chemical shifts in formaldehyde solutions prepared by dilution of the formaldehyde stock solutions with water and methanol by ^{13}C NMR.

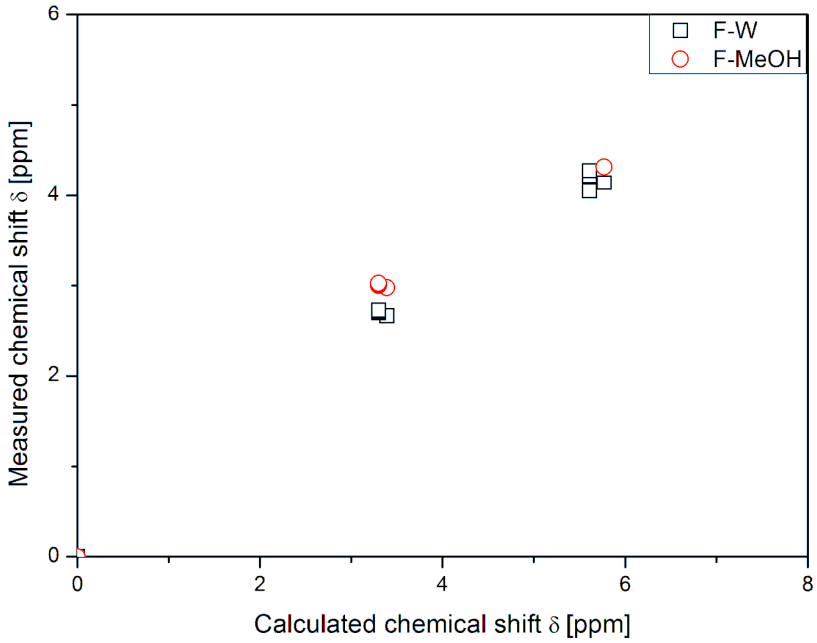

Figure 22. Correlation of assignments of chemical shifts in formaldehyde solutions prepared by dilution of the formaldehyde stock solutions with water and methanol by ^{1}H NMR.

The values of chemical shifts shown in Table 5 and Table 6 correspond to the calculated and measured values; please note that the latter ones are calculated as an arithmetic average from results for all solution compositions. As the results of experiments performed on formaldehyde-water and formaldehyde-methanol solutions showed, chemical shifts of certain species changed insignificantly with formaldehyde concentration. Chemical shifts of three major formaldehyde-related peaks (MG, DG, MMG) oscillated around the values shown in Table 6 and varied by no more than ±0.02 ppm. There was no clear tendency of the signals moving up- or downfield with increasing concentration. The only signal worth mentioning here was the one generated by CH_3-O- group. Its chemical shift in methanolic solution

decreased by nearly 0.2 ppm when formaldehyde concentration increased from 1.63%wt. to 11.66%wt. This is different from aqueous solution, where no such observation was made. It is difficult to assess whether this trend is identical for other formaldehyde-related species, as those are not visible in all formaldehyde-water solutions.

Table 5. Comparison of calculated chemical shifts for specific ^{13}C nuclei and values measured for formaldehyde solutions prepared by dilution of the formaldehyde stock solutions with water and methanol by ^{13}C NMR at 20°C (293K).

Name	**Assignment**	**Calculated δ [ppm]**	**Average measured δ [ppm]**	
			F-W	**F-MeOH**
TMS	TMS	0	0	0
MeOH	**C**H$_3$OH	46.7	48.99	48.89
MMG	**C**H$_3$O-CH$_2$-OH	55.3	54.61	54.38
MDG	**C**H$_3$O-CH$_2$-OCH$_2$-OH	55.6	55.34	55.21
MTG	**C**H$_3$O-CH$_2$-OCH$_2$-OCH$_2$-OH	55.6	55.52	55.41
MG	HO-**C**H$_2$-OH	82.0	81.91	82.43
DG	HO-**C**H$_2$-O-**C**H$_2$-OH	85.2	85.60	n/a
TG	HO-**C**H$_2$-O-CH$_2$-O-**C**H$_2$-OH	85.5	86.03	n/a
MDG	CH$_3$O-CH$_2$-O**C**H$_2$-OH	85.5	86.15	85.79
TG	HO-CH$_2$-O-**C**H$_2$-O-CH$_2$-OH	87.4	88.83	n/a
MTG	CH$_3$O-CH$_2$-O**C**H$_2$-OCH$_2$-OH	87.7	89.23	86.27
MMG	CH$_3$O-**C**H$_2$-OH	91.4	89.61	90.09
MDG	CH$_3$O-**C**H$_2$-OCH$_2$-OH	93.6	93.22	93.00

Table 6. Comparison of calculated chemical shifts for specific ^{1}H nuclei and values measured for formaldehyde solutions prepared by dilution of the formaldehyde stock solutions with water and methanol by ^{1}H NMR at 20°C (293K).

Type of group	Name	Assignment	Calculated δ [ppm]	Average measured δ [ppm]	
				F-W	F-MeOH
$Si(C\underline{\mathbf{H}}_3)_4$	TMS	TMS	0	0	0
-O$C\underline{\mathbf{H}}_3$	MeOH	$C\underline{\mathbf{H}}_3$-OH	3.39	2.66	3.08
	MMG	HO-CH_2-O$C\underline{\mathbf{H}}_3$	3.30	2.69	3.10
	MDG	HO-CH_2O-CH_2-O$C\underline{\mathbf{H}}_3$	3.30	2.71	3.01
	MTG	HO-CH_2O-CH_2O-CH_2-O$C\underline{\mathbf{H}}_3$	3.30	2.72	3.03
-$C\underline{\mathbf{H}}_2$-$OCH_3$	MMG	HO-$C\underline{\mathbf{H}}_2$-$OCH_3$	5.61	4.04	4.45
	MDG	HO-CH_2O-$C\underline{\mathbf{H}}_2$-$OCH_3$	4.50	4.11	n/a
-O-$C\underline{\mathbf{H}}_2$-OH	MG	HO-$C\underline{\mathbf{H}}_2$-OH	5.77	4.13	4.32
	MDG	HO-$C\underline{\mathbf{H}}_2$-O-$CH_2$-$OCH_3$	5.61	4.19	n/a
	DG	HO-$C\underline{\mathbf{H}}_2$-O-$C\underline{\mathbf{H}}_2$-OH	5.61	4.20	n/a
	TG	HO-$C\underline{\mathbf{H}}_2$-O-$CH_2$-O-$C\underline{\mathbf{H}}_2$-OH	5.61	4.24	n/a
-C-O$C\underline{\mathbf{H}}_2$-C-	TG	HO-CH_2-O$C\underline{\mathbf{H}}_2$-$OCH_2$-OH	4.50	4.27	n/a

Depending on the concentration of formaldehyde in a given solution, the appearance of a ^{13}C NMR spectrum can be more or less abundant in signals. An example of a typical spectrum of a formaldehyde-water solution is shown in Figure 23. At the same this, this is a spectrum of a solution with formaldehyde to water ratio (1:6 by volume) which resembles the composition of a reacting system. ^{13}C NMR spectra of formaldehyde and methanol solutions are very similar, however, chemical shifts are slightly higher (see Table 5).

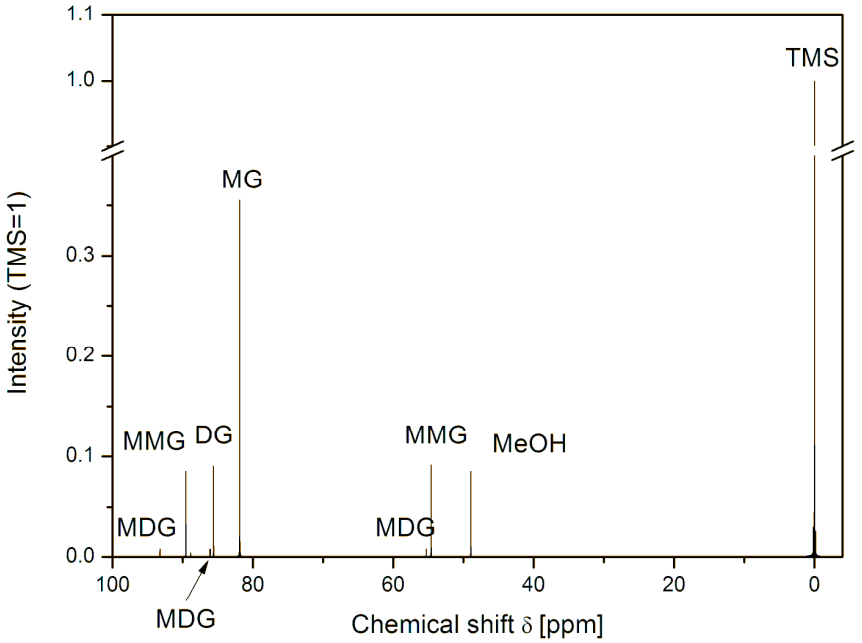

Figure 23. An example of ^{13}C NMR spectrum of formaldehyde-water solution (1:6 by volume, 20°C (293K)).

It can be clearly seen, when analysing data from Table 5, that the chemical shifts observed in results of ^{13}C NMR are more consistent in both methanolic and aqueous solutions of formaldehyde. They differ from calculated values but only by a small factor and the difference seems to be relatively constant for all signals. The situation is different with results from ^{1}H NMR. In this case the differences stand out more. Since we are dealing with solutions containing water (from formaldehyde stock solution or added in dilutions with water), the impact of hydrogen bonds is significant. This is especially the case for the -OH/D signal, which is observed at different chemical shift, depending on the amount of water. Additionally, it is as expected that positions of other peaks differ with the amount of water or methanol in the solution. It can be seen clearly from Figure 24, where chemical shift of -OH/D

peak is plotted against formaldehyde concentration. In case of formaldehyde stock solutions diluted with water, the increase of formaldehyde concentration also meant increasing methanol concentration, as it was a part of the formaldehyde stock solution. Whereas in case of formaldehyde stock solutions diluted with methanol the lower concentrations of formaldehyde were associated with higher methanol content. Therefore, one may conclude that an increase in methanol concentration leads to an increase in chemical shift values. At the same time, increasing the water content in the samples causes the –OH/D signal to move towards lower values of chemical shift.

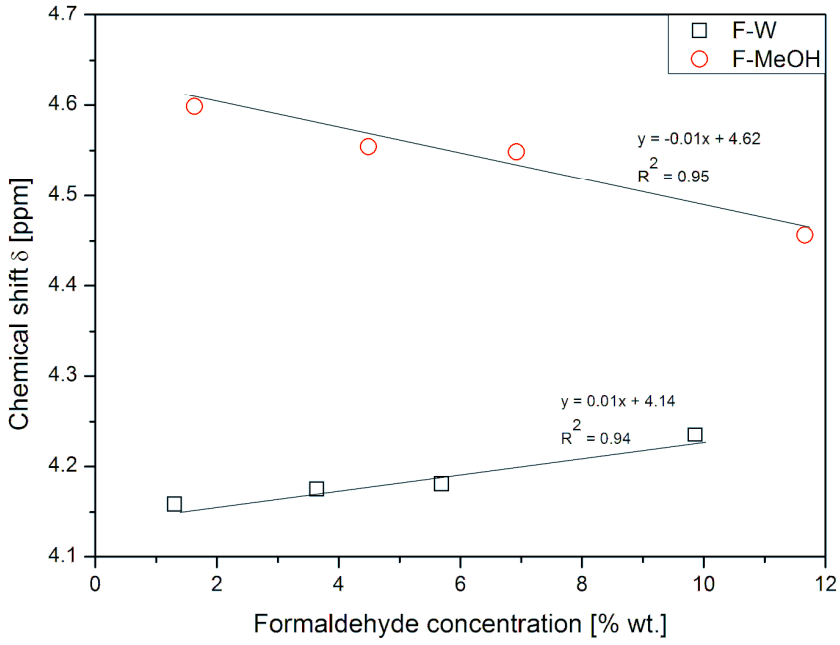

Figure 24. Values of chemical shift of the -OH/D peak versus total concentration of formaldehyde.

The influence of methanol and water concentrations is particularly strong on this peak, as it is associated with the hydroxyl groups. These are known to form weak hydrogen bonds and exchange the proton attached to the oxygen

atom. This is also the reason why this signal is much different in appearance than others – it is significantly broader. Positions and width of the remaining peaks are virtually unaffected by changes of solution concentrations.

The only way in which influence of the type of diluent on their chemical shift can be observed is when comparing samples with the same formaldehyde content but in a different diluent, as the average values indicate in Table 6.

The most significant difficulties with quantitative analysis using proton NMR spectra were due to the signal resulting from the hydroxyl groups in both glycols and water. The signal is very intensive due to high water content and very broad due to the chemical exchanges between proton and deuterium nuclei. The signal, as mentioned earlier, resonates at similar frequencies to the proton nuclei in the -CH_2 groups in glycols and methoxyglycols and unfortunately overlaps with those signals. There is a number of methods in which one can deal with this problem. One of them is solvent suppression or so-called solvent presaturation. In this type of experiments a long low-power pulse is applied on the solvent resonance frequency before the pulse sequence is used to excite the nuclei of the remaining species. The applied RF pulse tips the magnetization of the water solvent resonance to transverse plane, while the field gradient dephases magnetization, resulting in water signal being invisible in the spectrum [119]. There is a number of pulse programmes and methods which use this principle, however, they all suffer from one important flaw. Unfortunately, the resonating frequencies of -CH_2 groups overlap with -OH/D's, which means that the intensities and areas of these peaks may be compromised by the presaturation RF pulse. Another possibility to remove the -OH/D signal was using a ^{1}H-filtered-through-^{13}C NMR method. As it is obvious from its

name, it registers the ^{1}H nuclei which are attached to ^{13}C nuclei, therefore proton in the -OH/D is not registered. The idea behind this method is similar to the HSQC experiments, however it is considerably shorter and the resulting spectrum is not a plane but a typical spectrum of intensity plotted against chemical shift. The registered signals are split, i.e. for each detected proton there are two peaks and each of them constitutes to about half of the total signal for the proton. Moreover, since the signal is filtered through ^{13}C nuclei, the intensity is low and during concentration calculations one must remember that instead of assuming a 100% abundance, each peak is a signal proportional to $\frac{1.1\%}{2}$, as it is decreased significantly by low ^{13}C abundance. Despite a number of carefully ran test experiments and adjustments to the program, there was a small water-related signal visible as a wiggle in the baseline very close to the $-CH_2$ groups signal. The decision was made that this technique, despite having a good potential especially in the kinetics experiments would not be further developed. The main reason for this was that the risk of the intensities of $-CH_2$ groups peaks being affected by the residue of water signal was relatively high and there was no certainty that the residue did not contain by coincidence signals from $-CH_2$ groups. Eventually, successful deconvolutions of the -OH/D and $-CH_2$ signals were performed, allowing simple ^{1}H NMR experiments to be used in qualitative analysis. All spectra were deconvoluted using Origin 8.1 software and the shape of peaks was assumed to be Lorentzian [115]. For each spectrum, the range of chemical shifts containing the -OH/D and $-CH_2$ signals was closely investigated and using assignments discussed above, approximate positions of peaks were picked for species found by ^{13}C NMR at given solution concentrations. Should they be visible as shoulders or spikes on the -OH/D peak, they were picked for deconvolution. An example of deconvolution

performed on the discussed part of the ^{1}H NMR spectrum is shown in Figure 25.

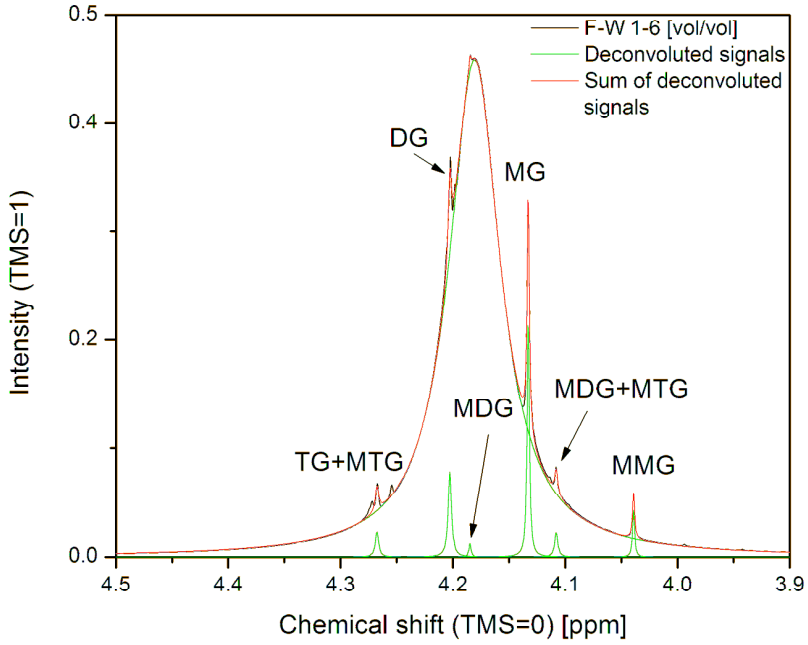

Figure 25. An example of deconvolution of -OH/D and -CH_2 region of ^{1}H NMR spectrum of formaldehyde-water solution (volumetric ratio 1:6).

The positions of the peaks fitted in the process of deconvolution (green lines in Figure 25) are found automatically by the software, basing on the estimate provided by the user. Unfortunately, in a number of situations peaks for species which according to the results from ^{13}C NMR were present in the solution but in very low concentrations, could not be found in ^{1}H NMR spectrum and therefore not taken into account for deconvolution, resulting in some error in quantitative analysis of proton spectra.

An additional factor determining the position of peaks in ^{1}H NMR spectra is the temperature. This factor had to be investigated due to the fact that the

experiments on kinetics of the reaction were performed at a higher temperature of 55°C (328K). Different insert was therefore required, as TMS has a boiling point at 25-26°C. The choice was made for non-deuterated benzene, which normally has a signal at 7.36 ppm (when $\delta_{TMS} = 0$ ppm). A coaxial insert containing this substance was prepared and then a number of ^{1}H NMR experiments in different temperatures was performed. The temperature range was chosen from 10°C (283K) to 55°C (328K) with increments of 5°C; this range covered temperatures above the melting point of benzene and reacting solution and below boiling point of these two and also covered the temperature in which reaction would be examined. It can be assumed that the distribution of the species found in formaldehyde and water solution differs with changing temperature, however this was not further investigated here since the purpose of these specific experiments was to observe the changes in chemical shift of the observed signals. It was observed that when increasing the temperature, it appeared that all peaks move to greater values of chemical shift, which is a sign of decreasing degree of shielding. This can be attributed to changes in the nature of hydrogen bonds in higher temperatures. However, in order to properly investigate the influence of the temperature on the migration rate of peaks other than benzene, the chemical shift of benzene was always set to 7 ppm and the intensity of this signal was set to 1. Figure 26 shows an example of three proton NMR spectra collected for the same sample in different temperatures. It can be clearly seen that the chemical shift of all peaks changes, also for the -OH/D peak.

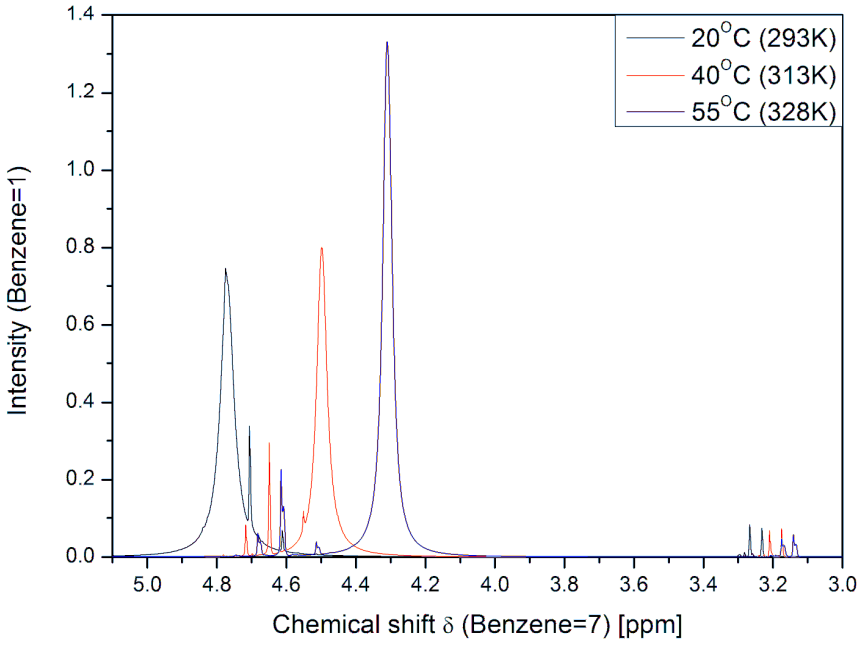

Figure 26. Example of three overlaid ^{1}H NMR spectra of formaldehyde stock solutions diluted with water at volumetric dilution 1:6 at three different temperatures.

The changes of chemical shift of the –OH/D peak are significant and linearly correlated with the changes of temperature, as it can be seen in Figure 27. Once the chemical shift of benzene was locked at a constant value, investigation of the relative migration of other peaks with temperature was possible. The signal of the –OH/D group travels to the lower values of the chemical shift – upfield, towards greater shielding. At 20°C the –OH/D peak overlaps with signals from -CH_2 groups but as it travels to lower values of chemical shift at higher temperatures, it overlaps less with them, despite the fact the whole group migrates. However, the rate at which peaks corresponding to glycols move with temperature appears much smaller than that for –OH/D. As it can be seen in Figure 27, the changes in chemical shift

values can be correlated linearly with temperature and the slopes of the linear regression compared, leading to an observation that the –OH/D peak moves nearly 5 times faster than MG signal (exactly 4.65, basing on the obtained spectra). The exactly same rate is observed for all other signals in the examined sample.

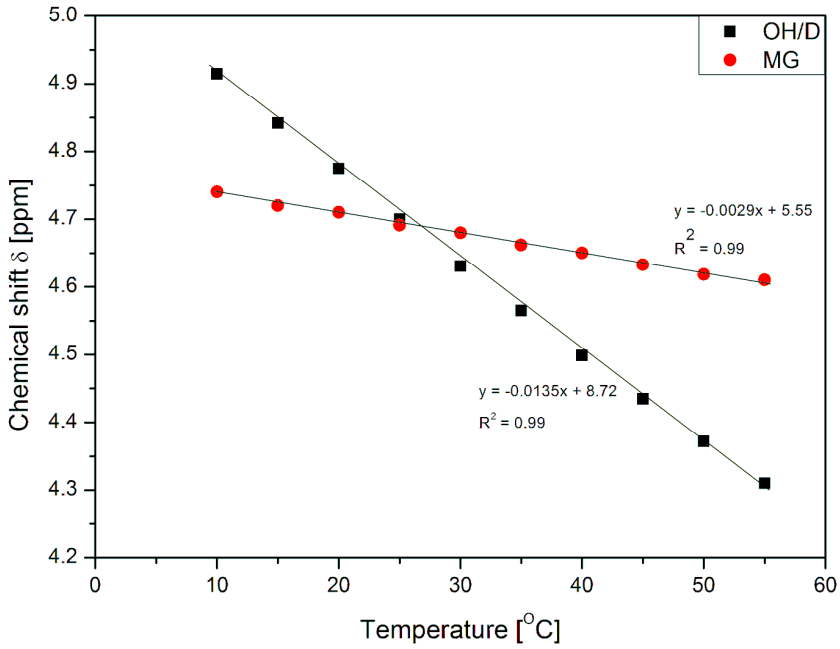

Figure 27. Changes of chemical shift of -OH/D and MG (HO-C**H**$_2$-OH) peaks in ^{1}H NMR caused by temperature increase.

Values of chemical sifts of all observed peaks for five chosen temperatures are compiled in Table 7. As it was mentioned earlier, the greatest changes are observed for the –OH/D peak, which migrated by 0.60 ppm in a temperature change of 45°. In practice this means that an increase of 1° causes the peak to move upfield by 0.01(3) ppm. The effect of a 45° increase in the temperature leads to change of chemical shift for other species by 0.12-0.14 ppm, which means 0.003 ppm per 1°, on average.

Table 7. Chemical shifts of observed peaks in five chosen temperatures.

Temperature [K] → Assignment ↓	**283**	**293**	**303**	**313**	**328**
Benzene	7.00				
C**H**$_3$-OH	3.26	3.23	3.20	3.18	3.14
HO-CH$_2$-O-C**H**$_3$	3.30	3.27	3.24	3.21	3.17
HO-C**H**$_2$-O-CH$_3$	4.64	4.61	4.58	4.55	4.51
HO-C**H**$_2$-OH	4.74	4.71	4.68	4.65	4.61
HO-C**H**$_2$-O-C**H**$_2$-OH	4.81	4.77	4.74	4.72	4.68
-O**H**/D	4.91	4.78	4.63	4.50	4.31

The assignment of peaks in the ^{1}H NMR spectra for the formaldehyde stock solutions diluted with water at volumetric ratio 1:6 at 55°C (328K) proved to be very valuable in the experiments involving kinetics at this temperature. Knowledge of the dependency of chemical shift on the temperature and its quantification permitted appropriate assignment of all formaldehyde-related peaks without any doubt and identification of the new ones, resulting mostly from CH_2 groups bound to resorcinol.

4.1.3. Quantitative analysis

Results obtained from ^{13}C NMR experiments allowed determination the quantitative speciation in formaldehyde-water-methanol solutions. It is known that during the manufacturing process, when formaldehyde is produced *via* methanol oxidation and is absorbed in water, it forms methylene glycol and its oligomeric forms. These forms are in mutual equilibria and the speciation in of aqueous or alcoholic solutions is dependent on the volumetric ratios of formaldehyde stock solution and diluent solvent.

For all solutions prepared by diluting formaldehyde stock solution, a calculation was performed in order to determine what should be the composition of each solution in terms of the total formaldehyde, methanol and water concentrations. The information provided by the manufacturer in the analysis of quality datasheets was treated as a basis for these calculations. The amount of formaldehyde is given as weight percentage corresponding to weight of formaldehyde as aldehyde absorbed in the resulting solution. This means that for purposes of transforming mass concentration of formaldehyde stock solution into molar concentration, the molar weight is to be taken as molar weight of formaldehyde, i.e. 30.03 g·mol^{-1}. The following equations can be used in order to convert mass concentration (C_p) into molar concentration (C_n): $C_p = \frac{m_{sub}}{m_{sol}} \cdot 100\%$, $C_n = \frac{n}{V}$ and $d = \frac{m}{V}$, where m_{sub} refers to the mass of substance dissolved in the mass of solution (m_{sol}); n is the number of mols and V is the volume. After rearranging these equations and unifying the units the following equation was obtained:

$$C_n = \frac{10 \cdot C_p \cdot d}{M_W} \tag{23}$$

where M_w is molecular weight of formaldehyde [g·mol^{-1}] and d is density of its solution [g·cm^{-3}].

Formaldehyde stock solution containing 37%wt. of formaldehyde, 13%wt. of methanol and having density equal to 1.09 g·cm^{-3} contains 13.43 mol·dm^{-3} formaldehyde and 4.16 mol·dm^{-3} methanol. When calculations of concentrations for each prepared solution were performed an approximation was made that the volume change upon mixing is not of significant magnitude. In practice this meant that the volume of the prepared solution is assumed to be equal to the sum of volumes of mixed fluids.

Calibration of NMR signals

As it was explained in the experimental procedures description, the ratio of signals resulting from the sample and from the coaxial insert containing reference substance needs to be taken into account when concentrations are being calculated basing on the values of measured areas. The measured signal is proportional to the number of atoms (or mols) of given nuclei, which means that if we consider a NMR tube with a coaxial insert of certain length (50 mm) inside, the ratio of signals from the sample and the reference should be the same as the ratio of volume of the sample and the volume of the reference, if they both contain the same solution. According to the specifications provided by the manufacturer, the volume of the sample is 530 μl and the volume of the reference is 60 μl, which means that the sample signal is 8.8(3) times greater than that of the reference for the same substance in both compartments. In order to confirm the ratio of sample to reference signals, two coaxial inserts were prepared: one containing TMS and the other 3.125 $mol \cdot dm^{-3}$ methanol in water and D_2O (volumetric ratio 7:3). One NMR tube was filled with TMS and then a coaxial insert containing 3.125 $mol \cdot dm^{-3}$ methanol solution was inserted, the tube securely sealed. The other NMR tube was filled with 3.125 $mol \cdot dm^{-3}$ methanol solution and an insert with TMS was inserted and the tube securely sealed. The samples were investigated using the same pulse program with long delay time and Nuclear Overhauser Effect removed and then the results were analysed. The theoretical ratio of signal areas resulting from ^{13}C nuclei in methanol and in TMS at these concentrations was calculated as follows:

$$Ratio = \frac{C_{n,TMS} \cdot N_{13C}}{C_{n,MeOH} \cdot N_{13C}} = \frac{7.345 \cdot 4}{3.125 \cdot 1} = 9.40 \qquad (24)$$

Where $C_{n,MeOH}$ and $C_{n,TMS}$ are molar concentrations of methanol and TMS, respectively, and N_{13C} is the number of carbon nuclei in the compound. The measured ratio of signals when methanol was the sample was equal to 84.08, which is 8.943 times more than expected if the both compartment volumes were the same. Similar result was obtained for sample containing TMS and methanol as an insert, however, this result was treated only as an indication due to high volatility of TMS which could not be prevented over 18 hours of experiment (the volume of the sample decreased). The value which was used to normalize the areas of peaks from the compounds in the sample was the experimental one (8.943); it is about 11% greater than theoretically calculated one based on volumes indicated by the manufacturer.

In order to determine the concentration of each detected compound in the examined solution a number of calculations were conducted. For each obtained spectrum the first step was to correct the baseline, phase and to set chemical shift of the reference signal to a given value (for TMS it was 0 ppm). After all peaks were found, manual integration of the areas beneath them was performed using either way Bruker® TopSpin ver. 2.0 or Origin 8.1 software. As it was explained above and in description of the experimental methods, the signal resulting from the sample is 8.943 times greater than the signal from the insert. Therefore, areas of all peaks need to be divided by this factor, in order to be proportional to the signal of reference. The area beneath TMS signal corresponds to four ^{13}C nuclei and to concentration equal to 7.345 mol·dm^{-3}. Since some of the detected peaks correspond to more than one ^{13}C nucleus, a unit area (U_A) corresponding to one ^{13}C nucleus at concentration equal to 1 mol·dm^{-3} was calculated:

$$U_A = \frac{Area\ of\ reference\ signal}{7.345 \cdot 4} \tag{25}$$

The average value of this area was $3.38 \cdot 10^8$ and it varied slightly across all measurements by ±1.9%. In order to provide the best accuracy of calculations, the value of U_A was calculated for every measurement. Once the value of U_A was established, calculations of concentrations for each compound were performed according to the following equation:

$$C_n = \frac{area\ of\ the\ peak}{8.943 \cdot U_A \cdot N_{13C}} \tag{26}$$

Where the area of the peak is a result of integration of the spectrum where peak was found, 8.9431 is used to normalize the signal from the sample to ensure proportionality to the reference signal, U_A is the area corresponding to 1 mol·dm^{-3} of ^{13}C nuclei and N_{13C} is the number of ^{13}C nuclei which resonate at frequency of a given peak.

Determination of species concentrations

The results obtained from ^{13}C NMR were compared with calculated concentrations. In each case two values were calculated: total formaldehyde and total methanol concentration. As it is shown further, the concentration of methanol specified by the manufacturer corresponds to the amount of methanol in forms of free methanol and methoxy groups attached to glycols. Total formaldehyde was calculated as a sum of concentrations of each chemical compound containing carbon atoms (but not methanol) multiplied by the number of carbon atoms in the molecule, as each carbon corresponds to one molecule of formaldehyde. Results of from measurements and the calculated concentrations were compared and then the difference was expressed as:

$$Difference = \left|\frac{calculated\ concentration - measured\ concentration}{calculated\ concentration}\right| \cdot 100\% \quad (27)$$

It is safe to assume that when dealing with samples which are not enriched in ^{13}C isotope, the difference between calculated and measured concentrations lower than 10% is very satisfactory. Table 8 and Table 9 present comparison between calculated and measured concentrations of formaldehyde-related species and total methanol along with the difference between them, expressed in per cent.

Table 8. Calculated and measured concentrations of total methanol (CH_3O-groups) and formaldehyde species in solutions prepared by dilution of formaldehyde stock solutions with water (^{13}C NMR).

F-W [vol/vol]	Total CH_3-groups - measured [mol/dm^3]	Total CH_3-groups - calculated [mol/dm^3]	Difference [%]	Total F-species - measured [mol/dm^3]	Total F-species - calculated [mol/dm^3]	Difference [%]
1/3	1.08	1.02	5.52	3.18	3.36	5.40
1/6	0.59	0.58	2.71	1.85	1.92	3.53
1/10	0.37	0.37	0.52	1.19	1.22	2.27
1/30	0.14	0.13	3.29	0.43	0.43	1.09
1/60	0.06	0.07	5.62	0.21	0.22	4.47

Table 9. Calculated and measured concentrations of total methanol (CH_3O groups) and formaldehyde species in solutions prepared by dilution of formaldehyde stock solutions with methanol (^{13}C NMR).

F-MeOH [vol/vol]	Total CH_3-groups - measured [mol/dm^3]	Total CH_3-groups - calculated [mol/dm^3]	Difference [%]	Total F-species - measured [mol/dm^3]	Total F-species - calculated [mol/dm^3]	Difference [%]
1/3	16.88	15.60	8.21	2.85	2.69	6.12
1/6	18.50	17.87	3.54	1.60	1.58	1.13
1/10	19.71	19.26	2.31	1.08	1.03	4.45
1/30	21.05	20.08	4.84	0.38	0.36	5.32
1/60	20.60	20.30	1.48	0.19	0.18	4.65

It can be clearly seen that the differences are all well below 10% (apart from F-W dilution 1/30) which leads to the conclusion that the method developed here is reliable and suitable for quantitative study of formaldehyde speciation. However, it is considerably time consuming, since due to very long relaxation times (see 4.1.1) a single experiment comprising of 1024 scans for good signal to noise ratio lasts approximately 18 hours, making ^{13}C NMR impractical in terms of kinetics analysis, despite excellent accuracy.

An important observation is that the concentration of methanol in its pure form (CH_3OH) is not a linear function of overall formaldehyde stock solution concentration, as can be seen clearly in Figure 28. The theoretical concentration of methanol was calculated under the assumption that it changes linearly with the dilution and that the starting concentration (at lowest dilution, in formaldehyde stock solution) is equal to the methanol concentration as specified by the manufacturer. When plotted against concentration of formaldehyde-related species, the total concentration of all methoxy groups overlaps with the calculated concentration for methanol. However, the data collected for methanol in its free form do not form a linear pattern. This confirms that the value specified by the manufacturer should be referred to as "overall methanol" and that it includes both free and bound methanol. The fact that the data points for free methanol do not form a straight line, like others do, proves that methoxylated formaldehyde-related species are in equilibria with free methanol and they are subject to water dilution.

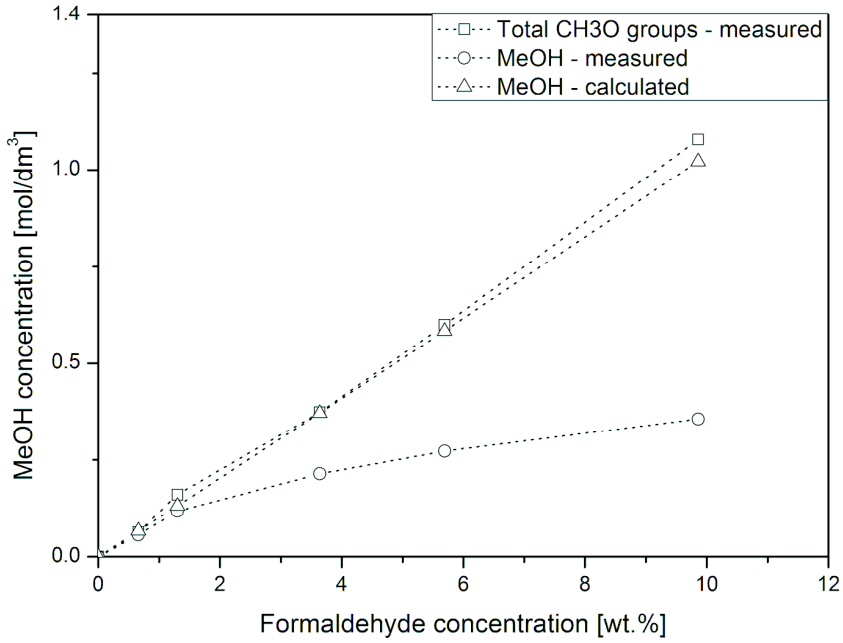

Figure 28. Methanol and methoxy groups concentrations calculated and measured by ^{13}C NMR against overall formaldehyde concentration.

Results obtained from ^{13}C NMR allowed not only to calculate the total concentrations resulting from formaldehyde and methanol-related species but also to describe the distribution of these species and the changes in speciation with changing amount of diluent, either water or methanol. The calculated concentrations of each species detected in the tested solutions are shown in Table 10 and Table 11. The Table 10 shows distribution of species found in solution prepared by dilution of formaldehyde stock solution with water. It can be seen that the total concentration of formaldehyde-related species changes proportionally with dilution, which is to be expected as the total mass balance of formaldehyde needs to be preserved. However, when analysing the data one will easily notice that the form of formaldehyde which remains in the solution when the concentration decreases to very low

values is the simplest one: methylene glycol (MG, HO-CH_2-OH). The more concentrated solution, the longer the chains of oligooxyglycols are present. Moreover, an increase in an overall concentration leads also to higher concentrations of methoxylated forms.

Table 10. Concentrations of formaldehyde-related species detected by ^{13}C NMR in formaldehyde-water solutions.

F-W						
Name	**Assignment**	**1-3**	**1-6**	**1-10**	**1-30**	**1-60**
		9.86 %wt. F	**5.69 %wt. F**	**3.64 %wt. F**	**1.30 % wt. F**	**0.66 %wt. F**
		Concentration [mol/dm^3]				
TMS	TMS	7.3454				
MeOH	**C**H_3OH	0.3562	0.2728	0.2141	0.1060	0.0565
MMG	**C**H_3O-CH_2-OH	0.5900	0.2947	0.1520	0.0302	0.0068
MDG	**C**H_3O-CH_2-OCH_2-OH	0.0955	0.0252	0.0074	0.0000	0.0000
MTG	**C**H_3O-CH_2-OCH_2-OCH_2-OH	0.0283	0.0071	0.0000	0.0000	0.0000
MG	HO-**C**H_2-OH	1.6769	1.1818	0.8747	0.3720	0.1975
DG	HO-**C**H_2-O-**C**H_2-OH	0.3392	0.1573	0.0752	0.0131	0.0030
TG	HO-**C**H_2-O-CH_2-O-**C**H_2-OH	0.0493	0.0137	0.0043	0.0000	0.0000

A more visual presentation of how the distribution of formaldehyde-related compounds changes with dilution can be done by analysing the molar fractions. Concentrations of all detected species were expressed as molar fractions of total formaldehyde (measured) and then these values were plotted against the total formaldehyde concentration and shown in Figure 29.

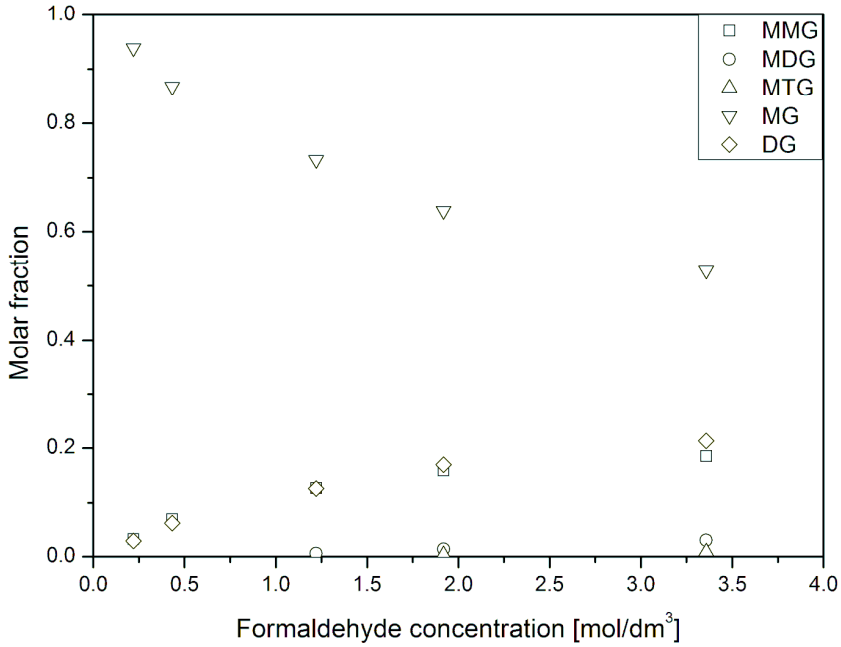

Figure 29. Concentration distribution of formaldehyde related species expressed by molar fractions against total formaldehyde concentration.

As it can be noticed when analysing the data for solutions prepared by dilution of the stock formaldehyde with methanol from Table 11, the speciation in more dilute samples is less complex than in corresponding aqueous dilutions. For example, let us compare the dilutions 1:30. In the aqueous one there are four detectable species: MG, DG, MMG and free methanol. The dominant species is MG, then four times less concentrated methanol. MMG concentration is as much as ten times lower than MG's and DG's concentration equals only 5% of MG's. Should the diluent be replaced by methanol, there are only two species: free methanol and MMG. The concentration of methanol is very high due to the fact it is added as the diluent, so it is not a value to be compared with aqueous dilutions. The concentration of MMG is relatively low, especially that it is the only

formaldehyde-related species that is detected in this dilution. Interestingly enough, dilutions at 1:60 in water and methanol consist of four and two species, respectively. Therefore, when forming the equilibria between all formaldehyde-related species and calculating their constants, it is more reliable to use data collected from the aqueous dilutions, as they allow to cover a wider range of species and concentrations. The results obtained from formaldehyde-methanol samples would allow to cover one of the equilibria at not more than three concentrations, as it is shown further on. For the same reasons representation of species distribution in terms of molar fractions is far less useful than in formaldehyde-water dilutions, and therefore is omitted.

Table 11. Concentrations of formaldehyde-related species detected by ^{13}C NMR in formaldehyde-methanol solutions.

F-MeOH						
Name	**Assignment**	**1-3**	**1-6**	**1-10**	**1-30**	**1-60**
		11.66 %wt. F	**6.92 %wt. F**	**4.49 %wt. F**	**1.63 %wt. F**	**0.83 %wt. F**
		Concentration [mol·dm^{-3}]				
TMS	TMS	7.34				
MeOH	**C**H$_3$OH	14.0912	17.0091	18.6359	20.6724	20.4091
MMG	**C**H$_3$O-CH$_2$-OH	2.7280	1.4185	1.0568	0.3823	0.1925
MDG	**C**H$_3$O-CH$_2$-OCH$_2$-OH	0.0562	0.0533	0.0133	0	0
MTG	**C**H$_3$O-CH$_2$-OCH$_2$-OCH$_2$-OH	0	0.01960	0	0	0
MG	HO-**C**H$_2$-OH	0.0433	0.0256	0.0089	0	0
DG	HO-**C**H$_2$-O-**C**H$_2$-OH	0.0068	0.0323	0	0	0
TG	HO-**C**H$_2$-O-CH$_2$-O-**C**H$_2$-OH	0.0045	0	0	0	0

4.1.4. Glycol and methoxyglycol equilibria and equilibria constants

The aim of quantitative analysis of data collected in NMR experiments has been to obtain the distribution of formaldehyde-related species concentrations. Knowledge of these allows determination of equilibria constants and thus may be useful in prediction of speciation in solutions of formaldehyde in a wide range of applications using formaldehyde as a reactant.

It is known that during the manufacturing process formaldehyde in the form of aldehyde is absorbed in water and reacts readily with it upon absorption [120]. The aldehyde compounds are solvated with water at mole ratio 1:1 and they form methylene glycol or its oligomers:

$$CH_2O + H_2O \rightleftharpoons \underset{\text{methylene glycol}}{HO(CH_2O)H}$$

$$HO(CH_2O)_{i-1}H + HO(CH_2O)H \rightleftharpoons \underset{\text{oligomeric methylene glycol}}{HO(CH_2O)_iH} + H_2O \qquad (28\&29)$$

Due to the fact that 100% conversion of methanol into formaldehyde in the production process is not attainable, it remains in the product stream leaving the reactor and is directed into the absorber with formaldehyde, where the latter one is absorbed in water. Since methanol is not removed at any stage preceding the absorption, it remains in the final solution. The actual concentration of methanol tends to vary, therefore the manufacturers usually specify a range of methanol concentration in their product. However, on request exact data is provided for a given batch. The presence of methanol in the formaldehyde solution is desired as it extends shelf life of the product by not allowing formaldehyde to polymerize into poly(oxymethylene) (POM).

Polymerization is suppressed by esterification of formaldehyde through reaction with methanol (or other alcohol):

$$CH_2O + CH_3OH \leftrightarrow H_3CO(CH_2O)H + H_2O \quad (30)$$

It is a reversible reaction and therefore it is the dilution that controls this reaction equilibrium.

Based on basic chemistry of formaldehyde-methanol aqueous solutions and qualitative information obtained from the NMR spectroscopy the following equilibrium model can be formed:

$$CH_2O + H_2O = MG \quad (31)$$

$$MG + MG = DG + H_2O \quad (32)$$

$$DG + MG = TG + H_2O \quad (33)$$

$$MG + MeOH = MMG + H_2O \quad (34)$$

$$DG + MeOH = MDG + H_2O \quad (35)$$

$$TG + MeOH = MTG + H_2O \quad (36)$$

Where:

MeOH - CH_3OH

MG - $HO\text{-}CH_2\text{-}OH$

DG - $HO\text{-}CH_2\text{-}O\text{-}CH_2\text{-}OH$

TG - $HO\text{-}CH_2\text{-}O\text{-}CH_2\text{-}O\text{-}CH_2\text{-}OH$

MMG - $CH_3O\text{-}CH_2\text{-}OH$

MDG - $CH_3O\text{-}CH_2\text{-}OCH_2\text{-}OH$

MTG - $CH_3O\text{-}CH_2\text{-}OCH_2\text{-}OCH_2\text{-}OH$

None of these reactions is isolated – they all take place in the same solution at the same time, therefore they are mutually related. In order to address this issue, the total molar concentration of water in the sample – W_{tot} – is introduced. This concentration includes water from the formaldehyde stock solution and water added as diluent (sum of these equal to W), minus the water which is the product of each reaction in which any glycol (MG, DG, TG) is produced. Since the stoichiometric ratio of water to any glycol produced is 1:1, then: $W_{tot} = W - MG - DG - TG$.

For each of the reaction written above, a concentration based equilibrium constant can be calculated using the following equations:

$$K_1 = \frac{C_{DG} \cdot W_{tot}}{C_{MG}^2} \tag{37}$$

$$K_2 = \frac{C_{TG} \cdot W_{tot}}{C_{MG} \cdot C_{DG}} \tag{38}$$

$$K_3 = \frac{C_{MMG} \cdot W_{tot}}{C_{MG} \cdot C_{MeOH}} \tag{39}$$

$$K_4 = \frac{C_{MDG} \cdot W_{tot}}{C_{DG} \cdot C_{MeOH}} \tag{40}$$

$$K_5 = \frac{C_{MTG} \cdot W_{tot}}{C_{TG} \cdot C_{MeOH}} \tag{41}$$

Where C_X refers to the molar concentration of a given species (X) in the state of equilibrium, i.e. the concentration measured using the ^{13}C NMR spectroscopy.

The values of these constants were calculated basing on concentrations measured in aqueous dilutions and the results of calculations are shown in Table 12. It is worth to underline that the equilibria constants calculated from formaldehyde-methanol dilutions would be based on only three dilutions, because in dilutions at formaldehyde to methanol ratio larger than 1:10 it is not possible to detect MG, DG or TG due to their extremely low concentrations caused by the fact that large amount of methanol present in the dilution shifts the equilibrium towards MMG.

Table 12. Equilibrium constants calculated basing on the concentration distributions measured by ^{13}C NMR at 293K.

	F-W					
Equilibrium constant	**1-3**	**1-6**	**1-10**	**1-30**	**1-60**	**Average value**
	9.86 %wt. F	**5.69 %wt. F**	**3.64 %wt. F**	**1.30 %wt. F**	**0.66 %wt. F**	
K_1	5.71	5.71	5.15	6.51	4.29†	5.77
K_2	4.11	3.73	3.45			3.76
K_3	46.8	46.4	42.5	46.4	33.5†	45.5
K_4	37.5	29.8	24.1			30.5
K_5	76.3	96.2				86.3

N.B.: † values not used to calculate average value (treated as subject to gross error)

By definition, the value of equilibrium constant should not depend on the concentration of the reactants, as it expresses the mutual dependency of concentrations in a state of equilibrium. In practice this means that altering the concentration of one of the reactants or the products, changes the concentrations of other species in a way in which the values of their mutual ratios (expressed by the equilibrium equations) are preserved. In light of this

fact, the results shown in Table 12 are consistent with expectations. The fluctuations in K values across concentrations are reasonable and result from errors in the quantitative analysis on the ^{13}C NMR spectra. Comparison of the K values results in very interesting observation. With methanol present in the solution, the values of K indicate that MG and oligooxyglycols are more susceptible of reacting with methanol and forming methoxylated forms like MMG, MGD and MTG rather than forming longer oligooxyglycols. Values of equilibrium constants for these reactions are 45.5, 30.5 and 86.2, respectively, while equilibrium constants of reactions leading to DG and TG formation are smaller by one order of magnitude – 5.77 and 3.76, respectively. Unfortunately, it is impossible to determine the equilibrium constant for MG formation, as no measurable amount of formaldehyde in the form of a glycol is detected in the solution. Therefore, this equilibrium constant is expected to be very high and indeed the equilibrium constant of formaldehyde hydration has been estimated to be around 2000 at ambient conditions [38]. Moreover, presence of methanol to aqueous solution certainly affects activity coefficients and this may explain the discrepancies between values of calculated Ks for methanolic and aqueous solutions, as these were calculated using concentrations only.

It was considered that the values of equilibrium constants K_1 and K_3 may be temperature dependent and therefore a series of ^{1}H NMR experiments on formaldehyde-water solution (1:6 by volume) was performed covering a range of temperatures from 283K to 328K (10-55°C) with an increment of 5 degrees. All spectra required the same processing as those obtained in experiments performed in 293K, i.e. deconvolution and integration. Absolute concentrations of MG, DG, MMG and MeOH were obtained and equilibrium constants K_1 and K_3 were calculated as previously, yielding values shown in

Table 13. It is clear that the equilibrium constant of DG formation (K_1) oscillates around a certain mean value of 4.1 while there is no obvious temperature-dependent trend discernible within margins of experimental errors. The values may vary mostly because the OH signal travelled with the temperature and in some cases may have caused deconvolution of the DG signal to be less accurate and therefore subject to greater error, which was then reflected in the calculated DG concentration. On the other hand, when analysing values for K_3, which corresponds to MMG formation, one may easily notice a trend which is also shown in Figure 30. It appears that the equilibrium constant K_3 decreases with increasing temperature, suggesting that less MMG is present in higher temperatures. As a result more MG and free MeOH is present. This phenomenon is favourable from the point of view of the resorcinol-formaldehyde reaction, as in higher temperatures more MG is available for reaction which would partially contribute to greater reaction rates in elevated temperatures.

Table 13. Values of K_1 and K_3 equilibrium constants in temperature range of 283-328K. N.B.: Deconvolution of signals at 328K was subject to gross error due to untypical shape of peaks caused by unresolvable issues with shimming.

Temperature [K]	**Equilibrium constant value**	
	K_1	**K_3**
283	3.85	53.81
288	3.53	45.44
293	5.71	46.37
298	3.17	43.07
303	2.52	37.61
308	5.16	36.31
313	-	34.83
318	2.06	33.22
323	4.52	30.91
328	*6.08*	*40.58*

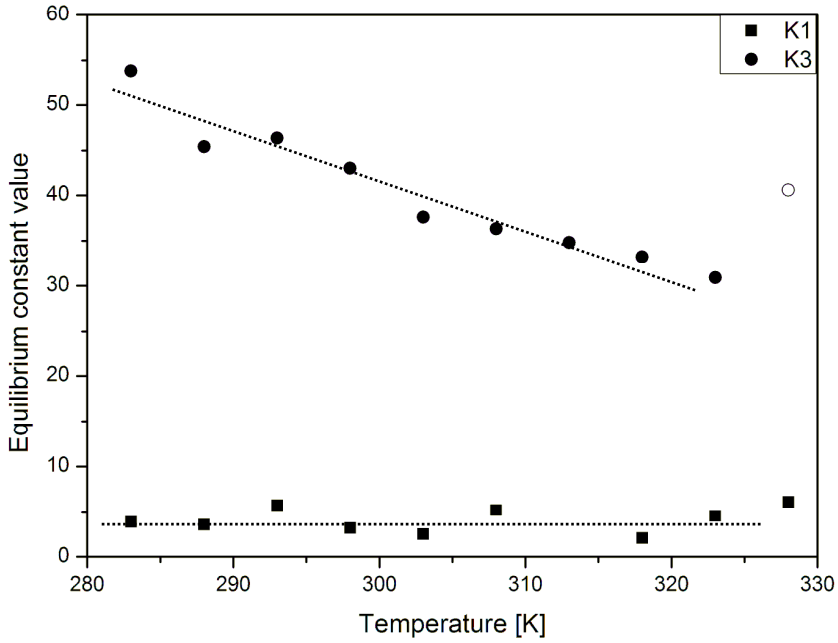

Figure 30. Temperature dependency of K_1 and K_3 equlibrium constants. The empty point for K_3 value at 328K represents value which was considered to be an outlayer in the trend and was not taken into consideration when defining a trendline (see N.B. in Table 13 for details).

Results obtained in this research work can be compared with those obtained by Hahnenstein et. al. [48]. In their work, the researchers focused on both ^{1}H and ^{13}C NMR investigations on formaldehyde-water and formaldehyde-methanol solutions prepared by depolymerisation of POM in an appropriate solvent. Therefore the composition of these solutions is different from the ones studied here because Hahnenstein et. al. did not add both methanol and water to formaldehyde but chose only one solvent at a time. At the same time, formaldehyde stock solution used in this research was aqueous and already contained a certain amount of methanol. The results obtained by Hahnenstein et. al. are comparable with those obtained in this work.

Equilibrium constants equivalent to K_1 and K_2 were 6.77 and 4.20, respectively, which makes them different by approximately 17% and 11%. These discrepancies are not significant and can be even considered very similar especially when the difference in compositions of the solutions is taken into consideration. This proves that the approach chosen by the author of this work proves valid also for mixed solvents solutions.

In the most popular method of formaldehyde production methanol is partially oxidised to form formaldehyde and some of the methanol remains in the product solution. The conversion rate is lower than 100% and varies from one installation to another, therefore the concentration of methanol can vary. Nonetheless, it is desirable for it to be present in the final product solution, as it prevents polymerization of formaldehyde into poly(oxymethylene), which in turn decreases the concentration of reactive species of formaldehyde in the solution, making it less valuable. The results shown in Table 12 help to explain why the addition of methanol prevents formaldehyde polymerization, as formation of methoxylated species is more favourable.

Identification of equilibrium constants of these reactions in formaldehyde-water-methanol solutions is very important, as most of the previous research on these equilibria was done for methanol-free dilutions. The practical application of these results is possibility of speciation prediction, where methanol concentration is taken into account.

4.2. IR and Raman spectroscopy

IR and Raman spectroscopies were used in addition to NMR to investigate formaldehyde solutions. The aim was to identify what information about

formaldehyde speciation in aqueous-methanolic solutions can be gained using these methods and to assess their potential for qualitative and quantitative analysis.

4.2.1. Qualitative analysis

As it was mentioned in the methodology section, certain molecules might be invisible in IR due to the fact they have no dipole moment but may be seen in Raman spectra due to their polarizability. Therefore Raman spectroscopy can be considered as complementary to IR. Signals for the same type of bonds may be observed at slightly different wavenumbers in spectra for both spectroscopies, however, for the system investigated here there are signals appearing at similar wavenumbers for both methods as discussed below. Figure 31 shows comparison of IR and Raman spectra for the stock formaldehyde solution, where one can see that there is a large number of resonance frequencies (corresponding to bands denoted A-O in Table 14) in the region of wavenumbers between 800 and 1700 cm^{-1}.

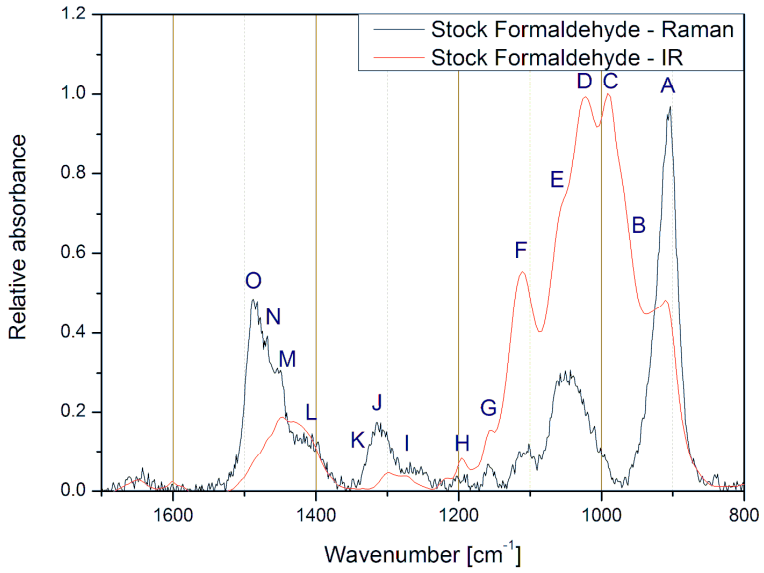

Figure 31. IR and Raman spectra of the stock formaldehyde solution.

Assignments of these bands were based on previously published literature [39] [121] for Raman spectroscopy analysis of aqueous formaldehyde solutions with or without methanol present, as well as limited information available from few previous IR spectroscopy studies [44] [122] [123].

Table 14. Assignments of signals in IR and Raman spectra in solutions prepared by dilution of formaldehyde stock solutions with water and methanol.

Band	Wavenumber [cm^{-1}]		Vibration assignment	Species
	IR	Raman		
A	910-915	905-910	C-O symmetric stretch (in O-C-O)	glycols/ methoxyglycols
B	~ 950	~ 950	C-O symmetric stretch (in O-C-O)	(oligo?)glycols/ methoxyglycols
C	990	995	C-O asymmetric stretch (in O-C-O)	glycols/ methoxyglycols
D	1025	1030	C-O asymmetric stretch (in C-OH)	methanol/glycols/ methoxyglycols
E	1060	1060	C-O asymmetric stretch (in C-OH)	glycols/ methoxyglycols
F	1115	1110	H-C-H out-of-plane (in CH_3)	methanol/ methoxyglycols
G	1160	1155	H-C-H out-of-plane (in CH_3)	methanol/ methoxyglycols
H	1195	1195	H-C-H out-of-plane (in CH_3)	methanol/ methoxyglycols
I	-	1265	H-C-H twisting or wagging (in CH_2)	(oligo?)glycols/ methoxyglycols
J	-	1310	H-C-H twisting or wagging (in CH_2)	(oligo?)glycols/ methoxyglycols
K	-	1320	H-C-H twisting or wagging (in CH_2)	(oligo?)glycols/ methoxyglycols
L	-	1410	C-O-H in-plane bend or H-C-H wagging	methanol/glycols/ methoxyglycols
M	-	1440	C-O-H in-plane bend or H-C-H wagging	methanol/glycols/ methoxyglycols
N	-	1460	C-O-H in-plane bend or H-C-H wagging	methanol/glycols/ methoxyglycols
O	-	1480	H-C-H bending (in CH_2)	glycols/ methoxyglycols

IR measurements

The data which was collected using an ATR probe during IR experiments suffers from a diamond resonance signal at ca. 2000 cm^{-1}, therefore it is reasonable to analyse spectrum below that value. The width of analysed part of the collected spectra ranges from 600 cm^{-1} to 1900 cm^{-1} and it covers the so-called fingerprint region which allows identification of species in the investigated sample. This region is probably the most abundant in information about the types of bonds present in the molecules in the examined sample, although it hardly ever allows to unanimously identify species, especially in complex solutions like those investigated here.

As it is with all spectroscopic techniques, data collected during the measurements was subject to errors caused by background subtraction and noise or drift in the baseline. Background subtraction was done automatically by the software which was used to collect the data during the measurements. In all cases pure distilled water was measured as background, as it was present in all solutions and could also affect the shape of the spectrum. In a number of samples after background subtraction, the baseline changed its shape and could become negative. This was because the signal from water collected at that particular wavenumber was greater than in the sample (this is related to differences in water concentration among various samples). Furthermore, baseline correction had to be performed; this was done semi-automatically using Origin 8.1 software. Baseline correction proved to be necessary in most cases, especially in very dilute solutions, where area integration errors caused by the baseline drift could be significant. The resulting spectra can be seen in Figure 32 and Figure 33.

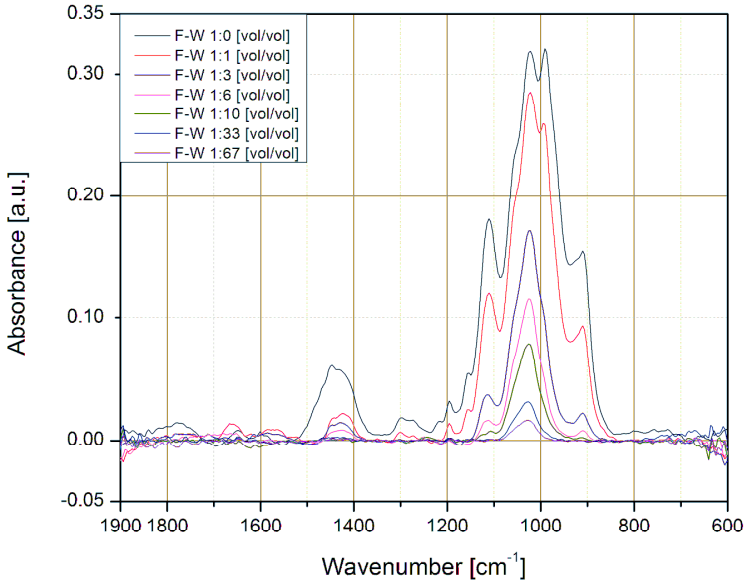

Figure 32. IR spectra (after subtraction of pure water spectrum and baseline correction) of formaldehyde-water solutions.

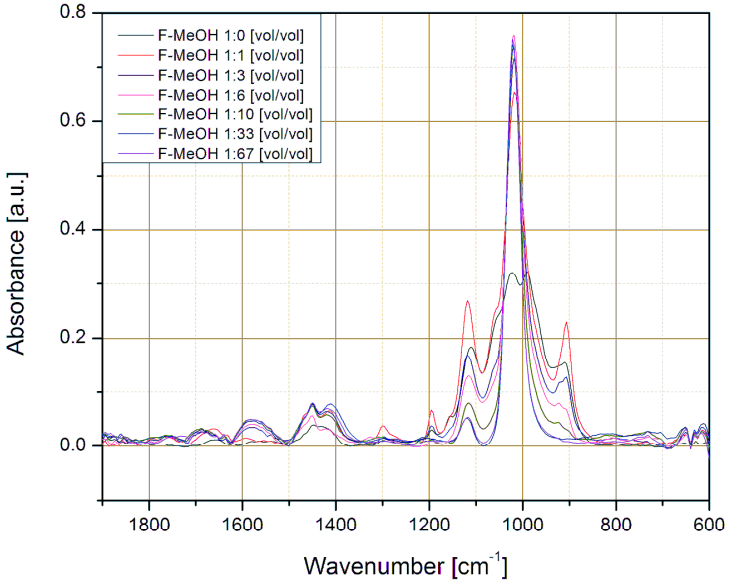

Figure 33. IR spectra (after subtraction of pure water spectrum and baseline correction) of formaldehyde-methanol solutions.

The reason for complexity of the 850-1200 cm^{-1} region is the fact that a number of bonds of very similar nature resonate at these frequencies. The most predominant group of signals at 990-1060 cm^{-1} corresponds to C-O asymmetric stretch vibrations of C-OH bond in primary alcohols, which in case of formaldehyde-water and formaldehyde-methanol solutions means signals from all glycols and methoxyglycols as well as from methanol. However, while methanol has only a single resonance frequency in this group at 1020 cm^{-1}, glycols and methoxyglycols have signals at all three frequencies, due to a different nature (dipole moment) of this bond in these molecules in comparison with methanol.

Raman measurements

Spectra collected in Raman measurements were – just as IR spectra – subject to processing prior to data analysis. In case of Raman spectroscopy the background which was subtracted automatically was also water but inside a polystyrene cuvette, due to the fact that all measurements were taken this way. Baseline correction was also considered important, however, it was not as critical as in case of IR spectra, as the negative intensities or drift in the baseline were less significant. Nonetheless, this was done and the resulting spectra which were analysed are shown in Figure 34 and Figure 35.

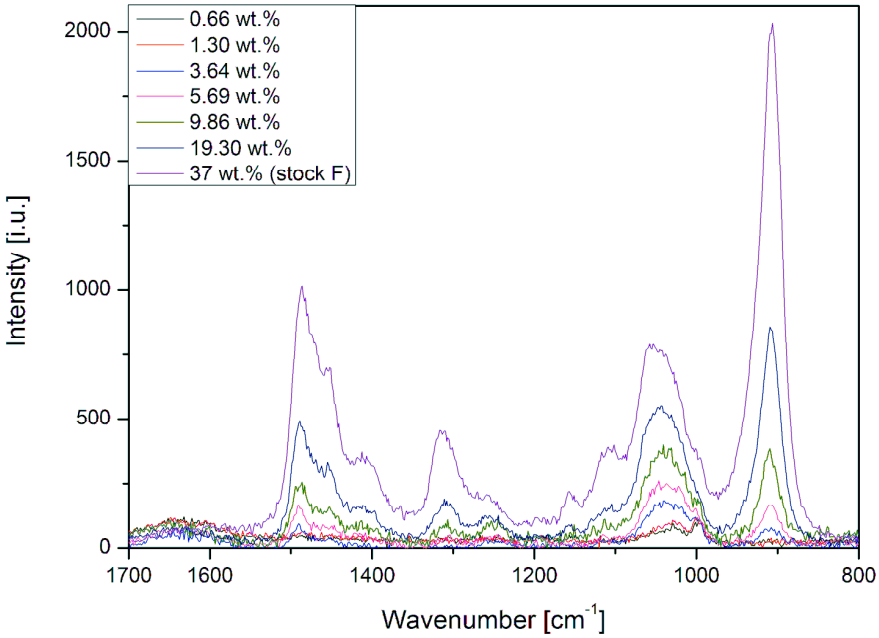

Figure 34. Raman spectra of formaldehyde-water solutions.

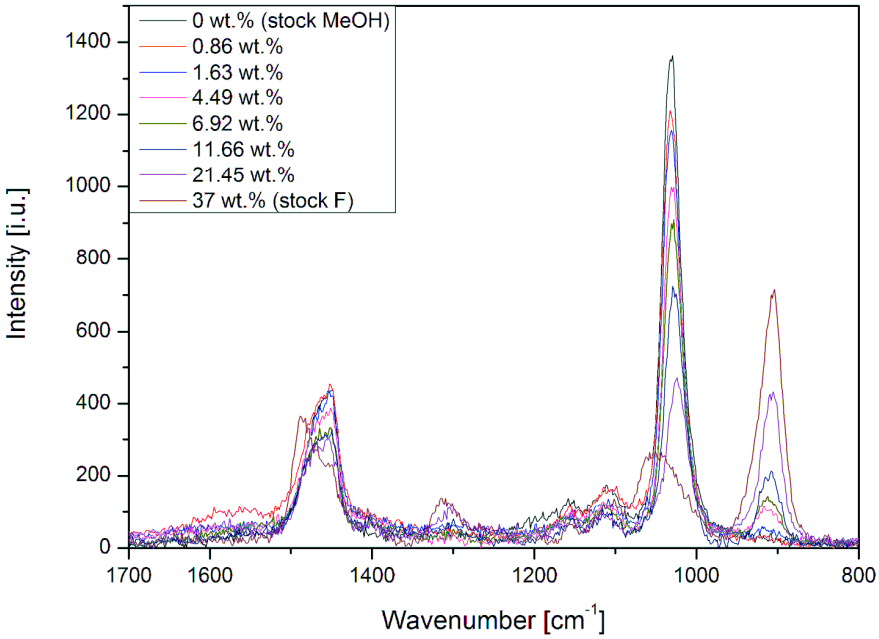

Figure 35. Raman spectra of formaldehyde-methanol solutions.

Just as this is the case for IR spectra, those obtained using Raman spectroscopy change their appearance with changes in formaldehyde concentration. In general, the higher the concentration, the more intense spectral peaks are obtained. This is obvious because the intensity of the signal is proportional to the concentration of a given bond/group. However, apart from the intensity, the shape of the spectra – especially for aqueous solutions – also changes because the speciation of the solution and thus relative amounts of given bonds change. For example, in both methanolic and aqueous solutions the region of ca. 1250-1350 cm^{-1} contains peaks which drastically decrease upon dilution. This is even more visible in case of methanolic solutions, as this region corresponds to different vibration modes in CH_2 groups which are present in oligooxyglycols. When comparing Raman spectra collected for methanolic and aqueous solutions, one can easily notice that in case of the latter ones the signal at 1030-1060 cm^{-1} is broader and less intensive, while the signal at 905-910 cm^{-1} is better defined. This observation confirms the assignments of these peaks, which are C-O asymmetric stretch (in C-OH of glycols) and C-O symmetric stretch (in O-C-O), respectively. Speciation determined by ^{13}C NMR proved that there are more glycols present in aqueous solutions, resulting in a more intensive signal at 910 cm^{-1}. In case of methanolic solutions, the peak at 1060 cm^{-1} is just a shoulder of another peak at 1030 cm^{-1}. In aqueous solutions the ratio of intensities of these two peaks is considerably smaller.

In order to better understand the differences of spectra of formaldehyde solutions in different solvents, spectra of formaldehyde-water, formaldehyde-methanol and methanol only were plotted together in Figure 36.

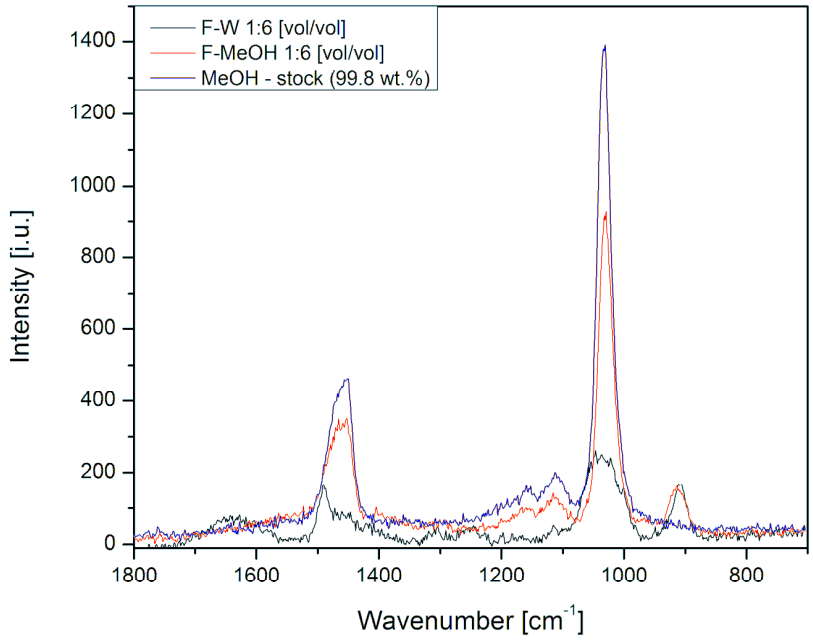

Figure 36. Overlaid Raman spectra of methanol, and both methanolic and aqueous solutions of formaldehyde.

One can easily see that the overall shape of these spectra is similar, regardless of the type of solvent. Region 1400-1500 cm^{-1} which corresponds to C-O-H and/or H-C-H bonds is more dominant in both formaldehyde-methanol and methanol only solution, while it is less intensive for aqueous solution. The signal at 1030 cm^{-1} is better defined when methanol is present, which is in agreement with this signal being assigned to C-OH bond in methanol. However, the most interesting peak is present at 905 cm^{-1}. It is missing in pure methanol spectrum but is present in both aqueous and methanolic solutions of formaldehyde. More importantly, it has practically identical intensity and shape for both solutions. The signal is assigned to symmetric stretching modes in O-C-O bonds in glycols and methoxyglycols. Basing on the results of ^{13}C NMR, in case of F-W at 1:6 volumetric ratio the

predominant species is MG (with methanol and minor MMG species), while for the F-W solution at the same dilution ratio, MMG dominates (with methanol). It is clear, when looking at Figure 36, that Raman spectroscopy fails to resolve differences between the respective species as well as NMR does. Because the overall concentration of formaldehyde-related species in both solutions presented in this figure is the same, one can say that the intensity of this peak corresponds to the total formaldehyde concentration.

The significant inconvenience of using either IR or Raman spectroscopy to determine the speciation in solutions as complex as the ones which were studied here is that the recorded signals can be assigned to certain types of bonds which are not specific for any of the compounds. Both these methods lack what is the greatest advantage of NMR, in which certain signal can be assigned to a specific nucleus rather than a type of bond. Moreover, the intensity of signals measured in NMR is proportional to the number of moles (or molar concentration) of specific nucleus, allowing straightforward quantitative analysis. This can also be done by IR or Raman spectroscopy, however, calibration curves should be made for quantitative analysis, as certain bonds give rise to more intensive signals than others and ratios of their intensities may vary with solvent composition. ^{13}C NMR which was very useful in terms of determination of speciation in the solutions – both quantitative and qualitative – suffers from a severe disadvantage though: length of the experiments, amounting to as long as 18 hours. However, ^{1}H NMR is a far more rapid method which gives results of the same quality as ^{13}C NMR spectroscopy, assuming that deconvolution of signals overlapping with the OH/D peak can be successfully accomplished.

Absolute concentrations were not determined from IR or Raman spectra due to the fact that calibration curves for isolated formaldehyde-related species could not be obtained. Nevertheless, since both IR and Raman spectroscopy were considered as possible methods of investigating the kinetics of reactions leading to formation of resorcinol-formaldehyde gels, experiments on a range of variously concentrated solutions were performed to allow detection of possible new peaks correlated to the products of reaction (see Chapter 6).

4.2.2. Quantitative analysis

IR measurements

When analysing IR spectra, it became evident that the signal in range between 850 and 1250 cm^{-1} required deconvolution to enable quantitative analysis of the overlapping signals. As in case of results obtained from ^{1}H NMR, the process of deconvolution was done using Origin 8.1 software but the shape of the peaks was assumed to be Gaussian. In certain cases deconvolution was not possible due to poorly defined peak shape, however, this was only an issue with the most dilute solutions in which it was expected that certain signals might be too weak and noisy to be picked up by the software accurately. Examples of deconvolution of the discussed mentioned region of IR spectrum are shown in Figure 37 and Figure 38 below.

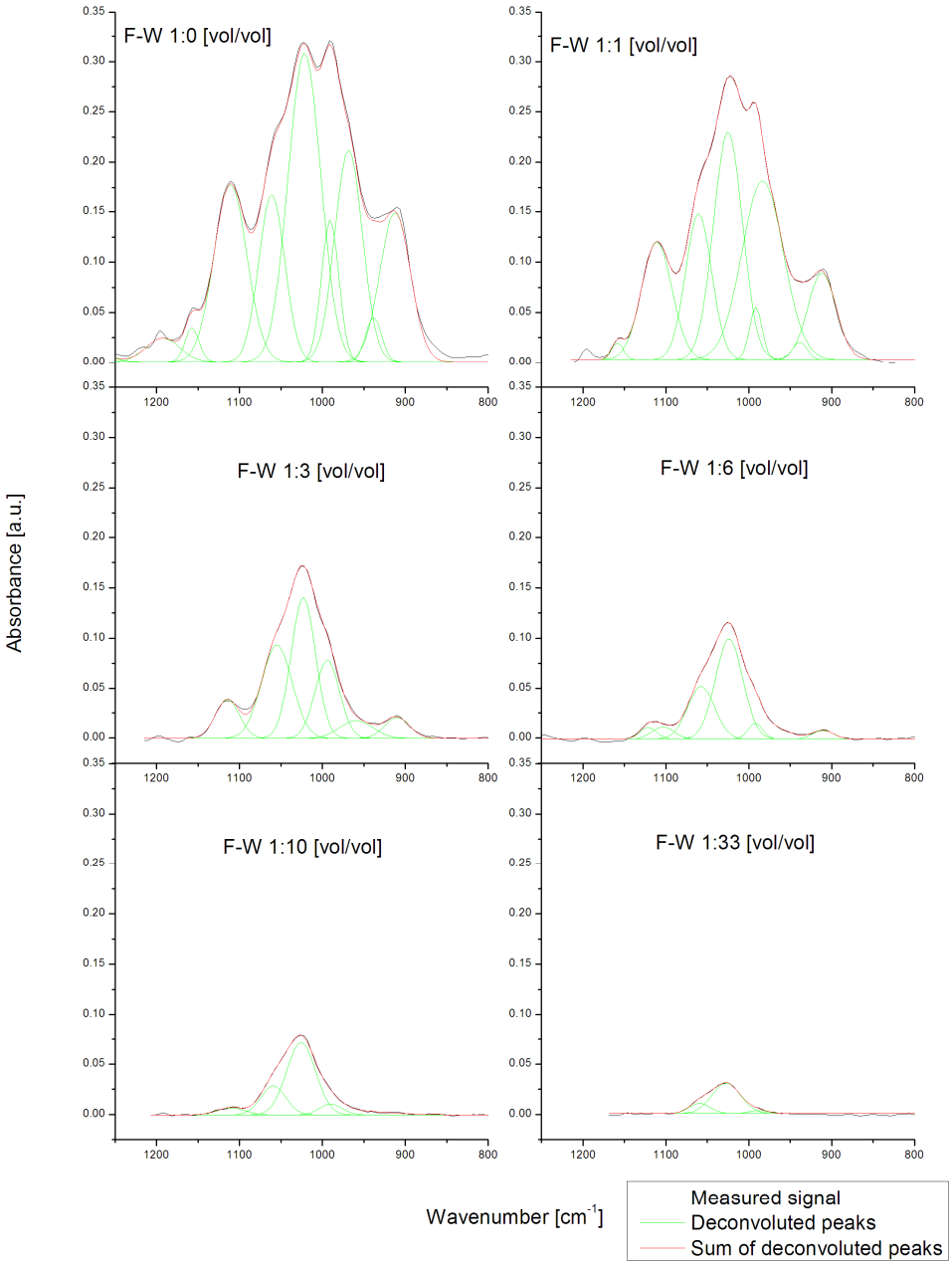

Figure 37. Deconvolution of the 850-1200 cm^{-1} region in IR spectrum of formaldehyde-water solutions at different volumetric dilution ratios.

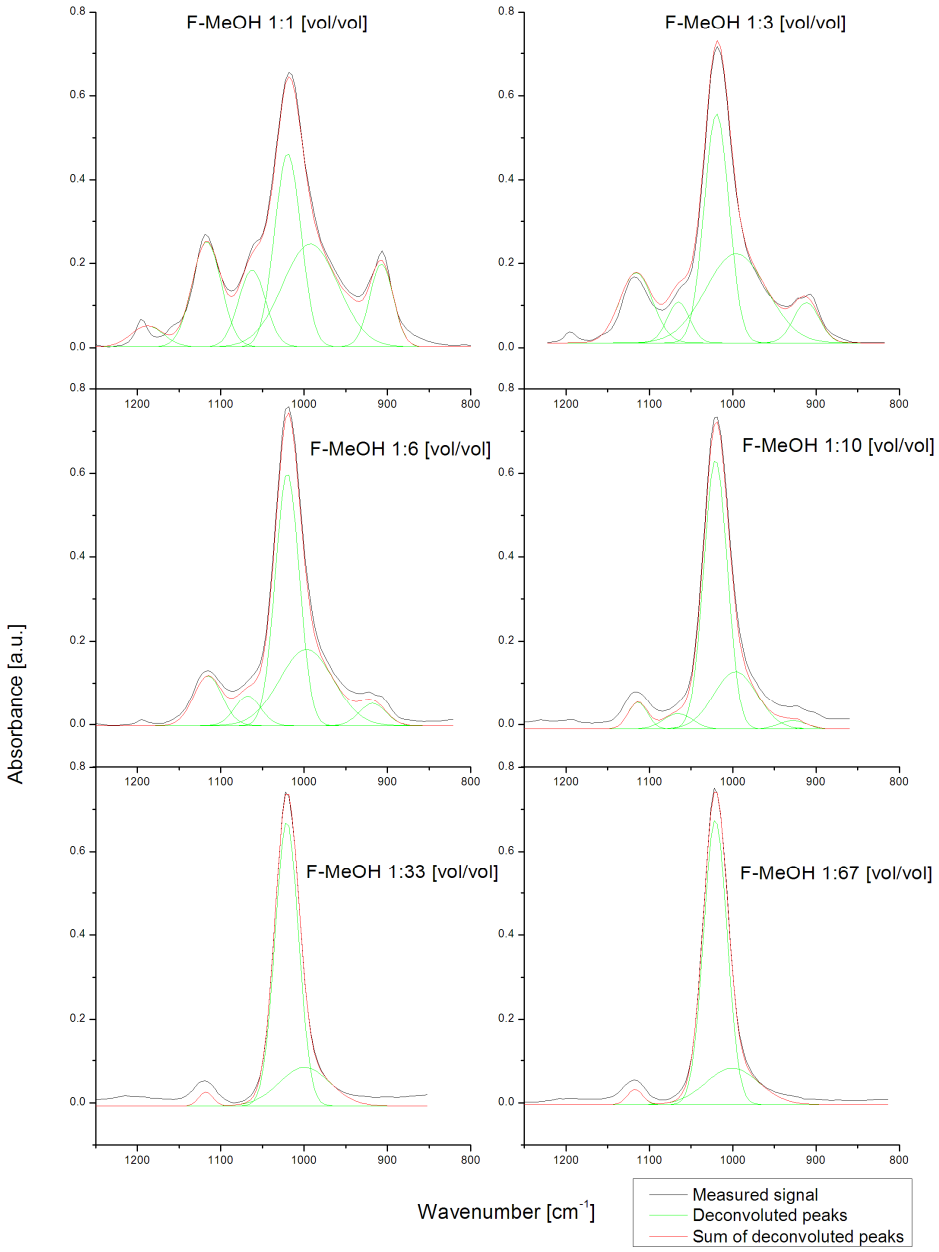

Figure 38. Deconvolution of the 850-1200 cm^{-1} region in IR spectrum of formaldehyde-methanol solutions at different volumetric dilution ratios.

Quantitative analysis of collected IR spectra was performed in terms of areas of peaks at given wavenumbers rather than absolute concentrations. This, combined with NMR results providing quantitative speciation in solutions at various dilutions allowed to confirm the assignments which were based on information found in the literature and in correlation tables. Plotting integrated areas of peaks deconvoluted in the most relevant bands covering C-O bonds vibrations (in the range of 900-1100 cm^{-1}) and H-C-H vibrations in CH_3 groups of methoxyglycols and methanol (at 1115 cm^{-1}) against concentrations of formaldehyde-related species obtained from the ^{13}C NMR experiments allowed to observe correlation or lack thereof, in order to test hypotheses regarding suggested assignments.

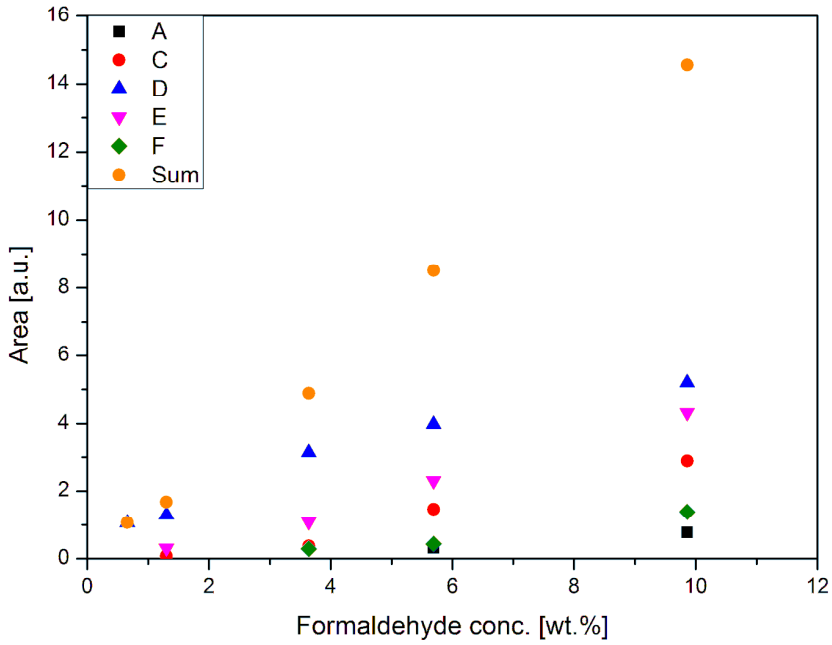

Figure 39. Areas of deconvoluted peaks in region 850-1200 cm^{-1} of the IR spectrum. Data for formaldehyde-water solutions.

The total sum of peak areas depends linearly on the total formaldehyde concentration, as it can be seen in Figure 39. It should be remembered that the resonances at 1020 and 1115 cm^{-1} also include methanol contributions, although in these solutions the methanol concentration is directly proportional to that of formaldehyde corresponding to the composition of the formaldehyde stock solution. Furthermore it can be seen that areas of some peaks do not decrease linearly with formaldehyde concentration, namely those at 910, 990 and 1115 cm^{-1} appear to decrease faster and that of the peak at 1020 cm^{-1} which decreases slower that the overall peak area. This will be further discussed below when relative areas of peaks are compared (see Figure 41).

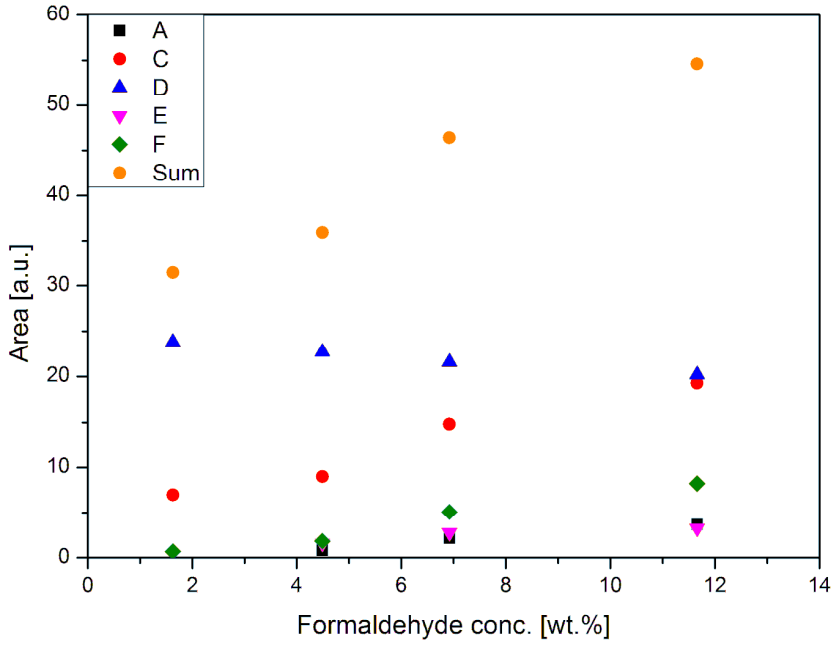

Figure 40. Areas of deconvoluted peaks in region 850-1200 cm^{-1} of the IR spectrum. Data for formaldehyde-methanol solutions.

In solutions obtained by dilution of formaldehyde stock solution with methanol the total peak area is not decreasing towards zero since the most dilute solutions are becoming close to pure methanol, so in the limit the spectrum of pure methanol should be obtained, with a single resonance at 1020 cm^{-1} for C-O vibrations and a smaller peak at 1115 cm^{-1} for H-C-H vibrations. It can be seen that peak areas for vibrations associated with formaldehyde related species, at 910, 990 and 1060 cm^{-1} decrease with decreasing formaldehyde concentration, but at the two lowest dilutions, peak areas for 990 cm^{-1} do not seem to change anymore. Since this resonance is not present in the methanol IR spectrum, it is concluded that this is an artefact resulting from baseline correction after subtraction of water background, which caused the peak asymmetry for the most dilute solutions in methanol (see Figure 32). The same problem appears to have led to an unsatisfactory baseline in the area around 1115 cm^{-1}, resulting in unreliable areas for that peak at the highest dilutions.

A useful way of representing the changes in areas of the deconvoluted peaks is to express them as fractions of the total area of the broad deconvoluted band and plot these values against total concentration of formaldehyde species in the samples, as it is done in for formaldehyde-water solutions (Figure 41) and for formaldehyde-methanol solutions (Figure 42).

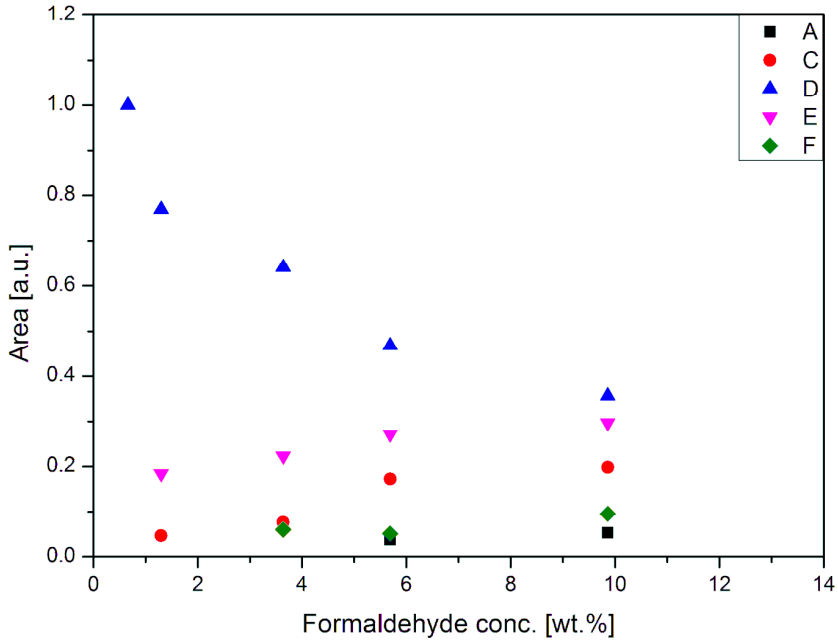

Figure 41. Areas of deconvoluted peaks in region 850-1200 cm^{-1} of the IR spectrum as fractions of their sum. Data for formaldehyde-water solutions.

It can be clearly seen that the signal at 1020 cm^{-1} corresponding to the vibrations of the C-OH bond in glycols and methoxyglycols (as well as methanol) is becoming more dominant at lower concentrations. At the same time, the peaks at 990 and 1060 cm^{-1} corresponding to O-C-O and C-OH bonds, respectively, in glycols and methoxyglycols becomes less dominant. At the same time, the proportions of these two peaks to the major peak at 1020 cm^{-1} is likely approaching certain limiting value corresponding to the spectrum of pure MG species, which is predominant in the most diluted aqueous solutions (as per ^{13}C NMR). This can also be seen from the asymmetric overall peak which is not changing its shape significantly with dilution for the most diluted solutions in water (Figure 32). In contrast, peaks at 1115 cm^{-1}, corresponding to methoxylated species and methanol, and at

910 cm^{-1}, corresponding to glycols (other than MG) and methoxyglycols are decaying to negligible area in comparison to the overall peak centred around 1020 cm^{-1}, since they correspond to oligomeric and methoxylated species which progressively decrease with dilution (compared to MG) due to de-oligomerization and hydrolysis of methoxy groups.

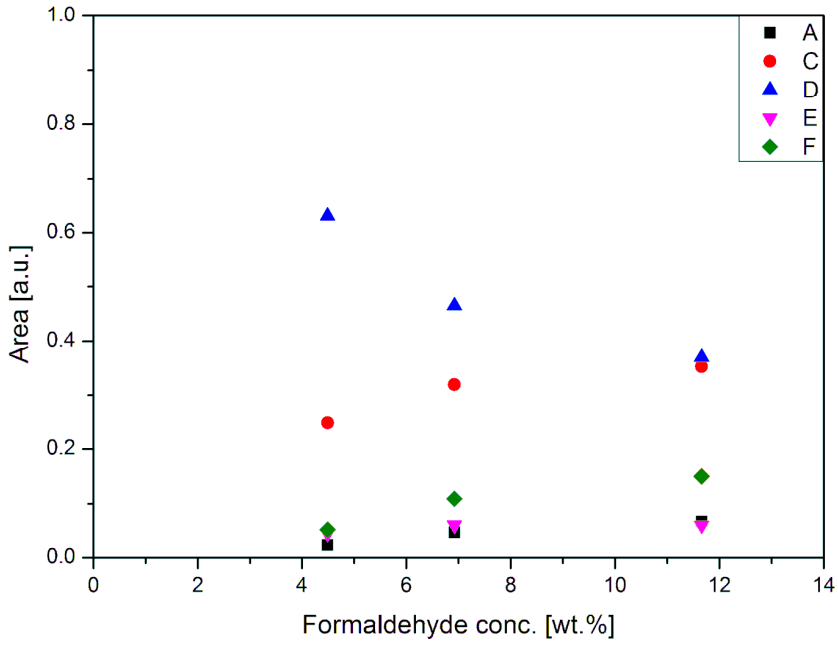

Figure 42. Areas of deconvoluted peaks in region 850-1200 cm^{-1} of the IR spectrum as fractions of their sum. Data for formaldehyde-methanol solutions.

Analysis of the data for the methanolic solutions (Figure 33) can be performed by contrasting it with results for the aqueous solutions (Figure 32). In the case of methanolic dilutions the signal at 1020 cm^{-1} becomes increasingly dominant since it corresponds to methanol which is the diluent solvent. The area of the peak at 1115 cm^{-1} (corresponding to CH_3 groups in methanol and methoxyglycols) decreases relatively to that at

1020 cm^{-1} since the overall concentration of methoxy species decreases upon dilution in methanol, and also because the ratio of the two peak areas changes with increasing methanol fraction in water-methanol mixtures (see below, Figure 43). Other peaks, namely at 910, 990 and 1060 cm^{-1} correspond to MMG, since these solutions contain predominantly this species as the only form of formaldehyde (as per ^{13}C NMR), and areas of these peaks appear to decrease in similar proportions with decreasing formaldehyde concentration.

Ratio of peak areas of the resonances at 1020 and 1115 cm^{-1} as a function of overall methanol concentration is shown in Figure 43 for three sets of data: formaldehyde stock solution diluted with water, formaldehyde stock solution diluted with methanol, and methanol-water mixtures.

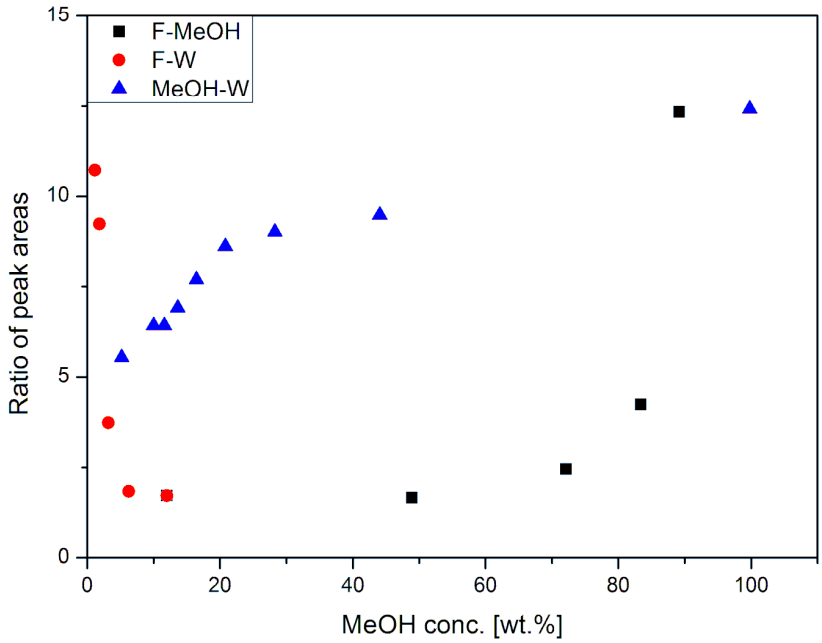

Figure 43. Ratio of areas of deconvoluted peaks at 1020 and 1115 cm^{-1} of the IR spectrum. Data from methanol-water mixtures together with those from formaldehyde-water and formaldehyde methanol solutions.

It can be seen that the ratio of areas of the two peaks for methanol itself varies with the methanol concentration in its aqueous solution from around 5 in dilute methanol solutions to about 12 in pure methanol. The ratio is around 2 in the formaldehyde stock solution, due to extensive contribution to the peak at 1115 cm^{-1} from methoxy groups of methoxyglycols (see IR spectrum of pure MMG in [44], where the peak at 1115 cm^{-1} is the second strongest after the peak centred at 1020 cm^{-1}). The peak ratio increases with dilution in methanol since the spectrum is evolving towards the one for pure methanol. On the other hand, the peak ratio also increases with dilution in water due to disappearance of methoxy groups via hydrolysis and dilution of total methanol and as overall methanol concentration decreases towards zero, the peak ratio increases sharply, since the peak at 1115 cm^{-1} eventually vanishes since it is not present in MG vibrations.

Raman measurements

Similar analysis can be performed using areas of peaks measured with Raman spectroscopy. Once again, these values were plotted against concentration of formaldehyde-related species in both aqueous (Figure 44) and methanolic solutions (Figure 45). Areas of relevant and easy to select and integrate peaks were chosen and due to the fact that the speciations of methanolic and aqueous solutions are different, those peaks were chosen as appropriate. Three bands were the same for both types of solutions and those were A (905-910 cm^{-1}), E (1060 cm^{-1}) and O (1480 cm^{-1}). The fourth one was different and for aqueous solutions the chosen band was I (1265 cm^{-1}), while for methanolic ones it was F (1110 cm^{-1}).

In case of formaldehyde-water solutions it can be clearly seen in Figure 44 that the sum of areas of all peaks is linearly proportional to formaldehyde concentration, as it was the case for IR spectra. As well as the sum, all signals seem to exhibit linear dependency on the formaldehyde concentration. All this was expected and in order to obtain more information from this data, analysis of areas expressed as fractions of their sum was done in the same way as for IR data. However, it did not reveal anything more than Figure 44, as expected, since all of the signals observed were specific for oligooxyglycols and their methoxylated forms. Therefore the distribution of their areas does not vary as they were changing proportionally to changes in concentration of the same group of molecules.

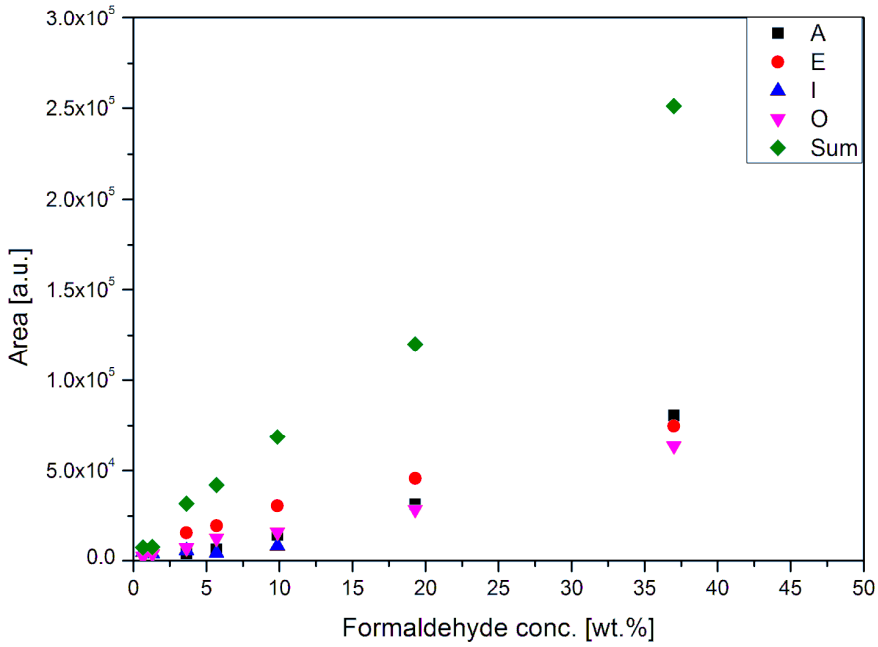

Figure 44. Areas of deconvoluted peaks in Raman spectrum. Data for formaldehyde-water solutions.

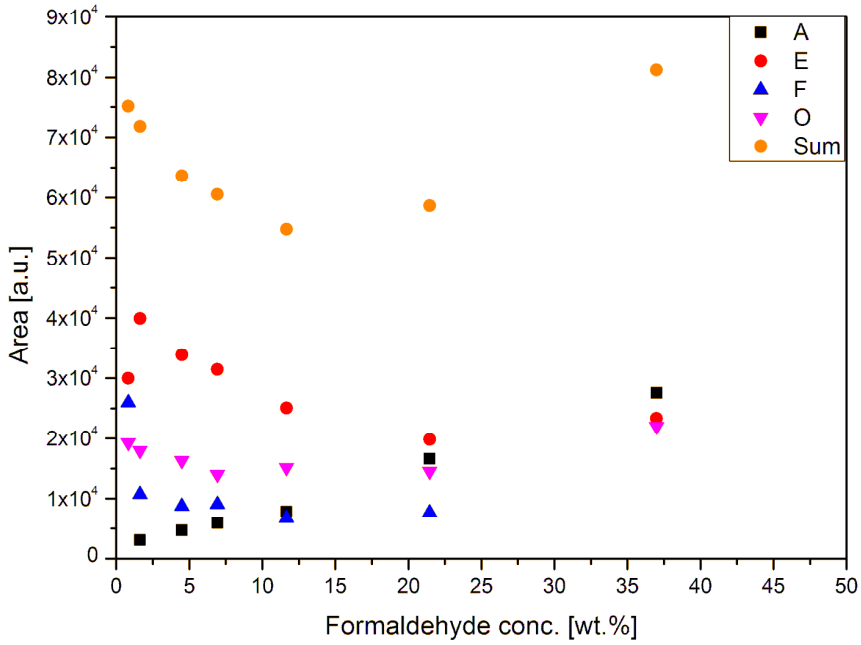

Figure 45. Areas of deconvoluted peaks in Raman spectrum. Data for formaldehyde-methanol solutions.

Analysis of formaldehyde-methanol spectra is more complex than that of formaldehyde-water solutions because changes in peak areas do not appear to be linear in all cases. Peaks E and O seem to form a curve with a minimum at ca. 10-20%wt. of formaldehyde. At the same time, area of peak A grows in a linear manner with increasing formaldehyde concentration, while peak E seems to decrease. Growth of band A, assigned to C-O symmetric stretches in O-C-O, is reasonable: with increasing concentration the degree of oligomerization of glycols and their methoxylated forms is higher. An increasing trend in changes of peak areas of bands E and O in more dilute formaldehyde solutions can be explained by increasing concentration of the diluent, which is methanol. It is difficult to explain the reason for formation of an apparent minimum in the shape of lines formed by these peaks. As it

was in case of formaldehyde-water dilutions analysis, plotting peak areas expressed as fractions of their sum was used to obtain additional information, but it did not provide any plausible explanation for this phenomenon. However, it may well be possible that relative intensities of some peaks with respect to each other vary with overall solvent composition in methanol-water solutions, which could be responsible for the observed discrepancies.

4.3. Dynamic Light Scattering

The primary application of DLS is determination of the mean hydrodynamic radii of sub-micron particles suspended in a continuous liquid phase where particles are freely diffusing. The detection of particles relies on elastically scattered light, which can be scattered by solid particles but also by polymeric chains or droplets of another fluid phase with a different refractive index from that of the suspending liquid. Therefore, it can be concluded that the DLS allows also detection of phase separation even at microscopic level. When suspended particles are interconnected into aggregates or more extensive networks or even form a gel, and primary particles are not freely diffusing anymore, DLS measurements indicate this through the autocorrelation function which does not decay exponentially, but much slower modes appear. Since there is an on-going discussion about the driving force for gel formation during the sol-gel polymerization of resorcinol and formaldehyde, it was worth to investigate if and at which stage this might occur. Additionally homogeneity of formaldehyde and water solutions is an important factor in NMR experiments, as inhomogeneous solutions lead to disturbance in homogeneity of the magnetic field, resulting in problems with

shimming, which – if not compensated for – lead to asymmetrical peaks and quantitative data of poor quality.

The DLS experiments were performed at room temperature (25°C) and for each formaldehyde solution three scans, each lasting 30 s, were performed. The resulting autocorrelation functions are shown in Figure 46. The shapes of obtained autocorrelation functions do not resemble the ones discussed earlier in the methodology (see Figure 12) – there is no distinguishable exponential decay, indicating that there are no suspended particles or droplets with a different refractive index from that of the suspending solution. This shows that there is no microphase separation in this type of solutions which appear to be fully homogeneous.

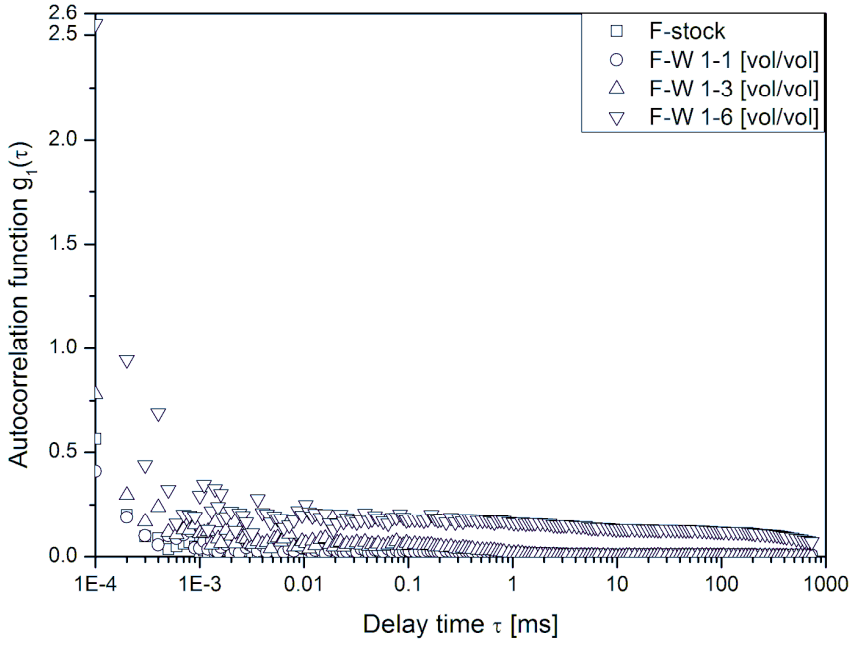

Figure 46. Autocorrelation function for formaldehyde solutions prepared by dilution of the stock formaldehyde solution with water.

If phase separation is the driving force behind gel formation, these results show that it is not caused by inhomogeneity of the formaldehyde-water solutions before adding resorcinol and sodium carbonate. However, since these experiments were performed only on non-reacting solutions, further experiments were carried out on solutions with sodium carbonate added (see Chapter 5) and finally on reacting solutions (Chapter 6).

4.4. pH measurements

Despite high concentration of oligooxyglycols, their methoxylated forms and methanol present in the aqueous solutions of formaldehyde, the measured pH value of 37%wt. formaldehyde solution containing 12%wt. of methanol is as low as 4.40±0.10. Judging by very high pK_a values of substances found in the solution (methanol – 15.54, glycols – comparable values), the expected pH of the formaldehyde solution would be much higher or at least near-neutral values, as aqueous environment without any acidity adjustment would not favour dissociation of these species. This discrepancy can be caused by presence of small amount of formic acid (up to 0.02%wt.), which can be a product of two different processes: oxidation of formaldehyde, which takes place to a limited degree during the production process of formaldehyde or the reaction of disproportionation between two formaldehyde molecules. The latter one is called the Cannizzaro reaction and it takes place in strongly basic conditions or at elevated temperatures. According to the information provided by the manufacturer of the formaldehyde stock solution, the concentration of formic acid is 0.02%wt., which corresponds to 4.74 mmol·dm^{-3} (d_{Fsol} = 1.09 g·cm^{-3}, Mw_{FA} = 46.02 g·mol^{-1}). Knowing that the pK_a of formic acid is 3.77, the calculated value of pH for aqueous solution of formic acid of this concentration is 4.21. This is slightly lower than the

measured value for the non-diluted formaldehyde stock solution and the discrepancy between measured and calculated value can be explained as being due to several factors, including presence of methanol (known to influence proton activity coefficients and also pH electrode membrane operation) in solutions and equilibria involving dissolved carbon dioxide.

An interesting trend is observed for pH values measured upon dilution of the formaldehyde stock solution in de-ionised water, which can be seen in Figure 47. The initial value of pH, i.e. of a 37%wt. stock solution, is 4.40 and it decreases as the concentration of formaldehyde decreases and pH reaches a minimum of 3.37 for 5.69%wt. of formaldehyde. Furthermore, as the concentration of formaldehyde decreases further, the pH of the solution starts to rise again and finally approach the measured pH value of pure water (5.0).

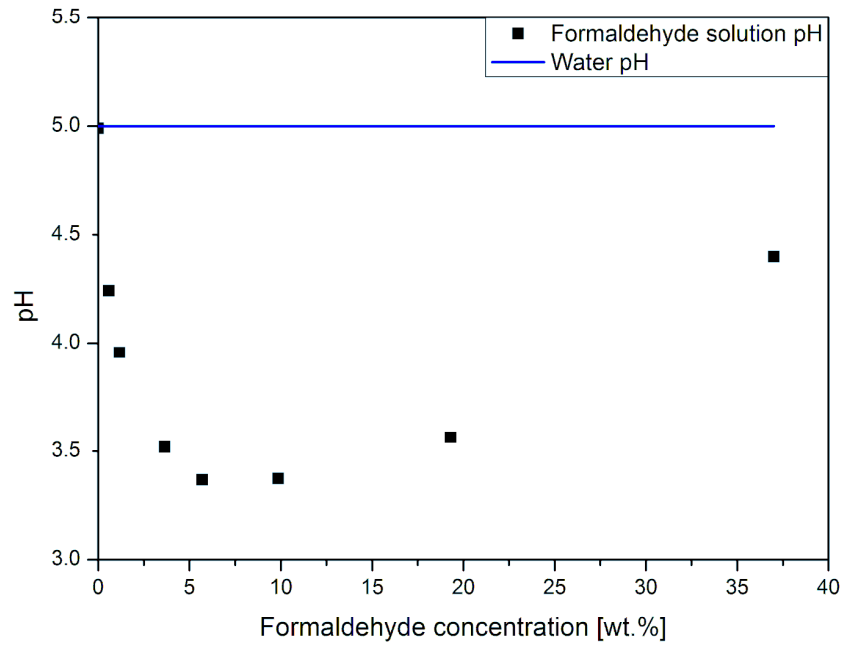

Figure 47. Changes of pH in formaldehyde-water solutions.

This effect cannot be solely attributed to the presence of formic acid in the solution, as its concentration in stock solution would cause pH to be equal to 4.21 and upon dilution the concentration would decrease and the pH value would increase. This is the case in very high dilutions, however it does not explain the phenomenon of the pH values reaching a plateau of minimum values at solutions containing approximately 5-10%wt. of formaldehyde. This most likely due to variation of activity coefficients of proton and other ionic species with varying concentration of methanol and glycolic species as the formaldehyde stock solution is being diluted by pure water.

Results of pH measurements of formaldehyde solutions prepared by dilution of the formaldehyde stock solution with methanol also show that the pH value varies with dilution, as it can be seen in Figure 48. The minimum value is recorded for the solution with 37%wt. of formaldehyde and it is equal to 4.40, while the highest value is 6.40 and recorded for 0.52%wt. solution. The absolute difference between these two is 2.00, while the difference between the minimum and maximum pH values (recorded at 5.69%wt. and 0.58%wt., respectively) in aqueous dilutions is 0.87. The difference between the behaviour of pH in these two types of dilutions is that the results obtained for methanolic dilutions seem to form a linear pattern, with pH increasing steadily towards lower formaldehyde concentrations, as expected. The pH measurements of aqueous dilutions form a pattern with a plateau of minimum values, which is not observed in the methanolic dilutions.

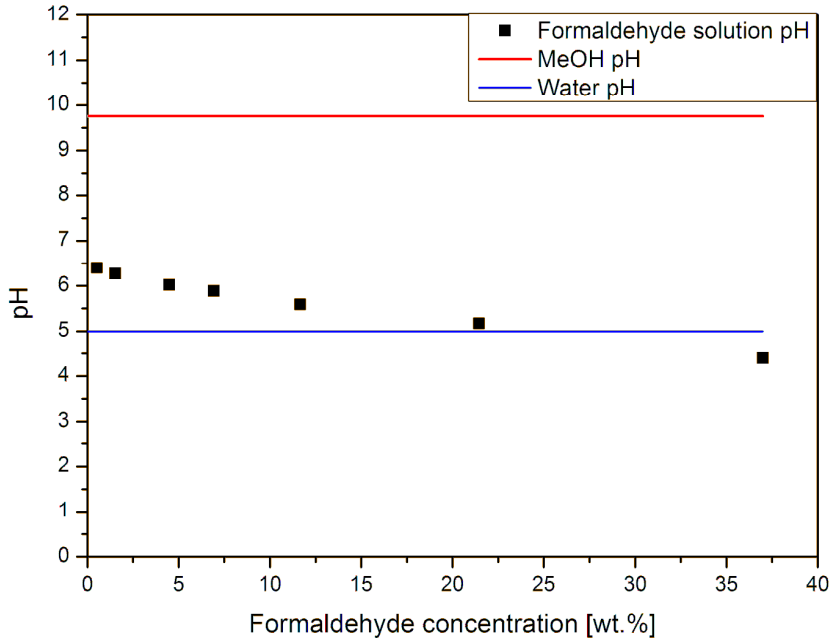

Figure 48. Changes of pH in formaldehyde-methanol solutions prepared by dilution of the formaldehyde stock solutions (37%wt. formaldehyde).

4.5. Main conclusions from Chapter 4

This Chapter summarizes the most important findings of this research regarding glycol equilibria in formaldehyde-water-methanol solutions. Methods used here were appropriately developed to allow a fully quantitative analysis within reasonable error margin.

The results of NMR, IR and Raman spectroscopies confirm lack of formaldehyde in the aldehyde form in detectable amounts in formaldehyde aqueous solutions. Instead three groups of species can be found, namely (a) methylene glycol and its oligomers, (b) methoxylated methylene glycol and its oligomers and (c) free methanol. All these species were found to be in mutual equilibria and the exact speciations of solutions of different

concentrations were determined. The main conclusion of the observations was that the more dilute the formaldehyde solution, the more simple (shorter) species are present. In case of water as diluent the speciation goes towards methylene glycol and free methanol, whereas in case of methanol as diluent, it is mostly methoxylated methylene glycol and free methanol. Based on the measured concentrations, equilibrium constants were calculated in a range of temperatures, allowing the future researchers and formaldehyde-based resin manufacturers to predict the speciation basing solely on the dilution of formaldehyde stock solution. From a practical point of view this is of great importance, as previous research did not deal with commercially available formaldehyde solutions which are used widely in all formaldehyde-based resins. It allows the potential manufacturers to predict the best dilution rate for the reaction, basing on the speciation of the formaldehyde solution.

In order to verify whether the investigated solutions exhibit mixing issues, a series of DLS experiments was performed. The obtained results proved that all solutions were uniform, therefore confirming that there are no difficulties regarding their miscibility.

It was found that pH depends on the dilution of formaldehyde stock solutions in water in a non-linear manner, while it is linear for methanol-based solutions. It is difficult to explain this phenomenon, however it may be assumed that the changes in distribution of formaldehyde-related species affect pH. Possibly also changes in formic acid concentration and absorption of carbon dioxide from ambient atmosphere contribute to this effect, as well as variation of activity coefficients in mixed water-methanol solutions.

CHAPTER 5. FORMALDEHYDE-WATER-SODIUM CARBONATE SOLUTIONS

This Chapter investigates the nature of formaldehyde and sodium carbonate solutions in water. The main purpose of this Chapter is to determine whether the catalyst affects the speciation of formaldehyde in these solutions and thus may influence subsequent reactions between formaldehyde and resorcinol. A number of formaldehyde-water and sodium carbonate solutions were prepared, with different catalyst concentrations.

In order to verify whether the dependency of formaldehyde-water solution speciation on sodium carbonate concentration exists, a series of quantitative ^{13}C NMR experiments was performed. These were expected to yield qualitative description of the solution and also to provide a description of formaldehyde-related species distribution. Based on the measured concentrations, equilibrium constants were calculated, as it was done in Chapter 4. This was done to confirm whether addition of a pH-altering agent affects the equilibria between species found in the solution. Additionally, since the polymerisation reaction normally takes place at temperatures higher than 20°C (293K), a series of ^{13}C NMR spectra were taken for one solution at various temperatures. This was expected to allow determination of temperature influence on speciation in these solutions.

IR spectroscopy was employed also to analyse the effects of catalyst addition on composition of the solution. Despite the fact that the formaldehyde-water spectra were expected to be complex and requiring deconvolution before further analysis, this spectroscopy method was used because it is well accessible and relatively easy to use. Results provided by the IR spectroscopy

were expected to be complementary to the information provided by the NMR.

Dynamic Light Scattering was used in order to assess whether addition of sodium carbonate or adjustment in the pH of the solution could cause changes in the homogeneity of the sample. DLS is typically used to measure the hydrodynamic radii of particles in colloidal suspensions, but it can also detect microphase separation, especially if the dispersed phase is in form of nanodroplets with a different refractive index. One of the theories on the role of catalyst was that it partially enhances microphase separation in the reacting resorcinol-formaldehyde mixtures. However, it was not examined previously whether the phase separation could be triggered in solutions without resorcinol.

Measurements of pH of these solutions were necessary to establish how does the addition of sodium carbonate affect acidity of formaldehyde-water solutions. It is crucial because it is currently assumed by majority of researchers that the primary role of the catalyst is adjustment of the pH, which leads to formation of resorcinol anion and which enhances reactions between formaldehyde and resorcinol. Since the pK_a values of species found in formaldehyde are very high and the solution equilibria are complex, it is difficult to predict how the addition of sodium carbonate does affect the acidity of the solution. Moreover, sodium carbonate undergoes a two-step dissociation process and the products of it are also in equilibrium with CO_2 in the atmosphere.

5.1. NMR results

Following experiments performed with a nuclear magnetic resonance (NMR) to quantitatively study speciation in formaldehyde-water and formaldehyde-methanol solutions, investigation of formaldehyde-water-sodium carbonate was conducted. This was done in order to obtain information whether addition of sodium carbonate and thus change in the pH, influences the composition and changes the distribution of formaldehyde-related species. The experiments were performed in the same manner as before, using the same spectrometer and pulse programs in order to ensure data consistency. As previously, inverse gated decoupling was applied during the experiment to eliminate nuclear Overhauser effect and a long delay time (60 s) was used to allow full relaxation. A typical number of 1024 scans was collected to provide a good signal-to-noise ratio and a coaxial insert with TMS was used for reference. Three solutions with different concentration of sodium carbonate were investigated at 293K and results were compared against formaldehyde-water solution spectra and data.

The amount of catalyst was chosen so that it would correspond to the composition of reacting mixture. Therefore the formaldehyde-water-catalyst solutions were prepared in the same way as reacting mixture would be but without adding resorcinol. The compositions of the investigated solutions are shown in Table 15.

Table 15. Composition of formaldehyde-water-sodium carbonate solutions examined by ^{13}C NMR.

Sample	**Water [ml]**	**D_2O [ml]**	**Formaldehyde stock solution [ml]**	**Na_2CO_3 [g]**
Eq. R/C 50	7.00	3.00	1.47	0.0192
Eq. R/C 100	7.00	3.00	1.47	0.0096
Eq. R/C 200	7.00	3.00	1.47	0.0048
Eq. R/C 500	7.00	3.00	1.47	0.0019

The spectra obtained in these experiments (see Figure 49) were not qualitatively different from those obtained for formaldehyde-water solutions. In terms of peak assignments and detected species no differences are observed; moreover, the chemical shifts of all peaks are unaffected by addition of sodium carbonate. This can be clearly seen when analysing the data in Table 16. However, due to an increase in the width of the peaks compared to those observed in the absence of sodium carbonate, the least intensive ones, like TG, MTG and MDG which were detected in formaldehyde-water dilutions, could not be detected and quantified in spectra collected for the samples with addition of the salt. These peaks appear as very small bulges in the baseline which did not allow these peaks to be quantified.

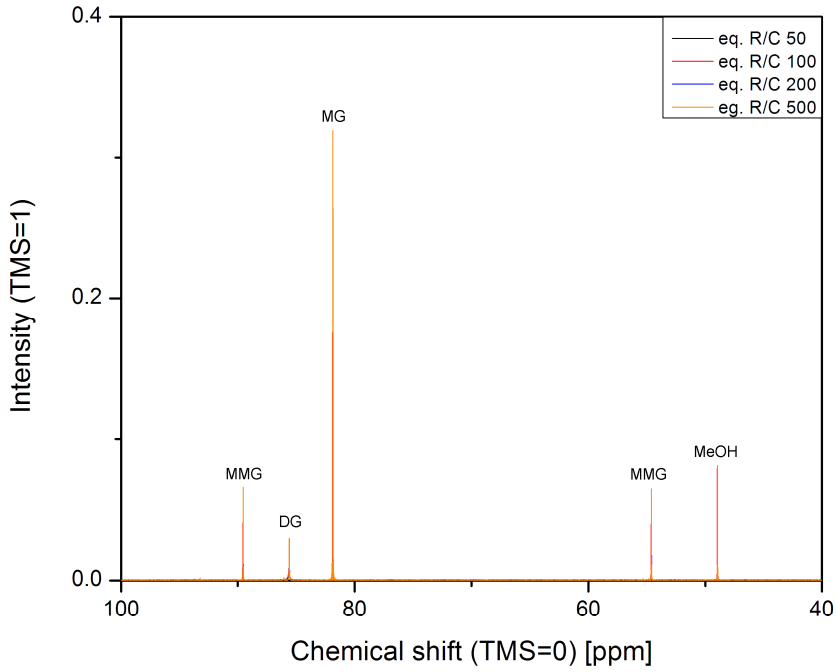

Figure 49. ^{13}C NMR spectra of formaldehyde-water-sodium carbonate solutions.

A closer analysis of the obtained spectra reveals the main difference in their appearance, namely the width of the peaks. As an example, peak corresponding to the ^{13}C nucleus in DG at 85.5 ppm was chosen and shown in Figure 50. The choice of this peak was motivated by two facts: its width changes are the most prominent and since it corresponds to a major formaldehyde-related species, it serves as a good indication of formaldehyde species behaviour in presence of a basifying agent.

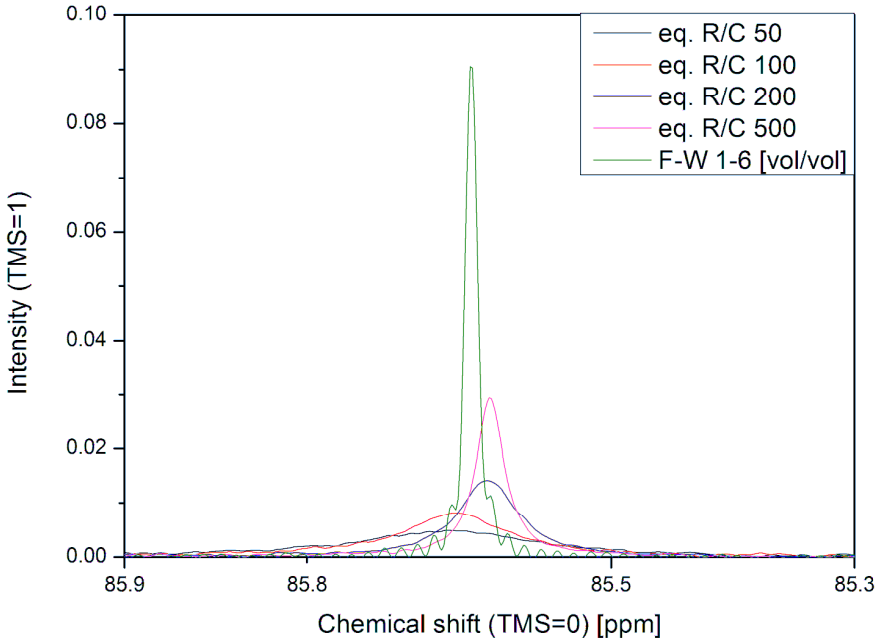

Figure 50. ^{13}C NMR spectra of formaldehyde-water-sodium carbonate: enlarged DG signal.

There is a clear relationship between concentration of sodium carbonate (corresponding to changing pH) and both width and intensity (height) of the peaks. The change in the intensity is linked with changes in the width of the peak, since the area under the peak remains approximately constant. Quantitative analysis of the data – performed further on – allowed to determine whether changes in the pH were causing changes in concentrations of species or not.

As concentration of sodium carbonate (and also pH) increases, the intensities of formaldehyde-related peaks decrease, as shown in Figure 51. Meanwhile, methanol signal intensity remains constant with changing sodium carbonate concentration. The intensity of the MG peak drops significantly – it decreases by a factor of two (from 0.32 at 0.0015 mol·dm^{-3} Na_2CO_3 to 0.15 at

0.0152 mol·dm^{-3} Na_2CO_3). A similar decrease is observed for the MMG peak, while the DG peak decreases its intensity six-fold. Since it is the peak area that is related to the species concentration, the broadening of the peaks must compensate for that since (as it is shown further on) the concentrations of species do not change significantly.

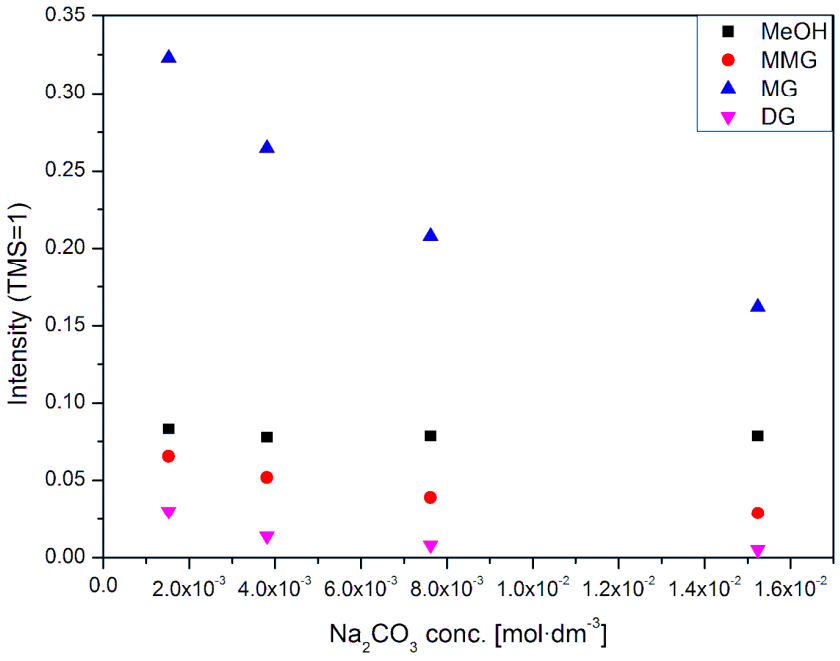

Figure 51. Dependency of NMR peak intensities for methanol and main formaldehyde-related species on sodium carbonate concentration in formaldehyde solutions.

There are at least two possible explanations for this phenomenon of peak broadening for formaldehyde-related species. According to one explanation, a chemical exchange can cause broadening of the peaks, while the other suggestion is change of T_2 spin-spin relaxation time caused by phase separation and migration of certain species into the other phase.

It is known that chemical exchange between two species can cause NMR peaks to broaden, especially if exchanging atoms have similar resonance frequencies [115] [116]. For slow chemical exchanges signals for both forms can be observed, though their linewidths at half of the maximum height are broadened proportionally to the rate constant *k* of the chemical exchange: $\Delta\nu = \frac{k}{\pi}$, where Δν is the linewidth broadening. In case of fast chemical exchange, the signals tend to blend into one, usually broad, peak. This is caused by the fact that the signal from a given nucleus is dependent on its magnetic environment. If it changes the environment quickly (on an NMR timescale) then only an averaged spectrum is observed. If the rate is low or none at all, individual peaks can be seen. A good example in proton NMR is the case of water (-OH/D) signal: it is broad and predominant in spectra of all aqueous solutions. In ^{13}C NMR spectra for all formaldehyde-water-sodium carbonate solutions this effect is observed for all peaks, therefore it is less probable that the broadening is caused by chemical exchange unless it is an exchange that affects all carbon atoms found in the solution. The rate of chemical exchange is subject to temperature, therefore one of the formaldehyde-water-sodium carbonate solutions (0.0152 mol·dm^3 Na_2CO_3) was examined using the same technique but in four different temperatures: 278K, 283K, 288K and 293K. Increase of temperature should increase rate of chemical exchange, therefore the signal is expected to be broader in higher temperatures and sharper in lower temperatures up to a point when – ideally – two separate peaks would appear. The results of these experiments revealed that this is the case. The intensity of the chosen peak at 85.5 ppm (DG) decreases when temperature increases, while its area remains approximately constant, suggesting that linewidth increased. Even though this can be caused by increased rate of chemical exchange, it may as well

partially support the phase-separation theory, as linewidth broadening is associated with changes in T_2 which may be related to phase changes which may also be temperature-dependent. However, more evidence is required.

The results obtained by ^{13}C NMR spectroscopy were interpreted and quantified in the same manner as formaldehyde-water and formaldehyde-methanol dilutions. This allows to assess the effect of adding sodium carbonate on formaldehyde speciation by comparing the obtained results with the ones for formaldehyde-water dilution with no sodium carbonate at all. Results of these calculations are shown in Table 16.

Table 16. Comparison of concentrations (A) and chemical shift changes (B) in formaldehyde-water-sodium carbonate solutions.

A					
Sample →	**eq. R/C**				**F-W 1-6 [vol/vol]**
	50	**100**	**200**	**500**	
	Na_2CO_3 concentration [mol·dm^{-3}]				
	0.0152	0.0076	0.0038	0.0015	0
Assignment	**Concentration [mol·dm^{-3}]**				
TMS	7.3454	7.3454	7.3454	7.3454	7.3454
MeOH	0.2541	0.2663	0.2608	0.2543	0.2728
MMG	0.2533	0.2489	0.2637	0.2380	0.2947
MG	1.0853	1.0967	1.1330	1.0933	1.1818
DG	0.1287	0.1293	0.1330	0.1284	0.1573
B					
Sample →	**eq. R/C**				**F-W 1-6 [vol/vol]**
	50	**100**	**200**	**500**	
	Na_2CO_3 concentration [mol·dm^{-3}]				
	0.0152	0.0076	0.0038	0.0015	0
Assignment	**Chemical shift - δ [ppm]**				
TMS	0.00	0.00	0.00	0.00	0.00
MeOH	48.96	48.96	48.95	48.95	48.98
MMG	54.61	54.62	54.60	54.60	54.62
MG	81.88	81.88	81.86	81.86	81.92
DG	85.63	85.63	85.60	85.60	85.58

The results show that in terms of species concentrations, the addition of sodium carbonate did not have a significant effect, i.e. all species detected in formaldehyde-water-sodium carbonate solution are also present in formaldehyde-water solutions.

In these solutions, equilibria among detected species are present as previously discussed for solutions in the absence of sodium carbonate. Addition of catalyst does not change the equilibrium equations, therefore the values of equilibrium constants can be calculated in the same way but using concentration values found in Table 16. Due to the fact that in formaldehyde-water-sodium carbonate solutions certain species (namely TG, MDG and MTG) were not quantitatively detected (due to much wider peaks), only two equilibrium constants could be calculated – K_1 and K_3, corresponding to equilibria of DG and MMG formation, respectively(see Table 17). As can be seen when analysing this data, the values of the equilibrium constants are not dependent on the sodium carbonate concentration. The values of K_1 and K_3 calculated basing on concentrations measured in simple formaldehyde-water dilutions were 5.8 and 45.5, while the corresponding values for the formaldehyde-water solutions containing sodium carbonate are 6.0 and 49.5. This means that these values differ by 5% and 8%, respectively, which can be regarded as not significant in the context of this data set.

Table 17. Equilibrium constants calculated basing on formaldehyde-related species' concentrations measured using ^{13}C NMR spectroscopy.

eq. R/C →	**50**	**100**	**200**	**500**		**-**
Na_2CO_3 concentration. [mol·dm^{-3}] →	0.0152	0.0076	0.0038	0.0015	**Average value**	0
K_1	6.14	6.04	5.82	6.04	6.01	5.77
K_3	51.66	47.92	50.16	48.14	49.47	45.53

Detection of possible (micro)phase separation is not an easy task, especially when relying on classic NMR spectroscopy methods. Results presented above do not rule out that addition of sodium carbonate is causing phase separation, in the similar way that addition of strong electrolytes causes de-mixing of alcohol and water dilutions. However, in order to confirm this with NMR spectroscopy, additional experiments need to be performed. One would be measurement of T_2 time-constants in formaldehyde-water and formaldehyde-water-sodium carbonate solutions, as the relaxation which T_2 describes depends on the composition as well. This could be in principle done by measuring the experimental line width (LW), which would in practice mean measuring the signal width at half height and then obtaining T_2 from the relationship: $LW = (\pi \cdot T_2)^{-1}$. This is unfortunately not the most precise method, as the experimental line width depends also on other factors, which include inhomogeneity of the field. However, for the purpose of this research, where the key is to prove if addition of sodium carbonate does cause the phases to separate, this method is sufficient. Moreover, due to time restrictions, this method is the most appropriate as it uses data already collected, which is additionally proved to be of high-quality, while other methods of T_2 measurement would need development and series of test runs before application.

Measurements of the linewidth proved that this value changes significantly with change of sodium carbonate concentration changes, as it is shown in Figure 52. Interestingly, the results prove the previous observations that the influence of the sodium carbonate concentration is not uniform for all species. It is strongly affecting the linewidth of the DG peak (observed at 85.5 ppm): in formaldehyde-water dilution with no salt addition, the linewidth is only 0.013 ppm (1.95 Hz), while in sample containing 0.0152 mol·dm^{-3} it is almost 13 times greater – 0.162 ppm (24.3 Hz).

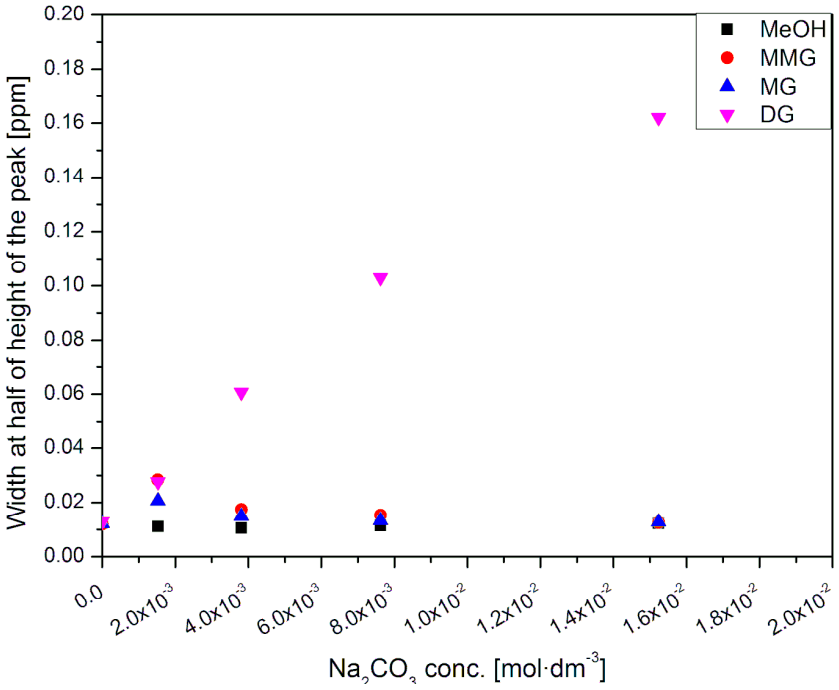

Figure 52. Changes of linewidth associated with variations of sodium carbonate concentration.

The linewidth (LW), as it was mentioned earlier, is closely related to the T_2, therefore an approximate values of T_2 can be calculated and then plotted against sodium carbonate concentration, as it is done in Figure 53. Linewidth

values were converted from ppm to Hz units and then T_2 values were calculated using the equation: $T_2 = \frac{1}{LW \cdot \pi}$.

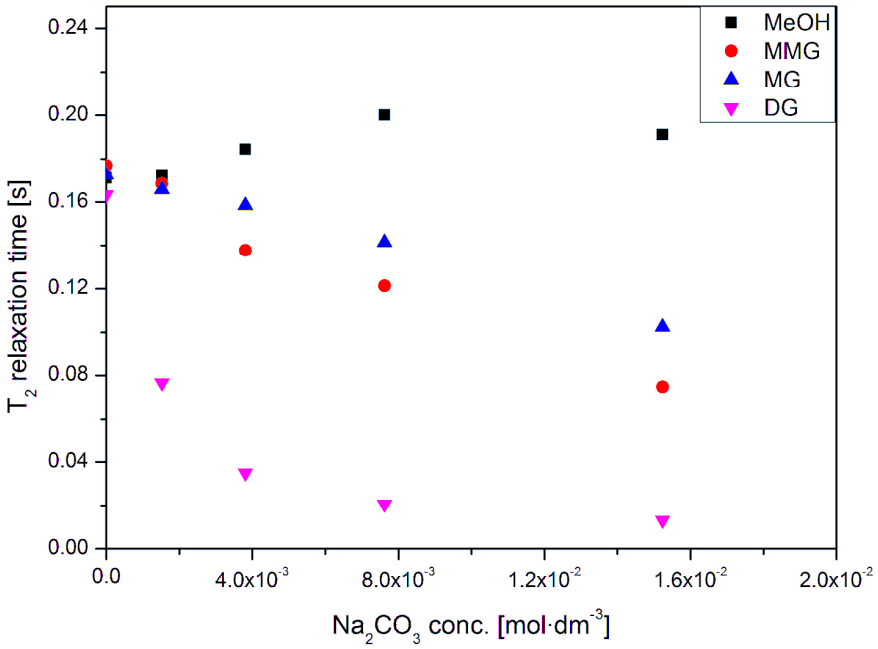

Figure 53. Changes of measured T_2 associated with variations of sodium carbonate concentration.

It can be clearly seen that the time constant for the spin-spin relaxation decreases significantly for all formaldehyde-related species, including the methoxylated ones. The greatest change is observed, once more, for the DG species: the T_2 for this molecule in formaldehyde-water dilution with no sodium carbonate is 0.163 s, while in solution containing the highest amount of the salt (0.0152 mol·dm^{-3}), the T_2 constant is 0.013 s. Though these values should be treated with caution, they do indicate a clear trend in T_2 dependency on amount of sodium carbonate. As it was mentioned before, the spin-spin relaxation process is dependent not on the arrangement of nuclei in the molecule but mostly on the environment in which the molecule

is found. Therefore, it is a constant more specific for the type of dilution rather than the chemical structure of investigated compounds. The fact that the T_2 changes for some of the species in a different manner, suggests that there is phase separation and that species tend to migrate into one or another, depending on a number of factors. Undoubtedly, this process is subject to diffusion (transport between two phases) and is governed by the Nernst distribution law. All formaldehyde-related species present a shorter T_2 relaxation constant values, while at the same time this increases slightly for methanol. This suggests that these species migrate to different phases and the lowering concentration of glycols or their methoxylated forms leads to faster spin-spin relaxation of methanol. It can be assumed that water is the dominating phase, however it is difficult to establish which species are present in which of the phases and if there are more than two present.

Further investigation of phase separation can be done by means of Dynamic Light Scattering. The results of experiments performed with this technique are described further below.

5.2. IR spectroscopy

The experiments performed using Fourier-Transform mid-IR spectroscopy included examination of five samples of formaldehyde-water-sodium carbonate solutions, with compositions similar to the ones examined by ^{13}C NMR. The composition of the samples was different only in respect to the addition of D_2O, as it can be seen in Table 18: all of D_2O was replaced with water, since the locking agent was not necessary.

Table 18. Composition of formaldehyde-water-sodium carbonate solutions investigated by IR.

Sample	**Water [ml]**	**Formaldehyde stock solution [ml]**	**Na_2CO_3 [g]**
Eq. R/C 50	10.00	1.47	0.0192
Eq. R/C 100	10.00	1.47	0.0096
Eq. R/C 200	10.00	1.47	0.0048
Eq. R/C 500	10.00	1.47	0.0019

The collected spectra were plotted together with a spectrum of formaldehyde-water solution without sodium carbonate in order to assess the impact of the salt on the appearance of the spectrum. The overall appearance of the spectrum remains unchanged, however, the signals at 1115 cm^{-1} and 910 cm^{-1} were significantly reduced upon addition of sodium carbonate. It is interesting that further addition of the salt did not proportionally affect the intensity of these signals. The peaks observed at 1115 cm^{-1} and 910 cm^{-1} are associated with C-H-C out of plane vibrations (in CH_3O- groups in methanol and methoxyglycols) and C-O symmetric stretch vibrations (in glycols and methoxyglycols), respectively. These differences can be seen in Figure 54, which shows this part of spectrum in detail.

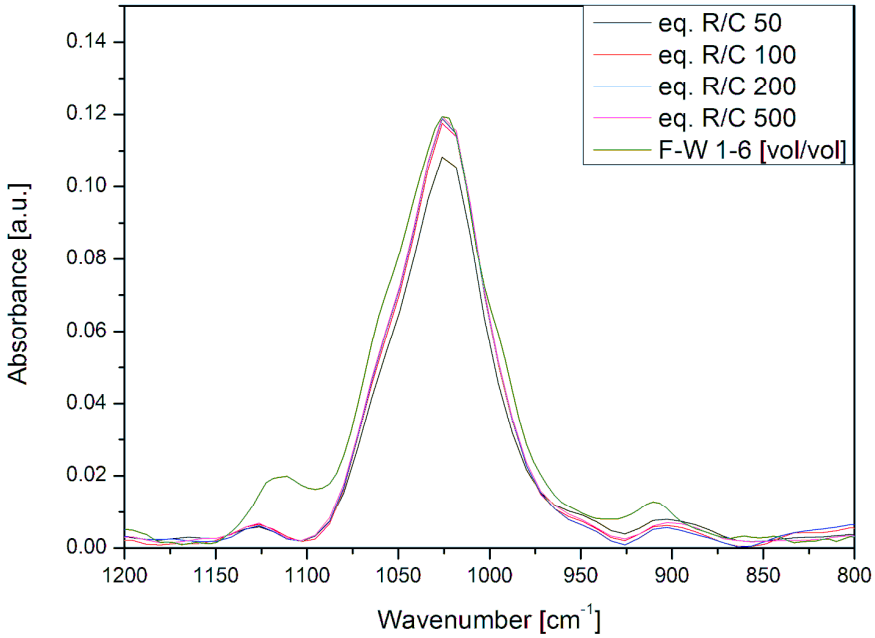

Figure 54. Section of IR spectra at 1200-800 cm^{-1} for formaldehyde-water-sodium carbonate solutions and formaldehyde-water solution.

Analysis, which included deconvolution of the peaks and integration of their area yielded information shown in Table 19. The most prominent differences in areas of peaks are between the formaldehyde-water solution without addition of the carbonate (the last column in Table 19) and formaldehyde-water-sodium carbonate solutions. Peak at 1025 cm^{-1} corresponds to the C-O asymmetric stretch vibrations in methanol as well as in glycols and methoxyglycols. Concentration of methanol, according to information obtained in ^{13}C NMR is not subject to significant changes with increasing concentration of sodium carbonate. The methanol concentration in formaldehyde-water dilution at 1:6 volumetric ratio is 0.27 $mol \cdot dm^{-3}$ and 0.25 $mol \cdot dm^{-3}$ in the formaldehyde-water-sodium carbonate solution with 0.0152 $mol \cdot dm^{-3}$ of the added salt. Similarly, concentrations of formaldehyde-

related species in sodium carbonate containing solutions are close to those in formaldehyde-water solution, as can be seen in Table 16. Since the species concentration are similar in all solutions regardless of sodium carbonate concentration, it appears that the presence of this salt affects the magnitude of IR signals in an unknown mechanism, as well as relative contributions of various vibrations to the overall IR spectra. This can be seen from Table 6, where relative areas of deconvoluted peaks are shown. Similarly, one would expect the area of the CH_3O^- peak in the sample with lowest sodium concentration to be the closest to the one in formaldehyde-water dilution without any salt. However, this is not the case. There is hardly any tendency in the dependency of the peak areas on the sodium carbonate concentration. This is interesting, as IR spectroscopy provided information on peak areas dependency on the dilution and there the trends were observed easily.

Table 19. Relative areas of deconvoluted peaks in IR spectra of formaldehyde-water-sodium carbonate solutions and formaldehyde-water dilution.

Wavenumber [cm^{-1}]	**Equivalent R/C ratio →**	**50**	**100**	**200**	**500**	**-**
	Sodium carbonate concentration [mol/dm^3] →	**0.0152**	**0.0076**	**0.0038**	**0.0015**	**0**
910	glycols/methoxyglycols	0.18	0.13	0.18	0.16	0.32
990	(oligo?)glycols/ methoxyglycols	1.24	1.92	2.44	2.11	1.47
1025	methanol/glycols/ methoxyglycols	4.37	3.99	3.26	3.83	3.99
1060	glycols/methoxyglycols	0.85	1.07	1.27	1.17	2.31
1115	methanol/ methoxyglycols	0.11	0.44	0.18	0.14	0.43

5.3. Dynamic Light Scattering

Since Dynamic Light Scattering is used to determine the mean hydrodynamic radius of submicron particulates in suspensions, appropriate filtering is essential. It allows to eliminate impurities from the reactants or solvents, which could then be mistakenly identified as products of reaction or new phases. Aqueous solutions of formaldehyde, water and sodium carbonate were filtered with 0.02 μm syringe filters as described in detail in the methodology section. A filter with this size of openings in the membrane removes all solid particulates which are larger than 20 nm in diameter, which means that virtually no solid impurities are left in the solution. It was decided that filtration would take place in several stages: each of the components of the solution was filtered separately and then mixed. Therefore no solid impurities were present and should phase separation occur, it would not be affected by the filtration process because the solution was not filtered after mixing. The filtration and handling process was conducted very carefully in order to minimise the risk of accidental pollution of the samples with dust. Control DLS measurements of the components prior to the mixing stage proved that virtually no submicron bodies were found, meaning that the filtration process was effective.

Two types of formaldehyde-water-sodium carbonate solutions were examined using DLS. The difference between them was that in one case D_2O was mixed with water used as a diluent at a 3:7 volumetric ratio in order to obtain solutions identical to those used for the ^{13}C NMR measurements. The other samples did not contain D_2O and were used as a control group in order to verify whether addition of D_2O would affect the phase separation.

Results obtained from experiments performed on solutions not containing D_2O prove that addition of sodium carbonate to the formaldehyde-water solution causes the shape of autocorrelation function to change. In samples containing sodium carbonate it is possible to observe a clear exponential decay shape, unlike in those without the added salt, as it can be seen in Figure 55. This indicates presence of domains of certain sort, with sufficient refractive index contrast, which were not observed in formaldehyde-water solutions. It is impossible to determine with DLS whether these objects are solid or liquid.

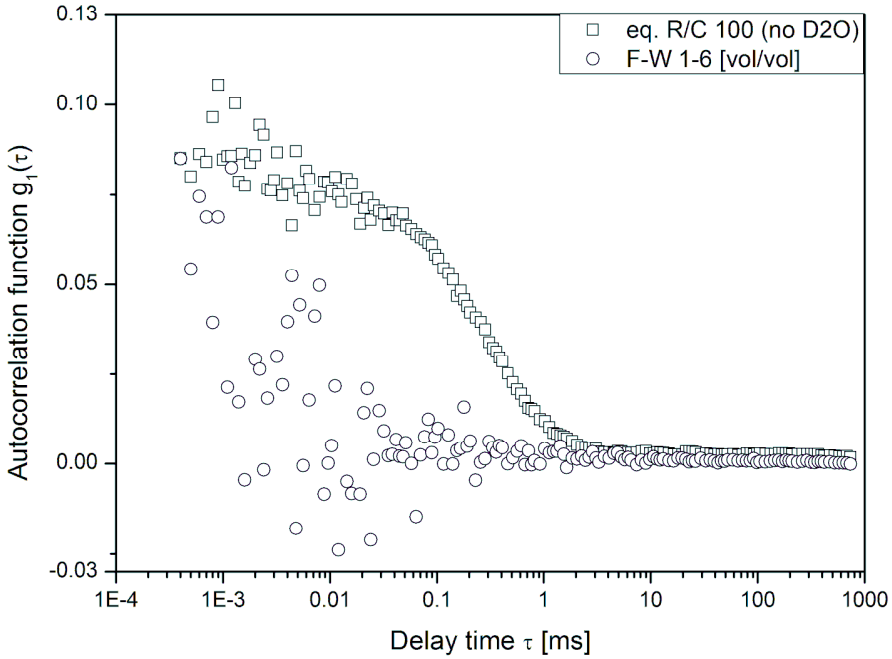

Figure 55. DLS autocorrelation function comparison between formaldehyde-water solutions (obtained by dilution of the formaldehyde stock solution with water at 1:6 volumetric ratio) with and without addition of sodium carbonate.

An interesting tendency was observed when autocorrelation functions for three solutions with different concentrations of sodium carbonate were plotted together, as it can be seen in Figure 56. First noticeable difference among all three curves is the delay time at which the exponential decay begins. This is correlated with the hydrodynamic radius of the observed objects and the later the decay begins, the larger size objects cause it due to its slower diffusive mobility. In this case, the slowest decay is corresponding to the highest sodium carbonate concentration, suggesting presence of the largest objects in this sample.

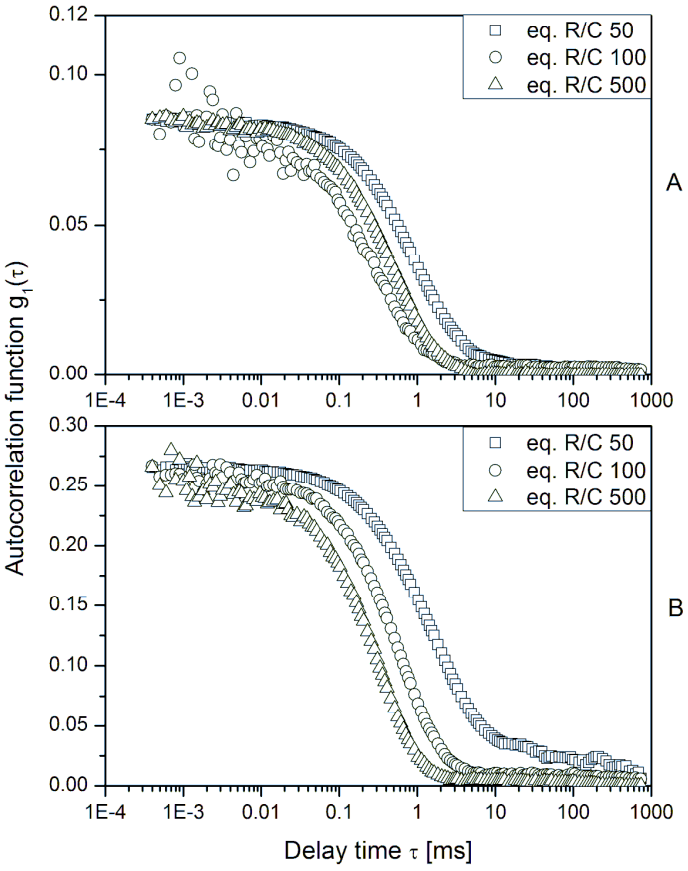

Figure 56. Autocorrelation functions for formaldehyde-water-sodium carbonate dilutions without D_2O (A) and with D_2O (B) as well as with different Na_2CO_3 concentrations (see Table 15 for details).

Numerical analysis of the autocorrelation functions seen in Figure 55 for solutions (formaldehyde-water-sodium carbonate solutions with formaldehyde to water volumetric ratio 1:6 and Na_2CO_3 concentrations equal to 0.0152 mol·dm^{-3}, 0.0076 mol·dm^{-3} and 0.0015 mol·dm^{-3}) with and without D_2O proved that addition of sodium carbonate lead to formation of objects with significant apparent hydrodynamic radius, as it can be seen in Table 20. It is clear that the higher the concentration of sodium carbonate, the greater hydrodynamic radius is observed. An increase in concentration by a factor of ten (0.0015 mol·dm^{-3} to 0.0152 mol·dm^{-3}) caused the hydrodynamic radius to increase almost three times – from 56 nm to 155 nm.

Table 20. Apparent hydrodynamic radii of particulates found in formaldehyde-water-sodium carbonate solutions with and without addition of D_2O.

Sample		**Na_2CO_3 [mol·dm^{-3}]**	**R_h [nm]**
eq. R/C 50	With D_2O	0.0152	236
	No D_2O		155
eq. R/C 100	With D_2O	0.0076	100
	No D_2O		59
eq. R/C 500	With D_2O	0.0015	85
	No D_2O		56

The comparison of these results proved that the presence of D_2O does not affect the fact of appearance of the submicron domains, however it does affect the apparent hydrodynamic radius of detected objects, as it can be seen in Table 20. The observed increase of hydrodynamic radius as a response to an increased concentration of sodium carbonate is the same as in solutions without D_2O, with the lowest radius reported for the lowest sodium carbonate concentration (0.0015 mol·dm^{-3}) and almost three times greater radius in solution with almost ten times greater salt concentration

(0.0152 mol·dm^{-3}). This confirms that addition of D_2O does not influence the relationship between the amount of catalyst and suspected microphase separation. Nonetheless, the results summarized in Table 20 prove that the D_2O addition has an effect on the dimensions of detected objects. Interestingly, in all examined solutions, regardless of the concentration of sodium carbonate, the hydrodynamic radius in solutions with D_2O is greater than in those without it by the factor of 1.5-1.7.

Due to the fact that all samples were carefully filtered, virtually no solid particulates of diameter greater than 20 nm were present in them prior to mixing, so it is safe to state that the large observed objects are droplets of a second phase which appears due to de-mixing process of the formaldehyde-water dilution. This is additionally supported by the fact that the sizes of these droplets are subject to sodium carbonate concentration and also the addition of D_2O.

5.4. pH measurements

Sodium carbonate is a salt of a weak acid and a strong base, therefore it can play a role of basifying component. In literature about polymerization of resorcinol and formaldehyde it is often replaced by other basic catalysts, including NaOH or KOH. It is assumed that the main role of the catalyst is to increase the pH value, so that resorcinol with a very high pK_a value can dissociate to a greater degree. Bearing in mind that in water the sodium ion is not attached to any particulate matter, while carbonate ions re-equilibrate until the following equilibria are reached:

$$HCO_3^- = CO_3^{2-} + H^+ \quad (42)$$

$$CO_2 + H_2O = HCO_3^- + H^+ \quad (43)$$

The pK_a values for these reactions are 10.35 and 6.33 for (42) and (43), respectively. The salt itself is regarded as strongly alkaline, with a pH value of a 0.1 mol·dm^{-3} solution measured to be 11.6. Therefore, it comes as no surprise that addition of even very small amount of sodium carbonate to a formaldehyde-water solution causes a significant increase of pH value, as it can be seen in Figure 57. The pH measured in formaldehyde-water dilution at volumetric ratio 1:6 is very low – only 3.37, however, when sodium carbonate is added, so that its molar concentration is as low as 0.0015 mol·dm^{-3}, the pH value soars to 9.69 (2.9 times greater). Further addition of the sodium carbonate does not cause such dramatic changes, nonetheless, a steady increase is observed, with pH values approaching 11.6, which was measured for a 0. 1 mol·dm^{-3} sodium carbonate aqueous solution without formaldehyde.

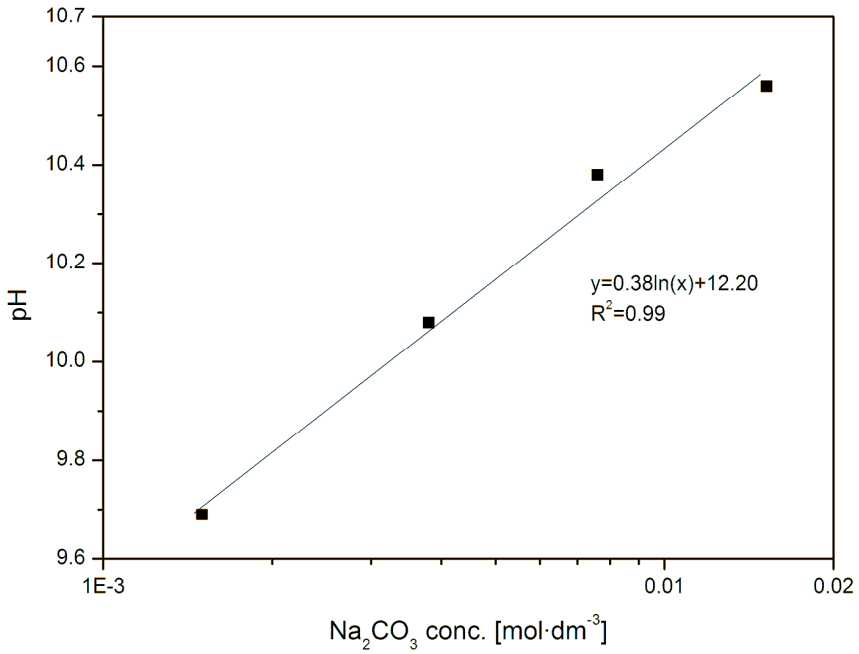

Figure 57. Changes in pH value of formaldehyde-water 1:6 by volume dilutions with addition of sodium carbonate.

5.5. Main conclusions from Chapter 5

Results of experiments described in Chapter 5 were very revealing in terms of determining the role of sodium carbonate as a catalyst. When added to formaldehyde solution, it did not affect the speciation of the solution despite affecting the pH. Although NMR was used primary to determine the effect of catalyst concentration on the speciation, it revealed a far more interesting phenomenon which was linewidth widening. This can be attributed to changes in T_2, which after a careful analysis and series of additional experiments were considered to be the effect of phase separation. Even after careful filtration and sample preparation, Dynamic Light Scattering confirmed presence of objects of diameter in range from a few tens to a couple hundred nanometres. The dimensions of these, most probably, droplets were enhanced by addition of D_2O by a constant factor. This previously not observed phenomenon clearly indicates that one of the roles of the catalyst is to induce phase separation, most probably through de-mixing of formaldehyde-water-methanol solution.

CHAPTER 6. KINETICS OF RESORCINOL-FORMALDEHYDE REACTIONS IN AQUEOUS SOLUTIONS

The main aim of this Chapter is to investigate the changes in the reacting mixtures in the course of the resorcinol-formaldehyde reaction in both room temperature and in elevated ones, in which the reactions are usually conducted for gel production.

The most straightforward method of assessing the overall influence of a given factor on the gel formation process is measurement of the gel time. These experiments were performed not only to determine how the temperature or the catalyst concentration influence the gel time, but also to determine the window of time for conducting NMR and DLS experiments to monitor reacting solutions before a gel forms.

Results of NMR experiments are presented and discussed here in terms of both qualitative and quantitative analyses. Assignments of ^{1}H and ^{13}C spectra were done with aid of those collected in 2D HSQC experiments. The focus was primarily on the initial stages of the reaction, in order to investigate the mechanism of formaldehyde addition to resorcinol and its dependency on the temperature and catalyst concentration. The main information which was sought after was identification of all products of the reaction between formaldehyde and resorcinol and, if present, products of condensation. It was of great importance to determine at which stage of the whole gel formation process these would be detected. Since fully quantitative ^{13}C NMR experiments are lengthy, they appear to be not at all practical in investigating kinetics of the reactions leading to gel formation. In most cases, a single experiment is considerably longer than the measured gelation time.

Therefore it was primarily the ^{1}H NMR spectroscopy method which was used to examine the kinetics of the reactions. The main advantage was very short acquisition time, which by far outweighed the issue of the –OH/D signal which made deconvolution essential.

IR spectroscopy is often used to monitor reactions in industrial processes as well as in laboratories. While this method provides less detailed information than NMR in case of non-reacting systems, it was used for kinetics investigation since the acquisition time of a good quality spectrum is very short and it allows monitoring of concentration changes of some reactants.

Dynamic Light Scattering experiments provided, along the NMR results, the most interesting and surprising results in this research. The main objective was to obtain information on the formation of primary particles in reacting solutions and their subsequent clustering and eventual gel formation. Measurements were performed in situ at 55°C and also at solutions undergoing reaction at 80°C, after their quenching to laboratory temperature. This allowed to determine the influence of both catalyst and temperature on the process of primary particle formation.

Time evolution of pH values in the course of the reaction was examined in order to further investigate the catalyst role in the resorcinol-formaldehyde reactions and subsequent gel formation. It was also confirmed that the addition of sodium carbonate can provide mildly basic or near-neutral conditions in which addition of formaldehyde to resorcinol is favoured.

6.1. Gelation time

A gel is a solid material which is substantially a dilute cross-linked system in which a solid macromolecule is immersed in a fluid. It can be said that gels are dispersion of liquid molecules in the solid phase with the latter one being the continuous phase. These materials show no flow when they are in steady state [124] and despite being mostly liquid by weight, they act as solids because the macromolecule constituting it is cross-linked. The properties of the gel, like its hardness and stickiness, strongly depend on the degree of cross-linking of the network. In case of resorcinol-formaldehyde gels the continuous (i.e. solid) phase is a macromolecule which is formed from polycondensation of various hydroxymethyl resorcinol derivatives. The exact mechanism of gel formation is not known, however there are a number of theories, which were discussed earlier in Chapter 2.

The gelation time is defined for the purpose of this research as the time measured from the moment the sample preparation is finished until it does not exhibit any flow when tilted to 45°. The method is described in Chapter 3. Measurements of the gelation time serve as an indication of overall rate of gel formation and its sensitivity to a variety of factors. There are several methods which can be used to determine the gelation time and these were discussed previously in Chapter 3. For purpose of this research, where mechanism of the early stages of resorcinol-formaldehyde reactions is studied rather than just overall gel formation process, a method to estimate gelation time based on visual observation was chosen. Since neither NMR nor DLS (which were the main experimental tools used in this work) were suitable to investigate gels, the gelation time determination was performed with the focus on specifying conditions to avoid gel formation during the

experiments and possible interference with measurements. The compositions of samples prepared and used to investigate the effects of reactants' and catalyst concentrations are presented in Table 21.

Table 21. Composition of samples used in gel time experiments.

R/W [g·cm^{-3}]	R/C [mol·mol^{-1}]	R/F [mol·mol^{-1}]	W [cm^3]	R [g]	C [g]	F [cm^{-3}]
0.10	50	0.5	10	1.00	0.0193	1.47
0.10	100	0.5	10	1.00	0.0096	1.47
0.10	150	0.5	10	1.00	0.0064	1.47
0.10	200	0.5	10	1.00	0.0048	1.47
0.10	250	0.5	10	1.00	0.0039	1.47
0.10	300	0.5	10	1.00	0.0032	1.47
0.10	350	0.5	10	1.00	0.0028	1.47
0.10	400	0.5	10	1.00	0.0024	1.47
0.10	450	0.5	10	1.00	0.0021	1.47
0.10	500	0.5	10	1.00	0.0019	1.47
0.10	550	0.5	10	1.00	0.0018	1.47
0.10	600	0.5	10	1.00	0.0016	1.47
0.10	100	0.5	10	1.00	0.0096	1.47
0.15	100	0.5	10	1.50	0.0144	2.21
0.20	100	0.5	10	2.00	0.0193	2.95
0.25	100	0.5	10	2.50	0.0241	3.69
0.30	100	0.5	10	3.00	0.0289	4.42
0.35	100	0.5	10	3.50	0.0337	5.16
0.40	100	0.5	10	4.00	0.0385	5.90

N.B.: W – water, R – resorcinol, C- catalyst (Na_2CO_3 – sodium carbonate), F - formaldehyde

Figure 58 shows results of measurement of gelation time for a range of catalyst concentrations (expressed as R/C ratio) at three different temperatures. It can be seen that both the temperature and the amount of catalyst influence greatly the resulting gelation time, as expected from previous reports in literature [9].

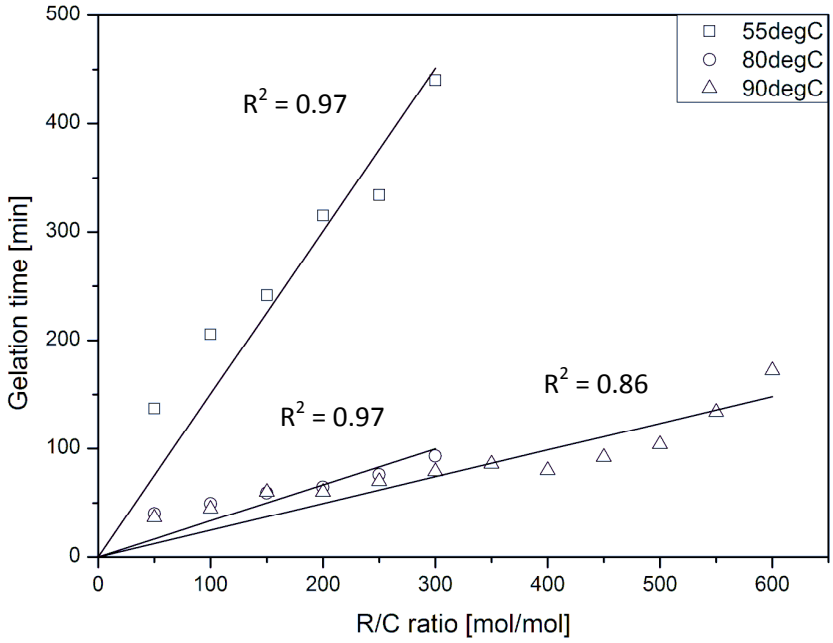

Figure 58. Dependence of gelation time on R/C ratio and temperature. R/C ratios as in the legend; R/W and R/F are equal to 0.10 g·cm^{-3} and 0.5 mol·mol^{-1}, respectively.

As can be seen from results in Figure 58 the higher R/C ratio at a given temperature results in longer time it takes for the gel to form. Interestingly, the observed gelation time varies linearly with the R/C ratio, so it is inversely proportional to the catalyst concentration in the solution (while the concentration of all other components of the solution is kept constant). The gelation time decreases with temperature: while these solutions do not appear to form gel at laboratory temperature, there is clear gelation time identifiable at 55°C for R/C ratios up to at least 300 and there is further decrease in gelation time by the factor of about 4 when temperature is increased to 80°C. However, gelation times are nearly identical at temperatures of 80°C (353K) and 90°C (363K).

Let us now explore a hypothesis that the influence of the catalyst on the gel formation kinetics is linked to the kinetics of the resorcinol-formaldehyde condensation reactions. In terms of gelation time dependency on the temperature, the results would be as expected. Higher temperatures increase the rate of condensation, which leads to faster formation of larger oligomers which are gradually interconnecting, thus increasing the viscosity of the solution. The gelation time is then expected to be inversely proportional to the rate of condensation reaction, which would be then proportional to the catalyst concentration, in agreement with results shown in Figure 58. The dependency of the inverse of the gelation time (proportional to the rate of condensation) on the temperature can then be described according to the Arrhenius equation $k = A \cdot e^{\left(\frac{-E_a}{RT}\right)}$, and the activation energy of the reaction leading to gel formation can be estimated. An Arrhenius plot of logarithm of gelation time versus 1/T has been done for each R/C ratio at all three investigated temperatures and the data was arranged linearly, therefore it was fitted with linear regression. The R^2 values for linear fitting were in range of 0.96-0.97 and the slopes of the obtained lines were equal to $-\frac{E_a}{R}$, from which activation energy (E_a) was determined. The values of this energy were between ca. 17 and 22 kJ·mol^{-1} and these were found to be subject to slight dependence on the amount of the catalyst but not significant enough to derive any solid conclusions. It appeared that the greater the concentration of sodium carbonate, the lower the activation energy. Apart from effects of temperature and R/C ratio, the concentration of resorcinol (expressed as R/W) was found to influence the rate of gel formation as well. Figure 59 shows results from gelation time measurements at 55°C and 80°C as a function of R/W ratio. The R/C and R/F ratios were kept constant and were 100 mol·mol^{-1} and 0.5 mol·mol^{-1}, respectively. However, it is important to

note that varying the R/W ratio while maintaining constant R/C and R/F ratios leads to samples with different catalyst and formaldehyde concentrations (see Table 21). Therefore, the results can be interpreted as influence of the overall concentration of reactants rather than just resorcinol concentration.

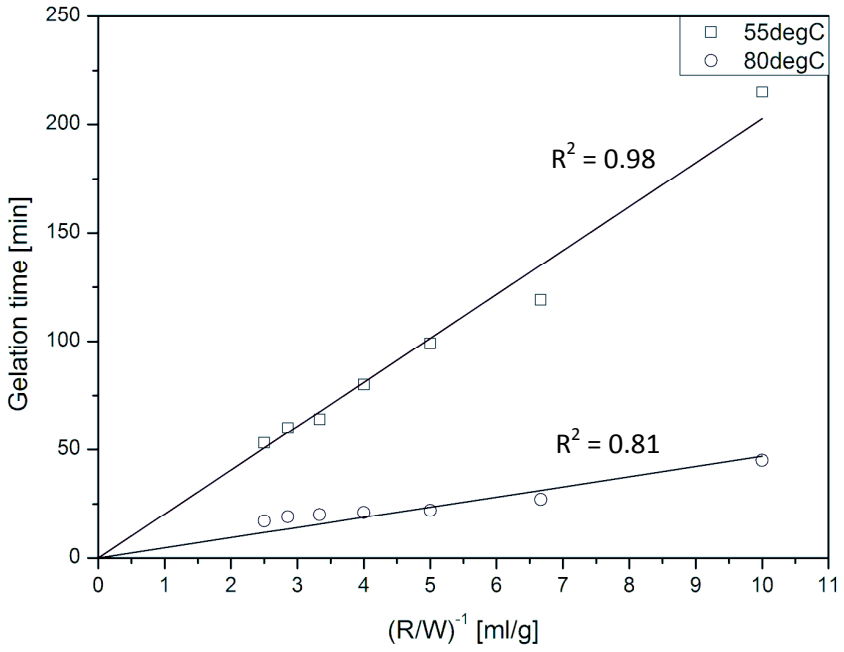

Figure 59. Dependence of gel time on R/W ratio and the reaction temperature. R/C and R/F were kept constant at 100 mol·mol^{-1} and 0.5 mol·mol^{-1}, respectively.

It can be seen that, just as this was the case in experiments in which R/C was varied, the gelation time varies linearly with the composition parameter R/W, while the gelation time at 55°C is about 4 times longer than that at 80°C at the same solution composition. The results from series of experiments investigating dependence of the gelation time on R/W ratio are consistent with the hypothesis that the gel formation kinetics is linked to reaction

kinetics of resorcinol-formaldehyde condensation. It would be expected that an increase in the reactant concentration would lead to faster condensation kinetics and shorter gelation times. This is because the number of effective collisions, which can lead to formation of new bonds and thus new species, is proportional to the concentration of colliding molecules. This effect is enhanced by temperature, which increases the energy and mobility of these atoms, making it more probable that the collision would take place and that it would be an effective one.

The main significance of these experiments for this research was the ability to determine a window of time available for experiments performed using DLS and NMR. The results allowed to establish the approximate time of the gel formation and thus enabled to select time during which the reacting solution was still in the initial stages with only insignificant changes in the viscosity caused by the reactions. The problem with increasing viscosity in the NMR experiments is that it is associated with changes in the relaxation times (T_2) which in turn leads to not fully relaxed and thus not fully quantitative spectra, and to problems with shimming which are reflected in the shapes of peaks. Therefore, it was necessary to establish the timeframe in which the collected data would not be affected by these changes.

6.2. Nuclear Magnetic Resonance

6.2.1. ^{13}C and ^{1}H NMR Qualitative Analysis

Due to the carbon-based nature of the reactants and the fact that the reaction between them is conducted in aqueous environment, the most preferable tool for qualitative investigation of reactant speciation and resulting products would be ^{13}C NMR. However, in order to get reasonable signal to noise

ratios, large number of scans is required, leading to very long acquisition times. This factor is unfortunately the greatest obstacle in employing ^{13}C NMR as a quantitative tool for examination of early stages of resorcinol-formaldehyde polymerisation. It fails to collect good quality and quantitative spectra in short periods of time, so that it could only be used to follow very slow reactions. As it was mentioned before, to obtain good quality and fully quantitative spectrum, an experiment lasting nearly 19h needs to be performed. In case of resorcinol and formaldehyde it is excessively long unless some form of reaction quenching is used. Shortening the acquisition time could be achieved by decreasing the number of scans but this would lead to lower signal-to-noise ratio and would cause greater error, especially when integrating the area of the low-intensity signals. Addition of relaxing agents, like $Cr(AcAc)_3$ would increase the rate of relaxation of carbon nuclei due to their paramagnetic enhancing effect, however, these agents can affect pH and one cannot exclude the possibility of the metal ion influencing the rate or even the mechanism of the reaction, making the experiment futile in terms of its interpretation. Another option considered was to use ^{13}C-enriched formaldehyde solution, however this was not pursued due to high costs. Nonetheless, ^{13}C NMR was used to study reacting solutions of formaldehyde and resorcinol but the main purpose of its application was to qualitatively identify reaction products and to facilitate the assignments of signals in the spectra collected with ^{1}H NMR (via HSQC experiments). The main advantage of ^{13}C NMR over ^{1}H NMR is the lack of water (-OH/D) peak, which overlaps with most of the -O-C**H**$_2$-O- groups signals in the aliphatic compounds. Additionally, the signals resulting from resorcinol (or any aromatic compound) are well separated from signals resulting from formaldehyde-related species like oligooxyglycols and their methoxylated

forms. The former ones are recorded at chemical shifts above 100 ppm, while chemical shifts from the latter ones are found in regions 81-94 ppm (-O-CH_2-O- groups) and 54-56 ppm (CH_3-O- groups). Additionally, the signals resulting from carbon nuclei in the hydroxymethyl groups attached to resorcinol should be found in region between 53 ppm and 70 ppm.

Resorcinol and substituted resorcinol species

Resorcinol has six carbon atoms, numbered from C(1) to C(6), where C(1) and C(3) carry one hydroxyl group each. As it can be seen in Table 22, the difference between chemical shift measured and calculated for carbon nuclei in resorcinol ring is 1.7 pm for hydroxyl-bound carbons C(1) and C(3) and 4.1 ppm for all other carbons. A plausible explanation for this would be the effect of water as the solvent and its interactions with hydroxyl groups of resorcinol. Formation of hydrogen bonds between water molecules and hydroxyl groups in resorcinol causes local changes in electron distributions, leading to changes in shielding of the nearest carbon nucleus and thus change in its chemical shift.

Table 22. Calculated and measured values of chemical shifts for resorcinol carbon nuclei.

Assignment	Calculated δ [ppm]	Measured δ [ppm]	Difference [ppm]
C(1)-OH	159.9	161.7	1.8
C(2)-H	103.6	107.7	4.1
C(3)-OH	159.9	161.7	1.8
C(4)-H	108.5	112.6	4.1
C(5)-H	131.5	135.6	4.1
C(6)-H	108.5	112.6	4.1

Substitution of resorcinol with formaldehyde should result in a number of changes in the spectra and it is worth to consider them before proceeding to assignment of the spectra. First of all, as it was previously reported [94], the chemical shift of carbon nuclei in unsubstituted resorcinol changes with the amount of catalyst added. More specifically, it was suggested that the position of the signals from resorcinol molecule in ^{13}C NMR spectra is dependent on the pH of the solution. The data presented in Table 23 shows that the chemical shift is affected by the amount of catalyst added to the resorcinol-water solution, however, in the considered pH interval (approximately 5.4-13.8), the extent of this influence is identical for all carbon nuclei in the resorcinol molecule. This is in accordance with the findings of Christiansen [94], who reported that the chemical shift can change by as much as 10 ppm for C(1) and C(3) when pH is increased from 9 to 12.5. More interestingly, according to the results of Christiansen's research, the pH affects positions of signals from C(1), C(3) and C(4/6), not C(5). This suggests that the effect is local and can be attributed to the specific nature of hydroxyl groups and their response to changing the concentration of hydrogen ions in the solution.

Table 23. Chemical shifts of carbon nuclei in resorcinol-water and resorcinol-water-sodium carbonate solutions at temperature 20°C.

Assignment	**Calculated δ [ppm]**	**Measured δ [ppm]**		**Difference**
		R/W 0.10 [g·ml^{-1}] no Na_2CO_3	**R/W 0.10 [g·cm^{-1}] R/C 50 [mol·mol^{-1}]**	
C(1)-OH	159.9	161.66	157.73	3.93
C(2)-H	103.6	107.67	103.53	4.14
C(3)-OH	159.9	161.66	157.73	3.93
C(4)-H	108.5	112.58	108.36	4.22
C(5)-H	131.5	135.60	131.51	4.09
C(6)-H	108.5	112.58	108.36	4.22

Secondly, reaction of resorcinol with formaldehyde results in substitution of hydrogen atoms with -CH_2OH groups on the resorcinol ring leading to important changes in the spectra of resorcinol in reacting solutions. There is a large number of possible substitutions of resorcinol and the chemical shifts of carbon nuclei in the most probable hydroxymethyl resorcinol species are shown in Table 24.

Table 24. Calculated chemical shifts of carbon nuclei in singly substituted hydroxymethyl resorcinol.

Assignment	**Calculated δ [ppm]**				
	Non-substituted	**C(2)-substituted**	**C(4)-substituted**	**C(5)-substituted**	**C(6)-substituted**
C(1)-OH	159.9	155.6	158.8	158.7	155.6
C(2)-H	103.6	121.4	103.8	102.5	103.8
C(3)-OH	159.9	155.6	155.6	158.7	158.8
C(4)-H	108.5	108.7	121.4	105.4	108.7
C(5)-H	131.5	130.4	129.9	144.0	129.9
C(6)-H	108.5	108.7	108.7	105.4	121.4

The most significant change in the values of chemical shift is related to the substitution of hydrogen atom with a hydroxymethyl group at any available carbon in resorcinol. In all cases the chemical shift of this specific carbon nucleus increases by 17.8 ppm, 12.9 ppm or 12.5 ppm (C(2), C(4/6), and C(5), respectively). It is worth mentioning that chemical shift of the C(1) and C(3), which are OH-bound, always decreases by 4.1-4.3 ppm when a directly neighbouring carbon atom is substituted, and by 1.1-1.2 ppm when a carbon atom further is substituted. The changes of the chemical shift of the H-bound carbon nuclei are less significant (from 3.1 ppm to 0.2 ppm), with decreasing magnitude as more distant carbon atoms are substituted.

Therefore the ^{13}C NMR spectra of reacting solutions of resorcinol and formaldehyde in the 100-200 ppm region should contain strong signals from H- and OH-bound carbon nuclei which should diminish in time, and series of small signals in their neighbourhood, corresponding to resonance frequencies of carbon nuclei altered by the substitution of hydrogen atoms with hydroxymethyl groups at neighbouring carbon atoms. Additionally, there should be a new peak detected at 121.4 ppm, which corresponds to the hydroxymethyl-substituted C(2,4,6) nuclei. Also possible would be presence of a signal at 144.0 ppm, corresponding to **C**(5)-hydroxymethyl substitution. Either of the signals at 121.4 ppm and 144.0 ppm has to be accompanied by groups of small peaks in the near proximity of the signals observed in unreacted resorcinol solutions.

In addition to changes in the resonance frequencies of carbons in resorcinol, substitution with hydroxymethyl groups causes also a prominent change in the ^{13}C NMR spectrum in the range partially overlapping with signals from methoxy groups in methoxylated glycols. Carbon nucleus in the hydroxymethyl group can be found in region of 53.6-65.3 ppm, as it can be seen in Table 25. Results of HSQC experiments allowed to unequivocally assign the signals in this region, due to the fact that the values of chemical shift of the protons in the methoxylated glycols are significantly different than in hydroxymethyl groups bound to resorcinol (see below).

Table 25. Calculated chemical shifts of carbon nuclei in hydroxymethyl groups bound to resorcinol.

Assignment	**δ [ppm]**
R(C2)-**C**H$_2$OH	53.6
R(C4/6)-**C**H$_2$OH	59.9
R(C5)-**C**H$_2$OH	65.3
HO**C**H$_2$-(C4/6)R(C2)-CH$_2$OH	60.2
HOCH$_2$-(C4/6)R(C2)-**C**H$_2$OH	53.9
HO**C**H$_2$-(C5)R(C2)-CH$_2$OH	65.3
HOCH$_2$-(C5)R(C2)-**C**H$_2$OH	53.6
HO**C**H$_2$-(C4)R(C6)-CH$_2$OH	60.2
HOCH$_2$-(C4)R(C6)-**C**H$_2$OH	60.2

In later stages of reacting resorcinol-formaldehyde systems, when resorcinol-formaldehyde undergoes water and/or formaldehyde producing condensation reactions, changes in the resorcinol and glycol related sections of the ^{13}C NMR are further accompanied by signals corresponding to aliphatic carbon atoms forming bridges between two or more resorcinol rings. There is a large number of possible structures formed by two hydroxymethyl resorcinol molecules condensing together. It is known that the aliphatic chain that links two resorcinol molecules is formed from hydroxymethyl groups condensing together producing either water or formaldehyde, as it can be seen in Figure 60.

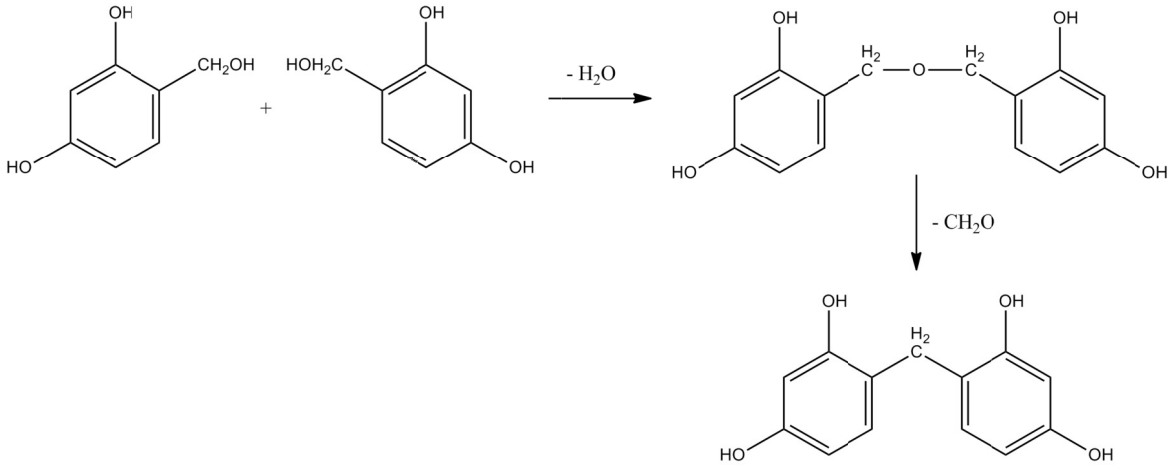

Figure 60. An example of hydroxymethyl resorcinol derivative condensation with water and formaldehyde as by-products.

Conveniently, ^{13}C NMR signals from carbons in both types of bridges between resorcinol molecules yield resonances in the region of significantly different chemical shifts than other species present, as can be seen in Table 26.

Table 26. Calculated ^{13}C NMR chemical shifts of carbon nuclei in aliphatic bridges linking resorcinol molecules.

B →	**δ [ppm]**		
	R^1-<u>C</u>H_2-O-CH_2-R^2	R^1-CH_2-O-<u>C</u>H_2-R^2	R-<u>C</u>H_2-R
C(2)-B-C(2)	62.1	62.1	16.5
C(2)-B-C(4/6)	62.1	69.7	22.7
C(2)-B-C(5)	62.1	73.1	28.1
C(4/6)-B-C(4/6)	69.7	69.7	28.9
C(4/6)-B-C(5)	69.7	73.1	35.7

Regardless of between which two resorcinol carbon atoms the methylene bridge is formed, the values of chemical shift of the carbon nucleus in the methylene bridge are significantly lower than any of the other observed signals. As discussed earlier, neither formaldehyde nor resorcinol spectra

have any peaks below 50 ppm (methanol in formaldehyde solutions), therefore, should these bridges be formed, their signals would be easily detected. The more likely type of linkage between resorcinol rings is the ether-like bridge, with carbons giving rise to signals at chemical shift similar to those of oligooxyglycols. Fortunately, proximity of the resorcinol rings influences their chemical shift and causes these signals to appear at chemical shifts smaller than those of oligooxyglycols (the lowest is 82.0 ppm but greater than from methoxylated oligooxyglycols (the highest of which is 55.6 ppm).

Experiments on reacting solutions

The greatest challenge in application of ^{13}C NMR to examine reaction kinetics in resorcinol-formaldehyde solutions was the very long acquisition time caused by long delay times, required to obtain a fully-relaxed and thus quantitative data. It was reasoned that since the gelation time, which is hypothesized to be an indicator of the overall reaction rate of resorcinol-formaldehyde polymerisation, decreases with both increased concentration of reactants and elevated temperature, increasing dilution and cooling down of the sample would have an opposite effect, resulting in quenching of the reacting system. Quenching by cooling, without additional dilution, was used in DLS experiments performed at temperatures above 55°C, which is the temperature limit of the DLS unit used here. The same samples were also investigated by ^{13}C NMR to provide some preliminary insight into processes happening in reacting solutions. The reaction mixture was prepared as usual and placed in a sealed vial in the electric oven preheated to 80°C or 90°C. At certain time intervals (0, 10, 20 and 30 min) a sample of 1 ml was taken by an automatic pipette, diluted in 3 ml of water-D_2O mixture (7:3 by volume)

which was kept in an ice bath (temperature above 0°C) to ensure the reacting mixture would be quenched immediately. The solution was then lightly shaken to mix and transferred into a clean and dry NMR tube equipped with a coaxial insert. The temperature during experiments was kept constant at 293K and both ^{13}C and HSQC (see the next subsection) spectra were collected. These experiments are further referred to as *snapshots*.

The spectra collected for t = 0 min, which correspond to no high-temperature treatment of a reacting mixture already had new peaks. New signals were observed in the 50-60 ppm region, as seen in Figure 61 (indicated by red arrows). The chemical shift values of these two signals are 59.2 ppm and 53.1 ppm, however, the latter signal has very low intensity and therefore its area is subject to large error which needs to be considered when performing quantitative analysis. At the same time, two signals, corresponding to methoxylated di- and triglycol (55.3 ppm and 55.5 ppm) are significantly decreased. Interestingly, even though the new signals are most surely related to the aliphatic carbon in the hydroxyl group attached to resorcinol, analysis of changes in their area in time prove that instead of increasing their abundance, they decrease gradually. The same observation was made for all other peaks, therefore it was concluded that most probably the solubility of the reacting species in water and D_2O mixture decreases as reaction progresses.

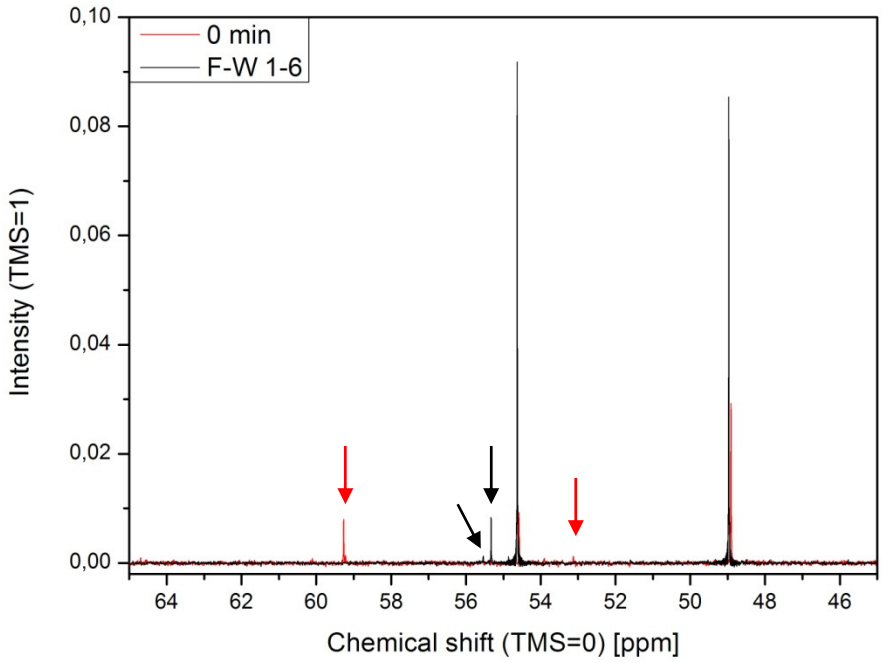

Figure 61. 45-65 ppm region of ^{13}C NMR spectrum of reacting mixture (R/C 200 mol·mol^{-1}, R/W 0.10 g·ml^{-1}, R/F 0.5 mol·mol^{-1}, see text for details) at t=0 min and formaldehyde-water solution (1:6 volumetric ratio).

The changes observed in the 45-65 ppm region are expected to be accompanied by changes in the 100-165 ppm region, which is assigned to carbon nuclei in aromatic compounds. As it is shown in Figure 61, there is a number of new peaks which correspond to carbons with resonance frequencies changed by the substitution of resorcinol. Signals originating from unsubstituted carbons in resorcinol rings are the most intense (ca. 0.04 to 0.085 of the reference TMS signal) and are accompanied by less intense signals of the same carbons in resorcinol molecules in which the neighbouring carbons were substituted and formed hydroxymethyl resorcinol. These are labelled with red arrows and appear at chemical shift lower by no more than 5 ppm from the unsubstituted signal, except for the

signal of the C(5). In this case when other carbons (C(2,4,6)) are substituted, the signal of this carbon nucleus is present at a higher chemical shift. This is unexpected, as calculated chemical shift is lower, just as it is for other carbon nuclei in resorcinol (see Table 24). Nonetheless, this is consisted with previous findings.

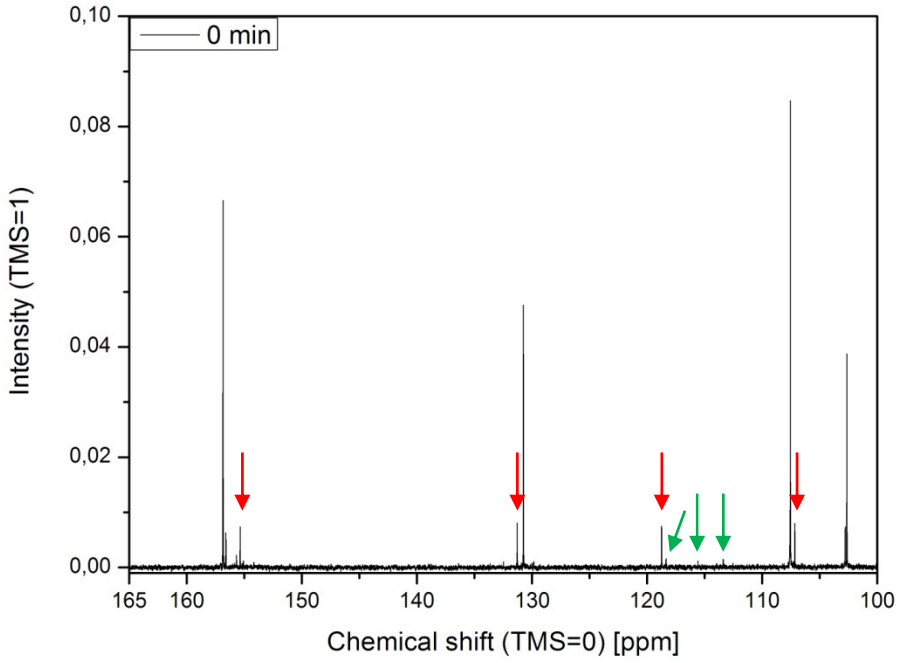

Figure 62. 100-165 ppm region of ^{13}C NMR spectrum of reacting mixture (R/C 200 mol·mol^{-1}, R/W 0.10 g·ml^{-1}, R/F 0.5 mol·mol^{-1}, see text for details) at t = 0 min.

The signal appearing at ca. 118 ppm is not observed in aqueous solution of resorcinol. It is considered to be the signal of either of the C(2) or C(4/6) when they are substituted with hydroxymethyl group. The calculated value of this specific chemical shift is 121.4 ppm, however it is experimentally observed at a lower value. It is discussed further on, along with assignment

and correlation of all other signals present in these spectra. The signal at ca. 118 ppm is accompanied by very small signals at lower chemical shift values (green arrows in Figure 62). It is possible that these correspond to substituted carbons C(2) or C(4/6), which do not appear in the signal at ca. 118 ppm. However, it is impossible to determine which peak corresponds to which specific carbon and if these small signals can indeed be assigned to any of these carbon nuclei. It is not expected that substituted carbons C(2) and C(4/6) resonate at different frequencies, however, given the nature of this reacting mixture it is possible that the chemical shift of these signals varies, as it does for certain species found in formaldehyde-water or formaldehyde-methanol dilutions. It is important to note that there is no signal at ca. 144.0 ppm, which would correspond to C(5) substituted with hydroxymethyl group. Organic chemistry predicts that hydroxyl group attached to a carbon atom in an aromatic ring directs the electrophilic substitution towards *para* and *ortho* carbon atoms. Resorcinol has two hydroxyl groups and their presence would direct the substitution towards carbons 2 and 4/6, which are in positions *para* and *ortho* with respect to each of the groups. It is therefore unlikely that the electrophilic substitution would take place at C(5), which appears to be confirmed by these experiments, although it is challenged by findings of the HSQC and ^{1}H NMR experiments (see below).

Table 27. Correlation of calculated and measured chemical shifts of signals detected in ^{13}C NMR experiments on reacting mixture (R/C 200 mol·mol^{-1}, R/W 0.10 g·ml^{-1}, R/F 0.5 mol·mol^{-1}; samples in water-D_2O solution; see text for details).

Assignment	**δ [ppm]**				
	Calculated	**Measured**			
		0 min	**10 min**	**20 min**	**30 min**
TMS	0	0	0	0	0
MeOH	46.70	48.91	48.91	48.91	48.90
R(C2)-<u>C</u>H_2OH	53.60	53.13	53.13	53.12	
MMG	55.30	54.58	54.57	54.56	54.55
R(C4/6)-<u>C</u>H_2OH	59.90	59.27	59.27	59.27	
MG	82.00	81.83	81.83	81.82	81.82
DG	85.20	85.59	85.59	85.59	85.59
MMG	91.40	89.51	89.51	89.50	89.49
R-C(2)	103.60	102.64	102.63	102.62	102.62
R-C(4),C(6) when C(2,5) subst.	107.05	107.17	107.16	107.17	
R-C(4,6)	108.50	107.56	107.55	107.55	107.56
R-C(2,4,6)-substituted	121.40	117.56	117.55	118.73	
R-C(5)	131.50	130.75	130.74	130.75	130.73
R-C(5), when (2,4,5,6) subst.	130.07	131.28	131.27	131.28	
R-C(1,3) when C(2,4,5,6) subst.	157.18	155.88	155.86	155.86	
R-C(1,3)	159.90	156.85	156.83	156.83	156.82

The analysis of spectra collected at different time intervals allowed assignment of all detected peaks and correlation of the calculated and measured chemical shifts. The results of this analysis are summarized in Table 26. Regardless of the length of the temperature treatment (0, 10, 20 and 30 min), the values of chemical shifts of the detected peaks were constant and varied by less than 1 ppm. Moreover, when measured values are plotted against the calculated ones, they show a good correlation pattern, as shown in Figure 63.

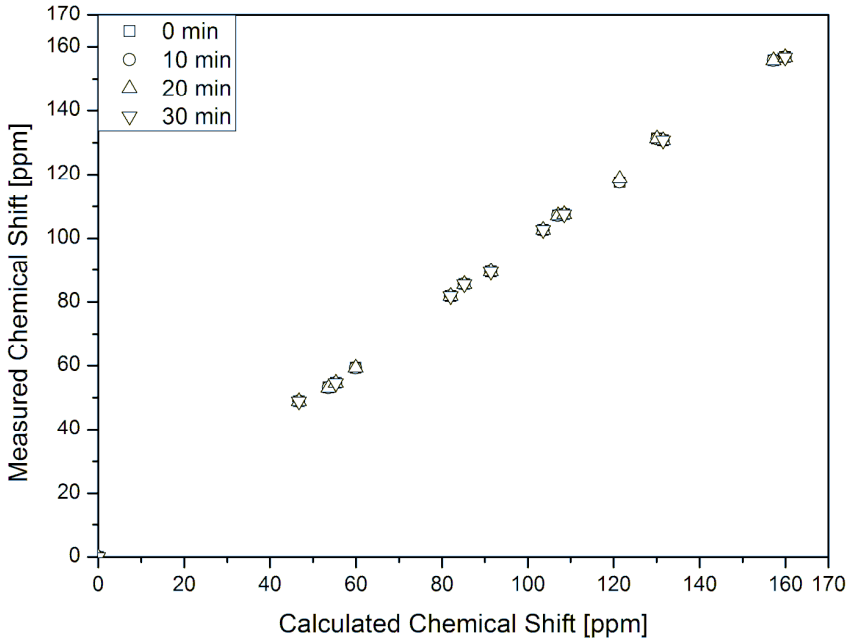

Figure 63. Correlation of chemical shifts of carbon nuclei in reacting mixture.

As can be observed from the data in Table 27, spectra collected after 30 min of high-temperature treatment contains fewer signals than spectra collected for samples which underwent shorter heating while areas under all peaks decreased over time. Surprisingly, the signals that disappeared completely are assigned to the products of resorcinol-formaldehyde reactions , while no other new signals were recorded. The signals of the reactants are still present, though are far less intense

HSQC measurements

A set of 2D NMR HSQC experiments was performed to aid the assignment of any new species produced by reactions of resorcinol and formaldehyde and/or their subsequent condensation reactions. The spectra resulting from these experiments are represented as planes with two axis corresponding to

appropriately scaled carbon or hydrogen spectra, respectively, while the plane contains signals of protons and carbons directly bound to each other. Each of the signals on the plane has two coordinates, with corresponding values of chemical shift (here x axis shows proton shift and y axis shows carbon shift). Just as it was done for formaldehyde-water and formaldehyde-methanol solutions, from the known assignment of carbon NMR chemical shifts, the hydrogen NMR chemical shifts can be assigned basing on the HSQC spectrum.

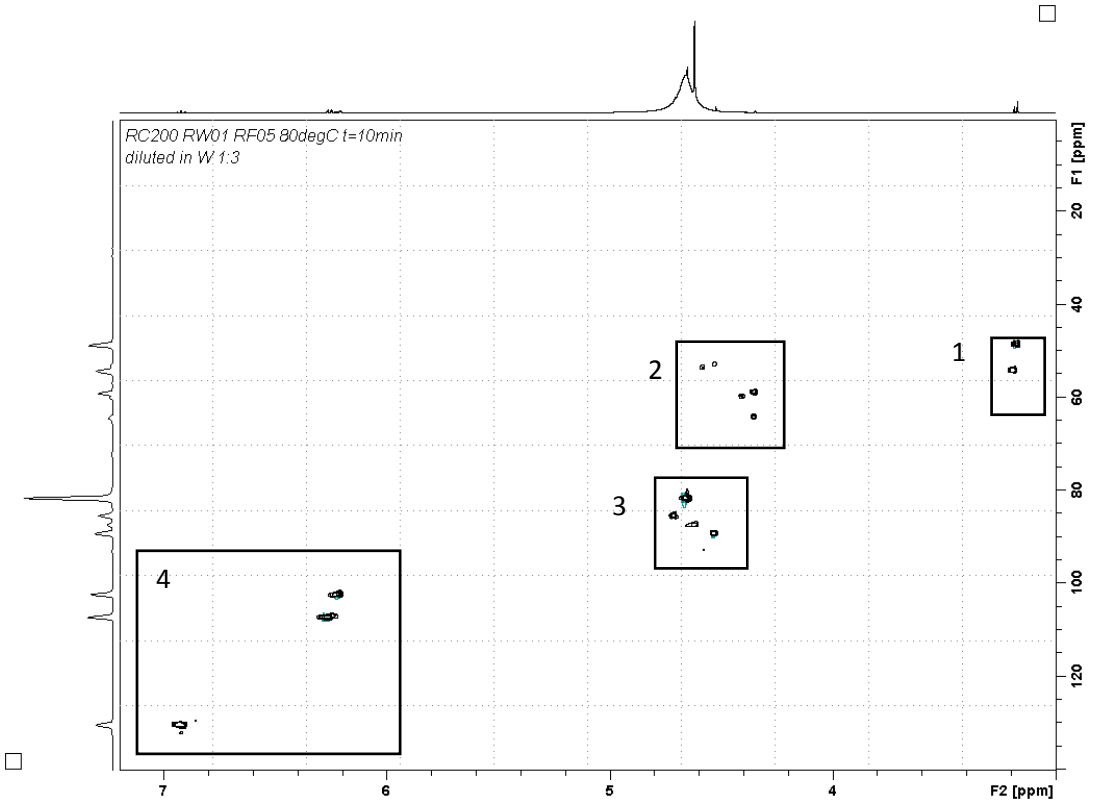

Figure 64. An HSQC spectrum collected after 10 min of temperature treatment (80°C) of a reacting mixture (R/C 200 mol·mol^{-1}, R/W 0.10 g·ml^{-1}, R/F 0.5 mol·mol^{-1}; water-D_2O solution; see text for details).

An HSQC spectrum shown in Figure 64 can be analysed in four sections, as marked in the figure. Sections 1 and 3 correspond to the signals originating

from the formaldehyde-related species, while Section 4 corresponds to resorcinol. The two peaks seen in Section 1 are due to the methoxy group **H**$_3$CO- in both methanol and MMG, as they were assigned previously in Chapter 4. Section 3 contains all the methylene group -C**H**$_2$O- signals, present in MG, oligooxyglycols and their methoxylated forms. Section 4 contains three signals, corresponding to carbon nuclei (C(2), C(4)&C(6) and C(3)) in resorcinol. There is an additional peak in the ^{13}C NMR spectrum at 160 ppm corresponding to C(1) and C(3), however since neither of these is directly bound to a hydrogen atom, the peak is not present in the HSQC spectrum. Section 2 contains new signals and is therefore the most interesting, as it can be seen in magnification in Figure 65. There are five new signals observed there and their assignment is based on comparison of the calculated and measured ^{13}C NMR chemical shifts. The number of peaks visible in this section is larger than it was observed in the classic 1D NMR experiment where only one signal was detected, and this is most probably due to greater sensitivity of HSQC experiments which rely on a much more abundant and faster-relaxing isotope (^{1}H).

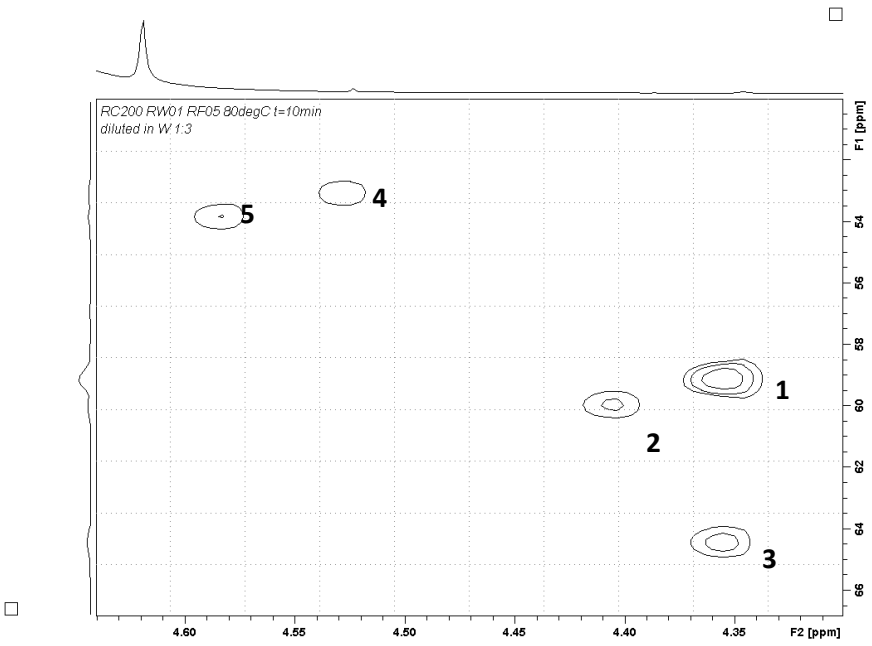

Figure 65. Magnification of Section 2 from Figure 64.

The assignment of peaks visible in Figure 65 is summarized in Table 28. As expected, there are signals originating from hydroxymethyl groups attached to the resorcinol ring at C(4/6) and basing on the peak areas for these signals, these are the most abundant species. Assignments of other peaks reveal interesting observations. Only after 10 min of temperature treatment, signals of di-substituted resorcinol are detected. At the same time, the Section 4 (see Figure 64) contains signals for hydrogen atoms attached to C(2,4,6), indicating that substitution at more than one site takes place simultaneously and not after the preferred carbon site is fully substituted. Moreover, presence of peak 3 shows that substitution takes place also at C(5), which has been previously considered to be an unfavourable site [126]. This signal can be assigned to both mono- and di-substituted resorcinol, however, in both cases it originates from hydrogen atoms bound to the carbon in hydroxymethyl group attached directly to C(5). As with the observation

regarding di-substitution, it is interesting that this site is substituted while others, considered to be preferable, are still available for substitution.

Table 28. Assignment of signals registered in Section 2 of an HSQC spectrum collected for reacting mixture (R/C 200 mol·mol^{-1}, R/W 0.10 g·ml^{-1}, R/F 0.5 mol·mol^{-1}; water-D_2O solution; see text for details; measured at 20°C) after 10 min of temperature treatment (80°C).

Peak	Assignment	Chemical shift [ppm]			
		Calculated		Measured	
		^{1}H	^{13}C	^{1}H	^{13}C
1	R(C4/6)-**C**H$_2$OH	4.61	59.9	4.35	59.1
2	HO**C**H$_2$-(C4/6)R(C2)-CH$_2$OH	4.61	53.9	4.58	53.8
3	R(C5)-**C**H$_2$OH and HO**C**H$_2$-(C5)R(C2)-CH$_2$OH	4.61	65.3	4.36	64.4
4	R(C2)-**C**H$_2$OH and HOCH$_2$-(C5)R(C2)-**C**H$_2$OH	4.61	53.6	4.53	53.1
5	HOCH$_2$-(C4/6)R(C2)-**C**H$_2$OH	4.61	60.2	4.58	59.9

Just as it was observed in 1D ^{13}C NMR experiment, an HSQC spectrum collected for a reacting mixture without any temperature treatment (i.e. referred to as t=0 min) revealed presence of a new signal at 3.81/59.42 ppm (δ_{1H}/δ_{13C}) (measured at 20°). It is a signal assigned to the hydroxymethyl group bound to resorcinol ring at C(4/6) and it proves that substitution can take place in room temperature.

Additional ^{13}C NMR experiment was performed for a different reacting mixture. In this case the R/C ratio was set to 100 mol·mol^{-1}, while R/W and R/F were the same as previously (0.10 g·ml^{-1} and 0.5 mol·mol^{-1}, respectively). The main difference was, except for doubling the concentration of the catalyst, that the sample was not diluted and the reaction was running *in situ* inside the NMR spectrometer probe, where temperature was kept constant at

20°C. As usual, each spectrum consisted of 1024 scans and during their collection there was a great chance of the composition changing and therefore making the final spectrum an averaged image of the composition of the sample. It is the case of all other NMR experiments presented here, however all effort was made to ensure that these changes would be minimal (i.e. dilution and cooling down the solution) or averaged over relatively short time, when the main goal of the experiment excluded the possibility of slowing down the reaction. The purpose of this experiment was to verify if any new signals would appear after a considerable amount of time, which was to compensate for lack of temperature treatment. Therefore it was only qualitative data that was sought after and a compromise had to be made between the number of scans and delay time. Reducing the number of scans would lead to spectrum with low signal-to-noise ratio and the possible new signals, which were expected not to be intensive, could be lost in the noise of the baseline. It would however allow to choose longer delay time, permitting a fuller relaxation and therefore more intensive signals. It was decided to run a pulse programme with considerably shorter delay times but with a high number of scans, allowing for a good signal-to-noise ratio. As a consequence, one spectrum was collected over approximately 1 h instead of nearly 19 h. The analysed spectrum was collected for approximately 60 min starting 790 min after the reactants were mixed together.

The most significant difference between the results of this experiment is different intensity and the number of the signals in the 45-65 ppm region, corresponding to carbon nuclei in the hydroxymethyl groups bound to resorcinol. There are new signals at 54.1 ppm, 59.3 ppm, 60.2 ppm and 64.6 ppm. All of these signals were also observed in the HSQC experiments of the diluted samples of the reacting mixture (R/C 200 $mol \cdot mol^{-1}$, R/W

0.10 g·ml^{-1} and R/F 0.5 mol·mol^{-1}) but were virtually shadowed by the noise in the ^{13}C NMR experiments. The assignment of these peaks is presented in Table 28. The region of 100-165 ppm of the spectrum is very similar but the signal-to-noise ratio is improved, so there are more signals observed. Groups of peaks in direct vicinity of signals corresponding to carbon nuclei in resorcinol bound to hydrogen atoms contain more peaks with low intensity. It is highly probable that these signals were also lost in the noise in the previous ^{13}C NMR experiments. Interesting observation is made in the 115-120 ppm region, where signals from resorcinol carbon C(2,4/6) nuclei substituted with hydroxymethyl group should be found. As previously, there is a relatively strong signal found at 118.6 ppm and it is accompanied by a smaller one at 118.2 ppm and then one more at 115.5 ppm. These are most probably the same peaks as those marked with green arrows in Figure 62. It can be concluded that the chemical shift of carbons C(2,4/6) can be differentiated between despite the fact that the calculated value of chemical shift is uniform for all these three and is equal to 121.4 ppm.

^{1}H NMR measurements

^{1}H NMR seems like a more obvious choice in terms of kinetics examination, as acquisition times are low (ca. 2 min) and certain techniques allow data collection in even shorter intervals. Moreover, despite short delay times (1 s compared to 60 min in ^{13}C NMR) this method provides quantitative data of good signal-to-noise ratio in a matter of minutes, which is crucial in this case. However, it is not ideal. The main problem is the presence of water which yields a very strong and broad signal, which is enhanced by signals of –OH groups in both glycols and resorcinol. Unfortunately, as discussed earlier, this peak covers a relatively wide chemical shift range and obstructs signals

of the CH_2-groups in oligooxyglycols. In most cases deconvolution can solve this problem, however it is only possible when the positions of the peaks beneath the –OH peak are known or when its shape indicates their whereabouts.

Resorcinol signals can be found in section of the spectra which is not assigned to any of the formaldehyde-related species, i.e. above 5 ppm, as it can be seen in Table 29. According to calculations, the smallest chemical shift assigned to resorcinol in proton spectra is 5.35 ppm and corresponds to the proton in –OH groups at carbon nuclei 1 and 3. The next signals are detected at 6.27, 6.51 and 7.11 ppm, corresponding to protons attached to carbons 2, 4/6 and 5, respectively. Presence of water in the solution changes these values slightly, as ^{1}H NMR spectrum collected for a solution containing 0.10 g·ml^{-1} resorcinol in water and D_2O (7:3 volumetric ratio) had peaks at 5.62, 5.67, 5.69 and 6.34 ppm. The registered values were smaller than expected, most probably due to the formation of hydrogen bonds, however, they are still well separated from formaldehyde-related signals and are not overlapped with the –OH peak. In terms of quantitative analysis based on this data, the concentration estimated from the area of the peaks in the spectrum – depending on which peak was used – differed from the calculated values by as little as 0.2-3.7%.

Table 29. Calculated and measured ^{1}H chemical shifts of 0.10 g·ml^{-1} resorcinol in water and D_2O.

Assignment	**δ [ppm]**		
	Calculated	**Measured**	**Difference**
C(2)-**H**	6.27	5.63	0.64
C(4)-**H** / C(6)-**H**	6.51	5.67	0.84
	6.51	5.68	0.83
C(5)-**H**	7.11	6.34	0.77

Similarly to the spectra collected with ^{13}C NMR, the proton spectra are expected to change in at least two regions. The primary change is the one resulting from alternating the chemical shift of protons attached to carbons of the resorcinol ring. Once resorcinol reacts with formaldehyde, proton bound to one of the available carbons (2, 4, 5, 6) is replaced and hydroxymethyl derivative is formed, thus the signal of this proton disappears. At the same time, the chemical shifts of other, remaining protons are changed, as it can be seen in Table 30. Since the substitution is a gradual process, the signal of a proton at a carbon susceptible to substitution decreases progressively in time, as not all resorcinol molecules are substituted at the same time. Therefore it is expected that signals assigned to protons bound to C(2,4,5,6) disappear in time and simultaneously new signals, with similar chemical shift, appear.

Table 30. Chemical shifts of proton nuclei in resorcinol ring of the hydroxymethyl derivatives.

Assignment	**Calculated δ [ppm]**				
	Non-substituted	**C(2)-substituted**	**C(4)-substituted**	**C(5)-substituted**	**C(6)-substituted**
C(2)-**H**	6.27	-	6.24	6.20	6.24
C(4)-**H**	6.51	6.44	-	6.66	6.24
C(5)-**H**	7.11	7.04	7.02	-	7.02
C(6)-**H**	6.51	6.44	6.24	6.66	-

Regardless of the position at which the hydroxymethyl group is attached and of the number of the groups attached to resorcinol ring, the chemical shift of the protons attached to the aliphatic carbon in this group (R-C**H**$_2$OH) is predicted to be 4.61 ppm. In this regard, ^{1}H NMR is of little use in determining the rate at which each position is substituted, however it

provides valuable information on the overall rate of reaction between formaldehyde and resorcinol.

Condensation of hydroxymethyl derivatives leads to formation of -CH_2-O-CH_2- or –CH_2- bridges between these molecules and chemical shifts of protons in these links were calculated and summarised in Table 31.

Table 31. ^{1}H NMR chemical shifts of atoms in bridges linking resorcinol molecules.

	Calculated δ [ppm]		
B →	R^1-C**H**$_2$-O-CH_2-R^2	R^1-CH_2-O-C**H**$_2$-R^2	R^1-C**H**$_2$- R^2
R^1C(2)-B- R^2C(2)	4.80	4.80	3.96
R^1C(2)-B- R^2C(4/6)	4.80	4.80	3.96
R^1C(2)-B- R^2C(5)	4.80	4.55	3.96
R^1C(4/6)-B- R^2C(4/6)	4.80	4.80	3.96
R^1C(4/6)-B- R^2C(5)	4.80	4.55	3.96

When comparing information from Table 26 and Table 31, one may notice that the chemical shifts of aliphatic carbons in the bridges are more sensitive to the resorcinol carbon atoms to which the bridges are attached. As it is seen in Table 31, the chemical shifts of protons in the aliphatic bridges linking resorcinol aromatic rings are almost uniform, except for bridges formed with C(5). Therefore, a far greater variety of signals can be recorded using ^{13}C NMR spectroscopy and due to the fact that methylene (CH_2) bridges resonate at characteristically low values of chemical shift, they are easy to detect unequivocally. Nonetheless, there were not observed in any of our experiments and previous literature [94] suggests that these can only be observed in far later stages of reaction, when the solution becomes a gel. Due to the fact that the probe in the NMR spectrometer was not applicable for

examining gels or solids but only liquids, the scope of kinetics experiments was limited to the time long before the gelation was expected to occur.

Assignment of ^{1}H NMR spectra is more complicated than the ^{13}C for a number of reasons. Most of all, the correlation between the calculated and measured chemical shifts is not necessarily linear and accurate for all peaks. An excellent example is the assignment of the position of proton in the hydroxyl groups, discussed in the previous sections. The correlation, not necessarily being linear for all signals, cannot be used to predict the chemical shift of new signals. Therefore, the most reasonable method of assigning the ^{1}H NMR spectra in reacting systems is the same way the non-reacting solutions were assigned: *via* HSQC and 13C NMR spectra. Just as this was the case in formaldehyde-water and formaldehyde-methanol dilutions, the broad water peak causes difficulties when assigning the spectrum, as it overlaps with the CH_2 signals and in the reacting mixture it may also overlap with new signals from hydroxymethyl resorcinol or the products of its condensation. This problem is solved by using the HSQC spectra, which was extensively discussed in previous sections. This solution addressed also another problem, which was that the proton signals from the hydroxymethyl groups attached to resorcinol all have the same calculated resonance frequency and therefore should appear at the same chemical shift. Similarly to the case of the 121.4 ppm peak (discussed earlier), it turned out that the nature of the solution causes that these measured chemical shifts are different for differently substituted resorcinol, making it possible to differentiate between the derivatives of resorcinol present in the reacting mixture at a given time. An appropriate assignment of HSQC spectrum using the knowledge of ^{13}C chemical shifts and verified by correlation of calculated and measured chemical shifts, proved to be possible.

Since the available probe in the NMR spectrometer allowed to investigate solutions only and a coaxial insert with reference substance was used, all effort had to be made in order to ensure that the solution would not form a gel during the experiments. Moreover, as it was discussed previously, it was reasonable to examine a slowly reacting mixture as the collected spectra were images of certain number of scans averaged over the acquisition time. Additionally, the assignment of the ^{1}H spectra was done for experiments performed in 20°C (293K) and – as it is explained further on – assignment of the spectra in higher temperature would require a number of additional lengthy experiments. Fortunately the overall rate of the reaction is increased in high temperatures, therefore monitoring the reaction in 20°C (293K) is reasonable and possibly would also shed light on the necessity of temperature treatment to form hydroxymethyl resorcinol derivatives.

A set of ^{1}H NMR experiments was performed on the reacting mixtures in which the R/C ratio was varied, while R/W and R/F ratios were kept constant at 0.10 $g \cdot ml^{-1}$ and 0.5 $mol \cdot mol^{-1}$, respectively. The R/C ratio was chosen to be 10, 25 and 50 $mol \cdot mol^{-1}$. These ratios are much smaller than those chosen in experiments performed in higher temperature but this was done in order to ensure reaction would proceed with observable rate in 20°C (293K). In order to examine what (if any) processes take place immediately after addition of formaldehyde in room temperature, i.e. during the typical preparation method, the experiments were started immediately after addition of formaldehyde to resorcinol and sodium carbonate solution, as described in the methods section. Therefore, instead of 30 min of stirring, the sample was shaken intensively in a sealed vial for approximately 30 s and then transferred into an NMR tube, equipped with a coaxial insert containing the reference substance. The sample was prepared in a room with constant

temperature, therefore the time required for the sample temperature to equilibrate with pre-set 20°C (293K) in the spectrometer probe was minimal and experiments began within approximately 4 minutes from the moment formaldehyde was added.

A region of 3.6-4.2 ppm in which the signals corresponding to protons in the hydroxymethyl groups are located is shown in Figure 66. It is a typical example of a proton NMR spectrum taken directly after addition of formaldehyde. It is interesting to see the presence of new peaks after only just a few minutes from addition of formaldehyde. When compared with signals from the formaldehyde species like MG, they are relatively intensive especially when taking into consideration that the spectrum was collected during what normally would still be called preparation of the solution and not "reaction" itself. Peaks labelled 1, 2, 3 and 5 in Figure 66 correspond to the nomenclature introduced in Figure 65 and Table 28. Peak 1 corresponds to the proton signals in aliphatic group in the hydroxymethyl resorcinol when the group is attached to carbons C(4) or C(6), while peak 3 corresponds to the same signals but from the group being bound to C(5) in two different species: mono-substituted resorcinol and di-substituted resorcinol (C(2) and C(5)). These two peaks have a significantly different ^{13}C chemical shift but their ^{1}H chemical shift overlaps, as it was shown earlier by HSQC. Peak 2 corresponds also to the protons in hydroxymethyl group but when it is attached to C(4/6) in di-substituted resorcinol (substituted at C(4/6) and C(2)), while signal labelled with number 5 corresponds to the protons in the hydroxymethyl group bound to C(2) in the same molecule. Therefore, presence of signal 2 has to be accompanied by peak number 5.

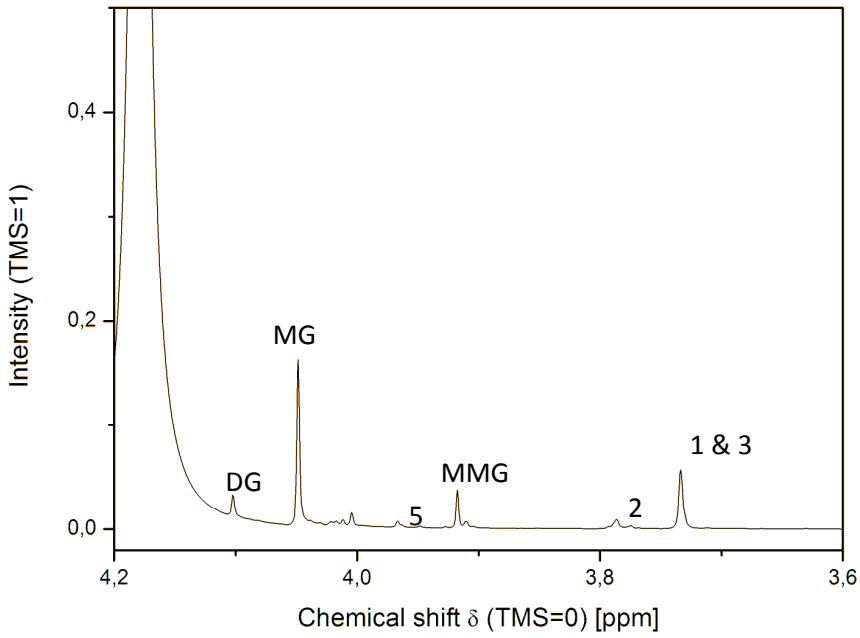

Figure 66. ^{1}H NMR spectrum of reacting mixture (R/C 10 mol·mol^{-1}, R/W 0.10 g·ml^{-1}, R/F 0.5 mol·mol^{-1}) taken immediately after formaldehyde addition (see text for explanation).

The signal present in the spectrum between MG and peak 5, at ca. 4.01 ppm cannot be unequivocally assigned as it changes its shape in the course of the reaction and the area underneath it does not represent any consistent tendency (i.e. does not increase or decrease, which would be the case of the reactant and product, respectively), so it may be a result of few different signals overlapping. The nature of its behaviour in time suggests that those signals are not only from the products (in this case the area would increase) but also from possible by-products or intermediate compounds, but a more specific assignment has not been possible.

6.2.2. ^{1}H NMR Quantitative Analysis

Quantitative analysis of the obtained results of ^{1}H NMR measurements is valuable because it allows to determine the relationship between the concentration of the catalyst and the rate of change of concentrations of reactants as well as products of resorcinol and formaldehyde reactions. This can provide insights into the mechanisms and processes involved in polymerisation and subsequent gelation in resorcinol-formaldehyde systems. Despite the presence of the water signal, it is possible to follow the changes in concentrations of the most important signals, which include most abundant formaldehyde species, resorcinol and certain products of addition of formaldehyde to resorcinol.

Experiments at 293K

Experiments at 293K were performed at three different catalyst concentrations, expressed as R/C ratios of 10, 25 and 50 [mol·mol^{-1}], corresponding to a five-fold increase in the catalyst concentration from R/C=50 to R/C=10, while keeping the reactant concentrations the same. Figure 67a shows time evolution of concentrations of total formaldehyde (obtained by summing the concentrations of MG, MMG and DG (counted twice since two formaldehyde molecules are involved)) determined by ^{1}H NMR. Figure 67b shows corresponding data for concentration of resorcinol in terms of C(2,4,6) carbon sites (which are expected to undergo reaction with formaldehyde species to form singly and multiply substituted products), also determined by ^{1}H NMR. It can be seen that both reactants undergo a rapid decrease in concentration in the first few minutes followed by a more gradual decrease afterwards. In contrast, resorcinol concentrations in terms

of the C(5) carbon site are staying constant over time as can be seen in Figure 67c, perhaps following a small initial decrease of not more that 10% of the total value of the total resorcinol concentration. This shows that C(5) sites are not significantly substituted by formaldehyde species under conditions investigated.

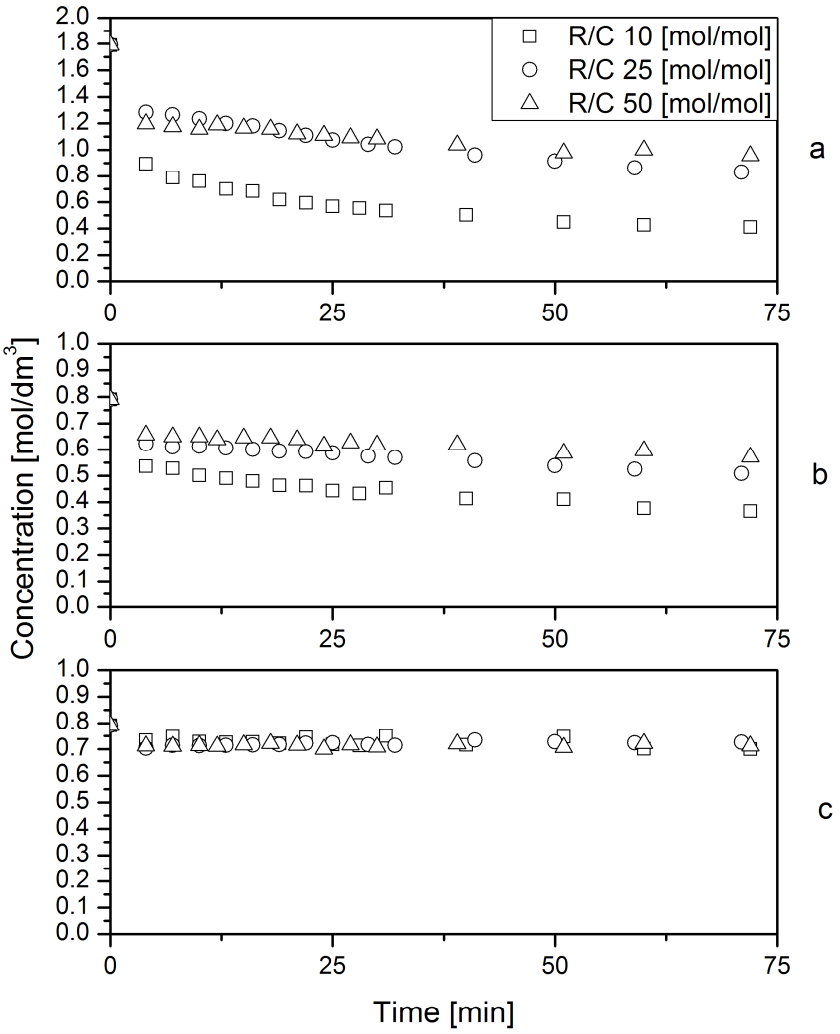

Figure 67. Time evolution of concentrations of total formaldehyde (a) and resorcinol, in terms of C(2,4,6) (b) and in terms of C(5) (c) at 20°C (293K) plotted in scaled time for three different catalyst concentrations.

Since the basic catalysts (Na_2CO_3) is expected to catalyse the reaction of resorcinol with formaldehyde species, the rate of reaction is expected to be proportional to the catalyst concentration. Therefore a plot of the experimental data in terms of scaled time $\tau = t/(R/C)$, which is proportional to the reaction time t multiplied by the catalyst concentration C, is done further on. Figure 68 shows concentrations of total formaldehyde and resorcinol (in terms of C(2,4,6) sites) plotted as a function of the scaled time τ and as one can see, the concentration data appear to follow a uniform dependence on the scaled time, as expected for the catalysed process (assuming that the rate of reaction is first order in the catalyst concentration, which is certainly reasonable).

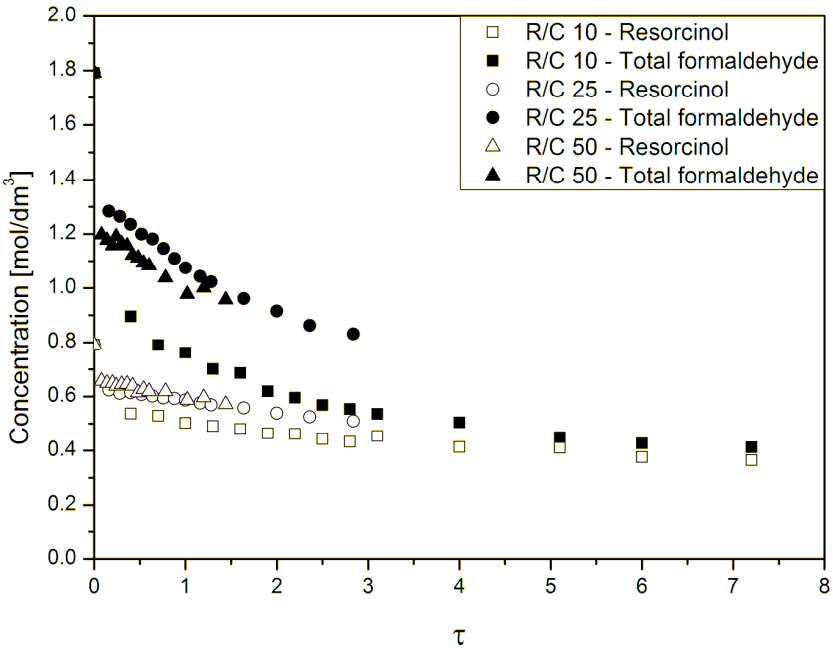

Figure 68. Molar concentrations of total formaldehyde and resorcinol (in terms of C(2,4,6) sites) plotted as a function of the scaled time τ during reaction in 20°C (293K).

The decrease of the total formaldehyde concentration, expressed as the sum of contributions corresponding to MG, MMG and DG species corresponds to decreasing concentrations of each of the species, as shown in Figure 69. This is expected, since these species are in mutual equilibrium as discussed in detail in Chapter 4.

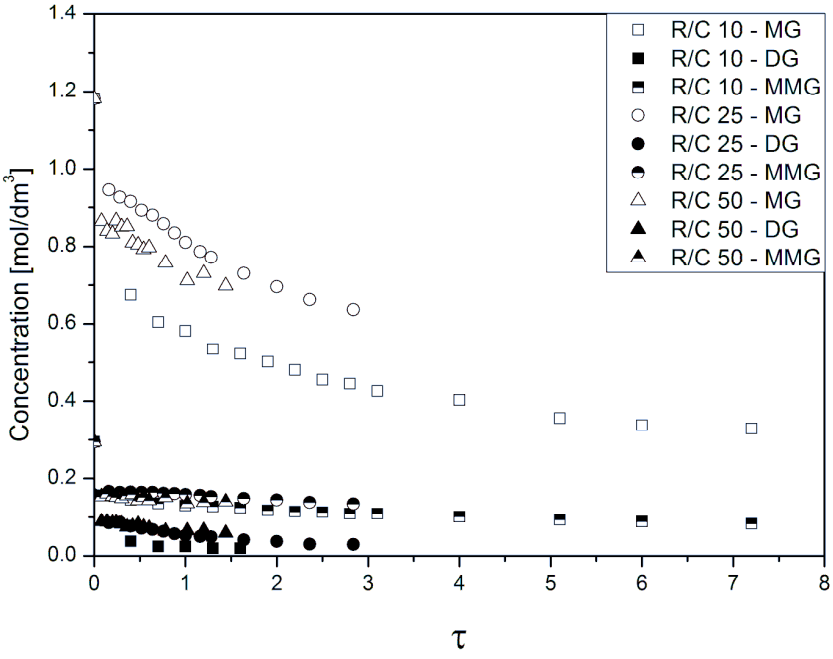

Figure 69. Time evolution of concentrations of MG, DG and MMG during reaction in 20°C.

In order to estimate the extent of substitution of resorcinol by formaldehyde species, in Figure 70 the time evolution of the molar ratio of formaldehyde consumed to the resorcinol (in terms of C(2,4,6) sites) consumed is shown. It turns out that from the very first measurement after the mixing of resorcinol and formaldehyde solutions the ratio is at least 3, which is the maximum value corresponding to the full substitution of C(2), C(4) and C(6) sites in every resorcinol molecule reacted. The value should not be much higher than

3, since C(5) sites do not appear to be reacting significantly, and certainly cannot be higher than 4, so the initial values for R/C=50, which exceed 4, appear to be inaccurate. The extensive substitution seems to indicate that the first substitution is the kinetically limiting step, after which the second and third substitutions are relatively fast and achieve completion once the first substitution on the resorcinol is accomplished.

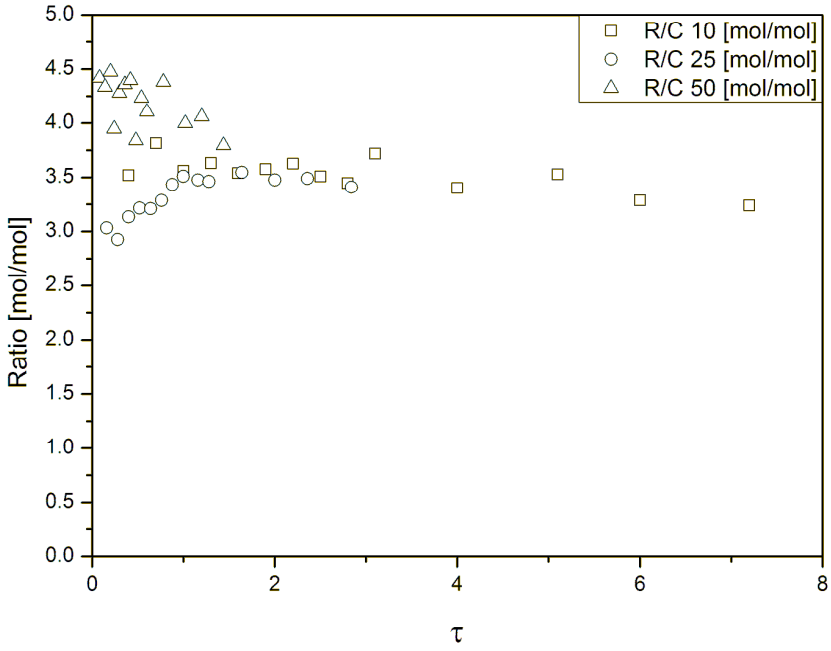

Figure 70. Time evolution of the molar ratio of formaldehyde consumed to the resorcinol (in terms of C(2,4,6) sites) consumed during reaction in 20°C (293K).

Observation of formaldehyde species is accompanied by changes in the resorcinol concentrations. The main issue in following these changes is that depending on the positions in which resorcinol is substituted, the chemical shifts or protons on the non-substituted carbon atoms change. These changes are very subtle and therefore the signals from substituted and unsubstituted

resorcinol molecules tend to overlap and it is not feasible to deconvolute these signals. It is possible to separate two regions in terms of resorcinol signals: the one associated with C(5) and with C(2,4,6). The first region contains signal from the proton attached to C(5) in both substituted and unsubstituted resorcinol. The other region contains signals from protons attached to carbons number 2, 4 and 6. It is obvious that if resorcinol molecule is substituted with formaldehyde-related molecule at e.g. C(2), then the signal from the proton which was attached at this carbon atom will disappear and since the peak is a sum of signals from all molecules, also those not substituted at this position, the area of the peak should only decrease. At the same time, the signal in region corresponding to C(5) should not decrease, as proton in that position is not substituted with a hydroxymethyl group. Bearing in mind that the most probable substitution due to presence of two hydroxyl groups at C(1) and C(3) is in positions C(2,4,6) one would expect the signals in region related to protons attached to those carbon atoms to decrease its area, while those in C(5) region to remain constant.

As expected, a decrease in concentrations of the reactants has to be accompanied by appearance of new signals corresponding to the products of reactions between formaldehyde and resorcinol and then by an increase in their concentrations. In all three investigated samples, signal labelled as peak 1 and 3 at ca. 3.73 ppm was detected, while signal at 3.78 ppm was seen only for sample with the highest amount of catalyst. It is understandable, as this signal corresponds to the protons in the hydroxymethyl group attached to C(4/6) in di-substituted resorcinol (at C(2) and C(4/6)). Di-substitution is generally considered to be less probable than mono-substitution and is to be

expected in later stages of reaction, when the most substitution-attractive spots in resorcinol ring are occupied.

Analysis of the collected spectra provided information on the absolute concentrations of the newly formed hydroxymethyl resorcinol derivatives. The results are shown in Figure 71a where a plot of time evolution of concentration of these new product species, together with the corresponding resorcinol reactant concentrations (in terms of C(2,4,6)) in the scaled time τ is shown. It can be seen that the decrease in reactant concentration is matched by the increase in product concentration, and this is quantitatively demonstrated in Figure 71b, where the total material balance of resorcinol is shown in terms of the sum of the unreacted resorcinol (C(2,4,6)) and the reacted resorcinol (hydroxymethyl derivatives) as being approximately constant over time. This shows that all resorcinol is accounted for and that no subsequent reactions (such as condensation/polymerisation) or phase separation processes are proceeding at these conditions (293K).

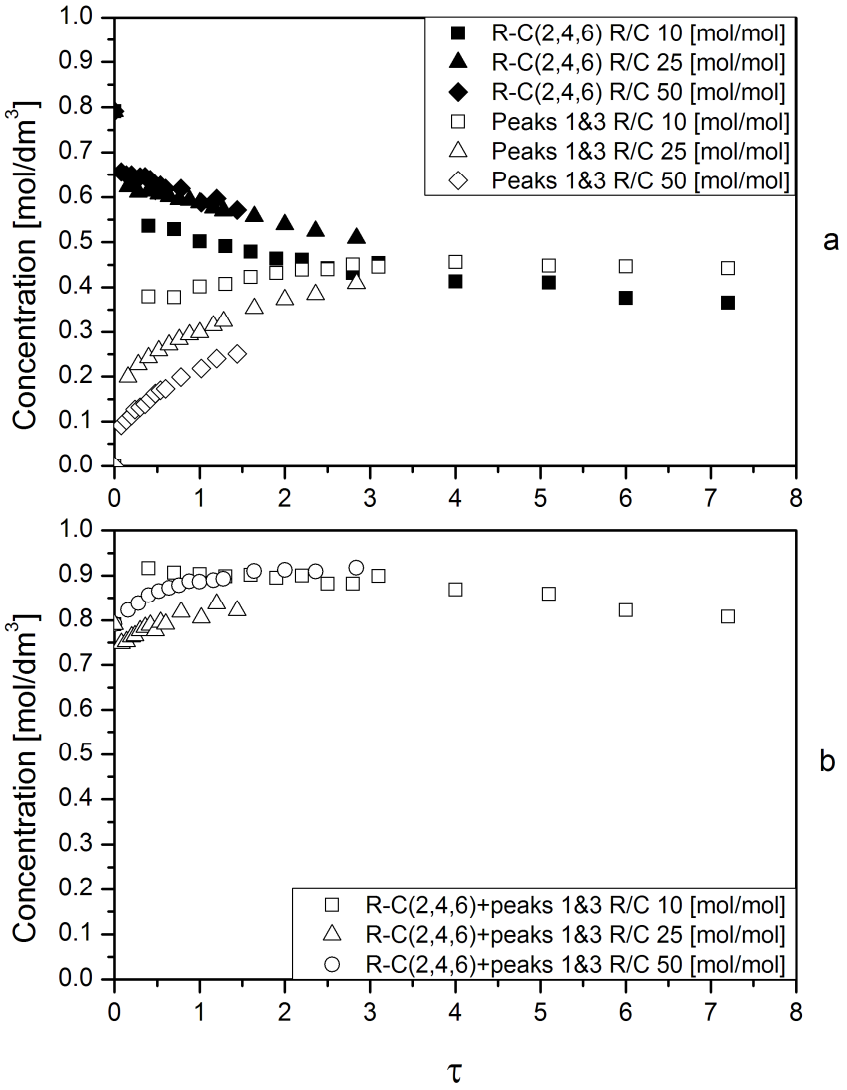

Figure 71. Scaled time evolution of concentration of (a) new product species with the corresponding resorcinol reactant concentrations (in terms of C(2,4,6)) and (b) total material balance of resorcinol as the sum of the unreacted resorcinol (C(2,4,6)) and the reacted resorcinol (hydroxymethyl derivatives, new species).

Again, it can be clearly seen that substantial amount of product was formed very rapidly after mixing the two solutions, followed by a slower rate of formation afterwards. Also it appears that a plateau in concentration of the product is achieved at the highest catalyst concentration (R/C=10). There is a number of possible explanations for this phenomenon. One possibility is that the apparent slowing down of the reaction is simply due to the second order of kinetics and gradual depletion of the reactants. This can be checked by running kinetic modelling in which the obtained data is fitted to kinetics equations of different order. The collected data on concentrations' evolution in time for both formaldehyde and resorcinol (represented by MG and C(2,4,6)) was processed using kinetic equations for first and second order reactions, shown below in Table 32.

Table 32. Kinetic equations for first and second order reactions

First order reaction	Second order reaction
$\frac{d[A]}{dt} = -k[A]$	$\frac{d[A]}{dt} = -k[A]^2$
$\frac{d[A]}{[A]} = -kdt$	$\frac{d[A]}{[A]^2} = -kdt$
$\int_{[A]_0}^{[A]} \frac{1}{[A]} d[A] = -k \int_0^t dt$	$\int_{[A]_0}^{[A]} \frac{1}{[A]^2} d[A] = -k \int_0^t dt$
$ln\left(\frac{[A]}{[A]_0}\right) = -kt$	$\frac{1}{[A]} - \frac{1}{[A]_0} = kt$

In the equation above [A] refers to concentration of a given reactant and $[A]_0$ refers to the concentration of this reactant at time zero which is the instant when the reaction begins. The last forms of the equations are linear with t

being the x and k being the coefficient a. If a reaction is of a given order then the concentration data ([A], $[A]_0$) inserted into the last form of an equation should produce a line in the graph of either way $\boldsymbol{ln}\left(\frac{[\boldsymbol{A}]}{[\boldsymbol{A}]_\mathbf{0}}\right)$ vs. t or $\frac{\mathbf{1}}{[\boldsymbol{A}]} - \frac{\mathbf{1}}{[\boldsymbol{A}]_\mathbf{0}}$ vs. t. Concentrations of MG and resorcinol (based on C(2,4,6)) were used in this way and the modelling proved that the reaction is of second order in respect to both MG and resorcinol. This is in accordance with a previous publications which relied on a far simpler and less accurate methods and suggested that the overall order of the reaction between formaldehyde and resorcinol is of second order. Another explanation can be that the effective concentration of catalyst and thus solution pH changes over time and therefore the initial rapid reaction stage is followed by a considerably slower reaction rate. This is supported by observations of the pH in the course of the reaction, which are discussed in this Chapter later on. It was discovered that the solution pH decreases over time for an unknown reason in all investigated reacting solutions. It is known that condensation of hydroxymethyl derivatives of resorcinol is catalysed by hydrogen cations, which explains why it is faster in acidic solutions. Decrease of the solution pH could enhance the condensation and thus cause a plateau in the discussed figures. Occurrence of this reaction in parallel to the resorcinol-formaldehyde substitution could also explain why the process might be of second order. The last possibility is that the substitution process of resorcinol with formaldehyde is reversible. Therefore the plateau could correspond to an equilibrium of the reaction, as it is observed in other reversible reactions. However, in the light of literature on fundamental chemistry and on resorcinol chemistry [126] this explanation appears highly unlikely.

There are several overall conclusions which can be made basing on the results of ^{1}H NMR spectroscopy experiments performed on the reacting systems in ambient temperature. The most significant observation is that even in the first few minutes after addition of formaldehyde into the resorcinol and sodium carbonate solution, the products of reactions between formaldehyde and resorcinol are visible. The concentrations of these hydroxymethyl derivatives are large enough not to be treated as an error or noise in the baseline of the spectra. Moreover, HSQC experiments proved that there are more than just one type of hydroxymethyl derivative and that di-substituted species are present in later stages (still, within less than one hour) despite lack of high temperature treatment. Another significant observation is the decreased concentrations of both reactants even at the beginning of the experiment. It is also clear that these concentrations decrease gradually in time, proving that the reaction between formaldehyde and resorcinol does not require elevated temperatures. This is very important when analysing results of other researchers' work and when considering the currently used gel preparation methods. All of the most popular methods require approximately 30-60 min of mixing the reactants in room temperature and most researchers assumed that this period of time is necessary to ensure homogeneity of the mixture rather than to perform reactions already. Very often, the time in which the sample is heated is referred to as *reaction time* – this seems to be inappropriate in the light of these results. The duration of the mixing time determines the concentration and the type of hydroxymethyl derivatives (mono- or di-substituted) and therefore, the mixtures which then undergo high temperature treatment most certainly have different concentrations, which affects the condensation and gel formation stages. The fact that the concentrations of both reactants and

products reach a seemingly steady values, which is reflected by a plateau in Figure 71, suggests that a few possibilities need to be considered and basing on the earlier discussion, two are the most reasonable. It might be that the overall order of the reactions is greater than one and/or that with time, when pH decreases, condensation of hydroxymethyl derivatives begins, thus changing the manner in which concentrations change over time.

Experiments at 328K

Experiments on reacting mixtures in ambient temperature (293K) were followed by those performed in 55°C (328K). This temperature was chosen for several reasons: it corresponds to the temperature which was chosen for the DLS experiments (see 6.4); it is significantly higher than ambient temperature and therefore it was expected that the reactions between resorcinol and formaldehyde and those leading to gel formation would take place at a much greater rate but still slow enough to perform experiments with a relatively low error of time-averaging of the collected spectra; and it was compatible with technical limitations of the probe used in the NMR spectrometer allowing in situ monitoring in real time.

Experiments were performed in an exactly same manner as those in 20°C (293K), however, a different substance had to be used as an external standard inside a coaxial insert due to the fact that TMS has a boiling point at ca. 26°C (299K). Just as it was done in case of non-reacting formaldehyde-water and formaldehyde-methanol dilutions, benzene was used to replace highly volatile TMS. In all collected and then analysed spectra the chemical shift of benzene was locked at 7 ppm to facilitate observation of the reactants' and products' signals, especially changes in peak positions and shapes in time.

Due to the fact that the temperature was increased, the amount of catalyst (R/C ratios) had to be adjusted so that the reacting mixture would not form a gel during the experiment. Instead of using very low R/C ratios, a set of mixtures with resorcinol to sodium carbonate ratios of 50, 100 and 300 $mol \cdot mol^{-1}$ were prepared and tested. The ratios of other reactants were as usual, meaning R/F 0.5 $mol \cdot mol^{-1}$ and R/W 0.10 $g \cdot ml^{-1}$.

Quantitative interpretation of results of experiments performed in 55°C (328K) was complicated by the signal of the hydroxyl groups obscuring most of the protons in CH_2 groups. However one can still use information from other, unobstructed parts of the spectra. The main challenge lies in assignment of the CH_2 signals. It is known that the chemical shift changes with the temperature, however, the rate at which peaks migrate (in terms of ppm per degree of temperature) is not uniform. Figure 72 shows ^1H NMR spectra collected for a sample with R/C 100 $mol \cdot mol^{-1}$. It can be clearly seen that the overall appearance of the spectra is comparable with that of those collected in 20°C (293K). The main difference is presence of a strong signal at 7 ppm resulting from benzene and the fact that the water signal is shifted towards smaller values of chemical shift. As a consequence, it is possible to see signals between 4.3 and 4.7 ppm, which are shown in Figure 73.

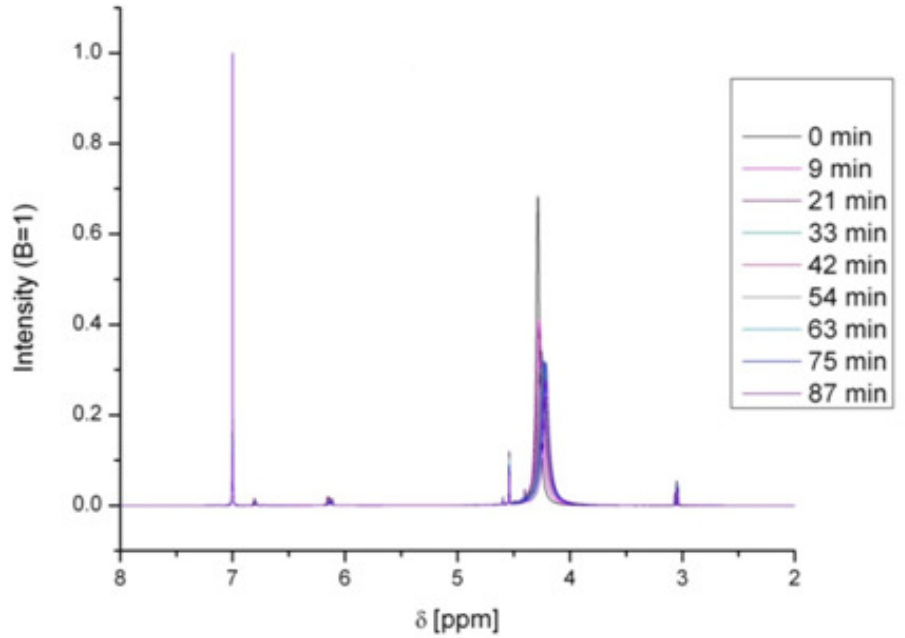

Figure 72. A selection of ^{1}H NMR spectra of a mixture reacting at 55°C (328K). R/W 0.10 g·ml^{-1}, R/F 0.5 mol·mol^{-1} and R/C 100 mol·mol^{-1}.

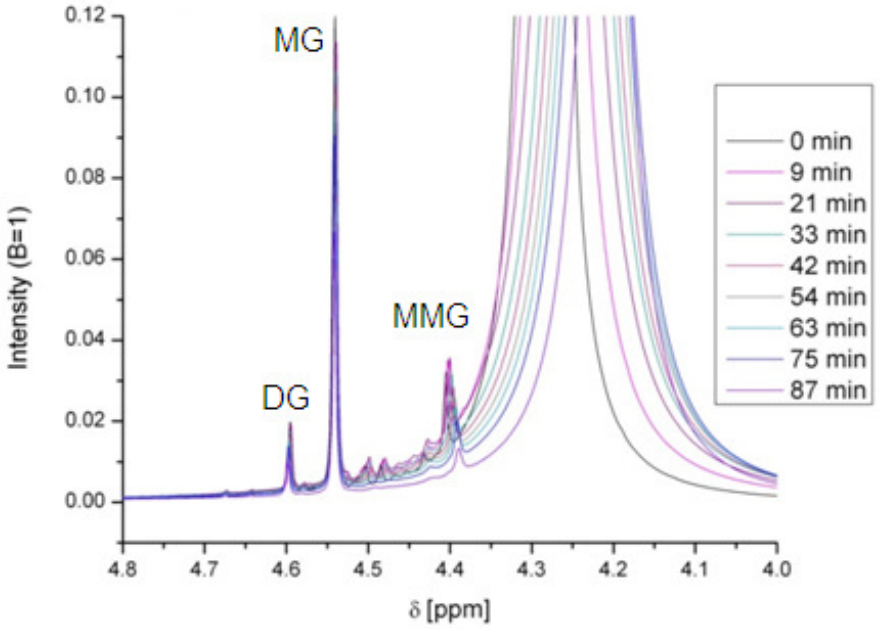

Figure 73. Expanded view of ^{1}H NMR spectra shown in Figure 72

The difficulty in assigning the signals shown in Figure 73 is that in 20°C (293K) this region of the spectrum is a flat line, without any other signals than the baseline. Spectra of formaldehyde and water dilutions in 55°C (328K) have signals present in this region and an attempt at the assignment was made. The assignment of the signals present in the same region in the spectra of reacting mixture can only be made under assumption that presence of sodium carbonate, resorcinol and severely changed pH do not significantly change chemical shifts. Additional help in assignment comes from the observation of the area changes in time and from the knowledge of an approximate composition (i.e. it is known that the predominant form of formaldehyde is MG). It is safe to assume that signals from reactants (i.e. CH_2 groups in glycols or methoxylated forms) will decrease in time, while signals related to products will increase, even if at an insignificant rate. Assignment of peaks found in majority of the collected spectra in 55°C (328K) was done under these assumptions and it is summarized in Table 33.

Table 33. Assignment of peaks found in ^1H NMR spectra of mixtures reacting in 55°C (328K).

Assignment	**δ [ppm]**	
	Calculated	**Measured**
C**H**$_3$-OH	3.39	3.04
C**H**$_3$O-CH$_2$-OH	3.30	3.05
CH$_3$O-C**H**$_2$-OH	5.61	4.39
HO-C**H**$_2$-OH	5.77	4.54
HO-C**H**$_2$-O-C**H**$_2$-OH	5.61	4.59
R-C(2,4,6) - substituted and unsubstituted neighbouring carbons	6.36	6.12
R-C(5) when C(2,4,6)-substituted	7.03	6.70
R-C(5)	7.11	6.79
Benzene – C_6H_6	7.26	7.00

The analysis of the data contained in spectra collected at 55°C (328K) was performed in a way analogous to the method in which data collected in 20°C (293K) was examined. The results of this analysis are subject to slightly more noise and errors than those obtained in experiments performed in 20°C (293K). This is mostly due to the fact that the shape of these peaks may undergo small changes in time, especially when the viscosity and temperature conductivity of the sample change. This was not an issue in ambient temperature, as reactions were proceeding very slowly then and the viscosity would not change in an extent that would cause problems with shimming of the sample and as a consequence with shapes of the peaks. In elevated temperature it is assumed that condensation takes place leading to formation of large clusters which may impede movement of other molecules and affect their relaxation time causing changes in the areas of their peaks. Another factor which may have contributed to these errors is the fact that despite using a fully thermostated probe, there is a risk of temperature gradient existing across the sample tube. This is caused by the fact that the heater and temperature control are located near the bottom of the probe meaning that depending on thermo-conductivity of the sample the temperature closer to the bottom of the sample might be greater. This may affect the shape of the signals in a way that chemical shift is temperature dependent and molecules located closer to the bottom will have a different chemical shift than those located at the top of the sample. This was also the case in formaldehyde-water dilutions investigated in 55°C (328K).

Experiments at 328K were performed at 3 different catalyst concentrations, expressed as R/C ratios of 50, 100 and 300 [$mol \cdot mol^{-1}$], corresponding to a 6-fold increase in the catalyst concentration from R/C=300 to R/C=50, while keeping the reactant concentrations the same. Similarly to the analysis of

results from experiments at 293K, plots data using the scaled time tau (see section 6.2.1.) are made. Figure 74a shows time evolution of concentrations of total formaldehyde (obtained by summing the concentrations of MG, MMG and DG (counted twice since two formaldehyde molecules are involved)) determined by ^{1}H NMR. Figure 74b shows corresponding data for concentration of resorcinol in terms of C(2,4,6) carbon sites (which are expected to undergo reaction with formaldehyde species to form singly and multiply substituted products), also determined by ^{1}H NMR. It can be seen that both reactants undergo a rapid decrease in concentration in the first few minutes followed by a more gradual decrease afterwards. In contrast to observations at 293K, resorcinol concentrations in terms of the C(5) carbon site are now significantly decreasing over time as well, see Figure 74c.

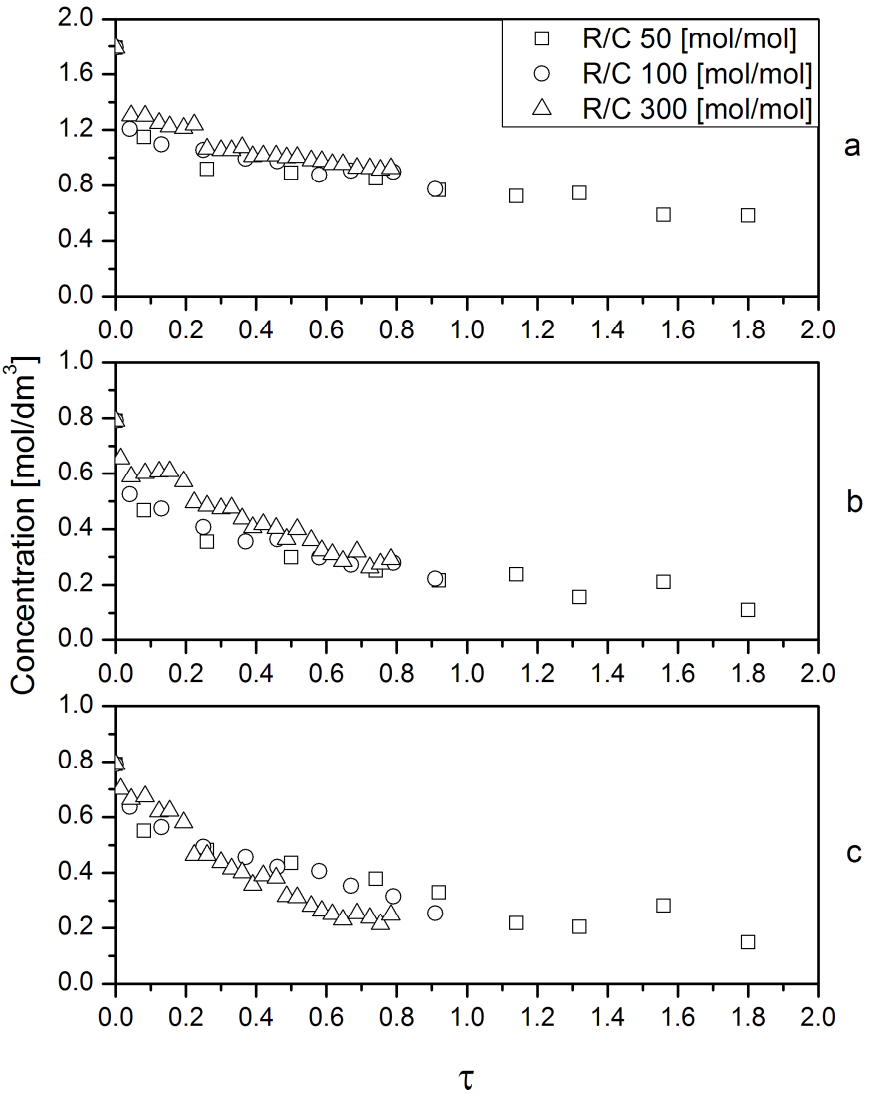

Figure 74. Time evolution of concentrations of total formaldehyde (a) and resorcinol, in terms of C(2,4,6) (b) and in terms of C(5) (c) at 55°C (328K) plotted in scaled time for three different catalyst concentrations.

It can be noted that the concentrations of DG and MMG decreases with time alongside MG, which is expected, since these species are in mutual equilibrium.

Analysis of the resorcinol region was done in the same way as it was done for experiments in 20°C (293K). This means that the whole resorcinol-related region was divided into two sections: one with signals from protons attached to carbons C(2,4,6) and another with signals from proton atom at C(5).

In order to estimate the extent of substitution of resorcinol by formaldehyde species, I show in Figure 75 the time evolution of the molar ratio of formaldehyde consumed to the resorcinol (in terms of C(2,4,6) sites) consumed. In contrast to results at 293 K, the ratio is now around 2 and remains steady over time. This indicates that while the second substitution of resorcinol proceeds readily at 328K, the triply substituted resorcinol is not present in the solution to a significant extent (see below for further discussion).

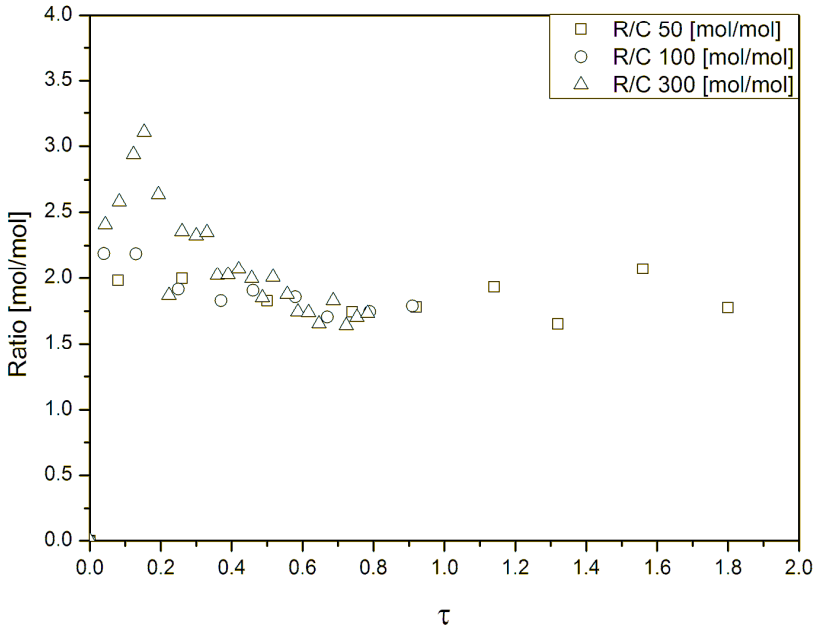

Figure 75. Time evolution of the molar ratio of formaldehyde consumed to the resorcinol (in terms of C(2,4,6) sites) consumed during reaction in 55°C (328K).

The only sample which can be directly compared at both temperatures is the one for R/C=50. where experiments were performed on samples with exactly the same compositions, i.e. R/C 50 mol·mol^{-1}, R/W 0.10 g·ml^{-1} and R/F 0.5 mol·mol^{-1}. The results of this comparison are shown in Figure 76. It can be seen that the initial decrease is very similar , which is expected since this happens almost immediately after the initial mixing which is done at lab temperature in both cases. Afterwards, the rate of total formaldehyde loss due to reaction with formaldehyde is very similar at both temperatures, indicating that the enthalpy of the reaction is not very large.

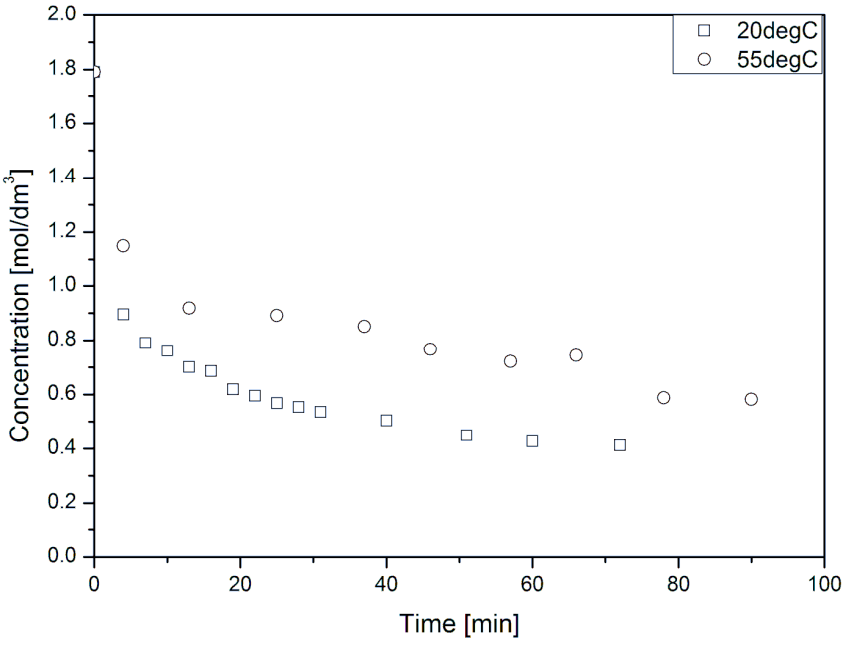

Figure 76. Comparison of changes in total formaldehyde concentrations in course of reaction in 20°C (293K) and 55°C (328K) in sample with R/C 50 mol·mol^{-1}, R/W 0.10 g·ml^{-1} and R/F 0.5 mol·mol^{-1}.

An interesting phenomenon which was observed during experiments in 55°C (328K). It appears that the signal generated by protons attached to C(5) of

resorcinol is diminishing in time at a rate comparable with the signals generated by protons at C(2,4,6). This could be observed when resorcinol undergoes substitution at these sites, which is expected for C(2,4,6) but is highly unlikely for C(5) on chemical reactivity grounds. It is known that C(2,4,6) sites are more susceptible for formaldehyde substitution and those should be substituted before substitution at C(5) could take place. Nonetheless, ratio of formaldehyde loss to resorcinol loss is around two, meaning that there are two formaldehyde molecules consumed per each molecule of resorcinol. This means that resorcinol is mostly doubly substituted, making C(5) substitution even less probable. Therefore the phenomenon of C(5) signal disappearance is unlikely to be caused by this and can be explained by two other possibilities. One is that doubly substituted resorcinol undergoes rapid condensation with another one and the product becomes insoluble in water and the solution undergoes (micro)phase separation. Another possibility is that resorcinol undergoes further substitution resulting in insoluble triply substituted resorcinol which promptly undergoes phase separation. It is very difficult to decide which of these two options is more likely the explanation. In ^{1}H NMR spectra one does not see the signals of species potentially bound to resorcinol at C(5) which can indicate that the condensed product (which is expected to have unsubstituted C(5) site) is not in the same phase as the reactants, therefore it is not visible in the spectrum. Should this be the case, one would not observe all other atoms in condensed hydromethoxyl resorcinol. For instance, aliphatic bridges should be visible in ranges different from the reactants' (Table 31) and these are not observed, suggesting that this theory is true. At the same time triply substituted resorcinol was not observed in any of the experiments in these conditions, suggesting that the second explanation can

also be true. One may debate as to which explanation is the more probable but the amount of information collected in this work does not allow to unanimously decide which one is true.

This is as far as analysis of the data collected during the reactions performed in 55°C (328K) can go because there are no new signals due to reaction products that can be detected quantitatively . The signal from hydroxyl groups obscures all CH_2 signals from hydroxymethyl derivatives making it impossible to determine the types and amounts of newly formed derivatives. It is without a doubt that those species are present in the solution, however, it is not possible to identify and quantify them.

It is worth mentioning that even though one could expect not to find products of condensation in samples which were reacting in ambient temperature, these were expected in experiments performed in 55°C (328K). It might be that these species are also located beneath the water peak and their detection is not possible in a 1D NMR experiment. Their presence could be confirmed with HSQC experiments but it was not done for reasons mentioned earlier in this Chapter. Another possibility is that the products of condensation are located in another phase which is not detectable with the NMR.

The signal of the hydroxyl group and the nature of its changes in the course of the reaction is a very important issue which calls for a thorough discussion. As it was mentioned earlier, this signal overlaps with proton signals in the CH_2 groups in formaldehyde-related species, namely methylene glycol and oligooxyglycols, as well as their methoxylated forms. Therefore, it may obscure signals which are of interest in terms of mechanism

and kinetics investigation. However, the water-related signal may reveal much information, and if studied closely may cease to seem as an obstruction and become very helpful.

The peak generated by the protons in hydroxyl groups generate a broad peak that changes its position with temperature and the composition of the sample. The change in the chemical shift can be caused by a number of factors which were discussed earlier but here the composition of the solution seems to be the most relevant. When the amounts and ratios of the chemical compounds in the solution change, the interactions between them may also be affected. Such is the case for the hydrogen bonds which are of special interest when dealing with aqueous solutions. If a hydroxyl group forms a hydrogen bond then the shielding of the proton in this group is changed. Since the position and the area of the hydroxyl group peak in the NMR spectrum is a cumulative value (i.e. it is a total of all OH peaks which may have different chemical shift and areas proportional to the number of mols of this specific hydroxyl group), the chemical shift of the peak will change if the amount of differently shielded groups changes. The amount of hydrogen bonds and thus the differently shielded groups can be altered in a number of ways, including changing the temperature and the concentration of water and all species with hydroxyl groups. The main reason for the width of the hydroxyl group peak is the chemical exchange which takes place between hydrogen atoms and because of the complex exchanges in hydrogen bonds.

In all investigated reacting mixtures, the position of the peak generated by the hydroxyl groups changed slightly in the course of the reaction. The chemical shift of this peak gradually travels towards greater values of the chemical shift, suggesting a very small de-shielding effect. Interestingly, the

same effect is observed for other signals, however, in case of those this effect is less significant. In order to compare these effects, rate of peak movement was calculated by dividing the change in the chemical shift of a given peak in a certain time interval. Peaks corresponding to the hydroxyl groups (OH), methylene glycol (MG), methanol (MeOH) and methoxymehtylene glycol (MMG) were chosen, their positions were recorder at two different times for a few reacting mixtures with different R/C ratios and the results are summarised in Table 34.

Table 34. Changes in chemical shifts of selected peaks visible in ^{1}H NMR investigations of reacting mixtures. N.B.: ratios R/W and R/F were 0.10 $g \cdot ml^{-1}$ and 0.5 $mol \cdot mol^{-1}$, respectively; experiments performed in 293K.

Peak	**R/C [mol·mol^{-1}]**	**δ_{start}**	**δ_{end}**	**Time [min]**	**Movement Rate x10^{3} [ppm/min]**
MeOH	10	2.5680	2.5552	42	0.3046
	25	2.5825	2.5743	43	0.1905
	50	2.5870	2.5824	41	0.1111
MG	10	4.0486	4.0363	42	0.2921
	25	4.0629	4.0545	43	0.1955
	50	4.0675	4.0627	41	0.1160
MMG (CH_2)	10	3.9174	3.9045	42	0.3074
	25	3.9296	3.9225	43	0.1653
	50	3.9335	3.9297	41	0.0917
OH	10	4.1792	4.1607	42	0.4408
	25	4.2003	4.1874	43	0.2988
	50	4.2064	4.1985	41	0.1927

When analysing the data from Table 34, it is easy to observe that the rate at which the peaks move strongly depends on the R/C ratio, regardless of the proton for which the signal is registered. The dependency of this rate on the amount of catalyst is similar for all selected peaks, which is pictured in

Figure 77. Another observation is that the movement rate is significantly greater for the hydroxyl group – even up to ca. 50% greater. Both of these observations can be explained by the theory on the hydrogen bonds and changing composition, which was described earlier. Moreover, these results are yet another proof that the rate in which the composition (expressed by changing amount of hydrogen bonds) of the reacting mixture changes, strongly depends on the amount of the catalyst.

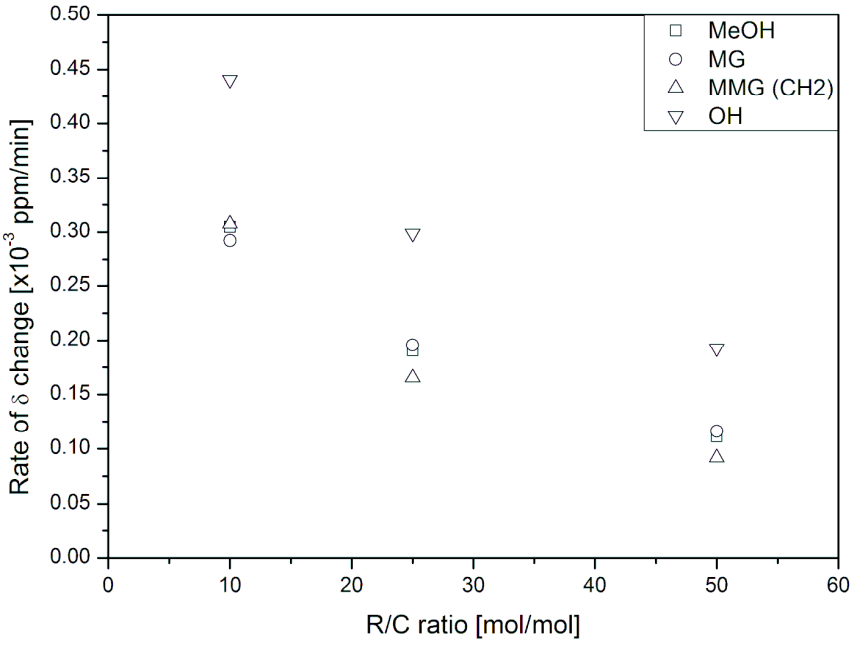

Figure 77. Dependency of the selected peak movement rates on the R/C ratio.

In terms of changes in the intensity or the area of the hydroxyl groups peak, the data analysis is less consistent. Overall, the intensity of the peak decreases and so does the area, however, the dependency on the catalyst concentration is not as obvious. It is not possible to relate the changes in the area or the intensity of the OH peak to absolute concentration of the hydrogen atoms of hydroxyl groups, therefore the only information which

can be obtained and analysed here is the overall rate of changes. Analysis comparing the rates of changes in intensity and the area of the hydroxyl groups signal is summarised in Table 35.

Table 35. Changes in intensity and area of the hydroxyl groups peak present in the ^{1}H NMR spectra of the reacting mixtures. N.B.: ratios R/W and R/F were 0.10 g·ml^{-1} and 0.5 mol·mol^{-1}, respectively; experiments performed in 293K.

R/C [mol·mol^{-1}]	Intensity		Area x10^{2}		Time [min]	Intensity change rate x10^{3} [i.u./min]	Area change rate x10^{3} [i.u./min]
	Start	End	Start	End			
10	1.28	1.21	3.29	3.23	42	1.7048	0.0151
25	1.12	1.12	3.43	3.38	43	0.0261	0.0116
50	0.97	0.89	3.05	2.94	41	1.9109	0.0276

The change in the width of the hydroxyl groups peak could be expected in later stages of the experiments. The reasoning for this expectation is that if large clusters are formed or even a gel network is formed, water molecules might be trapped in this structure and thus possibly have different relaxation time because of their movement restrictions, which would be observed in the spectrum as peak broadening. At the same time, formation of clusters or a polymeric network would result in an increased viscosity and would create more movement restrictions for all species in the solution, resulting in broadening of all signals. It is crucial to state that such observations were not made for experiments performed in 20°C (293K). This can be treated as confirmation that the process of gel formation requires elevated temperature and that in order to form it in ambient temperatures, considerably longer reaction time must be allowed.

6.3. IR Spectroscopy

IR spectroscopy was used to investigate aqueous solutions of all reactants individually (as reported in previous sections above) and then also to monitor the kinetics of the reactions in initial stages of resorcinol-formaldehyde polymerisation. The IR spectra of formaldehyde solutions were discussed extensively in previous Chapter, while spectrum of resorcinol solution in water is shown here in Figure 78. The spectrum is less complicated than those generated by formaldehyde solutions, as the composition is far more simple. Most peaks can be easily seen without the need to be deconvoluted and they can be easily assigned. The signals observed between 600 and 900 cm^{-1} are related to H-C-H out-of-plane bending vibrations, typical for aromatic rings. The signal at 965 cm^{-1} is caused by ring stretching and bending vibrations which are typical for 1,3-substitution. A couple of peaks observed at 1080 cm^{-1} (very weak signal) and 1170 cm^{-1} are related to the 1 and 3 type of substitution, which is naturally present in resorcinol solution. A couple of strong peaks at 1150 cm^{-1} and 1225 cm^{-1} are caused by stretching vibrations between aromatic carbon and oxygen atom – this is undoubtedly related to the hydroxyl groups attached at carbons 1 and 3. All signals above ca. 1250 cm^{-1} can be assigned to vibrations specific for the carbon atoms in phenolic ring except for the signal at 1400 cm^{-1} which is related to the C-O stretching vibrations.

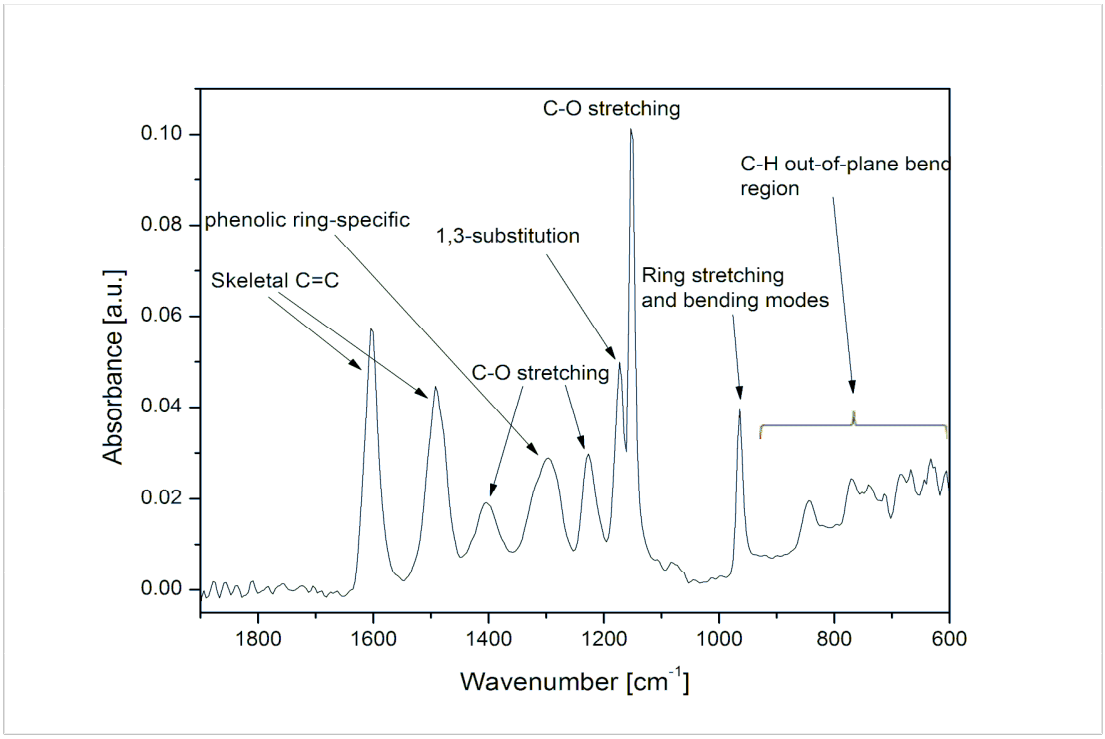

Figure 78. IR spectrum of aqueous resorcinol solution at 0.10 g·ml^{-1} concentration.

In order to assess whether the kinetics of the reaction could be followed by IR spectroscopy, spectra of two main components (resorcinol and formaldehyde) were overlapped and the result is shown in Figure 79. It can be clearly seen that in the most part of the spectra, the signals do not overlap significantly and therefore there is a possibility of following kinetics by either way observing the decrease in intensities or areas of resorcinol or formaldehyde related peaks or by detection and observation of new peaks, which should appear upon substitution of resorcinol.

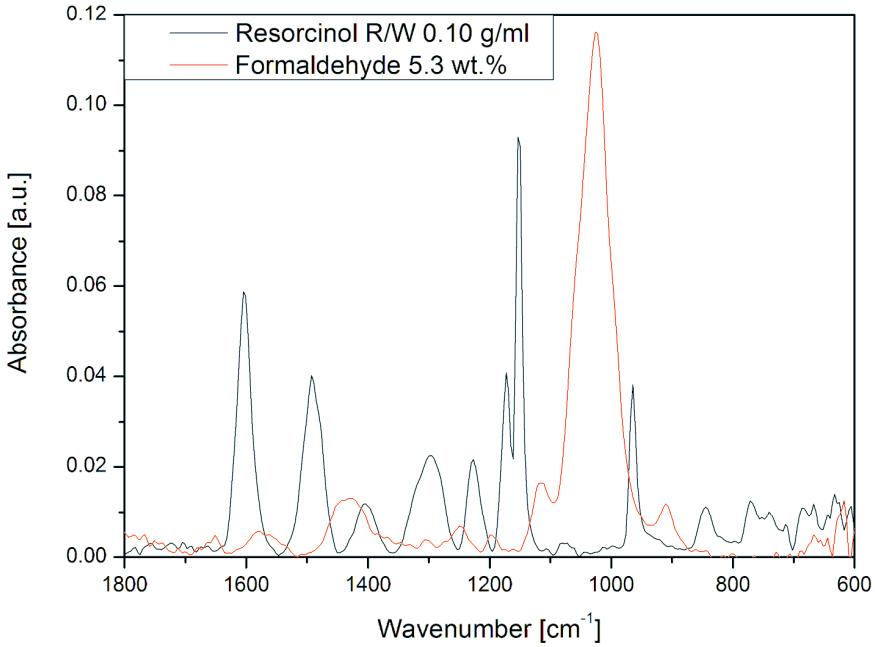

Figure 79. Overlaid IR spectra of formaldehyde and resorcinol at concentrations close to the reaction conditions.

Experiments performed for monitoring of the reaction were conducted for a number of samples with varied amount of catalysts, expressed by the R/C ratio. The other ratios – R/F and R/W – were kept constant at 0.5 mol·mol^{-1} and 0.10 g·ml^{-1}, respectively. The range of the R/C ratio was chosen to cover the most common composition used for synthesis of resorcinol-formaldehyde gels and was between 100 and 600 mol·mol^{-1}. The reaction was ran at 90°C in a sealed 25 ml poly(propylene) flask in an electric oven. The measurements were performed after the sample was taken out after a given time interval and cooled down to room temperature. The reason for cooling down the sample was that the probe in which the spectrometer operated had temperature limitations and that during the measurement in such high temperature, it would be expected that significant amounts of the reactants

or solvent (including) methanol could evaporate. Additionally, maintaining low temperature during measurements ensured that the results from ^{13}C NMR, IR and DLS would be consistent, as all these experiments were performed in the same manner.

As it was explained in the previous section, the IR spectra for formaldehyde solutions are fairly complex, require deconvolution and cannot provide detailed information on the specific chemical species in the sample. It can be expected that the spectra collected for reacting mixture are even more complicated. An example of spectra of a reacting mixture, taken at 10 min intervals, is shown in Figure 80.

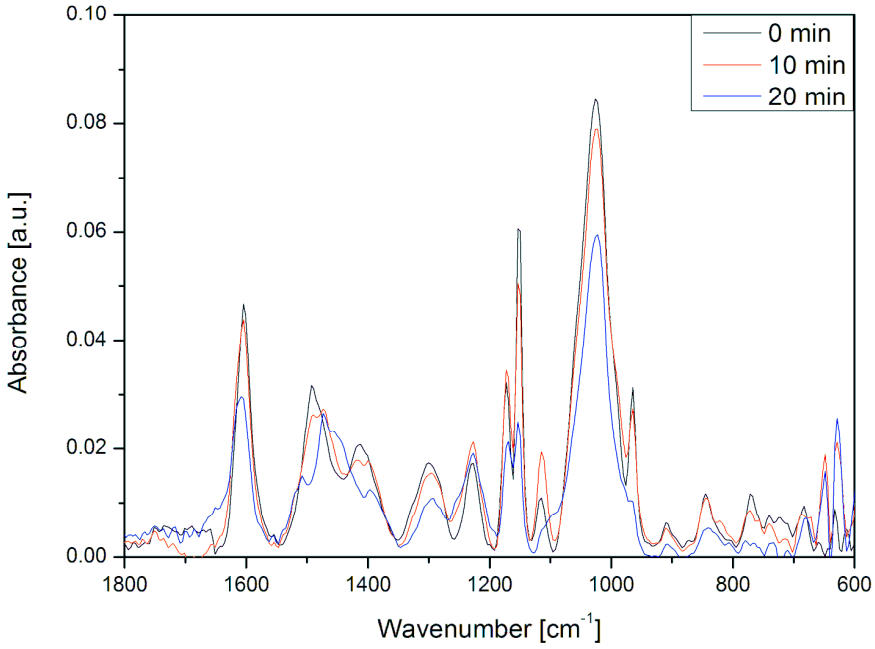

Figure 80. IR spectra of reacting mixture with the composition of R/C 100 mol·mol^{-1}, R/F 0.5 mol·mol^{-1}, R/W 0.10 g·ml^{-1} kept at 90°C for times as indicated.

Analysis of the spectra shown in Figure 80 results in a number of observations. Most of all, the spectrum taken at 0 min (which means no high temperature treatment) resembles very much the sum of spectra shown in Figure 79. This was expected, as the reaction proceeds very slowly in room temperature and the changes in the composition could be detected by the NMR but are far too small to be clearly seen in a convoluted IR spectrum. The overall shape of IR spectrum of reacting mixture does not change very much in time, even though the spectrum taken after 20 min of temperature treatment corresponds to a sample with a visual appearance significantly different from others. It is far more viscous and has an intensive orange tint, which is characteristic of a solution near the gelation point. It is not possible to point to a new signal, which would be caused by the newly formed molecules, clusters or gel network. Instead, the shape of the spectrum remains fairly similar in time and the main difference observed in the change in absorbance of individual peaks. These changes, associated with changes in concentration, are caused by the course of the reaction and gradual disappearance of the reactants.

Decreasing intensity of band at ca. 1000-1100 cm^{-1} is related to decreasing concentration of glycols and poly(oxymethylene glycols), which undergo reaction with resorcinol aromatic ring. Peaks within this wavenumber region corresponds to C-O asymmetric stretching vibrations of bonds between oxygen atom and aliphatic carbon atom. This region does not correspond to vibrations of hydroxymethyl group attached to resorcinol ring and can be used only to monitor the rate of formaldehyde-related species disappearance. However, one must bear in mind that this region also corresponds to signals from free methanol, which does not react with resorcinol and most probably also to the hydroxymethyl groups attached to resorcinol rings. One could

deliberate what should be the overall change in this region, as theoretically the overall concentration of aliphatic hydroxymethyl groups should be constant until the resorcinol derivatives condensate. Therefore, one may interpret the small difference of the overall shape and absorbance in this region between 0 and 10 min as indication that there is still a considerable amount of aliphatic hydroxyl groups in forms of glycols or hydroxymethyl resorcinol derivatives; however, the small decrease in the intensity clearly indicates that some of these groups are either way invisible (i.e. migrate to another phase) or disappear because the hydroxymethyl resorcinol derivatives condensate. Interestingly the difference between spectra taken at 10 and 20 min is far more significant than between 0 and 10 min. It is a clear indication that reaction rate increased greatly in this period of time. This can be supported by visual observation of the sample: viscosity increased and this can only be a consequence of growing molecular weight of the species or extent of clustering of primary particles in the solution.

The spectra change their shape mainly in the 1400-1550 cm^{-1} region, which is the area where peaks for O-H bending, CH_3 asymmetric bend and C=C stretching in ring vibrations appear. The change of this region can be caused by both the substitution of the aromatic ring and condensation of these derivatives.

Another change associated with proceeding substitution and condensation can be observed in the low wavenumbers region. A group of peaks which indicate 1,3-substitution is found at ca. 685 cm^{-1}, 740 cm^{-1} and 770 cm^{-1}. Absorbance at these wavenumbers decreases with time, as well as absorbance of the signal at 965 cm^{-1}. This indicates that resorcinol is substituted at other carbon atoms in aromatic ring than those which are

already substituted with hydroxyl groups and that the 1,3-substitution is accompanied by other species, namely by hydroxymethyl resorcinol derivatives. Decrease in intensity of peak at ca. 1175 cm^{-1} (characteristic for *para*-substitution pattern) is also caused by an increase in concentration of differently substituted resorcinol compounds.

An interesting observation can be made when analysing the changes in the absorbance of the signal at ca. 1150 cm^{-1}. This signal is associated with stretching vibrations between aromatic carbon and oxygen atom, which is thought to be between carbons 1 and 3 and the hydroxyl group in an unsubstituted resorcinol. The absorbance at this wavenumber decreases with time and it does not change proportionally to the changes in the other peak associated with this type of vibrations. In other words, the ratio of peaks at ca. 1150 cm^{-1} and ca. 1225 cm^{-1} changes with time, while it should be constant as both of them correspond to vibrations from the same type of bond.

In order to discuss the influence of the resorcinol to catalyst ratio on the rate of the reaction, a sample with a significantly different amount of catalyst was analysed. Out of all investigated compositions, the sample with R/C ratio of 500 was chosen and the resulting IR spectra are shown in Figure 81. The gelation time is much longer than for the sample with R/C 100 $mol \cdot mol^{-1}$, as the catalyst concentration is five times lower and this allowed for more spectra to be collected. The assignment of the peaks is the same as for the previous composition and same observations can be made as before. The overall tendency of the absorbance intensity of reactants' peaks to decrease is maintained. Moreover, the peaks at ca. 1150 cm^{-1} and 1225 cm^{-1} decrease in the same manner as in the sample with higher catalyst concentration, i.e. not proportionally. The decrease of absorbance intensity of the peak at

ca. 965 cm^{-1}, corresponding to the aromatic ring stretching and bending modes typical for 1,3-substitution, is also rapid.

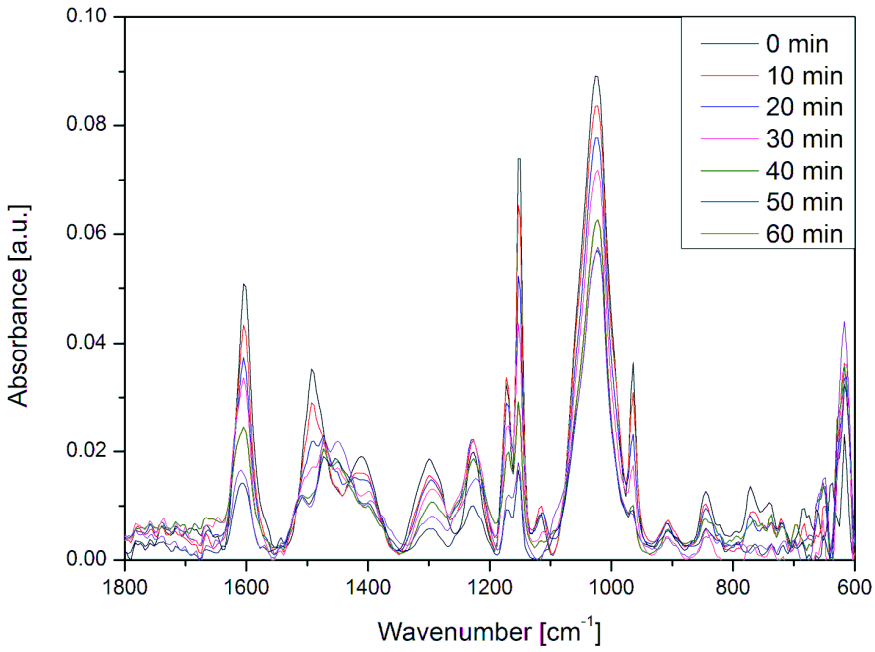

Figure 81. IR spectra of reacting mixture with the composition R/C 500 $mol \cdot mol^{-1}$, R/F 0.5 $mol \cdot mol^{-1}$, R/W 0.10 $g \cdot ml^{-1}$.kept at 90°C for times as indicated.

In order to establish whether any of these changes are dependent on the catalyst concentration, a comparison of absorbance intensities versus R/C ratio at given time intervals was made and is presented further on.

In order to perform a fully quantitative interpretation of the results a number of steps would be required. First of all, overlapping peaks in spectra should be deconvoluted, where necessary. This is a challenging task, especially in later stages, when the peaks become increasingly featureless, thus making

the deconvolution task difficult even for the specialised software and in certain cases the peaks cannot be separated.

Furthermore, should one wish to perform an analysis which provides information on changes in absolute concentrations of reactants or products, calibration should be performed in order to establish what is the relationship between the molar concentration and absorbance of the collected spectrum. Normally, this is done by collecting a set of IR spectra for a number of samples with different concentrations of the investigated sample and then plotting the response (absorbance) against the concentration values, thus forming a calibration curve which can allow to determine the concentration of the species in a sample with an unknown concentration. This can be easily done for resorcinol because its aqueous solution is very simple and the absorbance of each peak can be easily obtained. It is a much more complicated problem for formaldehyde solutions, as they are far more complex and deconvolution is required. This issue was actually overcome in the previous section, however, the fact that the composition of the sample depends strongly on the dilution, it is not possible to determine the absolute concentrations from this data. To be more precise, this is caused by the fact that none of the peaks can be assigned uniquely to one of the species and thus only the overall concentration could be determined. Furthermore, one must be aware of another obstacle, related to the ca. 1020-1050 cm^{-1} region corresponding to vibrations of various types of single bonds between carbon and oxygen atoms. When using this region to determine the disappearance of formaldehyde-related species in the course of reaction, one must remember that hydroxyl groups on the aliphatic chains in the hydroxymethyl resorcinol derivatives are also visible in this region. Therefore, this method of analysis in terms of absolute concentrations would only be viable for resorcinol.

Nonetheless, one must remember that certain signals should not disappear with time, as the bond from which vibrations they result should not decrease its concentration. Such is the case for peak representing the bond between aromatic carbon and oxygen atom: the hydroxyl groups at carbon atoms 1 and 3 in resorcinol are expected to remain unchanged. On the other hand, one would expect signals typical for 1,3-substitution to gradually disappear: this should take place for peaks at ca. 965 cm^{-1}, 1175 cm^{-1} and for the group of three peaks at ca. 685 cm^{-1}, 740 cm^{-1} and 770 cm^{-1}.

Ideally, in order to determine the absolute concentrations of species found in an examined sample one would use a standard, as it is done in NMR spectroscopy. However, this approach is questionable as the response of the signal from the standard may be stronger or weaker than that of the considered species. Additionally, one would have to choose an inert standard not to compromise the results of the experiments. Therefore it was decided that the results from IR would not be treated in terms of absolute concentrations. However, it is known that the absorbance intensity is proportional to the concentration, which allows to roughly assess the influence of catalyst concentration on the rate of the reactants' disappearance.

In order to minimise problems occurring in the deconvolution in later stages of the reaction and in order to minimise possible errors arising while forcing deconvolution on smooth peaks, only a few signals were chosen to be investigated. This is reasonable because the analysis of the influence of the catalyst concentration on the rate of reaction can be examined by comparing the signals corresponding to reactants and since their absorbance is proportional to their concentration, it should not matter which signal is

chosen. Therefore, the chosen peaks were located at 965 cm^{-1}, a pair at ca. 1150 and 1225 cm^{-1} and a single peak at 1175 cm^{-1}. The choice is justified by Figure 80 and Figure 81, where it can be seen that these signals are well visible and well separated. In case of the peak located at 964 cm^{-1}, deconvolution is necessary, however in this case it is a fairly simple procedure as this signal is always well visible and does not merge into a shoulder of the broad peak at ca. 1020-1050 cm^{-1}.

The deconvolution and integration of the selected peaks allows to investigate how the absorbance intensity and area of the selected peaks change in time for each reacting composition with different R/C ratio. The results proved that changes in the intensities of peaks are proportional to their area, therefore it can be assumed that the width of the peaks and their shape do not undergo any significant changes and hence only changes in the intensities are shown here.

Regardless of the R/C ratio, intensities of all selected peaks decrease in time, as it can be seen in Figure 82, where the time dependence of intensity of the peak at 965 cm^{-1} is plotted in scaled time $\tau = t/(R/C)$ The decrease of peak intensity corresponds to the decrease in the concentration of species with bonds related to this signal, in this case resorcinol (1,3-substituted aromatic ring). Although there is a substantial scatter of peak intensity values, it can be seen that the values are decreasing comparably when plotted in scaled time, in agreement with observation from ^{13}C NMR in the previous section. This is consistent with the rate of resorcinol consumption being proportional the concentration of sodium of carbonate, which is thus acting as the catalyst for the reaction of resorcinol with formaldehyde as expected.

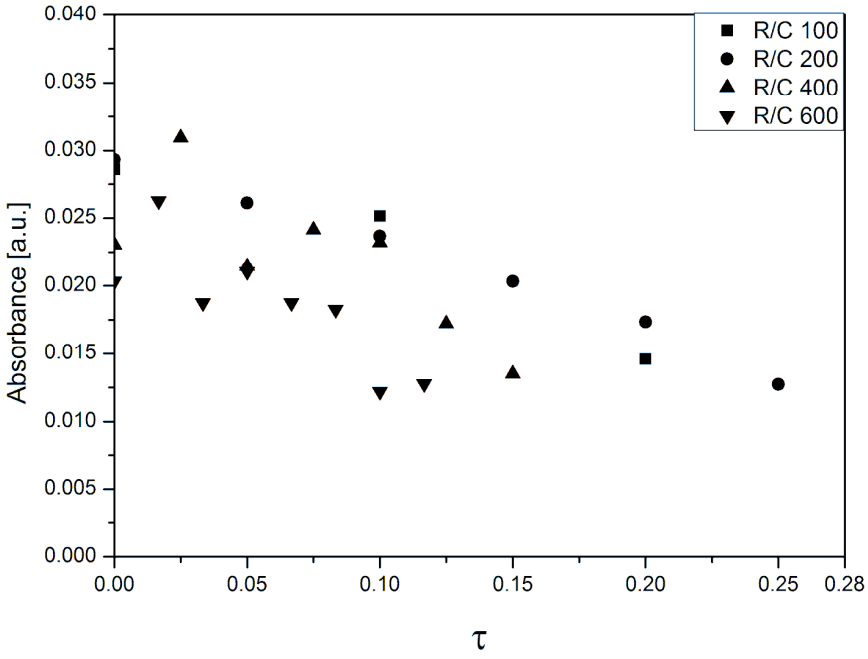

Figure 82. Time evolution of absorbance intensities of peak at 965 cm^{-1} expressed in scaled time τ for different sodium carbonate concentrations as indicated

The same tendency can be seen when analysing data collected for some other selected peaks, for example the one at 1150 cm^{-1}, as it can be seen in Figure 83. However, it can also be seen that another peak, the one at 1225 cm^{-1}, is hardly changing its intensity over time, which indicates that the same vibrational frequency is present in both reactants and reaction products, i.e., the substituted resorcinol.

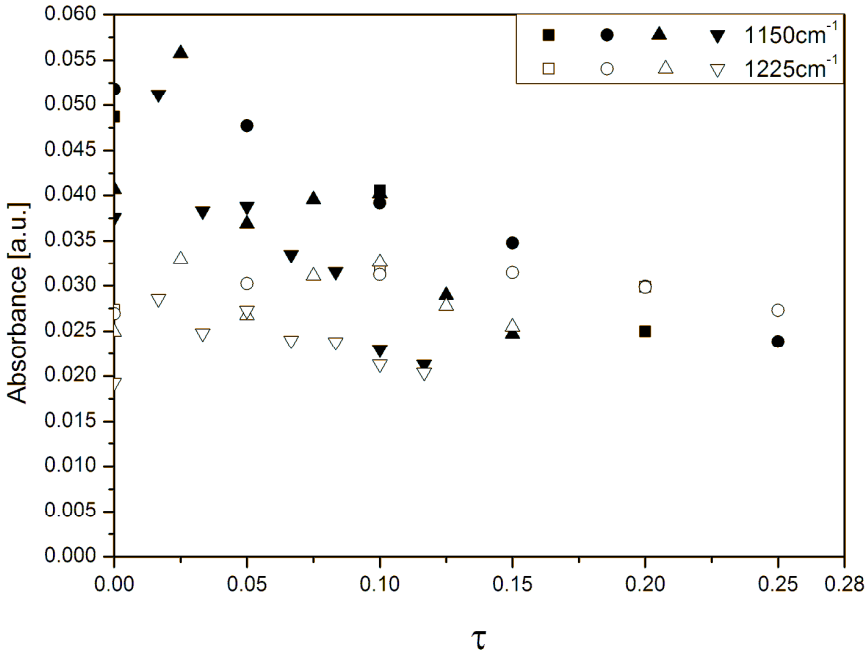

Figure 83. Time evolution of absorbance intensities of peaks at 1150 cm^{-1} and 1225 cm^{-1} expressed in scaled time τ for different sodium carbonate concentrations as indicated.

As it was explained earlier, IR spectroscopy is far from being an easily available quantitative tool for monitoring of reactions between formaldehyde and resorcinol leading to gel formation. Certain amount of information can be obtained but it is definitely not sufficient to draw quantitative conclusions without further investigation into IR spectroscopy of these solutions. It might be sufficient to monitor the overall rate of the reaction in the industry or to roughly define the composition of the mixture, but at the current state of knowledge it does not provide further quantitative information for the purpose of this research.

6.4. Dynamic Light Scattering

DLS experiments were used to monitor the influence of catalyst and temperature on the formation of the primary particles which are involved in the subsequent formation of the particulate gel structure. This method did not investigate the qualitative composition of the reacting mixture in the course of the reaction and it did not shed any light on the actual structure of forming clusters, but it did novel and surprising information on the formation of primary particles as small as few nanometres.

Series of *in situ* experiments were performed at 55°C, as it was described in the methods section. The data collected in these experiments can be presented in two ways: as autocorrelation functions and as development of hydrodynamic radius in time, which is determined by appropriate fitting of the initial decay of autocorrelation functions.

An example of how autocorrelation function changes in the course of the reaction is shown in Figure 84. Autocorrelation functions were measured every 3-5 minutes, however only three representative ones are shown here for clarity.

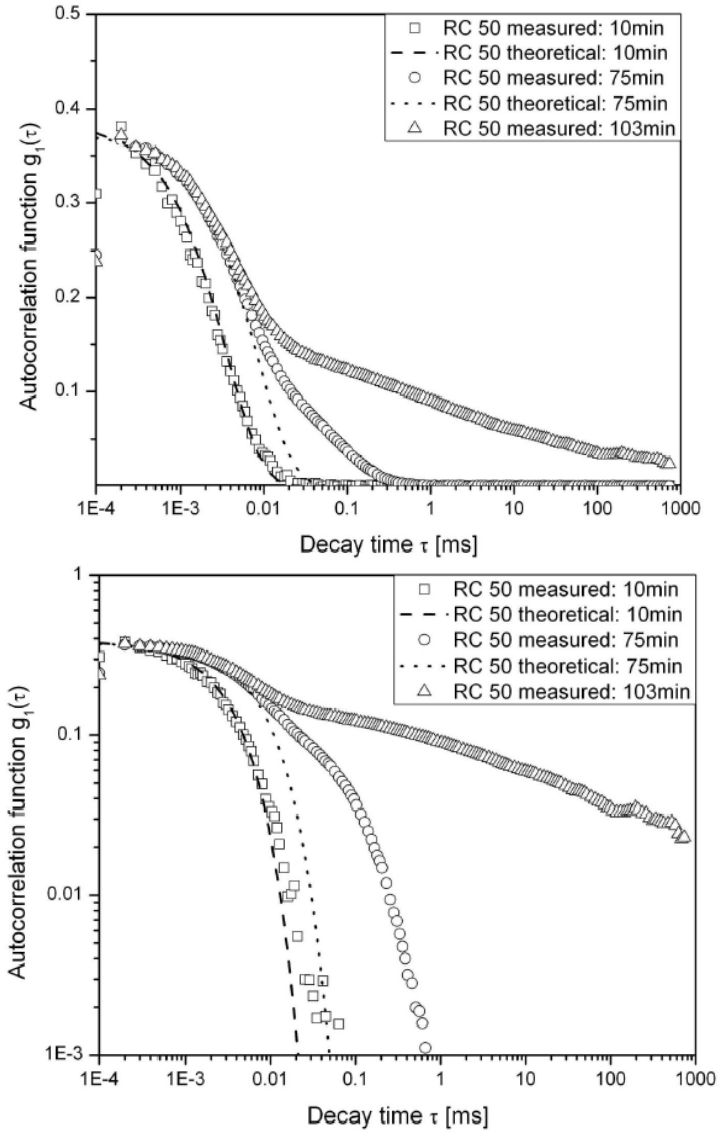

Figure 84. Selected autocorrelation functions for solutions with composition R/C, R/W and R/F ratios are 50 mol·mol^{-1}, 0.10 g·ml^{-1} and 0.5 mol·mol^{-1}, respectively, kept at 55°C for times as indicated.

It can be seen in Figure 84 that the autocorrelation function collected 10 min into the reaction has the shape which corresponds to the single exponential decay, meaning that the objects observed are subject to unhindered Brownian diffusion resulting in exponentially decaying autocorrelation function. The shape of the autocorrelation function changes in time due to the growth of the particles, which can be seen in the shape of the

autocorrelation function collected at 75 min, where the initial decay takes a longer time. Moreover, a secondary decay can be also seen at this time, corresponding to much slower relaxation most likely due to formation of larger clusters from some primary particles, while most of them still remain free to move around. This stage can be referred to as *transition* stage: the mixture is not yet gelled but it no longer is a suspension with particles which are all subject only to Brownian motions. The sample becomes a gel some time before 103 min and the shape of the autocorrelation function shown in Figure 84 for that time is no longer of an exponential decay shape but becomes more like a power law function, typical for gel-like networks, where mobility is strongly restricted. This would be expected for a gel network consists of a 3D structure of interconnected primary particles, where solvent and unconnected primary particles are still free to diffuse within the pores of the gel structure, as indicated by the still visible initial decay. The autocorrelation function can therefore be used to estimate the gelation time. In practical terms, however, it is not easily quantifiable because it adapts the shape of a power law gradually, therefore it can be used to indicate only an approximate gelation time.

In order to investigate the effect of temperature on the growth of primary particles, similar DLS experiments were performed for solutions reacting at 80°C, but samples were quickly quenched at specified times to 20°C where reactions are expected to be much slower and DLS measurements could be performed. The experimental procedure was similar to that used for sample preparation in the NMR experiments as described in the methodology section. Example of results from these experiments is shown in Figure 85. The composition of the sample is identical to the one for which autocorrelation functions were shown in Figure 85. Comparison of these two

figures leads to a conclusion that the evolution of the autocorrelation function follow exactly the same pattern – from being single exponential decay, through a transition stage to a power law. The significant difference is the time at which the autocorrelation function falls into one of these three stages. When reaction took place at 55°C, the transition stage was observed at ca. 100 min, while performing the reaction at 80°C caused this stage to appear as soon as within the first 10 min. The stage in which the solution was nearly gelled was observed at roughly 250 min into the reaction in case of experiments at 55°C, while the sample reacting at 80°C was almost a gel in time more than ten times shorter, i.e. in 20 min.

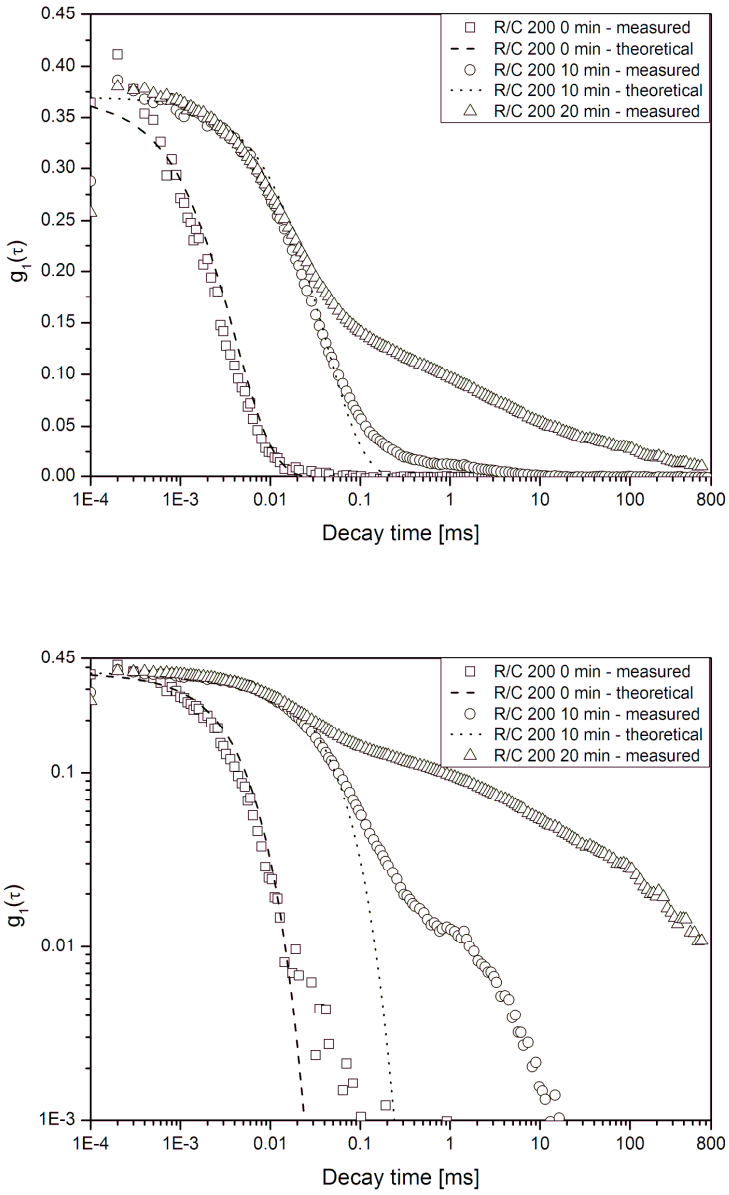

Figure 85. Selected autocorrelation functions for solutions with composition R/C, R/W and R/F ratios are 200 mol·mol^{-1}, 0.10 g·ml^{-1} and 0.5 mol·mol^{-1}, respectively, kept at 80°C for times as indicated.

The most significant conclusion from this comparison is confirmation of the visual observations of the gel formation *via* the gelation time measurements.

These experiments indicate that the temperature influences the rate of the gel formation but it does not influence the mechanism of its formation.

The autocorrelation functions can provide overall information on the growth of primary particles and their interconnection into larger networks and eventually forming a gel. If the autocorrelation function is in the form of a single exponential decay function (e.g. collected at 10 min in Figure 84), it can be interpreted as corresponding to a suspension with particles of approximately same hydrodynamic radius freely diffusing in suspension. If the particles have various radii, i.e. the suspension was polydisperse, the autocorrelation function would be a combination of multiple exponential decays – each for each hydrodynamic radius (providing the number of particles of this size is sufficiently large to scatter with measurable intensity). The shape of the autocorrelation function collected at 75 min into the reaction, shown in Figure 84, shows development of a second, slower decay mode, which can be attributed to formation to formation of larger clusters, but still being able to relax density fluctuations. It is an example of a size distribution that could be treated as bimodal, however, the appearance of the second step indicates that the clusters are likely to be polydisperse. At even longer times, the second decay mode changes from exponential to power law in decay time and does not manage to fully relax fluctuations, which is typical for gel-like networks.

The initial decays of measured autocorrelation functions were fitted in the way described earlier and the resulting initial decay rates (Γ) and corresponding apparent mean hydrodynamic radii are shown in Figure 86.

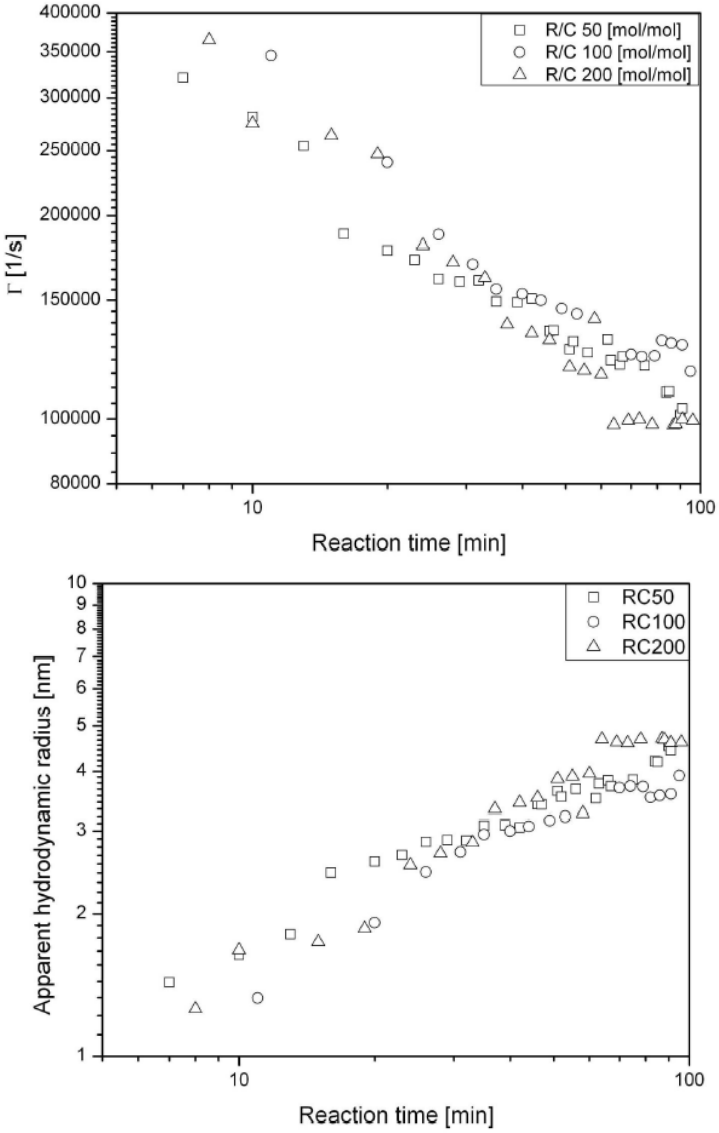

Figure 86. Time evolution of the initial decay rate (a) and apparent mean hydrodynamic radius (b) at 55°C. Ratios R/F and R/W are 0.5 mol·mol^{-1} and 0.10 g·ml^{-1}, respectively.

It can be clearly seen in Figure 86 that the mean hydrodynamic radius does not depend on the R/C ratio. In all cases the growth of the hydrodynamic radius follows identical pattern. Initially there is a relatively rapid growth of the sizes of the particles, from ca. 1-2 nm at 10 minutes to ca. 4 nm within the first 50 min. It is known that gelation does not occur within this timeframe. It should be noted that the calculated hydrodynamic radius of unhydrated

resorcinol molecule is ca. 0.3 nm and the radius of variously substituted hydroxymethyl derivatives of resorcinol varies between 0.3-0.4 nm. Therefore the measured values after first 10 minutes correspond to particles substantially larger than single resorcinol-formaldehyde molecules.

The rate of growth of the particles is not dependent on the concentration of the catalyst and, moreover, neither is the radius to which they initially grow. This suggests strongly that the catalyst does not play a decisive role in formation of the primary particles, which later on form a gel network. The second stage of the radius growth is a plateau: irrespectively of the R/C ratio, the growth of the particles slows down strongly and after ca. 100 min, the particles hardly grow any more. Their mean hydrodynamic radius changes from ca. 4 nm to 5-6 nm, which is significantly slower than within the first 50 min. Relatively rapid development of the secondary autocorrelation decay which follows after the plateau can be related to the gel formation.

Series of experiments with varied R/W ratios were also performed at 55°C in order to determine the influence of overall reactants concentration on the evolution of autocorrelation function and the apparent hydrodynamic radius. Ratio of resorcinol to formaldehyde was kept at 0.5 $mol \cdot mol^{-1}$ which means that when R/W was increased, also the concentration of formaldehyde was raised. In order to separate the effect of catalyst concentration R/C ratio was not kept constant, as with increasing R/W ratio the amount of added sodium carbonate would also increase and thus its concentration. Therefore the sodium carbonate concentration was kept constant and equal to 7.9 $mmol \cdot dm^{-3}$, ratios of resorcinol to water were changing from 0.10 $g \cdot ml^{-1}$ to 0.50 $g \cdot ml^{-1}$ at an increment equal to 0.10. Effectively, the first sample with R/W 0.10 $g \cdot ml^{-1}$ corresponds in composition to samples with R/C ratio

100 mol·mol^{-1}, R/W 0.10 g·ml^{-1} and R/F 0.5 mol·mol^{-1}. Figure 87 shows autocorrelation functions for a few selected measurement times for sample with R/W 0.50 g·ml^{-1}. The overall shape of the autocorrelation functions resembles the ones shown in Figure 84 and, interestingly enough, despite five times greater resorcinol concentration the decay times of each curve are comparable (see: curves for 10 min). This phenomenon is explored further on, when apparent hydrodynamic radii are calculated and compared.

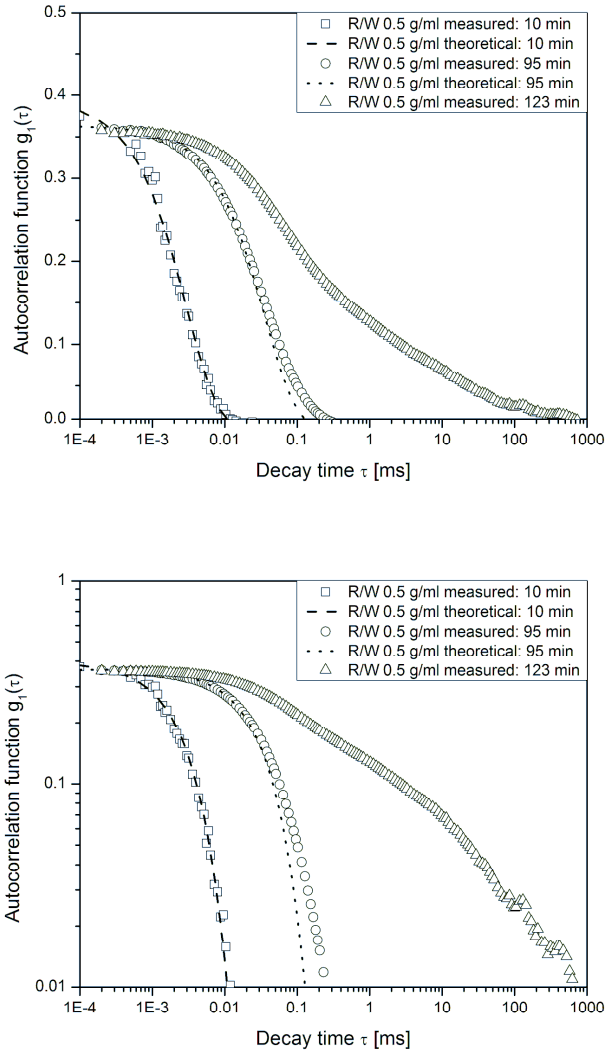

Figure 87. Selected autocorrelation functions for solutions with R/W and R/F ratios 0.50 g·ml^{-1} and 0.5 mol·mol^{-1}, respectively, and sodium carbonate concentration 7.9 mmol·dm^{-3} kept at 55°C for times as indicated.

In order to verify whether R/W ratio has any effect on the hydrodynamic radii of the particles formed during the reaction, a simple comparison of autocorrelation functions for five samples with varied R/W ratios was performed. The shapes of the initial section of the autocorrelation functions are shown in Figure 88. The measurements were taken at very similar times (ca. 10 min), which were long enough for the reactions to take place and short enough so that the autocorrelation functions would still exhibit an exponential shape. It can be clearly seen that despite the fact that the resorcinol concentration increases fivefold across these samples, the autocorrelation function remains virtually unchanged and starts to decay at the same time. Visual analysis of the autocorrelation functions is one way of comparing the growth of hydrodynamic radii, however, to perform a reliable analysis, apparent hydrodynamic radii need to be calculated from the autocorrelation functions and this is done further on.

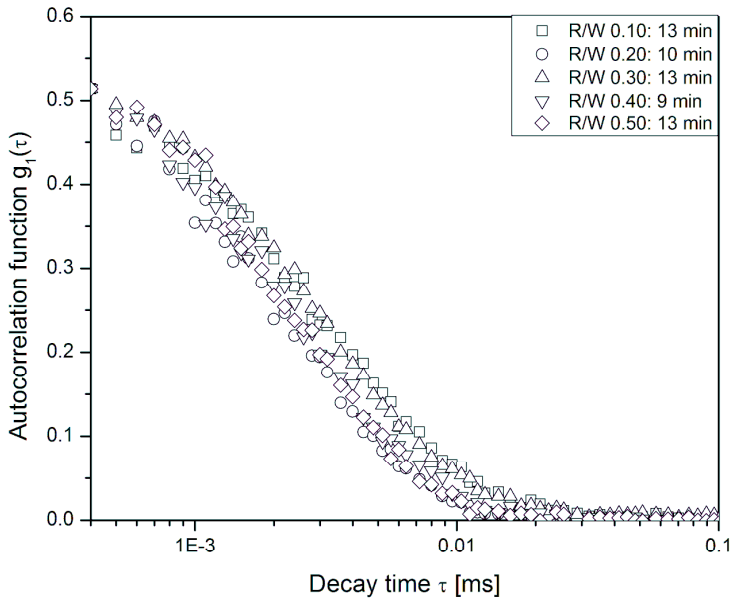

Figure 88. Comparison of initial sections of the autocorrelation functions for five samples with different R/W ratios. Data was collected at a similar time.

Just as it was done for samples with varied R/C ratios, hydrodynamic radii time evolution was calculated by first fitting the autocorrelation functions and then calculating the gamma coefficient (Γ) and finally the hydrodynamic radius. The results of this analysis are shown in Figure 89. It is clear that the rate in which apparent hydrodynamic radii grow in time is independent on the R/W ratio, meaning that the overall concentration of the reactants does not control the sizes of primary particles which then form a gel. When analyzing these plots, one can see that towards the greater reaction times, the lines formed by hydrodynamic radius datapoints start to separate and form a fan. This is especially true for samples with the two lowest R/W ratios and may be caused by the fact that these samples were very viscous and close to gelation, therefore their corresponding autocorrelation functions were not fully exponential and their fitting might have been less accurate and resulting in artificially increased radii.

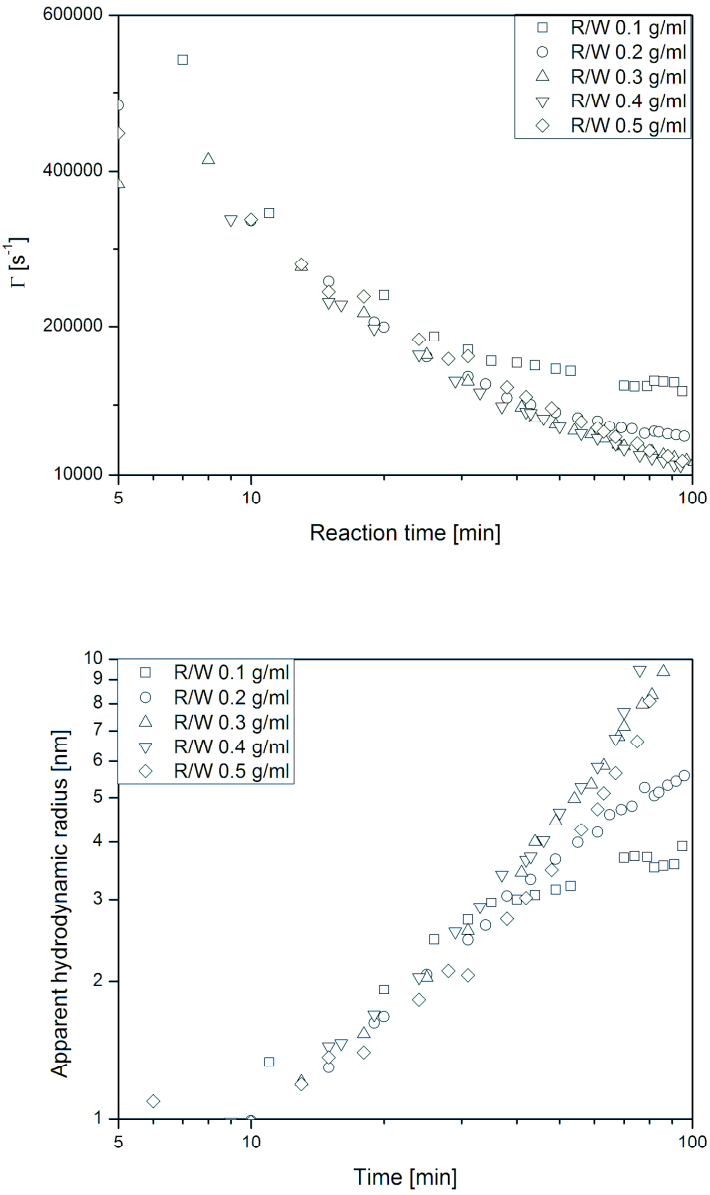

Figure 89. Time evolution of the initial decay rate (a) and apparent mean hydrodynamic radius (b) at 55°C. Ratio R/F is 0.5 mol·mol^{-1}, R/W as shown in the legends and sodium carbonate concentration is 7.9 mmol·dm^{-3}.

Analysis of the data from experiments performed in a continuous manner at 55°C proved that the R/C ratio does not control the hydrodynamic radius of the primary particles formed in the course of the reaction and neither does

R/W. Therefore, the results from a set of experiments performed at 80°C were also investigated and contrasted with those from 55°C to verify whether the temperature influences the rate of growth and the mean hydrodynamic radius. The comparison of these results is shown in Figure 90. In this figure, the hydrodynamic radii were grouped by temperature and not by the R/C ratio, because previous experiments proved that the R/C ratio does not affect the growth of particles. It can be seen in Figure 90 that the hydrodynamic radii detected at the same time at 80°C are greater than those at 55°C. This supports the conclusions from previous experiments that the temperature affects the rate of the reactions taking place in the mixture. It was observed that higher temperature leads to faster gel formation, expressed by shorter gelation time. It is now clear that higher temperature increases the rate of particles' growth in the reacting solution. This is observed throughout the whole reaction time until the gel is formed but the data shown in Figure 90 are only for the time when the gel is not yet formed. In other words, this means that the temperature affects not only the gel formation (polycondensation) but also the formation of clusters which then subsequently are joined to form a solid 3D structure immersed in the solvent and residues of reactants.

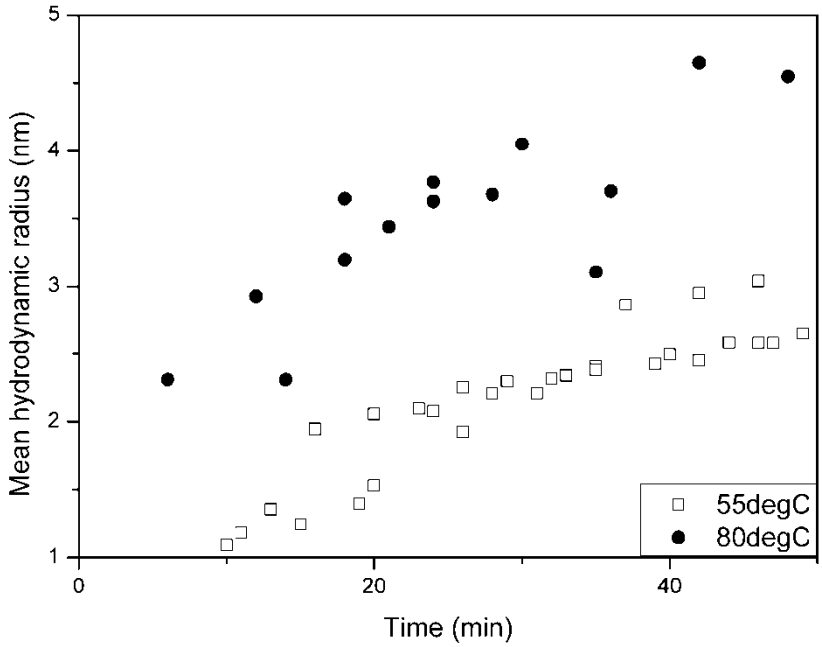

Figure 90. Early evolution of mean hydrodynamic radius independent of R/C ratio at two different temperatures. (R/C ratios 50, 100 and 200 mol·mol^{-1} ; R/F is 0.5 mol·mol^{-1}; R/W is 0.10 g·ml^{-1}).

An unexpected overall conclusion can be drawn from the DLS experiments. It appears that regardless of the concentration of the catalyst, primary particle formation is a process which follows the same pattern at a given temperature. In all cases the primary particles formed initially have very similar hydrodynamic radii and the amount of catalyst and the temperature only determine the time at which these particles form a solid network. In these experiments, it was not possible to determine the amount of the particles detected at a given time therefore it is hard to prove the following conclusion basing only on the above results. It appears that the gel is formed when there is a sufficient (critical) concentration of clusters. Possibly the addition of catalyst causes changes in distribution of charges on the surfaces

of these colloidal particles and instead of repulsing each other, they are attracted and start coagulating and forming much larger structures which eventually form a gel. The amount of catalyst seems to control the value of this critical concentration: the more catalyst, the lower the concentration required for gelation, which would explain why larger catalyst concentration leads to faster gelation. This process is also enhanced by an increased temperature, as expected for a kinetic process with an activation barrier (Arrhenius theory).

6.5. pH measurements

Measurements taken at room temperature right after mixing of samples after the final step of adding of resorcinol was finished (once the solution was divided into parallel samples) were performed in order to observe the effect of addition of resorcinol on the pH of the reacting mixture. There is a clear relationship between pH and the amount of sodium carbonate in the reacting mixtures, just as there was with formaldehyde-water dilutions. The main purpose of the catalyst is thought to be the adjustment of pH, therefore these results are as expected: the higher the R/C ratio, the lower catalyst concentration, therefore the value of pH increases as it can be seen in Figure 91. From measurements of non-reacting solutions of reactants and water, it is known that the pH value of the 0.1 $g \cdot ml^{-1}$ aqueous solution of resorcinol is 4.63 (theoretically predicted value based on pK_a of resorcinol is 4.66), the pH of formaldehyde at concentration similar to that used in most reacting solutions is 3.37 (concentration 5.69%wt., formaldehyde-water volumetric ratio 1:6). Measurements in formaldehyde-water-catalyst solutions (without resorcinol) at concentrations exactly same as in the reacting solutions in the range of R/C values between 50-700 resulted in pH

values between 10.56 and 9.18. The corresponding pH values in reacting solutions of the same overall composition (but including resorcinol) after 45 minutes of mixing at laboratory temperature but before any temperature treatment were about 3.2 pH units lower than those in the absence of resorcinol. This drop is caused by the addition of resorcinol, which is known to acidify the aqueous solutions. The effect of resorcinol addition on the pH is rather constant across all investigated samples with varied sodium carbonate concentration, which is as expected since the concentration of resorcinol remains constant.

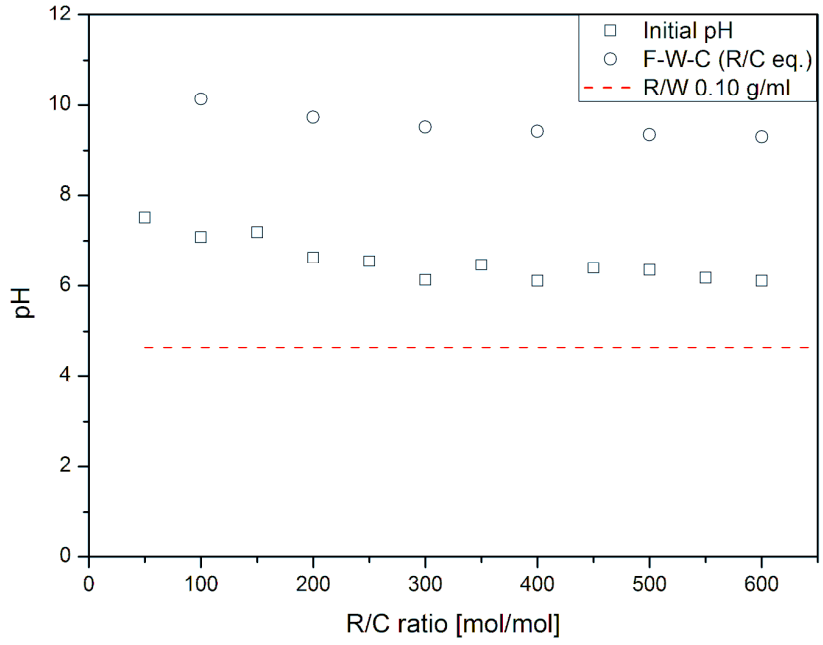

Figure 91. Initial values of pH of the reacting mixtures and corresponding formaldehyde-water-catalyst solutions (without resorcinol) at different R/C ratios. Measured pH value of aqueous resorcinol solution is shown by red line.

A set of pH measurements performed at room temperature without any temperature treatment of the reacting mixture shows a very slow decrease of pH over time, as can be seen in Figure 92. For most mixtures the decrease is not significant, being not more than about 0.1 pH unit. For example, the pH value of reacting mixture with R/C ratio equal to 50 mol·mol^{-1} (R/W 0.10 g·ml^{-1}, R/F 0.50 mol·mol^{-1}) changes from 7.51 to 7.38 within 30 minutes. Similar changes can be observed for R/C ratios of 100, 300 and 600: 7.08 to 6.95, 6.13 to 6.02 and 6.11 to 6.03, respectively. It is most likely that the slow pH decrease observed is caused by the carbon dioxide gradually absorbed from the atmosphere. However, as the NMR results showed above, the reactions take place in these solutions even at the room temperature and first products of addition of formaldehyde to resorcinol are seen almost instantly after the two are mixed. Therefore, it is also possible that these reactions can also contribute to the decrease of pH observed in Figure 92.

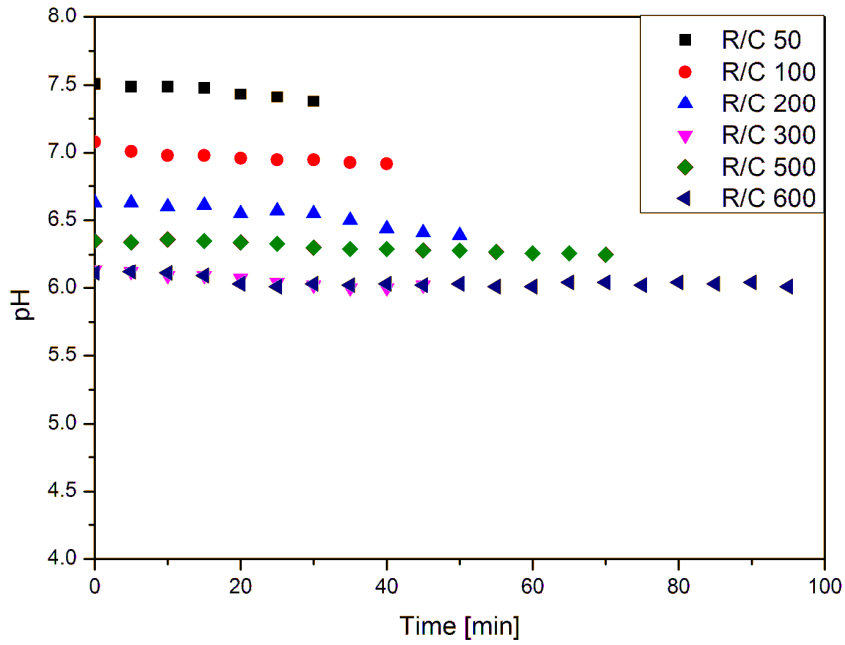

Figure 92. pH change in the course of reaction at room temperature.

More surprising results were obtained in experiments on samples reacting at 90°C. All pH measurements were performed at room temperature, after rapid cooling of samples, as it was described in the methodology section. Results of these measurements were plotted in Figure 93. in a similar way as those obtained in room temperature reaction experiments. One can clearly see that regardless of the catalyst concentration, all samples were subject to a significant pH drop within the first half an hour of the temperature treatment. In samples containing more sodium carbonate, the drop begins slightly earlier, at around 10 minutes, while for those with much lower catalyst content, the drop starts at approximately 20 minutes. Let us consider samples with R/C ratios 50 and 600, respectively. Even though the catalyst concentration decreases twelve times between the two samples, the time at which the pH drop starts is different only by a factor of approximately two: 10 and 20 minutes for R/C 50 and R/C 600, respectively. One would expect the catalyst concentration to have a greater impact on this. Moreover, for all samples the pH drop slows down dramatically – literally ends – after approximately 30 minutes from the beginning of the temperature treatment, indicating that whatever process or reaction triggered the pH drop, it was finished within the first 30 minutes. This is an interesting observation, as the gelation times for these conditions are considerably longer and the growth of primary particles in the solutions, observed by the DLS, did not cease at this time. Therefore, the pH drop surely cannot be associated with the primary particle formation or subsequent gelation.

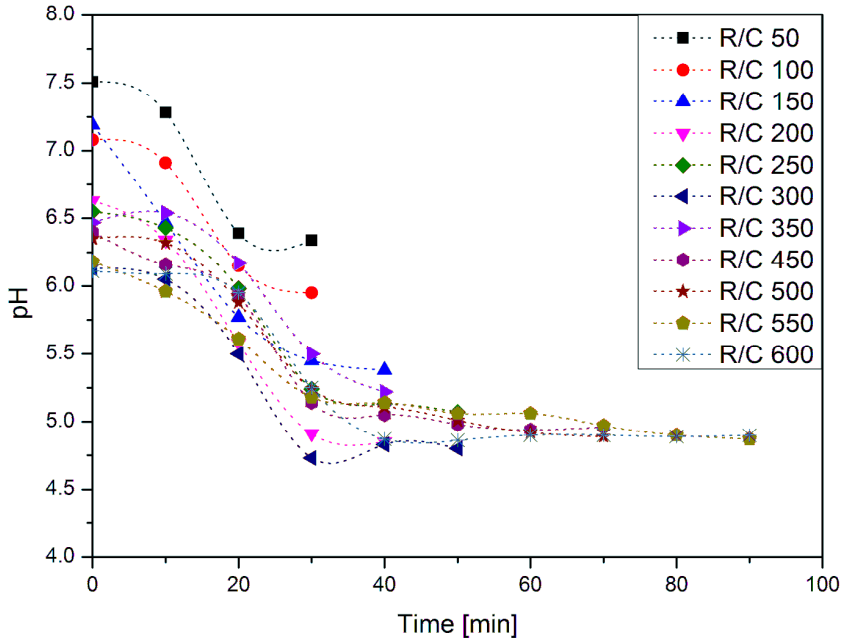

Figure 93. pH change in the course of reaction at 90°C.

Analysis of the data plotted in Figure 93 allows to quantify the pH change within the first 30 minutes. It would be reasonable to expect the overall concentration of sodium carbonate to affect either the rate of the observed pH changes or its magnitude. Analysis of the data showed that the rate is not affected significantly and, surprisingly, neither is the magnitude, as it can be seen from data in Table 36. In all cases, the decrease in pH values was very similar, being around 1 pH unit. When these pH changes are expressed as a fraction (%) of the initial pH value, it becomes clear that in case of all reacting mixtures, the pH drops by approximately 15% within the first 30 minutes. Two exceptions are for R/C 200 and 300, for which the pH drops by nearly 26% and 23%, respectively. It is unclear what caused this phenomenon, observed in a number of repetitions, but it is worth mentioning that it coincides with the fact that these two compositions are frequently chosen for

gel preparation, due to favourable properties of the resulting material (high surface area).

Table 36. Values of pH measured during the reaction in 90°C for selected times and R/C ratios.

R/C →	**50**	**100**	**200**	**300**	**500**	**600**
Time ↓	**pH**					
0	7.51	7.08	6.63	6.13	6.35	6.11
10	7.28	6.91	6.34	6.05	6.32	6.09
20	6.39	6.15	5.58	5.5	5.88	5.95
30	6.34	5.95	4.91	4.73	5.24	5.25
40			4.85	4.83	5.11	4.87
50					5.01	4.86
Total change	1.17	1.13	1.78	1.30	1.34	1.25
Change in first 30min	1.17	1.13	1.72	1.40	1.11	0.86
Change in first 30min as % of the initial pH	15.58	15.96	25.94	22.84	17.48	14.07

When results from Table 36 are compared with those observed in experiments involving pH measurements during the course of reaction in the room temperature, it is clear that heating of the solution increased both the rate and the magnitude of the pH decrease. It is worth to emphasise that all measurements were performed once the samples were quenched in an ice bath to room temperature, so that this did not affect the observed values. As it can be seen in Figure 92, there is no significant change in the pH within the first 30 minutes – all data points for each solution form a steadily decreasing linear pattern, unlike those pictured in Figure 93. The magnitude of pH changes differences between these two datasets is also clear: in experiments performed on the samples reacting in room temperature, the pH decrease amounted to no more than 2% of the initial value, while in solutions treated

at 90°C, the pH decrease was about 15% or more. Once more, this confirms the findings of other experiments, like gel time measurements, NMR spectroscopy and DLS, that the temperature greatly affects the rate of reactions and subsequently gel formation.

It is not clear what causes the decrease of pH during the reaction. Since all measurements were performed in the same conditions and temperature compensation was automatically done, these differences cannot be explained by inconsistencies in measurements. The pH was measured using a glass electrode which is smooth on the surface apart from a small (3-4 mm in diameter) round dot, called the key of the electrode. Its surface was not smooth, therefore could become clotted with the gelling solution and provide false results. This explanation is also not very probable, as all effort was made to clean the electrode thoroughly between measurement. Moreover, this particular part of the electrode was regularly checked and the results of measurements taken when the samples became more viscous and there were traces of gel on the key were not used (and are not shown in this work). As mentioned earlier, in Chapter 2, a special type of reaction called Cannizzaro reaction may take place in formaldehyde solutions. In this reaction two formaldehyde molecules react with each other and one is oxidized by the other and as a result a molecule of methanol and formic acid are formed. The latter one could contribute to the drop in the pH, however, this is highly doubtful mostly because the concentration of formic acid which would trigger such a change in pH would be seen in NMR spectroscopy (and it is not). Moreover, the concentration of formaldehyde as aldehyde is very low and the resorcinol-formaldehyde reaction requires conditions which are not favourable for the Cannizzaro reaction. The latter one requires strongly basic conditions and those provided here are doubtfully sufficient. Another theory

which was considered during this work is related to changing concentration of the carbonates in the samples. Addition of sodium carbonate to the solutions causes the concentration of both sodium and carbonates to increase. The latter ones can exists as carbonic acid or its partially or fully dissociated forms, therefore they contribute to decreasing pH, while sodium ions do otherwise. The carbonates are present in a few forms which are in mutual equilibria also with carbon dioxide. It is known that, unlike for most solids, solubility of gases in water decreases with increasing temperature. Therefore it is possible that when the samples were heated, carbon dioxide migrated into air above the sample, thus shifted the equilibria in the solution. However, this would most likely lead to an increase in the pH value of the solution. Moreover, solubility of carbon dioxide in water is relatively high (90 cm^{-3} per 100 ml at 20^{o}C), therefore it is doubtful that this explanation is true.

6.6. Main conclusions from Chapter 6

Results presented in this Chapter are relatively novel as there is a limited number of publications dedicated to NMR and DLS investigations of the resorcinol-formaldehyde polymerization.

As it was expected, the gelation time was found to be inversely proportional to the concentration of the catalyst, as well as to concentration of the reactants. Additionally, the gelation time was found to be shorter when the reaction temperature was elevated, although it seems that the correlation between these two is not linear.

The most interesting results were provided by the NMR spectroscopy. It revealed that substitution of resorcinol with formaldehyde takes place almost

instantaneously after addition of formaldehyde, even in room temperature which was previously regarded as highly improbable. Moreover, not only mono- but also di-substituted species of resorcinol were detected, including those substituted at C(5) position which is thought to be rather inactive for electrophilic substitution. Experiments performed at 293K and 328K revealed that the concentrations of both reactants decrease significantly within the first few minutes of the reaction and then a gradual decrease is observed over time. Plotting these values in scaled time showed that rates in which both reactants were consumed, were very similar at given temperatures, regardless of the catalyst concentrations. Such an observation confirms that sodium carbonate serves as a catalyst for the reaction of resorcinol substitution with formaldehyde. Whereas experiments performed in 293K showed insignificant changes in protons at resorcinol C(5) concentrations, those done at 328K revealed a decrease proportional to the one for C(2,4/6). This phenomenon may be explained by condensation or further substitution of di-substituted resorcinol in higher temperature, which then leads to formation of a highly reactive or insoluble species which then leaves the reacting solution and forms another (micro)phase. This can explain why signal from the C(5) protons is lost in the NMR in the course of the reaction.

The results from the Dynamic Light Scattering experiments were of significant importance in the light of previous research in the field. Most importantly, they proved that the growth of submicron identities, which in later stages form a solid network in the gel, follows the same pattern regardless of the R/W and R/C ratios. These results also revealed that the average hydrodynamic radius of these objects is very similar across all samples and the only effect concentrations of reactants and the catalyst have on their growth is how soon these particles reach given dimensions. It was

also found that when the temperature or the concentration of reactants or the catalyst were higher, the particles reached their final radius faster. Analysis of how the autocorrelation functions changed during the reaction, allowed to confirm the gelation times and to detect the intermediate stage between the *sol* and *gel* stages of the reaction. To some extent these results disprove previous suggestions on the role of the catalyst as a mean to directly control the dimensions of the particles forming the gel structure.

The reacting systems were also investigated in terms of pH changes during the reaction. As it was revealed, regardless of both the catalyst and reactants' concentration, within the first 30-40 minutes the pH decreased by the same amount in all reacting samples. Unfortunately, neither of the theories discussed here appears to fully explain this phenomenon.

CHAPTER 7. CONCLUSIONS AND RECOMMENDATIONS FOR FUTURE WORK

Overall aim of this research was to explore the mechanism of reactions and gel formation in initial steps of resorcinol-formaldehyde polymerization, as well as to determine the influence of catalyst on this process. Since formaldehyde undergoes hydration and subsequent oligomerisation and esterification in aqueous-methanolic solutions, such as those used in common resorcinol-formaldehyde sol-gel processes, quantification of formaldehyde-related species in these solutions was investigated in detail.

Formaldehyde-methanol-water solutions

Results provided by liquid ^{13}C NMR, ^{1}H NMR and both IR and Raman experiments allowed us to identify all formaldehyde-related species in examined solutions. First of all, our results confirmed that the aqueous-methanolic solutions of formaldehyde do not contain formaldehyde in form of an aldehyde (at least not in detectable amounts). Instead, these are complex solutions of oligooxyglycols and their methoxylated forms, which can be quantitatively identified using ^{13}C NMR. As expected, the greater the formaldehyde concentration, the larger oligomeric species are found. In case of solutions prepared by dilution of formaldehyde stock solutions with water, oligooxyglycols were dominant, however, a significant amount of their methoxylated forms was also found. This was due to the fact that methanol was present in the stock solution of formaldehyde as stabilizing agent. At lower concentrations of formaldehyde, the most dominant structure is monomeric glycol, MG, accompanied by a smaller amount of its methoxylated form, MMG. More generally, increasing amount of water in

the solutions leads to depolymerisation of longer oligooxyglycols and formation of smaller oligomers. Addition of methanol to formaldehyde solutions leads to formation of methoxylated species, rather than simple glycols. These results show that it is necessary to obtain information on the amount of methanol present in the formaldehyde stock solution when synthesising resorcinol-formaldehyde gels in order to know distribution of formaldehyde-related species in the reacting solution and to be able to assess how it effects the reaction with resorcinol and subsequent polymerisation and final properties of the resulting gel.

Using results provided by the NMR spectroscopies, equilibrium constants for MMG and DG species formation were calculated for a range of temperatures, indicating that the higher the temperature, the more MG should be found in reacting solutions. This is important from the reaction point of view, as in higher temperatures more MG is available which partially contributes to higher reaction rates.

Analysis of the results of experiments performed on formaldehyde-water-methanol solutions makes it clear that methanol concentration which is stated by the manufacturer of formaldehyde stock solution corresponds not to free methanol but also includes methanol bound in methoxylated oligooxyglycols. These can decompose under the influence of water and generate more free methanol and oligooxyglycols. At the same time, the total methanol amount measured in the solutions agrees with calculated (expected) values.

The results obtained from Dynamic Light Scattering for non-reacting solutions showed that the solutions of formaldehyde and water or methanol

do not form two phases. At the same time, this confirms that the process of mixing these liquids together and the filtration process was sufficient to ensure homogeneity of the sample.

Measurements of pH in both aqueous and methanolic formaldehyde solutions were performed in order to verify whether changes in distribution of formaldehyde-related species affect the acidity of these solutions. Basing on very high pK_a values for oligooxyglycols and their methoxylated forms in formaldehyde solutions, one would expect the pH of these solutions to be near neutral. However, the actual pH values are in the acidic range and this is most likely caused by presence of formic acid, since the manufacturer states that there can be up to 0.02%wt. of formic acid in the stock solution. The pH values calculated for aqueous solutions of formaldehyde based on theoretical formic acid concentration and its pK_a are slightly lower than the measured values, possibly suggesting that the pH of these solutions is subject to other factors. The dependency of pH on the dilution of formaldehyde stock solutions in water is not linear, therefore it can be assumed that the changes in distribution of formaldehyde-related species can affect it. Possibly changes in formic acid concentration and absorption of carbon dioxide from ambient atmosphere contribute to this effect, as well as variation of activity coefficients in mixed water-methanol solutions.

Formaldehyde-methanol-water-sodium carbonate solutions

Since the results of experiments performed on formaldehyde-water-methanol solutions proved that there is a dependency of speciation on the composition, it was hypothesized that the presence of basic catalyst (sodium carbonate) may as well affect this. Moreover, it is informative to examine formaldehyde-

water-methanol-sodium carbonate solution without resorcinol in order to verify whether the catalyst affects the solution in any other way than by influencing the chemical reactions between formaldehyde and resorcinol.

The results obtained from NMR spectroscopy from formaldehyde-water-methanol-sodium carbonate solutions were very informative in several aspects. Because a fully quantitative analysis was performed, information on exact speciation of all solutions was obtained and information on the dependency of composition on the concentration of sodium carbonate was assessed. Across all of the samples, the qualitative composition was the same, which means that addition of sodium carbonate did not lead to formation of any new species or to disappearance of any others. Quantitative analysis proved that, even when the catalyst concentration was increased ten times, the distribution of species remained constant and molar fractions of each specific compound remained substantially unchanged. Equilibrium constant values were calculated from concentrations of specific species, as it was done previously for formaldehyde solutions without sodium carbonate. This analysis proved that these values are very similar to the ones obtained for catalyst-free solutions and are in general greater by only 5-8%. Nonetheless, the addition of sodium carbonate affected the appearance of the spectra. The intensities of peaks generated by MG, DG and MMG decrease with increasing sodium carbonate concentration, while the area of these peaks remains constant. This could be caused by either chemical exchange between two signals being close together or by changes in the T_2 relaxation time, which could be triggered by changes in the physical or chemical properties of the solution. Changes in relaxation time would be due to some of the molecules migrating to another phase in which they possess a different T_2 relaxation time, therefore being present in the spectrum as broader peaks.

Measurements of linewidth proved that for all formaldehyde-related species the value of T_2 increases with an increasing sodium carbonate concentration, while for methanol this time shortens. It could indicate that methanol is the species migrating from one phase to another, leading to such changes.

Analysis of IR spectra of formaldehyde-water-sodium carbonate solutions included deconvolution of most of the peaks in order to properly assign and quantify them. It is reasonable to state that these results were less revealing than those obtained using the NMR technique. As previously, the assignment of the IR spectra allowed to determine the presence of certain groups in the solutions, however, none of the peaks could be assigned exclusively to one of the species.

The results obtained from the Dynamic Light Scattering experiments reveal that sodium carbonate addition to formaldehyde causes the microscopic appearance of the solution to change. A formaldehyde-water solution is normally homogeneous, as previously discussed results showed, however for solutions with sodium carbonate DLS revealed presence of submicron-scale domains. The range of hydrodynamic radii of these objects is quite wide and the values depend on both the concentration of sodium carbonate and on addition of D_2O. The solutions were filtered with 0.02 μm syringe filters, therefore objects with hydrodynamic radii in range of 50-250 nm, which were found in these solutions could not be particulates of undissolved solids from sodium carbonate or any other solids, hence must have a liquid-like form. The most plausible explanation is that addition of sodium carbonate causes microphase separation and the dispersed phase contains mostly a different solvent (possibly methanol in this case), which has a different refractive index, therefore its droplets are visible through light

scattering measurements. One cannot dismiss the possibility that because of complexity of the solutions speciation, certain formaldehyde-related species migrate into this phase while others remain in the aqueous phase, which would without a doubt have an effect on the mechanism on the gel formation. It also confirms that the catalyst plays an important role in microphase separation, therefore suggesting the gel formation process may involve mechanisms of a physical nature rather than be limited by chemical reactions.

Measurements of pH proved that addition of sodium carbonate strongly changes the acidity of the solution, which was expected. While at very low sodium carbonate concentrations pH increases very significantly, for more concentrated solutions the pH value seems to asymptotically approach certain value. This is very important to bear in mind when investigating the reacting systems. There is an assumption that addition of sodium carbonate causes the resorcinol to dissociate to a certain degree and the greater the pH value, the greater amount of resorcinol dissociates. These experiments prove that in the formaldehyde-water solutions certain amount of sodium carbonate is *consumed* because at a point further addition of the catalyst does not affect the pH anymore. Therefore, it has to be taken into consideration when analysing how much resorcinol is present in a form of ion in the reacting system – one cannot make such approximate calculations without taking this effect into consideration.

Reacting (formaldehyde-methanol-water-sodium carbonate-resorcinol) solutions

Examination of the reacting solutions is more complex than that of equilibrium (non-reacting) solutions as changes of their viscosity, pH and appearance need to be accounted for, especially when using sensitive spectroscopic methods. The formaldehyde-resorcinol polymerization process was investigated from two angles: one was to determine the chemical changes in the solution, while the other focused on physical changes like formation of nano-sized particulates and possible phase separation. In order to examine the chemical reactions between formaldehyde and resorcinol in aqueous solutions both ^{1}H and ^{13}C NMR were used, along with IR spectroscopy. Dynamic Light Scattering proved invaluable when investigating the physical changes occurring in the solution due to formation of formaldehyde-resorcinol reaction products.

The results of the gelation time measurements determined the timeframe in which experiments involving NMR or DLS could be performed. The results of the gel time measurements in 55°C allowed to make an informed decision about the duration of experiments performed in DLS and NMR at the highest permitted temperature. The set of gel time experiments performed in 55°C, 80°C and 90°C was used to compare the effect of the temperature on the overall gelation time. It was found that there is a strong dependency of the gelation time on the temperature and that it is not linear. The gelation times for the samples reacting in 80°C and 90°C are virtually identical, while for 55°C these values are as much as five times longer. The overall conclusion is that the gelation time is strongly decreasing with temperature. The relationship of the gelation time with the R/C ratio is similar. As expected, the greater the concentration of the catalyst, the shorter the gelation time. Interestingly, the effect of the catalyst concentration on the gelation time is relatively modest, as doubling the concentration leads to a decrease of

gelation time by only one third. Another interesting observation is that there appears to be a stronger dependency on the catalyst concentration in samples which were reacting in 55°C, rather than in 80°C. The results also show that an increase in the resorcinol concentration decreases the gelation time of the sample, as expected. However, this effect is very significant for lower R/W ratios and, as with the catalyst concentration influence, for samples reacting in 55°C.

The results obtained from the NMR spectroscopy experiments were the most informative. A series of experiments performed using ^{13}C NMR revealed presence of hydroxymethyl resorcinol derivatives even at a very early stage of the reaction, without any temperature treatment, which was confirmed by ^{1}H NMR spectroscopy. Moreover, the concentrations of these products at early stage are quite significant. This is very important, as previous research assumed that the rate of reaction between resorcinol and formaldehyde in presence of sodium carbonate in room temperature is very slow and it was not expected to find hydroxymethyl resorcinol derivatives only a few minutes after addition of formaldehyde. Therefore, one has to be aware that even during the preparation of the reacting solution, which usually involves long mixing time of all reactants in room temperature, products are already forming. Since subsequent condensation is triggered by higher temperatures, it is safe to assume that very little condensation – if any – will take place during the solution preparation stage.

Qualitative analysis of the ^{13}C NMR spectra involved their assignment basing on the calculated values of chemical shifts and on the values previously measured for the non-reacting solutions and also on previous literature. A series of ^{1}H NMR spectra were measured for the reacting solutions at room

temperature. Having the ^{13}C NMR spectra properly assigned, identification of peaks visible in the ^{1}H spectra was facilitated by using results of HSQC measurements. Presence of hydroxymethyl derivatives just a few minutes after addition of formaldehyde was confirmed with these experiments. The experiments performed on a sample which was heated for 10 min in 80°C and then cooled down to 20°C revealed presence of a number of products. Some of the identified species were expected, like mono-substituted hydroxymethylresorcinol with the hydroxymethyl group located at carbon atom 4 or 6. The product which was less expected to be found was a di-substituted hydroxymethylresorcinol with hydroxymethyl groups at carbon atoms 4 or 6 and 2. It was more surprising that the measured spectra confirmed presence of resorcinol substituted at carbon atom number 5. The species found were mono-substituted hydroxymethylresorcinol at carbon atom 5 and a di-substituted hydroxymethylresorcinol at carbons 2 and 5. Since some of these peaks may overlap on the ^{1}H NMR spectra, using HSQC and ^{13}C NMR spectra were invaluable in confirming these assignments.

^{1}H NMR experiments provided information on the changes in reactants' concentrations shedding light on the influence of the catalyst concentration and temperature on the rate of the reactions between them. The results of experiments performed at both temperatures investigated here (20°C and 55°C) showed that the concentrations of both total formaldehyde and resorcinol decreased rapidly within first few minutes of mixing the two solutions, followed by a more gradual decrease over time. When plotted in scaled time, accounting for catalyst concentrations, the rates of consumption of both reactants were found to be very similar for all catalyst concentrations at a given temperature, which is consistent with the role of sodium carbonate as a catalyst for the substitution reaction of resorcinol with formaldehyde.

Concentrations of all major formaldehyde-related species decrease in time in a similar manner as expected, since these species are in mutual equilibria. Peak corresponding to the protons in the hydroxymethyl group attached to resorcinol can be analysed to obtain additional information on the substitution reactions at 20°C, where deconvolution from the dominant –OH/D peak was possible. The concentration of substituted resorcinol species corresponding to this peak was found to correspond to loss of resorcinol concentration in terms of C(2,4,6) sites, indicating that no condensation reaction was taking place at this temperature. Furthermore, there was no significant loss of signal from C(5) sites of resorcinol, which shows that there was little or none substitution at this site and the substituted resorcinol was present in solution and completely visible to liquid NMR. Interestingly, the number of formaldehyde molecules consumed per resorcinol was 3 or more, indicating full substitution at all C(2,4,6) sites at all times.

In contrast, results from experiments at 55°C showed that while degree of formaldehyde substitution was around 2 formaldehyde molecules per resorcinol, the loss of signal from C(5) sites of resorcinol was very close to that from C(2,4,6) sites. This indicates that doubly substituted resorcinol appears to be subject to condensation or further substitution resulting in either highly reactive or insoluble intermediate which then leaves solution and forms another (micro)phase, since liquid NMR signal from C(5) sites is lost.

Experiments performed using the IR spectroscopy were not amenable to detailed quantitative analysis, especially in comparison with ^{1}H NMR results. However, since IR spectroscopy is a common technique widely used in industry and as a means of off-line and in-line quality monitoring, an

attempt was made to assess applicability of this method to provide insight into the resorcinol-formaldehyde sol-gel process. The IR spectra change their shape mainly in the 1400-1550 cm^{-1} region, i.e. the area where O-H bending, CH_3 asymmetric bend and C=C stretching in ring vibrations give rise to peaks. This is likely caused by both the substitution of the aromatic ring and condensation of hydroxymethyl resorcinol derivatives. Three of peaks characteristic for 1,3-substitution, found at 685 cm^{-1}, 740 cm^{-1} and 770 cm^{-1}, decrease their intensity in the course of the reaction. This proves that resorcinol is substituted at other carbon atoms in aromatic ring than those which are already substituted with hydroxyl groups and that the 1,3-substitution is accompanied by other species, namely by hydroxymethyl resorcinol derivatives. Decrease in intensity of peaks at 965 and 1150 cm^{-1} has been used to monitor consumption of resorcinol in substitution reaction with formaldehyde.

Results of the Dynamic Light Scattering experiments were very interesting in revealing the trends in growth of primary particles forming the gel network. Analysis of the shapes of the DLS autocorrelation functions allowed to see that during the early stages of reaction the primary particles were diffusing freely , showing single exponential decay, while at intermediate stages a power law decay was developing indicating growth and networking of clusters leading to eventual gelation. Comparison of the autocorrelation functions across temperatures and R/C ratios allowed to establish that the intermediate stage is reached much faster at elevated temperature and at higher catalyst concentration. Mathematical analysis of the autocorrelation functions allowed to estimate the mean apparent hydrodynamic radii of primary particles and it was found that their growth was independent of the catalyst concentration as well as resorcinol concentration at a given

temperature. At higher temperatures the primary particles grew faster and were subject to clustering and networking at earlier times. This confirms that the overall rate of gel formation is increased by higher temperature as expected. When the samples approach the gelation point, the apparent hydrodynamic radius grows rapidly until the sample becomes solid. However, since the measured autocorrelation function show power law secondary decay, this influences the initial decay rate so that the estimated hydrodynamic diameters at later times do not correspond to actual size of primary particle but rather reflect dynamics of clusters and networks incorporating them. Nevertheless, the key finding here is that sizes of the primary particles formed at the early stages of resorcinol-formaldehyde sol-gel process do not depend on the catalyst concentration. This suggests that the catalyst (sodium carbonate) plays a role in the gel formation process which is primarily related to clustering of primary particles and formation of the resulting physical particulate gel.

While pH measurements taken at room temperature in the reacting solution showed a very slow decrease of pH over timer, results from experiments performed in 90°C showed that all compositions, regardless of the R/C ratio, experienced a significant (about one pH unit) decrease of pH within the first 20-40 minutes. It is possible that the changes in the pH are caused by the reactions involving formaldehyde and/or resorcinol or by microphase separation, although no conclusive explanation for this phenomenon has yet been achieved.

Recommendations for future work

In the course of research that led to formation of this thesis many questions, doubts as well as theories were developed, although many of them are not included here. In most cases it was time and equipment limitations that prevented the author from expanding this work and venturing into their verification.

In terms of glycol equilibria it would be highly beneficial to expand the temperature range in which the speciation was determined and thus expand the temperature range in which equilibrium constants can be determined. The results proved that the pH changes with dilution of the formaldehyde solution in a rather unexpected manner and this would require confirmation by running experiments using a different type of electrode, though the one used here was attested for measurements in solutions containing alcohols.

In terms of formaldehyde-water-sodium carbonate solutions' investigations, it is highly recommended to further explore the possibility of phase separation by NMR techniques. There is a number of 2D methods which include precise measurements of T_2 and diffusion coefficients, however, their development and adjustments are time consuming and therefore they were not included in this research. Possibly also SAXS or SANS could also be used to further explore these solutions, however they were not available to the author.

In terms of experiments involving kinetics, there are a few questions that call for further exploration. Most of all, an explanation on the pH changes in the course of the reaction ought to be found. A number of theories was explored by the author, however none of them seemed to explain the phenomenon. It

was observed by the author that in higher temperatures concentration of protons at C(5) in resorcinol decreases proportionally with other resorcinol signals. The author's interpretation of this phenomenon is that in this temperature substituted resorcinol condenses or is further substituted and become insoluble in the reacting mixture and thus is invisible in the ^{1}H NMR spectra. Even though this theory is supported by the DLS results, its confirmation would be of great value. Following kinetics using NMR proved to be challenging, however, while this work was underway a number of publications of a new, highly advanced technique were released. An Ultrafast NMR method allows to follow in real time how the concentrations of species change in a reacting sample. Instead of measurements taking a couple of minutes, these last just tenths of minutes and can be ran continuously. As a result even 3D spectra can be obtained, with the z-axis being the reaction time. This method is relatively novel and requires both an experienced expert in the field as well as sufficient amount of adjustments and development of the process.

All of the experimental results presented in this work point to phase separation as the mechanism of gel formation, however it remains unknown what is the composition of each phase. It is without a doubt the greatest challenge of the future work.

CHAPTER 8. REFERENCES

1. **McNaught, A.D., Wilkinson, A.** *IUPAC. Compendium of Chemical Terminology.* 2nd. Oxford : Blackwell Scientific Publications, 1997.

2. **Brinker, C.J. and Scherer, G.W.** *Sol-gel science: the physics and chemistry of sol-gel processing.* s.l. : Gulf Professional Publishing, 1990.

3. **Pekala, R.W.** *4 873 218* USA, 1989.

4. **Scherdel, C. and Reichenauer, G.** Carbon xerogels synthesized via phenol–formaldehyde gels. *Microporous and Mesoporous Materials.* 2009, Vol. 126, pp. 133-142.

5. **du Fresne von Hohenesche, C., Schmidt, D.F. and Schädler, V.** Templating, Nanoporous Melamine−Formaldehyde Gels by Microemulsion. *Chemistry of Materials.* 2008, Vol. 20, pp. 6124-6129.

6. **Wu, D. and Fu, R.** Synthesis of organic and carbon aerogels from phenol–furfural by two-step polymerization. *Microporous and Mesoporous Materials.* 2006, Vol. 96, pp. 115-120.

7. **Guo, S-C.** Control of Mesoporous Structure of Aerogels Derived from Cresol-Formaldehyde. *Journal of Colloid and Interface Science.* 2002, Vol. 254, pp. 153-157.

8. **Sciarra, J.J. and Sciarra, C.J.** *Aerosols. Kirk-Othmer Encyclopedia of Chemical Technology.* s.l. : John Wiley & Sons, Inc., 2001.

9. **Al-Muhtaseb, S.A. and Ritter, J.A.** Preparation and Properties Resorcinol-Formaldehyde Organic and Carbon Gels. *Advanced Materials.* 2003, Vol. 15, pp. 101-114.

10. **Yamamoto, T., et al.** Evaluation of porous structure of resorcinol-formaldehyde hydrogels by thermoporometry. *Thermochimica Acta.* 2005, Vol. 439, pp. 74-79.

11. **Hüsing, N. and Schubert, U.** *Aerogels. Ullmann's Encyclopedia of Industrial Chemistry.* s.l. : Wiley-VCH Verlag GmbH & Co. KGaA, 2006.

12. **Pekala, R.W., et al.** Carbon aerogels for electrochemical applications. *Journal of Non-Crystalline Solids.* 1998, Vol. 225, pp. 74-80.

13. **Elkhatat, A.M. and Al-Muhtaseb, S.A.** Advances in tailoring resorcinol-formaldehyde organic and carbon gels. *Advanced materials.* 2011, Vol. 23, pp. 2887-2903.

14. **Contreras, M.S., et al.** A comparison of physical activation of carbon xerogels with carbon dioxide with chemical activation using hydroxides. *Carbon.* 2010, Vol. 48, pp. 3157-3168.

15. **Tian, H.Y., et al.** A synthesis method for cobalt doped carbon aerogels with high surface area and their hydrogen storage properties. *International Journal of Hydrogen Energy.* 2010, Vol. 35, pp. 13242-13246.

16. **Lee, Y.J., et al.** Nano-sized metal-doped carbon aerogel for pseudo-capacitive supercapacitor. *Current Applied Physics.* 2011, Vol. 11, pp. 631-635.

17. **Cotet, L.C., et al.** Structural properties of some transition metal highly doped carbon aerogels. *Journal of Alloys and Compounds.* 2007, Vol. 434, pp. 854-857.

18. **Halama, A. and Szubzda, B.: Pasciak, G.** Carbon aerogels as electrode material for electrical double layer supercapacitors—Synthesis and properties. *Electrochimica Acta.* 2010, Vol. 55, pp. 7501-7505.

19. **Li, W., Reichenauer, G. and Fricke, J.** Carbon aerogels derived from cresol–resorcinol–formaldehyde for supercapacitors. *Carbon.* 2002, Vol. 40, pp. 2955-2959.

20. **Saliger, R., et al.** High surface area carbon aerogels for supercapacitors. *Journal of Non-Crystalline Solids.* 1998, Vol. 225, pp. 81-85.

21. **Mirzaeian, M. and Hall, P.J.** Preparation of controlled porosity carbon aerogels for energy storage in rechargeable lithium oxygen batteries. *Electrochimica Acta.* 7444-7451, Vol. 54, pp. 7444-7451.

22. **Xu, P., et al.** Treatment of brackish produced water using carbon aerogel-based capacitive deionization technology. *Water Research.* 2008, Vol. 42, pp. 2605-2617.

23. **van den Berg, A.W.C. and Areán, C.O.** Materials for hydrogen storage: current research trends and perspectives. *Chemical Communications.* 2008, Vol. 6, pp. 668-681.

24. **Moreno-Castilla, C. and Maldonado-Hodar, F.J.** Carbon aerogels for catalysis applications: An overview. *Carbon.* 2005, Vol. 43, pp. 455-465.

25. **Tonanon, N., et al.** Preparation of resorcinol formaldehyde (RF) carbon gels: Use of ultrasonic irradiation followed by microwave drying. *Journal of Non-Crystalline Solids.* 2006, Vol. 352, pp. 5683-5686.

26. **Zhao, J., et al.** Preparation and electrical properties of SBN thin films derived from aqueous organic gels. *Materials Letters.* 2004, Vol. 58, pp. 1456-1460.

27. **Nie, F., et al.** Sol-gel synthesis of nano-composite crystalline HMX/AP coated by resorcinol-formaldehyde. *Journal of Physics and Chemistry of Solids.* 2010, Vol. 71, pp. 109-113.

28. **Gerberich, H.R. and Seaman, G.C.** *Formaldehyde. Kirk-Othmer Encyclopedia of Chemical Technology.* s.l. : John Wiley & Sons, Inc., 2008.

29. **Reuss, G., et al.** *Formaldehyde. Ullmann's Encyclopedia of Industrial Chemistry.* s.l. : Wiley-VCH Verlag GmbH & Co. KGaA, 2000.

30. **Walker, J.** *Formaldehyde.* 2nd ed. New York : Reinhold Publishing Corporation, 1953.

31. **Saliger, R., et al.** Carbon aerogels from dilute catalysis of resorcinol with formaldehyde. *Journal of Non-Crystalline Solids.* 1997, Vol. 221, pp. 144-150.

32. **Feng, Y.N., et al.** Effects of further adding of catalysts on nanostructures of carbon aerogels. *Materials Science and Engineering B.* 2008, Vol. 148, pp. 273–276.

33. **Zubizarreta, L., et al.** Development of microporous carbon xerogels by controlling synthesis conditions. *Journal of Non-Crystalline Solids.* 2008, Vol. 354, pp. 817–825.

34. **Tamon, H. and Ishizaka, H.** Influence of Gelation Temperature and Catalysts on the Mesoporous Structure of Resorcinol–Formaldehyde Aerogels. *Journal of Colloid and Interface Science.* 2000, Vol. 223, pp. 305-307.

35. **Mulik, S., Sotiriou-Leventis, C. and Levent, N.** Time-Efficient Acid-Catalyzed Synthesis of Resorcinol-Formaldehyde Aerogels. *Chemistry of Materials.* 2007, Vol. 19, pp. 6138–6144.

36. **Brandt, R., et al.** Acetic Acid Catalyzed Carbon Aerogels. *Journal of Porous Materials.* 2003, Vol. 10, pp. 171–178.

37. **Kirk-Othmer.** *Encyclopedia of Chemical Technology.* s.l. : John Wiley & Sons Inc., 2007.

38. *Kinetics and chemical equilibrium of the hydration of formaldehyde.* **Winkelman, J.G.M., et al.** 2002, Chemical Engineering Science, Vol. 57, pp. 4067-4076.

39. **Lebrun, N., et al.** Raman analysis of formaldehyde aqueous solutions as a function of concentration. *Journal of Raman Spectroscopy.* 2003, Vol. 34, pp. 459-464.

40. **Matsuura, H., Yamamoto, M. and Murata, H.** Raman spectra and normal vibrations of methylene glycol and its perdeuterated analogue. *Spectrochimica Acta Part A: Molecular Spectroscopy.* 1980, Vol. 36, pp. 321-327.

41. **Möhlmann, G.R.** Raman spectra of aqueous solutions of formaldehyde and its oligomers. *Journal of Raman Spectroscopy.* 1987, Vol. 18, pp. 199-203.

42. **Busca, G., et al.** FT-IR study of the adsorption and transformation of formaldehyde on oxide surfaces. *Journal of the American Chemical Society.* 1987, Vol. 109, pp. 5197-5202.

43. **Góra-Marek, K.** IR studies of the transformation of formaldehyde and methanol on Co-ferrierites. *Microporous and Mesoporous Materials.* 2011, Vol. 145, pp. 93-97.

44. **Johnson, R.A. and Stanley, A. E.** GC/MS and FT-IR Spectra of Methoxymethanol. *Applied Spectroscopy.* 1991, Vol. 45, pp. 218-222.

45. **Dankelman, W. and Daemen, J. M. H.** Gas chromatographic and nuclear magnetic resonance determination of linear formaldehyde oligomers in formalin. *Analytical Chemistry.* 1976, Vol. 48, pp. 401–404.

46. **Le Botlan, D.J., Mechln, B.G. and Martin, G.J.** Proton and Carbon-I 3 Nuclear Magnetic Resonance Spectrometry of Formaldehyde in Water. *Analytical Chemistry.* 1983, Vol. 55, pp. 587-591.

47. **Hasse, H. and Maurer, G.** Kinetics of the Poly(oxymethylene) Glycol Formation in Aqueous Formaldehyde Solutions. *Industrial & Engineering Chemistry Research.* 1991, Vol. 30, pp. 2195-2200.

48. **Hahnenstein, I., et al.** 1H- and 13C-NMR Spectroscopic Study of Chemical Equilibria in Solutions of Formaldehyde in Water, Deuterium Oxide, and Methanol. *Industrial & Engineering Chemistry Research.* 1994, Vol. 33, pp. 1022-1029.

49. **Hahnenstein, I., et al.** NMR Spectroscopic and Densimetric Study of Reaction Kinetics of Formaldehyde Polymer Formation in Water, Deuterium Oxide, and Methanol. *Industrial & Engineering Chemistry Research.* 1995, Vol. 34, pp. 440-450.

50. **Albert, M., et al.** Vapor-Liquid and Chemical Equilibria of Formaldehyde-Water Mixtures. *American Institute of Chemical Engineers Journal.* 1999, Vol. 45, pp. 2024-2033.

51. **Balashov, A.L., et al.** Association of Formaldehyde in Aqueous-Alcoholic Systems. *Russian Journal of General Chemistry.* 2002, Vol. 72, pp. 744-747.

52. **Maiwald, M., et al.** Quantitative NMR Spectroscopy of Complex Liquid Mixtures: Methods and Results for Chemical Equilibria in Formaldehyde-Water-Methanol at Temperatures up to 383 K. *Industrial & Engineering Chemistry Research.* 2003, Vol. 42, pp. 259-266.

53. **Maiwald, M., et al.** Quantitative high-resolution on-line NMR spectroscopy in reaction and process monitoring. *Journal of Magnetic Resonance.* 2004, Vol. 166, pp. 135-146.

54. **Ott, M., et al.** Kinetics of oligomerization reactions in formaldehyde solutions: NMR experiments up to 373K and thermodynamically consistent model. *Chemical Engineering and Processing.* 2005, Vol. 44, pp. 653–660.

55. **Maiwald, M., et al.** Quantitative NMR spectroscopy of complex technical mixtures using a virtual reference: chemical equilibria and reaction kinetics of formaldehyde–water–1,3,5-trioxane. *Analytical and Bioanalytical Chemistry.* 2006, Vol. 385, pp. 910-917.

56. **Durairaj, Raj B.** *Resorcinol: Chemistry, Technology and Applications.* 1st ed. s.l. : Springer, 2005.

57. **Weast, R.C.** *CRC Handbook of chemistry and physics.* 66. s.l. : CRC Press Inc., 1986.

58. **McKee, Wolf.** *Water quality criteria.* s.l. : California state water resources control board, 1963.

59. **Association, ESAPA – European Soda Ash Producers.** *Soda Ash Process BREF.* Brussels : European Chemical Industry Council, 2004.

60. **Pekala, R.W.** Organic aerogels from the polycondensation of resorcinol with formaldehyde. *Journal of Materials Science.* 1989, Vol. 24, p. 3221 3227.

61. **Gommes, C.J. and Roberts, A.P.** Structure development of resorcinol-formaldehyde gels: Microphase separation or colloid aggregation. *Physical Review E.* 2008, Vol. 77.

62. **Atkins, P.W. and de Paula, J.** *Elements of Physical Chemistry.* 5th Edition. Oxford : Oxford University Press, 2009.

63. **Wiener, M., et al.** Accelerating the synthesis of carbon aerogel precursors. *Journal of Non-Crystalline Solids.* 2004, Vol. 350, pp. 126–130.

64. **Yamamoto, T., et al.** Dynamic and Static Light Scattering Study on the Sol-Gel Transition of Resorcinol-Formaldehyde Aqueous Solution. *Journal of Colloid and Interface Science.* 2002, Vol. 245, pp. 391–396.

65. **Lin, C. and Ritter, J.A.** Effect of Synthesis pH on the Structure of Carbon Xerogels. *Carbon.* 1997, Vol. 35, pp. 1271-1278.

66. **Zanto, E.J., Al-Muhtaseb, S.A. and Ritter, J.A.** Sol-Gel-Derived Carbon Aerogels and Xerogels: Design of Experiments Approach to Materials Synthesis. *Industrial and Engineering Chemistry Research.* 2002, Vol. 41, pp. 3151-3162.

67. **Job, N., et al.** Porous carbon xerogels with texture tailored by pH control during sol–gel process. *Carbon.* 2004, Vol. 42, pp. 619–628.

68. **Pekala, R.W., et al.** Aerogels derived from multifunctional organic monomers. *Journal of Non-Crystalline Solids.* 1992, Vol. 145, pp. 90-98.

69. **Mayer, S.T., Kaschmitter, J.L. and Pekala, R.W.** *5 420 168* USA, 1995.

70. **Mayer, S.T., Kong, F. and Pekala, R.W., Kaschmitter, J.L.** *5 508 341* USA, 1996.

71. **Kaschmitter, J.L., Mayer, S.T. and Pekala, R.W.** *5 789 338* USA, 1998.

72. **Petričević, R., et al.** Structure of carbon aerogels neat the gelation limit of the resorcinol–formaldehyde precursor. *Journal of Non-Crystalline Solids.* 1998, Vol. 225, pp. 41-45.

73. **Coronado, P.R. and Poco, J.F.** *6 087 407* USA, 2000.

74. **Berthon, S., et al.** DLS and SAXS investigations of organic gels and aerogels. *Journal of Non-Crystalline Solids.* 2001, Vol. 285, pp. 154-161.

75. **Morales-Torres, S., et al.** Textural and mechanical characteristics of carbon aerogels synthesized by polymerization of resorcinol and formaldehyde using alkali carbonates as basification agents. *Physical Chemistry Chemical Physics.* 2010, Vol. 12, pp. 10365–10372.

76. **Horikawa, T., Hayashi, J. and Muroyama, K.** Controllability of pore characteristics of resorcinol–formaldehyde carbon aerogel. *Carbon.* 2004, Vol. 42, pp. 1625-1633.

77. **Fairen-Jimenez, D., Carrasco-Marin, F. and Moreno-Castilla, C.** Porosity and surface area of monolithic carbon aerogels prepared using alkaline carbonates and organic acids as polymerization catalysts. *Carbon.* 2006, Vol. 44, pp. 2301-2307.

78. **Job, N., et al.** Effect of the counter-ion of the basification agent on the pore texture of organic and carbon xerogels. *Journal of Non-Crystalline Solids.* 2008, Vol. 354, pp. 4698–4701.

79. **Grenier-Loustalot, M-F., et al.** Phenolic resins: 2. Influence of catalyst type on reaction mechanisms and kinetics. *Polymer.* 1996, Vol. 37, pp. 1363-1369.

80. **Bock, V., Emmerling, A. and Fricke, J.** Influence of monomer and catalyst concentration on RF and carbon aerogel structure. *Journal of Non-Crystalline Solids.* 1998, Vol. 225, pp. 69–73.

81. **Lu, X., et al.** Thermal Conductivity of Monolithic Organic Aerogels. *Science.* 1992, Vol. 255, pp. 971-972.

82. **Lu, X., et al.** Correlation between structure and thermal conductivity of organic aerogels. *Journal of Non-Crystalline Solids.* 1995, Vol. 188, pp. 226-234.

83. **Merzbacher, C.I., et al.** Carbon aerogels as broadband non-reflective materials. *Journal of Non-Crystalline Solids.* 2001, Vol. 285, pp. 210-215.

84. **Petričević, R., Glora, M. and Fricke, J.** Planar fibre reinforced carbon aerogels for application in PEM fuel cells. *Carbon.* 2001, Vol. 39, pp. 857-867.

85. **Yamamoto, Y., et al.** Control of mesoporosity of carbon gels prepared by sol–gel polycondensation and freeze drying. *Journal of Non-Crystalline Solids.* 2001, Vol. 288, pp. 46-55.

86. **Tamon, H., et al.** Porous structure of organic and carbon aerogels synthesized by sol-gel polycondensation of resorcinol with formaldehyde. *Carbon.* 1997, Vol. 35, pp. 791-796.

87. **Anderson, R., Haines, H. and Stark, P.** Analysis of Resorcinol-Phenol-Formaldehyde Resins by NMR Spectroscopy. *Die Angewandte Makromolekulare Chemie.* 1972, Vol. 26, pp. 171-176.

88. **Sojka, S.A., Wolfe, R.A. and Guenther, G.D.** Formation of Phenolic Resins: Mechanism and Time Dependence of the Reaction of Phenol and Hexamethylenetetramine As Studied by Carbon-13 Nuclear Magnetic

Resonance and Fourier Transform Infrared Spectroscopy. *Macromolecules.* 1981, Vol. 14, pp. 1539-1543.

89. **Kim, M.G., Amos, L.W. and Barnes, E.E.** Study of the Reaction Rates and Structures of a Phenol-Formaldehyde Resol Resin by Carbon-13 NMR and Gel Permeation Chromatography. *Industrial and Engineering Chemistry Research.* 1990, Vol. 29, pp. 2032-2037.

90. **Fisher, T.H., et al.** One- and Two-Dimensional NMR Study of Resol Phenol-Formaldehyde Prepolymer Resins. *Magnetic Resonance in Chemistry.* 1995, Vol. 33, pp. 717-723.

91. **Luukko, P., et al.** Optimizing the Conditions of Quantitative 13C-NMR Spectroscopy Analysis for Phenol-Formaldehyde Resol Resins. *Journal of Applied Polymer Science.* 1998, Vol. 69, pp. 1805-1812.

92. **Rego, R., et al.** Fully quantitative carbon-13 NMR characterization of resol phenol-formaldehyde prepolymer resins. *Polymer.* 2004, Vol. 45, pp. 33–38.

93. **Werstler, D.D.** Quantitative 13C n.m.r. characterization of aqueous formaldehyde resins: 2. Resorcinol-formaldehyde resins. *Polymer.* 1986, Vol. 27, pp. 757 -764.

94. **Christiansen, A.W.** Resorcinol-Formaldehyde Reactions in Dilute Solution Observed by Carbon-13 NMR Spectroscopy. *Journal of Applied Polymer Science,.* 2000, Vol. 75, pp. 1760-1768.

95. **Pizzi, A., et al.** Structure of Resorcinol, Phenol, and Furan Resins by MALDI-TOF Mass Spectrometry and 13C NMR. *Journal of Applied Polymer Science.* 2004, Vol. 92, pp. 2665–2674.

96. **Moudrakovski, I.L., et al.** Nuclear Magnetic Resonance Studies of Resorcinol-Formaldehyde Aerogels. *The Journal of Physical Chemistry B.* 2005, Vol. 109, pp. 11215-11222.

97. **Bock, V., et al.** Structural Investigation of Resorcinol Formaldehyde and Carbon Aerogels Using SAXS and BET. *Journal of Porous Materials.* 1997, Vol. 4, pp. 287–294.

98. **Melnichenko, Y.B. and Wignall, G.D.** Small-angle neutron scattering in materials science: Recent practical applications. *Journal of Applied Physics.* 2007, Vol. 102.

99. **Czakkel, O., et al.** Copper-containing resorcinol–formaldehyde networks. *Microporous and Mesoporous Materials.* 2009, Vol. 126, pp. 213–221.

100. *Effect of Container Size on Gelation Time: Experiments and Simulations.* **Anglaret, E., Hasmy, A. and Jullien, R.** 22, 1995, Physical review letters, Vol. 75, pp. 4059-4062.

101. *Rheological characterization of the gel point in sol–gel transition.* **Payro, E.R. and Llacuna, J.L.** 2006, Journal of Non-Crystalline Solids, Vol. 352, pp. 2220–2225.

102. *Detecting sol–gel transition using light transmission.* **Anderson, A.M., et al.** 2004, Journal of Non-Crystalline Solids, Vol. 350, pp. 259-265.

103. *Time-Resolved Dynamic Light Scattering Studies on Gelation Process of Organic–Inorganic Polymer Hybrids.* **Norisuye, T., et al.** 1999, Macromolecules, Vol. 32, pp. 1528-1533.

104. **Atkins, P.W.** *Physical Chemistry.* 6th Edition. s.l. : W.H. Freeman & Company, 1997.

105. **Miessler, L.M. and Tar, D.A.** *Inorganic Chemistry.* 2nd Edition. s.l. : Pearson Prentice-Hall, 1991.

106. **Williams, Dudley H. and Fleming, Ian.** *Spectroscopic Methods in Organic Chemistry.* s.l. : MacGraw-Hill Education, 2008.

107. **Smith, Brian C.** *Infrared Spectral Interpretation: A Systematic Approach.* s.l. : CRC Press LLC, 1999. 0-8493-2463-7.

108. **Kemp, William.** *Organic Spectroscopy.* s.l. : Palgrave Publishers Ltd., 1991. ISBN 0-333-51953-1.

109. **Sundin, Ch.E.** [Online] [Cited: 23 07 2011.] http://www.uwplatt.edu/~sundin/ir/irl.htm.

110. **PerkinElmer Life and Analytical Sciences.** *Technical Note: FT-IR Spectroscopy, Attenuated Total Reflectance (ATR).* Shelton, CT, USA : s.n., 2005.

111. **Hendra, P., Jones, C., Warness, G.** *Fourier Transform Raman Spectroscopy.* Chichester : Ellis Horwood Ltd., 1991.

112. **Smith, W.E. and Dent, G.** *Modern Raman Spectroscopy - A Practical Approach.* 2005.

113. *Particle Sizing by Quasi-Elastic Light Scattering.* **Finsy, Robert.** s.l. : Elsevier Science B.V., 1994, Advances in Colloid and Interface Science, Vol. 52, pp. 79-143.

114. **Smoluchowski, M.** O fluktuacjach termodynamicznych i ruchach Browna. *Prace matematyczno-fizyczne.* Warszawa : s.n., 1914, Vol. XXV, pp. 188-263.

115. **Hore, P.J.** *Nuclear Magnetic Resonance.* s.l. : Oxford University Press Inc., 1995.

116. **Keeler, J.** *Understanding NMR Spectroscopy.* 2nd Edition. Cambridge : John Wiley & Sons, Ltd., 2010.

117. **Sigma-Aldrich Company Ltd.** Safety Data Sheet. 21 07 2011.

118. **Parella, T.** Bruker TopSpin v2.0 NMR Guide. *Pulse Program Catalogue.* s.l. : Bruker BioSpin GmbH, 03 03 2006.

119. *Solvent peak saturation with single phase and quadrature Fourier transformation.* **Hoult, D.I.** 1976, Journal of Magnetic Resonance, Vol. 21, p. 337.

120. **Kirk-Othmer.** *Kirk-Othmer Encyclopedia of Chemical Technology.* 5. s.l. : John Wiley & Sons, Inc., 2006. Vol. 23.

121. *Online monitoring of synthesis and curing of phenol–formaldehyde resol resins by Raman spectroscopy.* **Monni, J., et al.** 2008, Polymer, Vol. 49, pp. 3865-3874.

122. *Equilibrium Composition of Formaldehyde Oligomers in Aqueous Solutions from IR Data.* **Ryabova, R.S., et al.** 2002, Russian Journal of Applied Chemistry, Vol. 75, pp. 22-24.

123. *Characterization of Phenol-Formaldehyde Prepolymer Resins by In Line FT-IR Spectroscopy.* **Poljanšek, I. and Krajnc, M.** 2005, Acta Chimica Slovenica, Vol. 52, pp. 238-244.

124. **Ferry, John D.** *Viscoelastic Properties of Polymers.* 3rd. s.l. : Wiley, 1980. 978-0471048947.

125. **Durairaj Raj B.** *Resorcinol: Chemistry, Technology and Applications.* 1st ed. brak miejsca : Springer, 2005.

APPENDIX A. COMPOSITIONS OF SAMPLES USED IN IR, DLS AND PH EXPERIMENTS

Formaldehyde-water			
Sample name	**Formaldehyde [ml]**	**Water [ml]**	
F-W 1-1	2.00	2.00	
F-W 1-3	2.00	6.00	
F-W 1-6	2.00	12.00	
F-W 1-10	1.00	10.00	
F-W 1-30	1.00	30.00	
F-W 1-60	1.00	60.00	
Formaldehyde-methanol			
Sample name	**Formaldehyde [ml]**	**Methanol [ml]**	
F-M 1-1	2.00	2.00	
F-M 1-3	1.00	3.00	
F-M 1-6	1.00	6.00	
F-M 1-10	1.00	10.00	
F-M 1-30	0.50	15.00	
F-M 1-60	0.50	30.00	
Formaldehyde-water-sodium carbonate (catalyst)			
Sample name	**Formaldehyde [ml]**	**Water [ml]**	**Sodium carbonate [g]**
FWC eq.50	1.47	7.00	0.0193
FWC eq.100	1.47	7.00	0.0096
FWC eq.200	1.47	7.00	0.0048
FWC eq.500	1.47	7.00	0.0019

Reacting solutions				
Sample name	**Formaldehyde [ml]**	**Water [ml]**	**Resorcinol [g]**	**Sodium carbonate [g]**
RC50 RW01 RF05	1.47	10.00	1.00	0.0193
RC100 RW01 RF05	1.47	10.00	1.00	0.0096
RC200 RW01 RF05	1.47	10.00	1.00	0.0048
RC300 RW01 RF05	1.47	10.00	1.00	0.0032
RC400 RW01 RF05	1.47	10.00	1.00	0.0024
RC500 RW01 RF05	1.47	10.00	1.00	0.0019
RC100 RW01 RF05	0.74	5.00	0.50	0.0048
RC178 RW02 RF05	1.47	5.00	1.00	0.0054
RC240 RW03 RF05	2.21	5.00	1.50	0.0060
RC292 RW04 RF05	2.95	5.00	2.00	0.0066
RC334 RW05 RF05	3.69	5.00	2.50	0.0072

APPENDIX B. COMPOSITIONS OF SAMPLES USED IN NMR EXPERIMENTS

Formaldehyde-water				
Sample name	**Formaldehyde [ml]**	**Water [ml]**	**Deuterium oxide [ml]**	
F-W 1-1	2.00	1.40	0.60	
F-W 1-3	1.00	2.10	0.90	
F-W 1-6	1.00	4.20	1.80	
F-W 1-10	1.00	7.00	3.00	
F-W 1-30	1.00	21.00	9.00	
F-W 1-60	1.00	42.00	18.00	
Formaldehyde-methanol				
Sample name	**Formaldehyde [ml]**	**Methanol [ml]**	**Deuterium oxide [ml]**	
F-M 1-1	2.00	2.00	1.00	
F-M 1-3	1.00	3.00	1.00	
F-M 1-6	1.00	6.00	1.50	
F-M 1-10	1.00	10.00	2.00	
F-M 1-30	0.50	15.00	3.00	
F-M 1-60	0.50	30.00	6.00	
Formaldehyde-water-sodium carbonate (catalyst)				
Sample name	**Formaldehyde [ml]**	**Water [ml]**	**Deuterium oxide [ml]**	**Sodium carbonate [g]**
FWC eq.50	1.47	7.00	3.00	0.0193
FWC eq.100	1.47	7.00	3.00	0.0096
FWC eq.200	1.47	7.00	3.00	0.0048
FWC eq.500	1.47	7.00	3.00	0.0019

Reacting solutions					
Sample name	**Formaldehyde [ml]**	**Water [ml]**	**Deuterium oxide [ml]**	**Resorcinol [g]**	**Sodium carbonate [g]**
RC50 RW01 RF05	1.47	7.00	3.00	1.00	0.0193
RC100 RW01 RF05	1.47	7.00	3.00	1.00	0.0096
RC200 RW01 RF05	1.47	7.00	3.00	1.00	0.0048
RC300 RW01 RF05	1.47	7.00	3.00	1.00	0.0032
RC400 RW01 RF05	1.47	7.00	3.00	1.00	0.0024
RC500 RW01 RF05	1.47	7.00	3.00	1.00	0.0019